Creation and exploration of single and multi antigen-targeting synthetic T cell immuno-stimulating treatments

BY ALEX SHEPHERD

Thesis Submitted to the University of Ottawa in partial Fulfillment of the requirements for the Doctorate in Immunology and Microbiology

Faculty of Medicine

University of Ottawa

COPYRIGHT PAGE

ACKNOWLEDGMENTS

I am exceedingly grateful to all of the people who have been there with me and helped me through my doctorate. First and foremost, is Dr. Scott McComb, my mentor and supervisor. Dr. McComb has given me countless opportunities to learn new things, encouraging me to explore new areas of study and expand my breadth of knowledge and experience, and continuously pushed me to my limits and beyond to become the scientist I am today. His support and belief in me are a large part of why I was able to come as far as I have.

Next, I want to acknowledge the work and support of my thesis advisory committee members, Dr. Subash Sad, Dr. Jennifer Hill and Dr. Shawn Beug. Their patience with me as I stumbled my way through TAC meeting, and their advice on improving my work and scientific communication has been invaluable over the course of this doctorate.

I also want to thank several different teams within the national research council. The cancer immunology team, the primary team I worked with for the past six years, for their patience and support. Being able to be apart of such a talented team and share in the amazing work that we have accomplished has been a tremendous honour. The proteomic team, specifically Dr. Jenniffer Hill, Dr. Rui Chen and Tammy-Lynn Tremblay for allowing me to use their space and their patience in teaching me proteomics. Finally, the genomic team, for all the work they have done to help me process the transcriptomic samples.

Finally, I want to acknowledge all of the amazing support from my family and friends and my wonderful partner. No matter how you supported me, know that I could not have done this without all of you.

This work was funded and supported by the Canadian National Research Council Human Health Therapeutics Division as well as BioCanRx.

Several of the figures included in this thesis were created using BioRender.Com

No Generative AI was used in the creation of this document

SUMMARY OF SCIENTIFIC CONTRIBUTIONS:

1. **Alex Shepherd**, Bigitha Bennychen, Anne Marcil, Darin Bloemberg, Rob Pon, Risini Weeratna, Scott McComb (2022) **A Simplified Function-First Method for the Discovery and Optimization of Bispecific Immune Engaging Antibodies,** PLoS One
2. Scott McComb, Tina Nguyen, **Alex Shepherd**, Kevin A Henry, Darin Bloemberg, Anne Marcil, Susanne Maclean, Ahmed Zafer, Rénald Gilbert, Christine Gadoury, Robert A Pon, Traian Sulea, Qin Zhu , Risini D Weeratna (2022) **Programmable Attenuation of Antigenic Sensitivity for a Nanobody-Based EGFR Chimeric Antigen Receptor Through Hinge Domain Truncation,** Frontiers Immunology Jul 22;13:8648681.
3. Scott McComb, Mehdi Arbabi-Ghahroudi, Kevin A Hay, Brian A Keller, Sharlene Faulkes, Michael Rutherford, Tina Nguyen, **Alex Shepherd**, Cunle Wu, Anne Marcil, Annie Aubry, Greg Hussack, Devanand M Pinto, Shannon Ryan, Shalini Raphael, Henk van Faassen, Ahmed Zafer, Qin Zhu, Susanne Maclean, Anindita Chattopadhyay, Komal Gurnani, Rénald Gilbert, Christine Gadoury, Umar Iqbal, Dorothy Fatehi, Anna Jezierski, Jez Huang, Robert A Pon, Mhairi Sigrist, Robert A Holt, Brad H Nelson, Harold Atkins, Natasha Kekre, Eric Yung, John Webb, Julie S Nielsen, Risini D Weeratna **Discovery and preclinical development of a therapeutically active nanobody-based chimeric antigen receptor targeting human CD22,** Molecular Therapy, Oncology
4. **Shepherd, A**., Bennychen, B., Ahmed, Z., Weeratna, R. D. and McComb, S. (2024). **A Flow Cytometry–Based Method for Assessing CAR Cell Binding Kinetics Using Stable CAR Jurkat Cells**. *Bio-protocol* 14(12): e5021. DOI: 10.21769/BioProtoc.5021.
5. Scott McComb, Bianca Dupont, **Alex Shepherd**, Bigitha Bennychen, et al**.** (2025) **Broadly Reactive Anti-VHH Antibodies for Characterizing, Blocking, or Activating Nanobody-Based CAR-T Cells, Antibody Therapeutics**
6. **Alex Shepherd,** Bigitha Bennychen, Laura Tamblyn, Shalini Raphael, Henk van Faassen, Greg Hussack, Mehdy Elahi, Nasha Nassoury, Jennifer J. Hill, Sameer Zulfiqar, Ahmed Zafer, Qin Zhu, Tina Nguyen, Robert A. Pon, Risini Weeratna, Mehdi Arbabi-Ghahroudi and Scott McComb, **Improving Solid Tumor Single Target Nano-CAR-T using a multi-antigen targeting platform,** Submitted to Frontiers in Immunology (October 2025)

ABSTRACT

The human body has developed many mechanisms and layers of defense against cancer, requiring multiple systems to fail for a malignancy to escape the immune system and pose a threat to the body. When cancers do develop, immunotherapy has emerged as a new potent way to harness these defense layers: using the body's own immune system, reprogramming a patient's immune cells using synthetically designed proteins that can stimulate T cells to attach to and kill cancerous cells. Here, I have explored the development and results of two distinct technological approaches for creating synthetic T cell stimulants: (1) Bi-specific T cell engagers (bTCEs); fusion proteins that combine multiple antibody-binding domains to simultaneously engage both T-cells and cancer cells in the body; and (2) Chimeric antigen receptors (CARs), fusion proteins that combine antigen targeting and immune cell stimulating domains that remain tethered to patient T cells, resulting in a living cell that can directly detect and respond to cancer cells.

I created two interoperable platforms to quickly and efficiently identify promising therapeutic TCE or CAR molecules. For TCEs, I established a high throughput function-first screening platform, allowing identification of effective TCE molecules without the need for protein purification. The second platform looked to expand a pre-existing CAR platform towards exploration of multi-antigen targeting CAR therapeutics. Specifically, two high-throughput molecular platforms were created to allow screening of multi-antigen CARs in either co-expression or tandem-CAR formats. I found that regardless of molecular strategy, multi antigen CARs maintained the ability to engage both targeted antigens and successfully suppressed tumor growth *in vitro*. In contrast to in vitro findings, co-

expression of CARs showed superior responses in a murine xenograft model of human lung cancer, relative to tandem CAR. Despite this clear superiority of co-expression in our experiments, I do not expect this finding to generalize to all multi-antigen targeting CARs, rather these results underline the need to approach multi-antigen CARs as unique entities.

In order to expand our screening methods for CAR-T, we developed two novel assays for CAR assessment. The first assessed the avidity of CAR-Jurkat cells using flow cytometry by assessing doublet formation of CAR-target pairs. When tested using CD22 CARs, we observed unique binding maximums for each CAR which appear to be enforce by an equilibrium in a biologically driven interaction. The second is an ongoing study using cell surface proteomics, phosphoproteomics and transcriptomics to better understand why the CD22 lead 1ug36 was superior to the other CD22 CARs tested along side it. Although still ongoing, this study has revealed potentially relevant differences in signaling through LCK, LAT, CD28 and the MAPK pathways.

As a whole, this work presents novel methods and findings related to the creation and assessment of synthetic T cell immuno-stimulating treatments.

TABLE OF CONTENTS

LIST OF TABLES AND FIGURES

Chapter 1

Chapter 2

Chapter 3

Chapter 4

Chapter 5

Chapter 6

CHAPTER 1: INTRODUCTION

1.1 – Overview of Cancer Immunology

1.1.1 – A Brief History of Immunotherapy and Oncology

Traditional cancer treatment options have been classified by the three pillars of cancer therapy: surgery, chemotherapy and radiation therapy for most its history. Starting with surgery, the resection of tumor was and still is the therapy with the highest survival rate when performed correctly, with the first radical mastectomy being performed in 1882 by William Halsted.[1] Next, radiation therapy: concentrated ionizing radiation directly to the tumor was first recorded in 1899 by Swedish physicians Tor Stenbeck and Tage Sjogren.[1] Finally, chemotherapeutics emerged post world war two with the use of mustard gas (mechlorethamine) being approved to treat malignancies.[1] However, decades of concerted effort have added a new pillar: immunotherapy.[2] Immunotherapy involves harnessing the bodies own innate ability to detect and kill cancer cells through methods like retargeting immune cells like T cells or NK cells, or by supplying the body with tumor specific antibodies either through a generic monoclonal antibody (mAb) produced in a lab, or a cancer vaccine.

While oft thought of as a recent achievement in oncology, harnessing the immune systems in an attempt to treat cancer was first pioneered in 1891. Here, the father of immunology, William Bradely Coley attempted, and in some cases succeeded, to cure patients using an injection of weakened/attenuated *Streptococcus pyogenes* and *Serratia marcescens,* after noting remissions in patients that had become sick during treatment.[3–6] While this treatment did succeed in causing over 1000 partial responses in patients, the lack of

understanding of the mechanism of action as well as the potential risk of infecting an already sick patient caused this work to be largely forgotten until the mid 1900s.[4–6] Cancer immunology remerged in the 1950s with a number of notable discoveries including: the discovery of interferon[7], the immune surveillance of cancer theory[8], acquired immunological tolerance[9], immune rejection of transplanted syngeneic tumors[10], and the use of the tuberculosis vaccine BGC to treat bladder cancer[11]. Our knowledge of the immune system and its relationship with cancer continued to grow throughout the latter half of the 1900s with the discovery of the genetic structure of the TCR[12], the ability to manufacture monoclonal antibodies using hybridomas[13], and tumor antigen recognition from a T cell.[14] These discoveries, among others, laid the groundwork for the birth of modern immunotherapy in the 2000s.

1.1.2 – Current Targeted Cancer Immunotherapy

Cancer immunotherapy broke through as a major branch of cancer therapeutics in 1998 with the United States' food and drug administration's approval of rituximab (Rituxan) to treat metastatic melanoma by targeting CD20, with several other targeted antibody therapies following in its wake.[15–17] These antibodies use a wide variety of mechanisms to induce direct killing and combat cancer growth such as signal mediated death; wherein binding to the target antigen can induce apoptotic pathways, blocking proliferative pathways, antibody-dependant cellular toxicity (ADCC) and/or cell-mediated cytotoxicity (CMC) allowing for targeted, cancer specific therapy.[18,19] Adjacent to mAbs, antibody drug conjugates (ADCs) were also first approved in the early 2000s with gemtuzumab ozogamicin (Mylotarg) allowed for target toxin delivery directly to the tumor by way of

antibody delivery by targeting CD33.[19,20] Unlike mAbs therapeutics, ADCs acts as a targeted delivery method, bringing a cytotoxic payload which has been conjugated to the antibody directly to cancerous cells. The ability of mAbs to internalize allows for a highly specific toxin delivery, while reducing the system toxicity.[21] The 2010s brought landmark achievements with the approval of sipuleucel-T (provenge) and ipilimumab (Yervoy) in 2010 and 2011 respectively, marking the first cancer vaccine and immune checkpoint inhibitors (ICI) therapies to pass clinical trials. [22,23] Since then ICI has risen to become a major therapeutic, giving some patients a level of survival that was previously impossible. Primarily targeting cytotoxic T lymphocyte associated protein 4 (CTLA-4) and programmed cell death protein 1 (PD-1), ICIs modulate the immunosuppressive environment by binding the immunomodulatory receptors, preventing cells from interacting with them and ensuring that the active T cells actively engaging the tumor aren't redirected to apoptosis.[24] Oncolytic vaccines only have three approved therapies as of the writing of this thesis, although the advent of oncolytic viruses and further categorization of cancer neoantigens may provide the boost necessary to bring this therapeutic to the forefront.[25] Instead of directly stimulating cytotoxic cells, cancer vaccines utilize a more indirect route, combining an injection of an immunogen, sometimes along side dendritic cells (DCs) adjuvants or patient DCs themselves to stimulate or restimulate the immune system through MHC antigen presentation or antibody mediated T cell activation.[26] This is achieved through the activation of pattern recognition receptors (PRRs) which in turn promote local inflammation and triggering type 1 IFN and cytokine production. This leads to the recruitment of antigen presenting cells (APCs) but particularly DCs, allowing target

antigens to be presented to other immune cells.[27] Oncolytic viruses provide a non-targeted method to this, targeting the tumors and in so doing causing immunogenic cell death (ICD), releasing the target antigens and danger associated molecular patterns, which the DC can use to activate T cells.[26,28]

The final kind of modern targeted immunotherapy is adoptive cell therapy (ACT), which an infusion of the patients own T cells is administered, often with modifications, as a therapeutic agent. The use of cells as a therapeutic presents several notable advantages over small molecules or biologics such as mAbs. Cells in their unmodified state are already capable of performing therapeutic functions such as interleukin or interferon production, recruitment and pathogen destruction through granzyme/perforin release or engulfment.[29] These preexisting mechanisms allow for more precise engineering opportunities such as more specific trigger conditions, modifications of existing production mechanisms or entirely novel cells combinations. Unlike synthetic molecules, living cells are highly dynamic and use complex signaling pathways to monitor and respond to both internal and external stimuli.[30] The receptors which control these signal pathways are extremely sensitive and specific, allowing for more precise control over specific pathways, and therefore downstream results with the correct modification.[31] With enough understanding, this could potentially allow for highly specific, synthetic cells designed to fill a niche the body lacks or can no longer effectively fulfill. While the primary subject of this document, Chimeric Antigen Receptors (CAR) is an obvious example of this, it does not fully illustrate the future potential treatments these modifications could produce. An excellent example is one put forth by Fischbach et al. in which a T cell has been modified with pancreatic DNA

and instead of patrolling for pathogen, sits in the bloodstream monitoring glucose levels and secreting insulin when the blood sugar level reaches a certain threshold.[29]

A method of using a patients cells as a therapeutic was first pioneered in attempts to treat patients with cancer in the late 1980s with cytotoxic lymphocytes (CTL), an infusion with no modifications from the general lymphocyte population and tumor infiltrating lymphocytes (TIL) therapy, an infusion of lymphocytes taken from within the patients own tumor and expanded to moderate success, although the first and only TIL therapy to make it through clinical testing thus far did not do so until 2024 with Afami-cel (Tecelra).[32,33] The first therapeutic modifications to patients cells appeared later with the first CAR-T treatment tisgenlecleucel (Kymriah) being approved in the United States in 2017 and the first TIL and TCR therapeutics in 2024, being Lifileucel (Amtagvi).[34–36] As of the writing of this thesis, all available CAR-T and TIL therapies exclusively target hematological malignancies, although there are many candidates in clinical trials for solid tumor cancers such as non-small cell lung cancer, ovarian or pancreatic.

1.1.3 - T cell biology and the TCR

T cells are a critical piece of the immune system, being a the major cell component of adaptive immunity and responsible for mediating cell-based immune responses to combat disease and infection.[37] T cell development begins in the thymus, with bone marrow derived thymic seeding progenitors, which then undergo three major steps to become T cells: T cell linage commitment, β-selection, and CD4/CD8 choice.[38] The first, in which the progenitor commits to becoming a T cells, occurs in four steps known as double negative, or DN, phases; referring the cells lack of either CD8 or CD4 receptors. Here, the early T-cell

precursor, or DN1 ($CD4^-CD8^-CD25^-CD44^-$)interacts with Notch, a critical protein in lymphocyte linage commitment, and acquire CD25 becoming DN2a.[38,39] From here, the cell either becomes a γδ T cell, or an αβ as it moved from DN2a to DN2b and DN3, upregulating either TCRγ and δ or TCRβ and an α precursor known as platelet and T cell antigen (PTCRA) as well as bringing CD3 to the cell membrane. This forms a pre-TCR complex whose signaling marks the beginning of β-selection step, in a process called V(D)J recombination.[40] Here the cells proliferate and undergo allelic exclusion, facilitated with Notch again, along side the pre-TCR . This process, wherein the cell arranges its β chain alleles such that only a one of the two is functional, is an essential step in generation of specific immune responses, as well as for ensure self-nonself discrimination.[41] Finally, the cell acquires both CD4 and CD8 moving from double negative cells to double positive (DP) cells. At this stage the T cells undergo T cell selection; a presentation of various antigen to ensure proper T cell function. Selection occurs in two independent steps: positive selection and negative selection. Positive selection marks the transition from DP to single positive (SP) cells, being tested on their ability to binding to MHC molecules, as presented by cortical epithelial cells.[42] Successful cells then undergo a CD4/CD8 choice and fully develop TCRα, now having a complete TCRαβ complex. While this process is not yet fully understood, one currently supported theory names interleukin-7 and other gamma chain cytokine stimulation alongside TCR signalling as a requirement for CD8 selection.[43,44] This theory posits that strong TCR signaling and IL-7 inhibition drive DP cells towards CD4+CD8- SP cells, while weaker or transient TCR signaling drives DP cells towards CD4-CD8+ SP cells, which rely on IL-7 and other gamma chain cytokines to complete the

differentiation.[45,46] Another key contributor in the CD4/CD8 choice are the transcription factors Thpok and Runx3, the former serving as a master regulator for CD4 lineage commitment and the latter downregulating Thpok and CD4 expression, leading to CD8 commitment.[37,47–50] The pathways containing these transcription factors also support the TCR IL-7 theory above: TCR signaling induces GATA-3, which enhances Thpok expression, while IL-7-STAT5 acts upstream of Runx3.[51,52] The other selection, negative selection, ensures that the resulting T cells are not reactive to healthy tissue. DP or SP cells are presented with a variety of self antigens through the autoimmune regulator gene (AIRE), a transcription factor which controls the local transcription of organ-specific proteins, through a process known as promiscuous gene expression.[53] Cells that fail either selection process die, either through death by neglect should they fail positive selection, or apoptosis should they fail negative selection.[42]

T cells come in one of two varieties based on what kind of SP cell they become. The first of these is the CD4 T cells also know as helper T cells. While there have been many different subsets of CD4 T cells identified, this document will mainly be discussing the classical Th1 and regulatory CD4 T cells, or Tregs. Th1 cells are primarily involved with intracellular pathogens and aids in the growth and activation of certain immune cells through the production interferon gamma (IFNγ), IL-2 and tumour necrosis factors alpha and beta (TNF-α/β).[54,55] IFNγ specifically is essential for the activation of mononuclear phagocytes, such as macrophages, and plays a key role in phagocytic activity.[56] IFNγ and IL-2 are also stimulatory cytokines for other T cells, activating proliferative pathways and driving naïve T cells towards effector memory phenotypes and help to amplify surface antigen expression

of antigen presenting cells.[57] Th1 cells response is contributed to through the upregulation of co-stimulatory B7 proteins, mainly CD80 and CD86, which facilitates further T cell responses.[57] Additionally, Th1 cells help to activate and prime the other form of CD4 T cells discussed here, Tregs, with downstream IL-2 pathways, enhancing FOXP3 in naïve CD4 T cells, causing them to differentiate into regulatory T cells.[58] Tregs are the foil to Th1 cells immune stimulation, keeping immune activity in check, regulating immune response and preventing the immune system from attacking healthy cells. This is achieved through a number of mechanisms such as the secretion of inhibitory cytokines IL-10 and 35 and transforming growth factor beta (TGF-β), killing effector cells through cytolysis or metabolic disruption and immunosuppressive receptor like cytotoxic T-lymphocyte associate protein -4 (CTLA-4) or lymphocyte activation gene 3 (LAG3)[59]

The other type of T cell is the CD8 cytotoxic lymphocyte (CTL). As the name suggests CTLs directly engage and kill target cells through three distinct pathways. The first is through cytokine secretion, such as tumor necrosis factor-α, which cause a caspase cascade when binding to its receptor, leading to apoptosis.[60] CTLs also produce immune stimulating cytokines such as IFNγ, similar to CD4 T cells, which can enhance cytotoxic function, proliferation and motility.[61] The second and third cytotoxic pathways are driven through direct cell-to-cell contact, either through binding to the Fas receptor, which also triggers a caspase cascade induced apoptosis, or through binding to the MCH class 1 receptor presenting a non-self antigen, through the TCR. [60,62] This causes a release of cytotoxic lysosomes containing perforin and granzyme B.

The primary trigger mechanism for T cell activation is the T cell receptor (TCR). The human

TCR is primary composed of αβ heterodimers (except in the case of γδ T cells), which are then assembled into the TCR, held together by disulphide bonds.[63,64] Like antibodies, άβ pairs are unique, target specific antigens and have an astronomical number of potential parings, with the likelihood of any random pairing being formed being less that 10^{-12}.[65] This variability is determined by Complementarity-Determining Regions (CDRs), the most diverse of which being CDR3, which primarily interacts with peptides of interest.[66] The resulting receptor regulates the T cells function and dictates the response to non-self antigens through binding and recognition, however the TCR cannot fully signal without the addition of CD3.

When the TCR is combined with CD3εδ and CD3εγ heterodimers and a CD3ζζ homodimer it forms a complete TCR-CD3 complex.[63,67] This complex is required for any form of TCR response, stabilising the TCR, and allowing for the recruitment and transport of the necessary proteins to the cell surface in order for a TCR-based response to occur.[68] This, alongside a co-receptor in CD4 or CD8, allows for foreign antigen recognition through the MHC, who's class is determined by which co-receptor is present.[63] (Figure 1.1) Signaling through the TCR is controlled through immunoreceptor tyrosine-based activation motifs (ITAMs) found within the CD3 subunits, with γ,δ and ε containing a single ITAM motif and ζ containing 3 (a,b and c) for 6 unique sequences and 10 total ITAMs per TCR-CD3 complex.[69] Upon binding to a target antigen through TCR:pMHC, human c-SRC kinase (CSK) and several phosphatases are suppressed, allowing these motifs to be phosphorylated through the kinase LCK, which is recruited by the co-localization of either CD4 or CD8.[70] Once phosphorylated, ITAMs become binding sites which allow for the tandem SH2 sites of

Zap70 to bind and become phosphorylated.[67] Once activated Zap70 then phosphorylates LAT, a signaling hub for T cell activations, phosphorylating sites Y132, Y171, Y191 and Y226.[71,72] Phospho-Y132 recruits PLC1, which in turn provides for calcium and Ras/MAPK pathways.[72,73] Phospho-Y171, Y191 and Y226 recruit Grb2 and Gads, which in turn bind to SOS and SLP-76 which in turn stimulate effector response from Ras, Rac and Rho among others.[72–75] In addition to LAT, the TCR and a co-stimulatory molecule CD28, activate PI3K. PI3K phosphorylates PIP_2, which then becomes PIP_3 with the addition of the extra phosphate, which is then used to phosphorylate ITK kinase.[76] ITK binds to SLP-76, pulling it to the plasma membrane and causing its activation. Additionally, ITK can also phosphorylate PLC 1, which can then hydrolyze PIP_2 into secondary messengers IP_3 and DAG. IP_3 causes calcium release, diffusing within the cytoplasm and binding is receptor IP_3R in the endoplasmic reticulum, causing a release of the stored Ca^+ ions through calcium channels such as Orai1. This increase in calcium can then cause the activation of several pathways, including transcriptional factor NFAT1. DAG remains in the plasma membrane and activates protein kinase C (PKC) and RasGRP.[67,76] The combined effects of RasGRP and SOS lead to rapid, bistable amplification of Ras. This then activates Raf which then leads to MEK activation, and culminates in MAP kinase ERK.[67,77] The MAP kinases then regulate transcription factors, which results in a T cell signal.

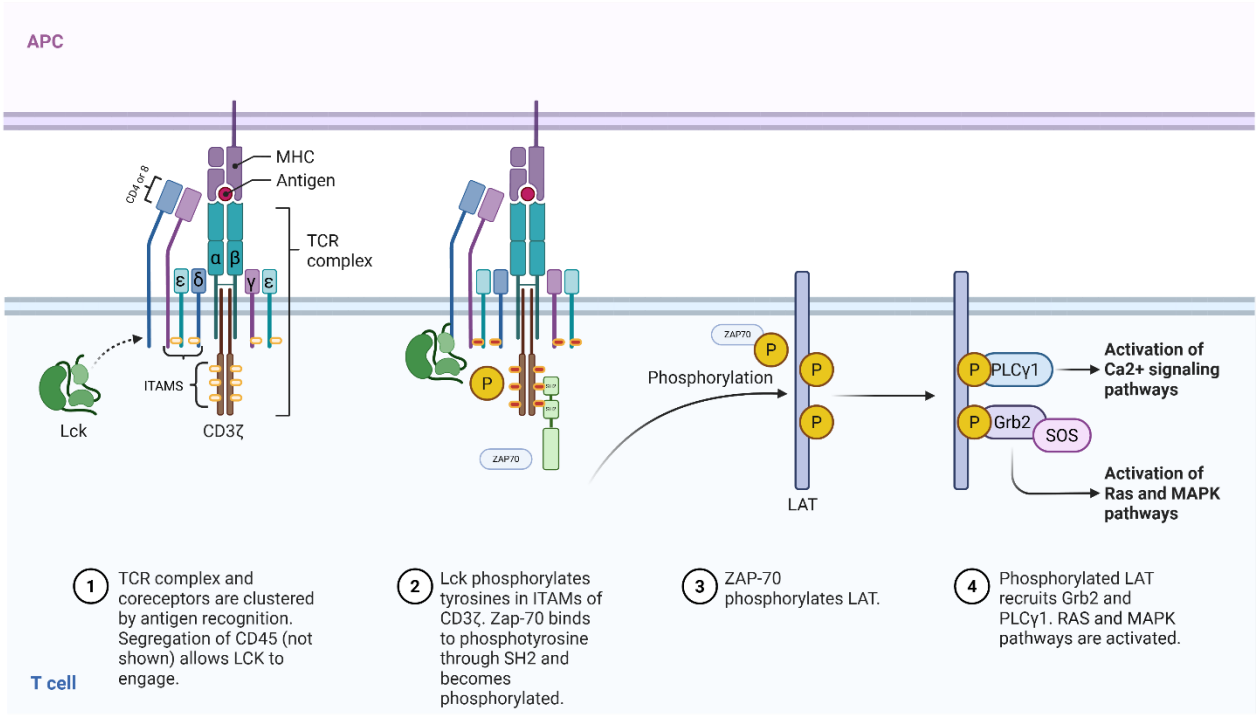

Figure 1.1. *Overview of TCR signal initiations. Adapted from a biorender template created by Ruslan Medzhitov, Akiki Iwasaki and Jung-Hee Lee.*

As previously alluded to, these signals are not simply the result of TCR:pMHC reaction. This signal is modulated through a number of co-stimulatory, inhibitory or structural molecules such as CD28, CD45, 4-1BB, OX-40, CTLA-4 and LFA-1, among others, forming a complex, multi layered system. The entirety of this signal begins with the initiation of TCR signaling through the formation of an immune synapse (IS). When the TCR:pMHC interaction occurs a full TCR mediated T cell response leads to the recruitment of additional TCRs forming TCR microcluster.[78] This microcluster rests at the center of the immunological synapse, a large multilayered structure that encompasses the whole of the TCR reaction and either priming the response of the T cell when receiving information, or modulating effector function when the T cell is communicating information.[79] This

structure is composed of three main layers, or supramolecular activation complexes (SMACs) which rapidly polarize to the site of contact and undergo differential clustering and rearrangement, forming a bullseye shape the IS is known for.[79–81] The central area of the IS, or the central SMAC (cSMAC) is marked by the previously mentioned TCR microcluster, as well as a centralized LCK cluster and ZAP-70 and LAT microclusters upon activation.[80,82,83] The peripheral SMAC (pSMAC) surrounds the cSMAC and is primarily marked by clusters of leukocyte function-associated antigen 1 (LFA-1) which binds to intercellular adhesion molecule 1 (ICAM1), physically binding the cells together.[83,84] While originally thought to be the central driver of activation, recent studies have argued that while the activation signal originates at point of first contact and disseminated by LCK clustering in the cSMAC, once the synapse in formed it is the pSMAC that facilitates continued T cell response, while the cSMAC is actually responsible for the downregulation and control of the longer term signal, through a combination of ubiquitination and receptor degradation and internalisation for recycling.[79,80,85–88] Past 2 minutes and especially after 5 minutes pSMAC is the primary facilitator of TCR signaling, but appears to be reliant on both actin, particularly WASP family WAVE/Scar proteins, and plasma membrane calcium levels in order to continue signaling.[83,89] A large portion of the cytoskeleton rearrangement and IS formation is thought to be facilitated by CD2, co-stimulatory module which stimulates both WASP and the microtubule organizing centre (MTOC).[90] The exact mechanisms of these interactions are unknown, CD2 has been shown to crosslink to actin and moves to the lipid bilayer where it becomes immobilized, aiding in the cytoskeletal formation of the IS and facilitating calcium mediated signaling.[91] While not entirely confirmed, the short distance

between CD2 and its receptors CD58 and CD59 supports kinetic segregation theory, where it helps segregate membrane bound phosphatases with large extra cellular domains (ECD) allowing LCK to phosphorylate CD3 ITAMS.[92] Finally, the last layer, the distal SMAC (dSMAC) primarily appears to form the structures known as the lamellipodia alongside the pSMACs lamellae, acting as a major component in the physical structure of the IS.[79,80] The dSMAC also contains the membrane bound proteins with large ECDs mentioned above, such as CD45, discussed below, CD44, a multifunction receptor involved in extracellular matrix interactions, transmission of growth signals and hyaluronic acid uptake and CD43 an adhesion and regulatory protein which controls proliferation and IL-2 production.[93–95]

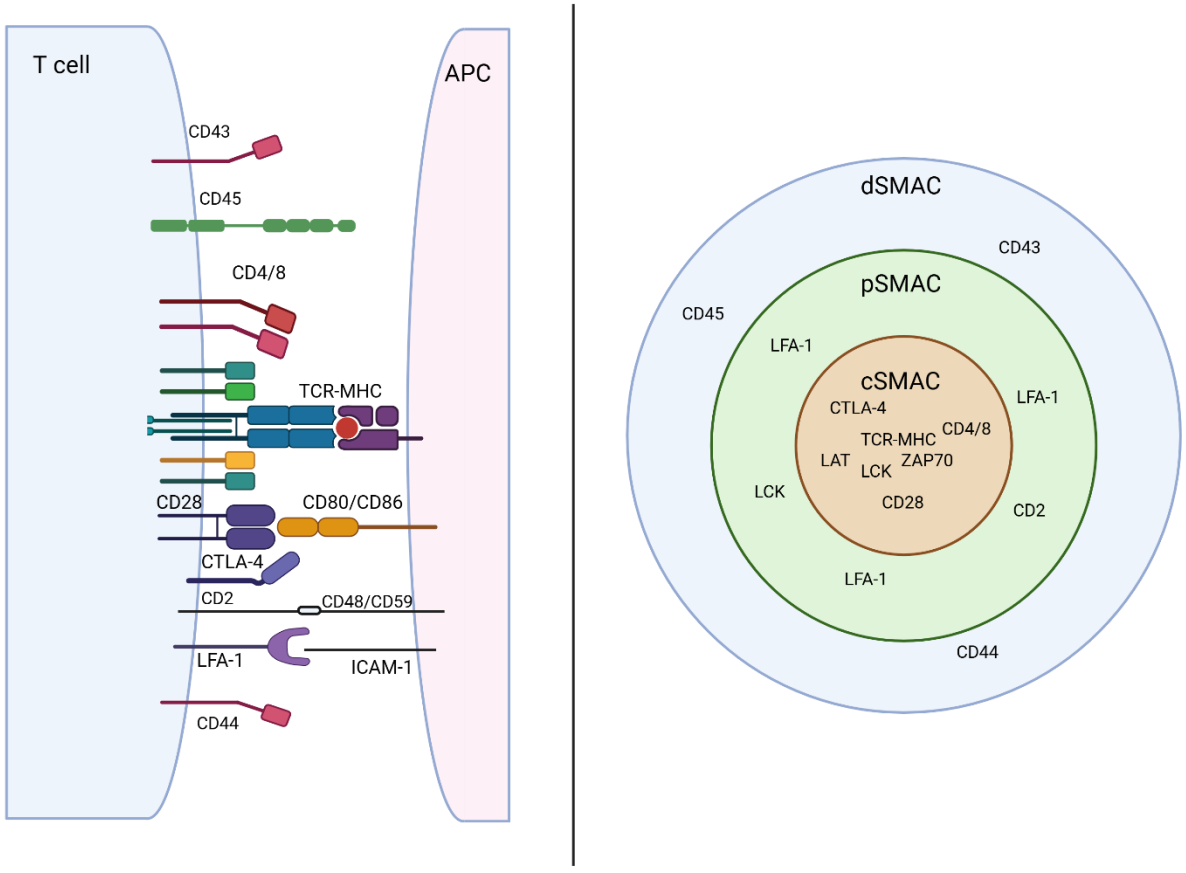

***Figure 1.2**. TCR Binding and SMAC formation*

One of the many functions of the immunological synapse is the segregation of CD45. CD45 is a tyrosine phosphatase, expressed in high amount of the surface of T cells and likely plays a major role in preventing resting cells from tonically activating.[96,97] However, T cells also cannot activate without the presence of CD45, likely due to CD45 dephosphorylating an inhibitory tyrosine on the C-terminus on LCK (Y505), as LCK becomes hyperphosphorylated at this site and can no longer activate.[96,98–100] When the SMACs form during TCR stimulation, the resulting polarization and actin structures physically segregate CD45 from the rest of the TCR complex, allowing for LCKs phosphorylation and subsequent T cell activation.

The TCR signal is also modulated by a number of co-stimulatory molecules, one of the most important of which is the previously mentioned CD28. CD28, while being an independent signal from the TCR, has an impact on cytokine expression, proliferation and survival and differentiation, even when not actively engaging. Binding to its associated ligand CD80/86, CD28-mediated signals upregulates cytokine expression, such as IL-2,4 and IFN-γ, chemokine expression such MIP1α or CCL3, and other co-stimulatory receptors such CD40L, CTLA4, ICOS and 4-1BB.[101,102] This not only ensures a continued T cell response after the initial contact, it is also critical for effector T cell function and T cell differentiation into long-term memory.[103] When resting post stimulation, T cell proliferation is partially driven by CD28 signaling strongly upregulating D cyclins, activating CDK4/CD6 which result in the phosphorylation of retinoblastoma proteins; which, when inactive, prevent T cells from progressing from G_0 to G_1 phase of proliferation.[104–107] Additionally, CD28 signaling increases the degradation of cyclin-dependant kinase inhibitors (CDKIs) which negatively control G_1, through the PI3K-AKT pathway, as well through INK4C, and CDK inhibitor.[108,109] Despite the vast amount of influence CD28 appears to have over the fate of TCR signaling, it is important to remember that it is a co-receptor, a receptor which serves to amplify and facilitate the main TCR signal and that no unique signalling pathways have been identified for it.[103]

Another co-stimulatory receptor that is highly relevant to understand in the context of CAR-T therapies is 4-1BB (CD137). Part of the tumor necrosis factor receptor superfamily, a group of immune ligand and receptors with a wide variety of functions which primarily

involve host defence and inflammation, 4-1BB becomes rapidly expressed on the surface after antigen induced activation.[110,111] 4-1BB co-stimulation provides signals through the activation of NF-κB, c-Jun and p38 pathways, through the recruitment of TRAF2, resulting in IL-4 secretion as well as long term proliferatory signals.[112] Notably, while both CD28 and 4-1BB are co-receptor independent, 4-1BB expression is more prominently and sustained in CD8 T cells[113] 4-1BB signaling has been shown to enhance expression of CD45RO and CCR6, both of which are important memory markers for T cells, as well as increased granzyme B.[113] 4-1BB also promotes survival of CD8 T cells by increasing the expression of antiapoptotic genes bcl-X_L and bfl-l through NF-κB, preventing activation induced cell death (AICD) and allowing for continued cell division and survival after the regulation provided in the initial signal from CD28 has ceased.[114,115] The pathways of both CD28 and 4-1BB can be seen in Figure 1.3.

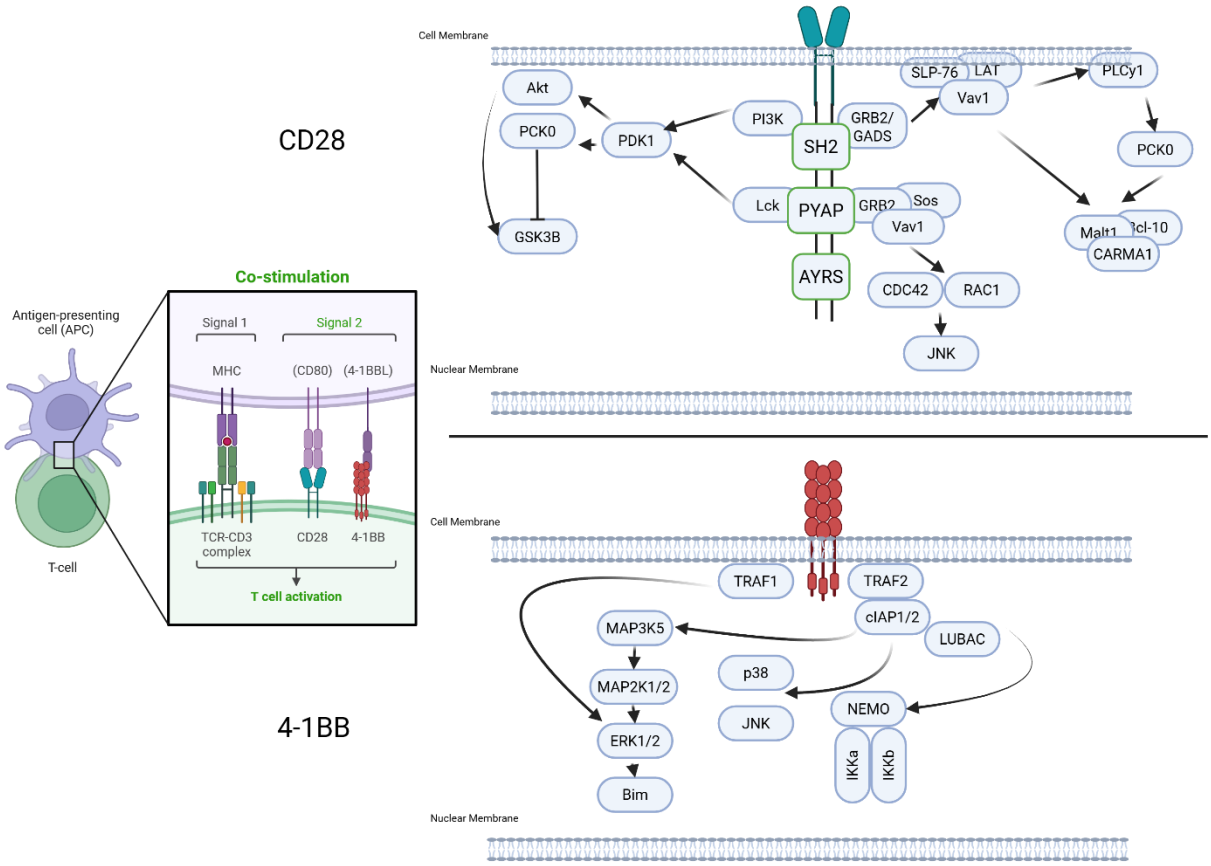

Figure 1.3. *Co-Stimulatory pathways of CD28 and 4-1BB*

It is important to note that although the receptors and complexes discussed above play an important role in TCR signaling and response, they are signal modulators and not the primary source of the TCR response. They aid and modify the function of an extremely complicated series of interaction resulting in a response from a cell. Additionally, due to the limitation of a thesis the entirety of the T cell cannot be comprehensively discussed here. While CD28 and 4-1BB play an undeniably important role in T cell function, they are by no means the only important receptor for T cell signaling and are highlighted here because of their role in CAR-T signaling.

1.1.4 - B cell biology and antibodies

Similar to the T cell, B cells form another critical piece of the human immune system. While the B cells do not actively kill targets during an infection, they play an integral role in both during and after, creating antibodies that inactivate and kill pathogens, recruit and activate T cells and safeguard the body against reinfection. B cells begin life in the bone marrow as a hematopoietic precursor cell.[116] Here, recombination-activating gene (RAG) 1 and 2 being the rearrangement of immunoglobulin gene segments, rearranging V_H, D_H and J_H in the heavy chain and V_L-J_L in the light chain. VDJ are rearranged first, pairing with V-preB and λlike to form the pre-B cell receptor (BCR). The pre-BCR signal temporarily halts the RAG signal, causing proliferation and preventing the second H-chain allele from being rearranged. Then RAG reactivates, rearranging the V_L-J_L in the light chain and combining λ or κ light chain segments with and μ-H-chain segments to create IgM on the cell surface. This creates a B cell repertoire capable of recognizing upwards of $5x10^{13}$ different antigens.[116] The cell is now an immature B cell and migrates to the spleen. Once in the spleen, the fate of the B cell, now known as a transitional B cell receives survival signals through B cell activating factor receptor (BAFF-R), and differentiate base on BCR specificity, either becoming a marginal zone B cell or a follicular B cell, the former becoming short-lived plasma cells, and the latter split into long-lived plasma cells and memory B cells when stimulated.[116]

While the limitations of this document mean that the intricacies of B cells will not be discussed in full, one important facet of B cells that is required for CAR-T is antibodies. Produced exclusively by B cells, antibodies, or immunoglobulin (Ig), are proteins that are

present on the cell surface of B cells, as well a secreted into the blood stream to mediate adaptive immune response. Each B cell produces a unique antibody, with a unique binding site, which can be produced at a rapid rate to combat infection when presented with a matching antigen with the help of CD4 helper T cell.[117] These antibodies come in five different forms, IgM, IgG, IgE, IgD and IgA, each of which fulfills a different function.[118] For our purposes, the form we are most interested in is IgG. IgG is the most abundant antibody in serum, and is major part of the complement system; interacting with the MB-lectin pathway and the alternative pathway to recruit immune cells, opsonize bacteria and neutralize toxins.[118,119] IgG are relatively large molecules, with a molecular weight around 150kDa and is comprised of two identical heavy chains and two identical light chains bound together with a disulphide bond. (Figure 1.4) As shown above with the formation of surface IgM in B cell maturation, light chains are either a κ or λ chains.[120] The antibody as a whole in comprised of two parts, two fragment antigen binding or Fab and the fragment crystallizable or Fc. While the Fc plays its own role in immunity our interests lie with the Fab region. This region is responsible for antibody recognition and binding and is comprised of two variable regions V_H and V_L, which are unique to the antibody and two constant regions C_L and C_H1, which are conserved between proteins. Each variable region is comprised of three hypervariable loops or complementary determining regions (CDRs) which determine which determine antigen specificity and determine when and how an antibody binds its target.[120,121] This variable regions specificity and the immune systems previously mentioned ability to target upwards of $5x10^{13}$ unique targets makes it an excellent candidate as an immunotherapeutic. Antibodies themselves also contain no host specific material

meaning they pose very little risk of immunogenicity.[122] For our purposes, however, our interest lies in the antibodies ability to specifically target an antigen. When isolated and bound together, the V_H and V_L regions form a single-chain variable fragment (scFv); a small highly specific antibody region which can be used to target specific therapeutics like CAR-T, to a specific target.

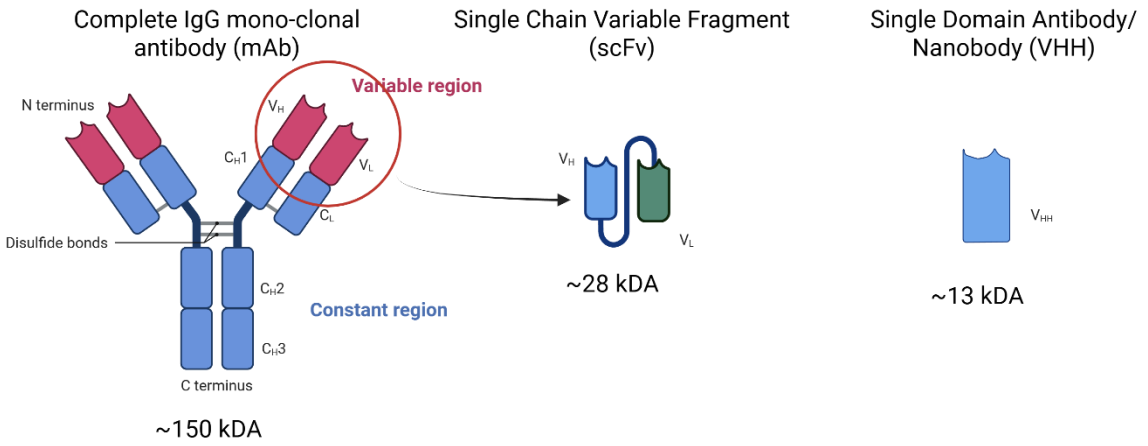

Figure 1.4. *mAb, scFv and VHH structure and weight*

1.1.5 - ScFv, VHH and their uses in immunotherapy

As introduced above scFvs are comprised of the variable regions of both the heavy and light chain of an antibody. These regions are typically bound together using a short linker, typically a series GGGGS animo acids, usually in triplicate also known as $(G4S)_3$.[123] Recently, however, the design of these linkers has been improved with the use of computation algorithms which optimize the linker based on the sequences of the regions in questions, improving flexibility, solubility and stability.[124]

Nanobodies, or variable heavy chain of heavy chain only (VHH) use a variable domain from a heavy chain only Ig. Standard scFv production uses murine hybridoma, mouse B cells that produce antibodies against a chosen target fused with immortal myeloma lines. While VHH could be produced in this manner, nanobodies are typically generated through antigen immunization of camelids such as llamas or alpacas, with the resulting mRNA from the B cells being isolated, reverse transcribed into cDNA and amplified using stepwise PCR.[125–127] The gene fragment is then typically sequenced, then inserted into a phage display vector and expressed in host cells (usually *e. coli*) and phage panning is performed to isolate relevant binders.[128] Unlike conventional vertebrate Igs, which combine a heavy chain and a light chain to create a variable region, these camelid antibodies instead produce antibodies that contain only heavy chains, and contain only two constant domain, with C_H1 being absent. Additionally, the VHH is only comprised of three complementary determining regions, as opposed to the standard six found in human or murine Ig due to the lack of light chain.[126]

VHHs have some advantages over traditional monoclonal antibodies (mAb) and scFv, namely epitope access and tissue penetration. Due to their size VHH can reach harder to access epitopes, and have shown to have superior diffusion rates across tumor stroma and higher perfusion rates across endothelial and epithelial barriers than both standard mAbs and scFvs, as antibody size was shown to have a negative linear correlation with tissue diffusion.[129,130] This size does have some disadvantages, however, significantly diminishing the half life of these molecules in the body, resulting in modifications such as fusion with a bacterial immunoglobulin binding domain being required to extend the half life for effective

therapy.[131,132] ScFvs lack of Fc region also makes them comparatively unstable, and prone to aggregation while VHHs, notably, do not suffer from this issue and are less susceptible to aggregation and more stable under worse conditions due to an extra disulphide bond.[133,134] Despite their low half life, VHHs are also more resistant to denaturants and enzymes, and are more stable in harsh pH.[135,136] Their less complex form also makes concatenation, and genetic manipulation, such as integration into TCEs or CARs, easier.[137]

ScFvs and VHHs have a wide variety of uses in healthcare. Both can be used as a direct therapeutic, similar to mAbs, or conjugated to a toxin from direct killing as an ADC, although modifications are often needed first. However, another key use is in diagnostics and detection: given their rapid clearance rate, scFvs and VHHs can be used as imaging tracers to without the risk of toxicity from accumulation or delayed clearance from the body.[134,138] The specificity of both scFvs and VHHs also makes them ideal for directing targeted therapy. Antibody based therapeutic such as TCEs (Bi-specific T cell engagers) or BIKES (Bi-specific killer cell engagers) use both scFvs or VHHs to simultaneously engage a target cell and an effector T or NK cell respectively..[139,140] Most targeted cellular therapeutics, such as CAR-T also use them for the binding region. The majority of CAR-T use scFv, however VHH-CARs have several advantages. In addition to those listed above, scFvs are about twice the size of a VHH by weight (15kD to 30kD), allowing even further increased access to difficult to reach epitopes increasing the range of VHH based CARs.[18,141] The reduced size also makes them ideal for combination therapies such a Tandem CAR.

1.2 Chimeric Antigen Receptor (CAR) T Cells

1.2.1 – A Brief History of CAR-T

While CAR-T is oft thought of as a modern invention, origination of CAR-T traces back to 1985, with T.H Rabbitt et al's *Fusion of an immunoglobulin variable gene and a T cell receptor constant gene in the chromosome 14 inversion associated with T cell tumors,* marking the first published combination of an antibody derived receptor and TCR derived signaling regions.[142] Next, in 1987 Y. Kuwana et al's *Expression of chimeric receptor composed of immunoglobulin-derived V regions and T-cell receptor-derived C regions* further expanded upon the idea of a combination of an antibody derived receptor and TCR derived signaling regions, creating a synthetic receptor capable of targeting a specific antigen and coining the term 'chimeric' for a fusion of a TCR constant domain with the variable domain of an antibody, and is likely the first instance of a CAR-like fusion protein.[143] This is swiftly followed by Gross, Waks, and Eshhar's *Expression of immunoglobulin-T-cell receptor chimeric molecules as functional receptors with antibody-type specificity,* which although widely recognized as the first instance of CAR-T published, is actually the second.[144] Testing and development of these CARs continued to progress, being championed by Carl June[145] and Michele Sadelin[146] among others until the approval of tisagenlecleucel for B-cell precursor acute lymphoblastic leukemia in 2017.[147] As of today, there are seven approved CAR-T therapies, and thousands of CAR based therapies in preclinical or clinical trials.

1.2.2 - CAR Structure and Function

Chimeric Antigen Receptors (CAR)s are synthetic fusion proteins which, when expressed on an immune cell, reprogram the cell to respond to a certain antigen. Like a TCR, CARs interact with its target antigen through a hyper specific extracellular domain, although unlike the specialised TCR, the CAR uses a preselected antibody that specifically targets the antigen in question. This antibody makes up the ectodomain of a CAR, also know as the binding domain. This is followed by a hinge or a spacer which is attached to the transmembrane domain. This is followed by the endodomain, which contains the stimulatory domains which fill a role similar to that of the CD3 domains in the TCR-CD3 complex. Typically, a CARs endodomain contains a CD3ζ signaling domain, which acts as the primary stimulatory domain and contains the ITAMs necessary for a signal to occur. Some CARs contain either a singular co-stimulatory domain or two different co-stimulatory domains, usually CD28 and 4-1BB, alongside the CD3ζ. Further modifications to CARs do exist, but are generally significantly different from the CAR structure discussed here, containing NFAT activating cassettes and IL-2Rβ binding sites respectively to enhance and modulate the signal for a more direct cytokine response and are generally referred to as T cells redirected for universal cytokine-mediated killing or TRUCKS.[148,149] All of the CARs used and discussed in this thesis contain only a single co-stimulatory domain. It also should be noted that despite the addition of a second co-stimulatory domain, little therapeutic difference has been noted between second and third generation CARs, often showing higher risk of adverse effects with dual co-stimulation[150,151].

While changing the binding domain has obvious impacts on how the CAR functions, and will be discussed at length, the other domains within the structure of the CAR can have a significant impact on CAR-T function and downstream signal as seen in Table 1.1. To start, the hinge domain, commonly IgG4, CD28 or CD8α derived, can impact CAR expression and signaling. Hinge length positively correlates with both CAR activation, to fixed maximum, and scFv folding, leading to higher CAR protein surface expression.[152,153] Additionally, the hinge domain appears to have an impact on the localization and transport of CAR proteins to the cell surface.[152] The transmembrane domain, again usually derived from CD8α or CD28, has been reported to impact CAR-T cell signaling through endogenous CD28, with the transmembrane domains dimerizing with the native receptors and blocking signaling through CD80/86 interaction.[154] This was also shown to significantly reduce CD28 surface expression, which can be confirmed with our own internal testing. CD8 transmembrane domains also show lower levels of cytokine response and activation induced cell death (AICD) *in vivo*. [155]

CAR Domain	Common Variants	Known Physical Function	Effects on CAR function
Binding Domain	scFv, VHH, Receptor ligands	Engages selected antigen epitope and binds, initiates CAR based signaling	Avidity, Epitope selection, antigen selection, cytotoxicity, proliferation, cytokine release, exhaustion, tonic signaling
Transmembrane domain and hinge	CD8α, CD28	Anchors CAR protein to the cell surface, determines ECD flexibility	Epitope accessibility, cytotoxicity, quorum sensing and proliferation, protein localization, cytokine release, exhaustion, tonic signaling
Co-Stimulatory domain	4-1BB, CD28	Stimulates one or more TCR co-receptors to	Cytotoxicity, Proliferation and

		achieve a more complete T cell response	survival, persistence, cytokine release, exhaustion, tonic signaling
Stimulatory domain	CD3ζ	Recruits LCK to CD3 ITAMs, begins downstream signaling	Activation and activation potential, cytotoxicity, cytokine response, cellular metabolism, exhaustion, tonic signaling

Table 1.1 – Known characteristics of structure-function relationship in CAR domains.

The co-stimulatory domains are the subject of a large amount of study for their impacts on CAR signal, survival and persistence. Most CARs that have been clinically tested are either produced with a CD28 transmembrane domain or a 4-1BB transmembrane domain, although other receptors such as ICOS or OX-40 have been used. CD28 co-stimulation in CAR-T has been shown to produce faster, stronger signals and higher cytokine expression, and promote differentiation into central memory cells. 4-1BB co-stimulation contrasts this with slower, longer lasting signaling, with higher observed persistence, sensitivity, and effector memory differentiation.[156–158] Another important difference between the two domains is safety profile. In a head-to-head using a CD19 CAR performed by Zhitao Ying et al, showed significantly lower occurrence rates and severity of cytokine release syndrome (CRS) and immune effector cell-associated neurotoxicity syndrome (ICANS) toxicity profiles from 4-1BB CARs than CD28 ones, with Grade 2 or higher events only occurring in CD28 patients, despite similar level of disease regression in patients.[156] While little therapeutic difference has been shown in 3rd generation CARs with both CD28 and 4-1BB,

some reports show that CAR-T can be improved with the two domains combined, such as improved proliferation, antigen selection and anti-tumor function.[159–161]

Currently, the vast majority of CARs including those used in other cells such as NK or Macrophages use a CD3ζ as its primary signaling domain. This does not mean that alternative activation domains have not been studied. One study by Velasco Cárdenas et al. showed that CAR-T is functional with all forms of CD3 intracellular domains, not just CD3ζ, and found that in some cases, hybrid non-zeta domains showed better performance in mice.[162] Another study showed enhanced safety in γδ T cells, that lacks a signaling domain entirely.[163]

As will become abundantly clear through the information presented in this thesis, all of these domains and the choices made during the design and construction of the CAR are important and do impact the how a CAR responds to a target cell, however, there is no objectively correct choice for CAR design. While the knowledge and data are not yet present to make objective decisions for CAR design, the eventual goal of CAR design should be to create design a CAR for a specific function, and choose the domains based on the disease in question.

All of the CAR molecules discussed in this thesis are single co-stimulatory (4-1BB) CARs of two varieties. The first is known as Quick Change 5 (QC5), which uses a VHH binding domain, (G4S)3+CD8hinge, CD28 transmembrane domain, 4-1BB co-stimulatory domain and CD3ζ stimulation domain and is the standard CAR layout for most screening and testing. The plasmid encoding these CARs is designed for rapid recombination of the

binding domain(s) to enable single pot screening. The second is referred to as BCRx plasmid, which was created to align structurally with a CAR plasmid used in a previous clinical trial.[164] This plasmid uses a VHH binding domain, CD8-hinge, CD8α transmembrane domain, 4-1BB co-stimulatory domain and CD3ζ stimulation domain. This layout is the one used in the current CD22-CAR clinical trial NCT06208735.

1.2.3 - CAR-T Therapy against blood cancers

As of the writing of this thesis (October, 2025), all seven CAR-T therapies which have been approved for public use target blood cancers. These are idecabtagene vicleucel (Abecma), lisocabtagene maraleucel (Breyanzi), ciltacabtagene autoleucel (Carvykti), tisagenlecleucel (Kymriah), brexucabtagene autoleucel (Tecartus), axicabtagene ciloleuce (Yescarta) and obecabtagene autoleucel (Aucatzl). The cancers currently targeted are acute lymphoblastic leukemia (ALL), chronic lymphocytic leukemia, mantle cell lymphoma, non-Hodgkins lymphoma (both Large B cell and follicular), small lymphocytic leukemia and multiple myeloma, only approved for relapsed or refractory cancers after multiple failed therapies.[165–172] These therapies only span two antigens, being CD19 and BCMA, and still present multiple problems with therapy, with patients reacting with cytokine release syndrome, immune effector cell associated neurotoxicity syndrome and specific to hematological malignancies, B cell aplasia, due to on target, off tumor toxicity from the CAR-T.[173,174] Despite the potential downsides and risks, CAR-T therapy still presents a significantly better survival rate for late stage hematological malignancies than traditional therapies with initial CR rates ranging from 40-81% for CD19 targeting CARs, depending on the cancer being treated. This increases when looking at BCMA targeting

CARs with overall response rates of 73-98%.[175] Long term follow-up with these patients showed a mean progression free survival of around ~48% of patients when combined allogenic haematopoietic stem cell transplant (HSCT) for CD19 patients, and ~55% in BMCA patients at 3 years and 27 months respectively.[176,177]

1.2.4 - CAR-T Therapy against solid tumors

CAR-T has seen much less success in solid tumors than it has in hematological malignancies due to a myriad of issues and complexities not found in liquid tumors. For one, while on target, off tumor toxicity can be largely dealt with in liquid cancers, as the aforementioned B cell aplasia is manageable with treatment; common solid tumor targets like HER2, or EGFR have significantly higher risk, with potentially lethal toxicities should the CAR attack healthy tissue.[178,179] Additionally, the tumor microenvironment poses significant challenged to any therapy, especially those that utilize immune cells as a primary method of attack. These tumors are often hypoxic and filled with toxic metabolites such as kynurenine and lactic acid.[180,181] This oppressive environment limits T cells access to amino acids, as well as immunostimulatory factors, causing T cell disfunction and making sustained T cell activity a challenge.[179,182] Tumors also erect physical barriers for immune cell trafficking and infiltration, limiting access through angiogenesis factors such as VEGF and tumoral stroma.[183] Finally, the tumor and the TME are filled with immune suppressive receptors such as PD-1 which prevent CAR-T cell activation or recruitment to the site.[184,185] Additionally, as CAR-T is generally a later stage therapy the majority of the malignancies are metastatic or advanced and thus are often immunologically cold and genetically diverse making a single target, immune based therapy like CAR-T much less effective.[186] Despite

these challenges, however, there are many potential CAR-T candidates. As of the completion of this thesis (October 2025) clinicaltrials.gov currently lists 291 clinical studies with CAR-T targeting solid tumors, more that one third of which are in phase II.

Drug or Trial name	Target	Diseases Targeted	Reference/Trial Number
Yescarta, Breyanzi, Tecartus, Kymriah, Aucatzyl, CLIC-1901, Various Clinical trials	CD19	Diffuse Large B-cell lymphoma* (DLBCL), transformed follicular lymphoma*, primary, mediastinal B-cell lymphoma*, Non-Hodgkin's lymphoma (NHL)*, Large B-cell lymphoma*, Acute lymphoblastic leukemia (ALL)	[166,168–170,172,187] NCT04271800 NCT04271410
Various Clinical trials	CD20	B-cell lymphoma, DBCLC, ALL, NHL	NCT04169932 NCT04160195 NCT03576807
CLIC-2202, Various Clinical trials	CD22	Multiple myeloma (MM),NHL, B cell lymphoma, ALL,	NCT06208735 NCT04546906 NCT07135466 NCT04163575
Abecma, Carvykti, Various Clinical trials	BCMA	MM*, mantle cell lymphoma (MCL)*, ALL*	[167,171] NCT03931421 NCT05767359
Various Clinical trials	MSLN	Non-small-cell lung cancer (NSCLC), colorectal cancer , pancreatic cancer, colon cancer, ovarian, malignant pleural mesothelioma	NCT05089266 NCT06054308 NCT05693844 NCT07030907 NCT06051695
Various Clinical trials	EGFR	Triple negative breast cancer, NSCLC, liver cancer, stomach cancer	NCT06682793 NCT02862028
Various Clinical trials	HER2	Breast cancer, osteosarcoma, rhabdomyosarcoma.	NCT06658951 NCT04995003 NCT05745454

*Approved by FDA

Table 1.2 – List of some ongoing studies and FDA approved CAR-T for common targets

1.2.5 - Weakness in current CAR-T design

As shown in the above section regarding solid tumors, the current CAR-T design and approach, while revolutionary, is still flawed. Like all single target, antigen-based therapies, CAR-T patients can often suffer from antigen negative relapse, wherein the selective pressure from the targeted therapy results in the downregulation, shedding or internalization of the target antigen, rendering the therapy useless of often actively harmful to the patient.[188,189] Additionally, as previously discussed, on target, off tumor toxicity poses a real hurdle to making solid tumor CAR-T a reality, severely limiting the range of viable CAR-T. Even in liquid tumors, B cell aplasia is still a severe condition.[174,178,190] This combined with the numerous toxicity issues, that while often manageable with medications like the IL-6 targeting tocilizumab, can still do permanent damage to patients' bodies and can severely affect quality of life.[191,192]

CAR-Ts current administration regimen is also flawed. As previously stated, CAR-T is an endline therapy, often used as a last resort and usually only approved in the case of relapsed (reoccurring) or refractory (treatment resistant) cancer. While this treatment method can be, and often is, lifesaving and can treat an otherwise untreatable patient, studies have shown that the damage done to the patients' body and notably, the patients' immune system can severely impact the efficacy of the treatment.[193] A large amount of effort has gone into bridging therapies; treatments used to the prepare the patients' body for the therapy, such as corticosteroids or combinations of mAbs and lose dose chemotherapeutics.[194] Additionally, research and physicians are pushing for CAR-T to

move up in the treatment regiment, as there is mounting evidence that the sooner the treatment is administered within the patient's cancer journey the better.[195,196]

Currently CAR-T remains less accessible than many other therapies due to the production process and cost of the therapeutic. Being a 'living drug', CAR-T therapies must be made with the patients own cells, or autologously, in order to avoid graft vs host disease (GVHD).[197] This means that although the virus necessary to transform the cells can be mass produced, the therapy as it currently exists cannot be off the shelf and must be manufactured each time it is to be administered. The production, like most therapies, must be manufactured in GMP3 facilities, a health standard set forth by the government.[198] While this is important, it limits the facilities that can manufacture these drugs. All in all, the average dose of a CAR-T costs somewhere close to ~$420000 USD[199], making it in accessible to most people, and a large expense for most governments.[200]

Finally, although CAR-T is referred to as a personalized therapy, that is only due to the fact that the therapy is autologous and can only be taken by a single patient. Like most drugs, CAR-T is a one size fits all option; assuming a patient fits the criteria required for administration they can receive essentially the same drug that all CAR-T patients of the same kind receive, just on their own unique cells. In order for the drug to be truly personalized more options, designs and a better understanding of both cancer physiology and CAR-T are required.

1.2.6 – The complex role of the binding domain in a CAR

A large portion of this document is dedicated to the examination of the CARs antibody binding domain and its impact on CAR efficacy and function. This domain is what directly

interacts the target cells, binding to the targeted antigen and initiating the signal that eventually leads to a CAR driven T cell response. This domain has been shown to dictate or at least partially dictate, length of binding, cellular avidity, T cell proliferation, efficacy of response and antigen sensitivity among others. Our own previously reported work has shown that the correct binding domain can mean the difference between full tumor clearance and minimal effect on tumor growth in mice.[201] Despite how important the domain is many groups still neglect to report on their scFv or VHH selection process either choosing a preexisting antibody that is successful as a mAb, selecting antibody based on characteristics that define a good antibody (affinity, antigen specific and sensitivity etc.) or not disclosing the reasoning behind their choice at all. While this can and has worked to produce at least somewhat successful CARs, this approach diminishes the role and impact of the binding region on CAR as a whole with these studies often only examining how the CAR performs with little to no examination of how the antibody in question affects the signal or how to optimize it. This approach has also made increasingly clear that the qualities that define a successful mAb do not apply to a successful CAR binding domain. When considering these parameters in the context of a CAR-T cell, a living cell as a therapeutic, this makes sense. The binding domain does not just interact with its antigen, it begins a cell-to-cell interaction, and as such defines how the interaction takes place from beginning to end. The binding domain effects which epitope of the antigen is being targeted, impacting cytokine release, downstream surface marker expression, the strength of the resulting signal, higher levels of degranulation and likely CD45 segregation.[202,203] As seen in Chapter 4, the binding domain also directly impacts cellular avidity as well as the

number of actively bound CAR cells at any given moment. This also likely impact dwell time, which has been shown to directly impact TCR signaling.[204] Binding domain selection also impacts tonic signalling, which has been shown to be beneficial to CAR-T in some cases.[205] Overall, what scFv or VHH is chosen to target the CAR plays a central role in helping define how it interacts with its targets and other cells. It is not simply an antibody; it is part of a complex system that triggers a cell to kill a target when bound, interacting with several different cellular systems to create a unique T cell signal. The full extent of this relationship, however, is still unknown and is part of a larger gap within our base of knowledge for CAR-T in understanding the relationship between a CARs structure and function. While filling this gap completely is well beyond the scope of this thesis, or any one project for that matter, it is my hope that this thesis will aid in furthering our understanding of CAR-T and its design.

1.3 Lentiviral Vectors

1.3.1 Overview of lentivirus

Viruses are infection agents composed of nucleic acids protected by a protein coat, which hijack the host's own replication machinery in order to copy themselves.[206] While primarily known for causing disease, their natural ability to supplement or modify genetic baseline genetic code have made them excellent tools for genetic engineering.[207] Of the options available, lentiviruses (LV) and Gamma Retrovirus (GRV) are the most widely used in research, and for the purposes of encoding CAR-T, lentivirus is the standard given their recorded ability to make stable, long term transgene expression.[206,208] Lentivirus requires three basic genes to survival and function – *gag, pol* and *env. Gag* codes for structural

proteins, *pol* for the enzymes required for reverse transcription and *env* for the viral envelope glycoproteins.[209] The lentivirus life cycle, and consequentially the modification of the host DNA, begins when the virus enters the cell, either through direct membrane fusion or receptor mediated endocytosis.[208,210] Next, viral proteins dissociate from the core, allowing the viral RNA to be converted into proviral double-stranded DNA through reverse transcription.[211] This DNA is then imported into the cells nucleus and integrated into the hosts genome through the assembly of a pre-integration complex (PIC) and the activity of viral integrase.[212] Once integrated, the virus relies upon the hosts own machinery to assemble new infectious particles which then exit the cell through the process known as budding.[213]

1.3.2 pHIV non replicating lentiviral vectors

Due to the infectious nature of wild lentivirus, lentiviral vectors have been engineered to reduce the amount of risk while still enabling them to modify cells. In current generation lentiviral vectors, the complete vector is split between four plasmids which need to be combined during transfection. These four plasmids are- two packaging plasmids one containing *gag/pol* and other regulatory proteins and the other containing *rev* which enables viral replication, an envelope plasmid(usually glycoprotein of vesicular stomach virus or VSV-G), and a transfer plasmid which contains the genetic modification of interest, a promoter region and the long terminal repeats (LTRs) which are required for intergration.[206,214] The combined plasmids also remove the accessory proteins or Nef, Vpr, Vif, and Vpu, all of which are associated with disease progression and pathogenicity, and

do not impact essential viral functions.[215] The transfer plasmid also replaces one of the HIV LTRs with a CMV viral promoter, allowing the removal of *tat*.[206,216]

The virus and viral plasmids used with this thesis utilize a three plasmid system, combining psPAX2 packaging vector, pCMV-VSVG envelope and and pCMV-Rev transfer plasmid containing a self inactivating LTR, which prevents replication competent lentivirus (RCL) from forming.[214]

1.4 Multitargeting therapeutics and CAR-T

1.4.1 Bi-specific T cell Engagers (TCE)

Similar to CAR-T, bi-specific T cell engagers (TCEs) also redirect T cells to kill tumor cells using an antibody to trigger an immune response when in the presence of a target antigen. Unlike a standard monoclonal antibody, TCEs gain their specificity through two separate binding regions: one targeting a tumor antigen and the other directly engaging the T cell, usually through anti-CD3.[217] While structure can vary, standard TCEs are composed of either two scFvs or VHHs bound together using a linker, usually a series of serine-glycine $(SGGGG)_n$ linkers.[217,218] In the case of scFvs the heavy and light chains are usually also connected in the same way. When engaging their targets, TCEs physically bridge the gap between effector and target, activating the T cell through the TCR-CD3 complex causing a cytotoxic reaction. It is important to note that TCEs will only produce this reaction when bound to both cells and will not cause a reaction in the absence of the selected tumor antigen, limiting the risk of nonspecific T cell activation.[219,220]

Notably, TCE mediated T cell activation induces the formation of the immune synapse, with the synapse formation reported to look the same under confocal microscopy as canonical

TCR synapse formation, displaying central and peripheral SMAC formation and localization of CD3, LCK and perforin.[221] This suggests that the underlying mechanism behind the subsequent tumor death is site specific degranulation, a theory supported by the fact that TCE specific toxicity can be blocked *in vitro* by calcium ion chelation through ethylene glycol tetra acetic acid.[222]

TCEs, similar to CARs, mediate specific T cell activation without the need for MHC-TCR interaction, however, TCE-mediate T-cell activation is also independent of T cell costimulation.[223] Why this is the case in unclear, as other bispecific formats require some form of co-stimulation to activate, although it has been postulated that it is because TCEs favour the stimulation of previously primed CD45RO positive effector memory cells, which require less stimulation to fully activate.[223,224]

1.4.2 Dual/Multi CARs

The first kind of multi-targeting CAR-T is the dual or multi- CAR wherein two separate CAR-T proteins are expressed on cell surface simultaneously. This can be achieved in several ways: co-transduction – where two separate lentiviruses are used to co-transduced the donor T cells at the same time, and a bi/multi-cistronic lentiviral vector which encodes for each CAR with a P2A or IRES separating each CAR.[225,226] These CARs are both methods of creating a multi-antigen targeting CAR with separate CAR proteins, however it should be noted that co-transduced CAR and bicistronic CARs produce different end products: co-transduced CARs contain multiple different populations: double expressing population and single expressing populations of both types, in which the dual expressing CAR usually diminishes over time and eventually becomes a CAR-POOL while bi-cistronic CARs are

entirely comprised of dual expression CAR-T.[227,228] While both methods are effective, the larger viral load required for bi-cistronic vectors can also reduce transduction efficiency and CAR expression.[229] This has been shown to have impacts on persistence, and toxicity, but is also important to consider from the perspective of regulation. Conversely, CAR-T is approved based on the process and final product; and co-transduced mixed culture makes the approval process significantly harder.[230] While neither of these combination types has received approval from the FDA or similar entities, these CARs, usually in the form of Dual CAR often appear in clinical trials as a form of secondary treatment to combat antigen negative relapse.[231] This makes it difficult to evaluate multi-CAR as its own stand-alone therapy as the context in which it is being evaluated is one in which at least one of its single target components is expected to fail when used alone. What data is available does show some promise showing good ORR and no reported antigen negative relapse as of yet but so far does not seem to be consistently better than any existing single target treatment of the same type.[232]

1.4.3 Tandem CAR

The other heavily used method of CAR-T combination is Tandem CAR, in which a secondary binder is attached to the end of the first binding region using a linker, allowing the CAR in question to bind to two separate targets, but signal through the same body.[233] This combinations has several variations – with binder order and composition and linker length and flexibility influencing the end product.[228] Given the increased customization, tandems often require more testing and are more difficult to optimize.[234] Like Dual CAR a true bi-specific Tandem CAR has not been approved by any regulatory entity, however unlike co-

transduced or Dual CAR, these CAR-T are tested as a novel therapeutic and therefore have more data available. These studies report that the tandem format are capable of adding a second functional target to a CAR-T without a negative impact on safety or *in vivo* efficacy in mouse models of hematological malignancies.[235,236] Similar to Dual CAR, tandem CAR has yet to be shown to be consistently more better than any existing single target treatment.

1.4.4 CAR-POOL

The final method of combination that will be discussed here is CAR-POOL. CAR-POOL is either a co-infusion, or a series of sequential infusions of single target CAR-T targeting different antigens into a patient. Similar to Dual CAR, CAR-POOL is frequently tested as salvage therapy, attempting to halt the progression of a malignancy after a single target CAR has failed.[237] The decision to administer as a co-infusion or a sequential infusions is often determined by the toxicity of individual therapies, as synergistic toxicities can limit the efficacy of treatments and the amount of each CAR that can be administered.[238] Optimizing the time, if any, between infusions has also been hypothesized to prolong peak expansion of CAR-T.[239]

1.4.5 Engineering opportunities with Multi-CAR

The introduction of a secondary binder or CAR into a single target CAR-T also allows for more potential for customization and specificity of treatment, controlling signaling and activation requirements while reducing potential risks. From a clinical efficacy perspective, multi-CAR has seen varying levels of success in all formats but has not consistently shown superiority to single target CAR as of yet. Despite the lack of clear advantage over single

target in clinical results, the increased potential for improved design, specificity and safety is where multi-CAR truly shines.

One of the primary potential benefits of multi-antigen targeting is protection from selective pressure resulting in antigen loss, downregulation or masking.[240] Lineage switching can also result in antigen negative relapse as seen in CD19 targeting CAR-T causing blasts to switch from lymphoid to myeloid phenotypes, removing CD19.[241,242] Having multiple different targets ensures that even in the case of the loss or downregulation of a single antigen, the CAR-T remains, in theory, an effective treatment. While multi-antigen downregulation has been recorded, this form of protection makes a primary failure condition of the treatment less likely.[230] The selective pressure of CAR-T also impacts how targeted antigens are expressed and how accessible they are. While not all patients who relapse post single target CAR-T have antigen negative tumors, studies on CD19-CAR patients show that the vast majority contain mutated CD19.[243,244] These mutations often truncate CD19, removing the epitope that the binding region of the CAR binds, or accumulating small mutations through alternative splicing, resulting an modified or inaccessible binding site.[243,244] Additionally, late stage or refractory/relapsed cancers are often heterogeneous, meaning that a small percentage of the targets mass many not contain the targeted antigen, making targeting multiple antigen necessary for any hope of a successful treatment.[240,245] All of these contributing factors indicate that for a large number of patients, especially those having gone through many lines of previous therapy, multi-targeting CAR-T may be a necessity to ensure a complete response (CR) and progression free survival (PFS).

Another issue that plagues targeted therapy like CAR-T is on target, off tumor toxicity. As previously discussed, while B cell targeting CAR-T can skirt this issue resulting only in B cell aplasia, solid tumor targets are much riskier to target. Severe toxicities have been reported in several solid tumor clinical trials, ultimately leading to the failure and often times death.[151,246] In theory, this can be addressed by targeting multiple antigens, as this presents additional space to engineer more specific activation conditions through logic gating. Without any additional modification a standard multi-antigen targeting CAR presents an OR gate: meaning that both antigen 1 or antigen 2 can trigger a T cell response independantly.[247,248] OR gates can be used to combat antigen loss or tumor heterogeneity as mentioned above, however properly tested OR combinations can impact all part of a CARs response as will be shown in chapter 3. Other studies have also shown enhanced cytotoxicity from OR gated CARs.[249]

By engineering the bodies of the receptors, you can instead create an AND gate: meaning both antigen 1 and antigen 2 must be present in order to trigger a response. A standard TCE would be an example of an AND gated T cell engager, however in the context of CAR-T this can be achieved through splitting activation signals across both CAR proteins, meaning that only the activation of both would result in a complete CAR response. While this is often done by splitting the co-stimulatory domain and CD3ζ across two separate CARs or a split-CAR, a much better example would be the Logic-gate Intracellular NetworK CARs or LINK CARs developed by Tousley et al.[247,250] These CARs replace the CD3ζ component of each receptor with the downstream components LAT and SLP-76 on two CARs which when combined allow for a complete T cell signal to occur.[250] Another proposed modification to

AND gates is what is referred to as a contextual AND wherein a CAR-T is instead paired with a TME specific receptor which allows for activity when the appropriate context is met. Examples of this would be an inhibitory cytokine or receptor, or a tumor associated protease or receptor preferentially binds at low pH or oxygen.[248,251,252]

The final applicable logic gate is NOT. As the name suggests a NOT gate would instead halt a T cell signal in the event of that particular receptor being bound. The first iteration of this is the inhibitor CAR-T or iCAR which uses an immunoreceptor tyrosine-based inhibitory motif or ITIM to trigger T cell inhibition allowing for selective, temporary T cell regulation.[253] Another approach it the Tmod CAR developed by Manry et al.[254] This blocker targets tumor loss of heterozygosity, blocking activation of CAR-T cells that target cells with a selected level of a chosen HLA-A type using LIR-1.[254]

Finally, even with no direct modification of the CAR protein, multi antigen CAR-T can be engineered simply by understanding the interactions between the two CARs used and the cancer being targeted. For example, pairing a super aggressive, cytotoxic CAR with low persistence with a less potent, longer lasting CAR may result in an optimized treatment, allowing the two opposing phenotypes to balance each other out. Even antagonistic behaviour could be exploited: two CARs that are too toxic as a single target product may antagonize each other when combined, resulting in an overall more manageable treatment. By having a better understanding the interactions and signaling capabilities of each CARs, combinations can be optimized to better fit the scenario in which they are needed.

1.5 Discussion of key cell lines

1.5.1 Jurkat e6.1

Jurkat e6.1 is T cell lymphocyte line, established from the peripheral blood of a 14-year-old male patient with acute T-cell leukemia.[255] Jurkat is probably best known as one of the most used T cell model systems, initially obtained for their ability to produce large amount of IL-2 when stimulated with phytohemagglutinin, the e6.1 line came about from the process of removing mycoplasma from the cells, and ultimately became the standard Jurkat line used today.[256] Since being established Jurkats have been wide used in immunology leading to insights into T cell calcium signaling and pathways, PTK signaling and the derivation of TCR signaling mutants to name a few.[257,258] For the purposes of this thesis the Jurkat cell line is used as a surrogate T cell, as many of the important pathways remain intact such as NFAT and NFκB.[259] This allows for metrics such as T cell activation and T cell binding to be assessed through a consistent, immortal cell line without the issues or normally associated with human donor T cells. Jurkat cells are not without flaw however; the e6.1 is incapable of any cytotoxic response and lack several key signaling factors such as PTEN and SHIP, leading to the PI3K pathway being always active.[260–262]

1.5.2 Blood cancer lines

Ramos (RA 1) is a B cell lymphocyte line derived from the ascites fluid of a 3-year-old boy with Burkitt's lymphoma. While Ramos is frequently used as a model for B cells, its use in this thesis is as a B cell lymphoma target line, as it overexpresses CD22, CD20 and CD19 on its cell surface. [263] Raji is another B cell lymphoma derived from Burkitt's Lymphoma. Both of these cell lines are usually used for their extremely high CD19 surface expression,

but also expression CD22, CD20 and BCMA. Unlike Ramos, Raji cells do not secret IGM but do express it on the cell surface.[264,265]

1.5.3 HEK293T

HEK293T is a highly versatile human embryonic kidney cell line, and is a modified version of the original HEK293 line that has been transfected with SV40 large T antigen, which assists in the production of VLPs.[266] HEK293 is one of two main animal cell-based expression platforms for large scale industrial production, the other being Chinese hamster ovary (CHO) cells. Unlike CHOs, HEK293s human origin allows for human specific post-translational modification. All of the non-commercial virus used and produced in this thesis was produced using HEK293T, and the virus for several approved CAR-T products is also produced using this line.[267] Importantly, HEK293T does not express any of the antigens being targeted here.

1.5.4 Solid tumor lines

H292 is a tumor cell line derived from a lung mucoepidermoid carcinoma.[268] It overexpresses MSLN and EGFR on its cell surface. Skov3 is a highly used ovarian cancer line, isolated from 64 year old with ovarian adenocarcinoma. Skov3 cells are resistant to a number of established treatment methods, such as adriamycin and cis-platinum, as well as tumor necrosis factors.[269] It also overexpresses MSLN and EGFR but not as high as H292. Next is MCF7, the most commonly used breast cancer model worldwide. While very high characterized, especially for its interactions with estrogen and progesterone, this thesis uses it as a solid tumor line which expresses low levels of both EGFR and MSLN.[270] Finally, U87vIII is a modified version of the standard glioblastoma multiforme (GBM) like

U87 which has been mutated to express EGFRvIII, and GBM specific neoantigen. The addition of EGFRvIII grants radioresistance, modifies the cellular proteasome and seems to be a part of the immune escape pathway that leads to GBM development.[271]

1.6 Discussion of Key Antigen Targets

1.6.1 Blood cancer lines

CD19 is a B cell restricted protein that encodes for a member of the immunoglobulin gene superfamily. CD19 forms a complex with complement receptor type 2 (CD21) and tetraspanin (CD81) in order to reduce the threshold of antigen-mediated B cell activation, and activates signaling pathways to activate PI3K and calcium signaling.[272–274] CD19 is also the most prevalent approved CAR-T target, due to its specificity and tissue exclusion as well as CD19 overexpression being extremely common on B cell leukemias and can be used as a potential marker for lymphoma development.[275,276]

Conversely CD22, another highly expressed B cell restricted antigen, in an inhibitory co-receptor. CD22 is the most highly expressed sialic acid-binding immunoglobulin-like receptor (siglec) on B cells which inhibits B cell activation through the inhibition of calcium pathways as well as the activation of SHP-1/PTPN6.[277] CD22 is also involved in B cell differentiation and trafficking to the bone marrow.[278] Overstimulation of CD22 in healthy B cells can result in apoptosis.[279] CD22 is also highly expressed in several types of cancers and has emerged as a potential target for targeted immunotherapy.[280] While there are no approved CD22 targeting therapy currently on the market, as of the writing of this thesis there are currently 217 ongoing trials targeting CD22 including CLIC-2201 using the CAR 1ug36 which will be discussed in Chapter 5.[281]

Finally, B cell maturation antigen (BCMA) or tumor necrosis factor receptor superfamily member 17 (TNFRSF17) is directly related B cell activating factor receptor (BAFF-R) and transmembrane activator and CAML interactor (TACI). These receptors promote B cell survival through the engagement of a proliferation inducing ligand (APRIL) and BAFF. It is also important to note that BCMA is only expressed on B cell lineage cells, plasmablasts and differentiated PCs but its absent from naïve and memory B cells.[282] Multiple myeloma, the approved target for BCMA targeting therapies shows high levels of BCMA across the majority of *in vitro* cells as well as clinical patients, making for an ideal target.[283]

1.6.2 Solid tumor lines

Epidermal Growth Factor Receptor (EGFR) is part of a family of receptor tyrosine kinase (RTK) proteins and is in the same family as HER2, one of the first immunotherapy targets. EGFR is a fully functional receptor which binds to a ligand and undergoes autophosphorylation, creating binding sites for Grb2 and SHC2 and activating the Ras pathway through SOS, leading to cell proliferation.[284] EGFR is expressed throughout the body being found on endothelial cells, lung and respiratory tissue, uterine and ovarian tissue, and several parts of the digestive system to name a few, with the average healthy tissue expression being around 40000-100000 receptors per cell.[284,285] Tumor cells express significantly more EGFR with the average tumor cell expressing an average of two million EGFR receptors, likely due to its role in pro-proliferatory stimulation. [286] Overexpressed and uncontrolled EGFR has been shown to be heavily involved in cancer progression, influencing cellular growth, metabolic pathway reprogramming, cell death and chemotherapy resistance, and notability metastasis.[287] RTKs such as EGFR play a critical

role in the formation of secondary tumors through the regulation of soluble factors and actin mediated cell migration.[288] These factors and its high expression on solid tumor tissue make EGFR and attractive target, however given how commonly EGFR on healthy tissue, targeting poses risks. While no EGFR based CAR-T therapeutics are on the market, EGFR inhibitors are used to treat non-small cell lung cancer and cetuximab, an anti-EGFR monoclonal antibody, is used to treat colorectal and head and neck cancer. These treatments often come with adverse side effects including: rash, blister, hives and other skin damage, arrythmia, vision damage, and bladder or urinary tract swelling and damage.[289,290] Given the potential for off tumor effects, EGFR treatment poses significant risk without precise target density control.

This issue is somewhat mitigated with the EGFR mutant EGFRvIII, commonly found in glioblastoma multiform tumors. EGFRvIII is an oncogene or neoantigen, meaning it does not naturally occur in the body and is unique to cancer, making it a much safer target for immunotherapy. EGFRvIII contains an in-frame deletion of exons 2 to 7, resulting in a truncated version of EGFR that is weakly phosphorylated in a ligand-independent manor, meaning that it can no longer be blocked.[291–293] Additional, EGFRvIII has been shown to confer radioresistance and further enhances its immune evasion.[271]

Finally, Mesothelin (MSLN) is a cell marker first discovered through the search for new cancer target. While is exact role in healthy tissue is unknown, MSLN appears to have a role in cellular adhesion and proliferation, mainly defined through its interactions with MUC16/CA125.[294] Mesothelin mainly appears in mesothelial tissues, but also appears in lungs, female reproductive system and GI tract.[295] MSLNs overall lack of expression in

healthy tissue makes it an attractive target, however current attempts to target it are often met with lung toxicity issues, or antigen escape through shedding.[246,296]

1.7 Summary and Key Aims

This thesis and the studies described herein attempt to contribute to solving a problem alluded to in the introduction above: CAR-T, while promising, is flawed and more importantly poorly understood. Modern T cell based therapeutic development, and screening consists of the scientific equivalent of firing blindly in the dark, you'll probably hit your target eventually, but you'll waste of a lot of time and energy before you do and even more of both before you find out whether you just grazed them or not. The screening process, as outlined in Chapters 2 and 3, consists of mainly functionality testing, and correlates poorly to actual *in vivo* results and often clinical trial findings, specifically when it comes to CAR-T. We have successful CARs targeting blood cancers, but we lack the understanding as to why those CARs are successful, and what makes them better than the thousands of CARs that fail in the clinical and preclinical testing that precedes them. We have begun to form CAR combinations, but we are unable to make informed decisions regarding what combinations we should pick and how we should combine them for the best possible results. While this thesis will not answer these questions, it aims to provide some measure of progress towards a better more complete understanding of CAR development and function by addressing the following aims:

Aim 1: Evaluate how synthetic immune stimulating treatment's signaling and interactions change when moved from a single target to a multi-target format.

Aim 2: Investigate early CAR to target binding and avidity and it effect on downstream T cell signaling

Aim 3: Evaluate CD22 CAR design variations using multi-parametric approaches to identify key signaling pathway variation between CARs.

CHAPTER 2: CREATING AND SCREENING BISPECIFIC T CELL ENGAGERS (TCEs)

Note: The following chapter is a manuscript published in Public Library of Science (PLOS one) on June 22, 2023. Please note that due to the nature of this document supplementary data included in the paper in video or excel table format have not been included but can be found at https://journals.plos.org/plosone/article?id=10.1371/journal.pone.0273884#sec017.

A Simplified Function-First Method for the Discovery and Optimization of Bispecific Immune Engaging Antibodies

Alex Shepherd[1,3], Bigitha Bennychen[1,3], Anne Marcil[1], Darin Bloemberg[1], Rob Pon[1], Risini Weeratna[1], Scott McComb[1-3]*

[1]Human Health Therapeutics Research Centre, National Research Council, Canada
[2]Centre for Infection, Immunity and Inflammation, University of Ottawa, Ottawa, Canada
[3]Department of Biochemistry, Microbiology, and Immunology, University of Ottawa, Ottawa, Canada

*Correspondence: scott.mccomb@nrc-cnrc.gc.ca

2.1 Abstract

Bi-specific T-cell engager antibodies (TCEs) are synthetic fusion molecules that combine multiple antibody-binding domains to induce active contact between T-cells and antigen expressing cells in the body. Blinatumomab, a CD19-CD3 TCE is now a widely used therapy for relapsed B-cell malignancies, and similar TCE therapeutics have shown promise for treating various other forms of cancer. The current process for new TCE development is time consuming and costly, requiring characterization of the individual antigen binding domains, followed by bi-specific design, protein production, purification, and eventually functional screening. Here, we sought to establish a more cost-efficient approach for generating novel TCE sequences and assessing bioactivity through a function first approach without purification. We generate a plasmid with a bi-modular structure to allow

high-throughput exchange of either binding arm, enabling rapid screening of novel tumour-targeting single chain variable (scFv) domains in combination with the well-characterized OKT3 scFv CD3-targeting domain. We also demonstrate two systems for high throughput functional screening of TCE proteins based on Jurkat T cells (referred to as TCE-J). Using TCE-J we evaluate four EGFRvIII-scFv sequenced in TCE format, identifying two constructs with superior activity for redirecting T-cells against the EGFRvIII-tumour specific antigen. We also confirm activity in primary T cells, where novel EGFRvIII-TCEs induced T cell activation and antigen selective tumor killing. We finally demonstrate similar exchange the CD3-interacting element of our bi-modular plasmid. By testing several novel CD3-targeting scFv elements for activity in EGFRvIII-targeted TCEs, we were able to identify highly active TCE molecules with desirable functional activity for downstream development. In summary, TCE-J presents a low cost, high-throughput method for the rapid assessment of novel TCE molecules without the need for purification and quantification.

2.2 Introduction

Monoclonal antibody (mAb) technology can be used to create biological molecules with high binding affinity and specificity for antigenic targets. In the case of immunomodulatory or cancer targeted therapeutics these antigens are typically on the surface of cells. Through binding, such antibodies can induce a variety of direct and indirect biological effects on the target proteins, such as agonistic or antagonistic receptor modulation[297]. In addition to these direct effects, antibodies can also recruit immune cells through interactions with the antibody Fc domain, creating a connection between target cells and certain types of immune cells that can lead to phagocytosis or antibody-dependent

cytotoxicity[297]. Synthetic immunology approaches have been developed to broaden the effects of antibodies and derivative molecules in immune cell activation, including the development of bi-specific T-cell engager (TCE) antibodies that can induce strong antigen-targeted T cell responses[298]. The most clinically advanced of such therapies is Blinatumomab, a CD19xCD3 antibody [299]used in the treatment of acute lymphoblastic B-cell leukemia[300].

To further broaden the types of cancer that can be effectively targeted using TCE therapeutics, optimize TCE biological activity, and explore additional modalities for other types of bi-specific antibodies, there is a need for cost-effective high-throughput platforms for TCE discovery and development. TCE molecular development begins with the identification of two antigen-binding molecules, most typically single chain variable fragments (scFv) derived from monoclonal antibodies (mAb) isolated from mouse, human, or other animals. One scFv must bind an antigen on a target cell, with the other binding a T cell specific protein, with the most common T-cell target being CD3 [217](see Figure 2.1A). These scFvs are connected using a linker, usually composed of a flexible amino acid sequence (GGGGS) length as seen in Blinatumomab[301], though this spacer element can be repeated or of varying composition to create a longer spacing between engager domains (GGGGS x 2, 3 etc.). In the presence of a TCE molecule, T cells and target cells expressing the target antigen should form a strong interaction, prompting both T cell activation and target cell killing[302,303].

Here we outline a complete, high-throughput method for generating novel bi-specific antibody plasmids, rapidly producing TCE proteins, and performing function first activity

screening in the human Jurkat T cell line with no antibody preparation, purification or characterization. This allows for immediate functional insight for TCE candidates following DNA assembly, reducing the time and cost associated with finding a lead candidate. Using the tools and techniques outlined in this paper, researchers can quickly discover and optimize ideal candidates for further clinical development or incorporation into more complex synthetic therapeutics.

2.3 Materials and Methods

2.3.1 Construction of pTCE modular plasmid

A synthetic plasmid modeled on blinatumomab[304] with modularized binding domains to allow low-cost single-pot restriction ligation recombination of either binding arm was designed in silico using A plasmid Editor[305]. The design contains a IgG1 signal peptide, modularized CD19-scFv (OKT3HD37), linker, modularized CD3-scFv (OKT3), and P2A-NeonGreen (see S1 Table for DNA and amino acid sequences used, see Fig 1B for a schematic of the sequence design). To build the pTCE plasmid, CAR-specific domains were removed from pSLCAR-CD19 (Addgene #135992), leaving a linearized plasmid containing a short EF1a promoter and a P2A-NeonGreen reporter sequence within a linearized lentiviral plasmid backbone. Next, a custom DNA fragment was synthesized (Twist Bioscience, USA) coding for the HD37 anti-CD19 scFV, linker, OKT3 anti-CD3 scFv and adapter sequences to allow cloning into the linearized plasmid using Gibson assembly [306]. Gibson assembly was performed using either the GeneArt™ Gibson Assembly HiFi Master Mix (ThermoFisher A46627) or an in house “DIY Gibson” assembly mixture using the RFC57 recipe [12]. Custom fragments (1uL), linearized backbone (1ul) and Gibson Assembly Mix (5ul) were

combined and filled to 10ul with molecular grade water. The Gibson reaction was run in a thermocycler at 50°C for 45 minutes before transformation. The reaction mix was then stored at -20°C for an undefined period before proceeding to bacterial transformation.

The final plasmid incorporates modular restriction sites to allow swapping of the tumour engager arm (using BpiI) and the CD3 binding arm (using Esp3I), as well as the linker arm between the two (see Fig 1B). The constructed TCE plasmid was transformed into DH5a chemically competent *E. coli*. To confirm successful cloning, individual transformed colonies were analyzed via direct colony PCR using backbone or scFv-specific primers. Colonies which contain predicted PCR products are grown overnight in normal lysogeny broth (LB) with 1% ampicillin. Plasmid DNA was purified using standard mini-plasmid or midi-plasmid purification kits (Cat#K0502 or #K0481, Thermo Fisher, USA) and then sequenced via Sanger sequencing to ensure accurate sequence construction. This plasmid, known as BMv4 can be found in the S1 Table t or on Addgene (Addgene #190677—Non His, or #190678—With His tag).

2.3.2 Tumor antigen binding domain or CD3-binding domain exchange

When designing scFv inserts for "Golden-Gate" single-pot restriction/ligation[307], the 5' and 3' ends are structured depending on the cloning site used. Typically, scFv sequences were synthesized based on antibody heavy and light chain sequences to create a VH-linker-VL sequence that is approximately 600–800 bp long. For swapping of the N-terminal tumour-antigen binding domain in pTCE the following BpiI restriction site containing sequence design was used: 5'–NNN**GAAGAC**NNAGGA—*VH or VL sequence—Linker—VH or VL sequence*—NNCCTTNN**GTCTTC**NNN-3'. For swapping of the C-terminal immune cell

engaging domain using Esp3I the following sequence design was used 5'–NNN**CGTCTC**NAAGT—*VH or VL sequence—Linker—VH or VL sequence*—GCTAN**GAGACG**NNN-3'. Any internal Esp3I or BpiI sites in the scFv were altered with silent mutations. Specific primers we used for sub-cloning scFv sequences from previous EGFRvIII-CAR constructs can be found in S2 Table. In this manuscript a VH-Linker-VL orientation was used for all scFvs tested, though the reverse orientation has been shown to produce functional scFv molecules as well[308]. Once assembled in silico, scFv sequences were generated through PCR subcloning or synthesized via commercial DNA synthesis company (Twist Bioscience, USA).

To swap either scFv, the following reaction conditions were used: 250ng of pTCE, 50ng of new scFv DNA fragment, 0.25ul BpiI or Esp3I, 0.25ul T4 ligase, 4ul T4 reaction buffer and filled to 20ul with molecular grade H_2O. The scFv insertion reaction is run on a thermocycler under the following protocol: (37°C for 10 min, 16°C for 10 min) 10 cycles, 37°C for 60 min, 80°C for 5 min to inactivate enzymes, and 4°C indefinitely. 2 to 5ul of this reaction was then transformed into chemically competent DH5α *E. coli*, which were then plated on ampicillin containing agar plates and grown overnight at 37°C. To confirm successful cloning, individual transformed colonies were analyzed with PCR using backbone or scFv specific primers (see S2 Table for primers used). Colonies which contained predicted PCR products are grown overnight in normal lysogeny broth (LB) with 1% ampicillin. Plasmid DNA was then purified using standard mini- or midi-prep purification kits (Qiagen, USA). It is recommended that purified plasmids are sequenced to ensure correct construction, sequencing primers used for Sanger sequencing of the

plasmid can we found in the S2 Table. EGFRvIII-specific scFv sequences used for cloning can be found in[309,310], and can be found in the S1 Table or on the Addgene repository (F263-4E11 Addgene #190680, F265-5B7 Addgene #190679, F269-3D12 Addgene #190681, and F271-1D2 Addgene #190682). Swapping CD3-targeting domains was performed similarly as described above using Esp3I enzyme to integrate synthetic CD3-scFv fragments (Twist Biosciences, USA), derived from in-house generated CD3-specific murine monoclonal antibodies, into the pTCE construct. Novel CD3 monoclonal antibody and scFv sequences can be found in[311]. Plasmids encoding novel CD3 TCEs can be obtained under MTA with the National Research Council Canada.

2.3.3 Cell lines

All cell lines were monitored regularly for mycoplasma contamination using in-house PCR assay[312]. In preparation of cell assays, healthy cultures of Jurkat E6-1 cells (ATCC#TIB-152) were maintained in complete RPMI (RPMI1640 supplemented with 10% FBS, 2mM L-glutamine, 1mM sodium pyruvate and 100 µg/mL penicillin/streptomycin) with cell density between 0.25 and 1×10^6 cells/mL for several weeks; we have found that maintenance conditions are critical for consistent results in Jurkat activation assays. All target cell lines described in this paper were modified using Nuclight-Red Lentiviral reagent (Cat#4625, Sartorius, USA) to generate stable red-fluorescent cells which can be easily differentiated from effector cells in FACS or live microscopy analyses. Specific target lines used were as follows: Raji (CD19+, ATCC#CCL-86), Nalm6 (CD19+, a gift from Dr. Beat Bornhauser, Kinderspital Zürich, Switzerland), MCF7 (CD19-, ATCC#HTB-22), U87MG-vIII (EGFRvIII+, a gift from Prof. Cavnee, Ludwig Cancer Institute, USA), U87MG (EGFRvIII -, also a gift from

Prof. Cavnee), DKMG (EGFRvIII^{low}, DSMZ#ACC277). Target cell lines were grown in varying media conditions, as recommended by cell repository.

2.3.4 Jurkat directed TCE electroporated protocol

Healthy cultures of Jurkat cells with cell density between 0.25 and 1×10^6 cells/mL were maintained in culture for several weeks. Prior to electroporation, a recovery plate was prepared using pre-warmed RPMI 1640 supplemented with 20% fetal bovine serum and 100 ug/ml of L-glutamate. Jurkat cells were pelleted via centrifugation, then resuspended in 100ul of 1SM buffer (as per [313]) and 2ug of plasmid and brought to room temperature. Cells were then placed into a 0.2cm electroporation cuvette (Cat#1652086, Bio-Rad, USA) and electroporated using a Lonza Nuceleofactor Electroporator using X4 settings. Cells were then immediately transferred to the recovery plate. Cells were allowed to recover for 4 hours prior to analysis or use in an assay. Post-recovery Jurkat cells and target cells were then resuspended in complete RPMI and placed in 96-well plates at varying ratios of Jurkat and target cells as shown in the text. If adherent target cells were used, cells were first treated with Accutase (Cat#A1110501, Thermo Fisher, USA) to create a single cell suspension. Plates were incubated at 37°C, 5% CO_2 for either 16 to 40 hours. Plates was then stained with anti-CD69 APC (Cat#340560, BD Bioscience, USA) at 0.25ul per well in no-wash format. Plates were then incubated in the dark at RT for 15 minutes and analyzed via flow cytometry using a BD Fortessa device (BD Bioscience, USA).

2.3.5 HEK293T transfection for TCE supernatant production

HEK293T cells were plated in a 6 well plate at approximately 150k cell per well and allowed to grow overnight before transfection. The following transfection mixture was prepared:

1.2ml of serum free DMEM 200ul/well, 9ug/well linear polyethyleneimine (PEI; Cat#765090-1G, Sigma-Aldrich, USA), and 12ug (2ug/well) of pTCE plasmid. The tube containing the transfection mix was vortexed and incubated at RT for 10 minutes. 200ul of the solution was added drop wise to each well incubated at RT for 20 minutes. Cells were then incubated at 37°C for 4 hours. After 4 hours, media was removed and replaced with 2-3ml of fresh DMEM media supplemented with 10% Fetal Bovine Serum (FBS), 1% L-Glutamate (Cat#25030081, Gibco, USA) and 1% Penicillin-Streptomycin (Pen-Strep; Cat#15070063, Gibco, USA) (referred to as DMEM complete below). After 5–7 days, transfected HEK293T supernatant was removed and filtered using 0.45-micron filter to remove any excess cells. TCE-containing supernatant was then frozen at -80°C and thawed prior to TCE-Jurkat assay as described below. We confirmed that freezing resulted in no loss of TCE activity for the active TCE molecules reported in this manuscript.

2.3.6 Indirect HEK supernatant TCE-Jurkat activation assay

If adherent target cells were used, target cells were first treated with accutase (Cat#A1110501, Thermo Fisher, USA) to create a single cell suspension. Jurkat cells and target cells were then resuspended in complete RPMI and placed in 96-well plates at varying ratios of Jurkat and target cells as shown in the text. Unless otherwise stated in the text, 50ul of TCE containing HEK supernatant were added to appropriate wells. Complete media was then added to equalize plating volume. Plates were incubated at 37°C, 5% CO_2 for either 16 or 40 hours, followed by staining with anti-CD69 APC (Cat#340560, BD Bioscience, USA) at 0.25ul per well in no-wash format. Plates were incubated in the dark at

RT for 15 minutes and analyzed via flow cytometry using BC Fortessa device (BD Bioscience, USA).

2.3.7 Primary T cell culture preparation

To prepare T cells, healthy donor blood samples were obtained under appropriate safety and ethics approvals by the Ottawa Hospital Research Institute (Ottawa, Canada). Whole blood was diluted 1:1 with Hank's balanced salt solution (HBSS) and PBMCs were isolated by Ficoll-Paque™ density gradient centrifugation, centrifuging for 20 min at 700 × g without applying a brake. The PBMC interface was carefully removed by pipetting and was washed twice with HBSS by stepwise centrifugation for 15 min at 300 × g. PBMCs were resuspended and counted by mixing 1:1 with Cellometer ViaStain™ acridine orange/propidium iodide (AOPI) staining solution and counted using a Nexcelom Cellometer Auto 2000 (Nexcelom BioScience, Lawrence, Massachusetts, USA). T cells from were then activated with Miltenyi MACS GMP T cell TransAct™ CD3/CD28 beads and seeded 1×10^6 T cells/ml in serum-free StemCell Immunocult™-XF media (Cat#10981, StemCell Technologies, Vancouver, Canada) with 20U/ml clinical grade human IL-2 (Novartis). T cells were then polyclonally expanded for 7 to 10 days in culture before cryopreservation of aliquots using complete media + 10%DMSO.

2.3.8 TCE-Induced target cell killing assessment via live fluorescence microscopy

Cryopreserved polyclonally expanded primary human T cells (frozen on day 7–14 post activation), were thawed on the day of the experiment and counted and assessed for viability using Nexcelom Cellometer Auto 2000 (Nexcelom BioScience, Lawrence, MA, USA). Human T cells and red-fluorescent target cells were then resuspended in

Immunocult-XF media supplemented with 100U/mL IL2. Cells were then transferred to a 96-well culture plate at 10 000 T cells per well and 2000 target cells per well. Plates were then placed in an S3 Incucyte Live Cell Imagine system (Sartorius, USA) and incubated at 37°C and 5% CO_2 for up to 140 hours. Images were taken every 2 to 4 hours. Target cell growth was tracked using automated assessment of red fluorescent area percentage using the accompanying Incucyte analysis software. Final data was assembled and analyzed using Graphpad Prism.

2.4 Results

2.4.1 Creating a modularized plasmid

Previously we reported on a Jurkat based platform for screening novel chimeric antigen receptor molecules[314], here we wished to create a similarly flexible plasmid which could be used for functional screening of single-chain variable fragments (scFv) in a soluble bi-specific antibody molecules (Fig 1A). We based our plasmid design on the amino acid sequence for blinatumomab[304], adding type-IIs restriction sites to allow for simplified cloning of either binding arm of the molecule (Fig 1B). The modularized blinatumomab biosimilar plasmid (pTCE) allows either end of the TCE DNA to be swapped for an alternative scFv in a single pot restriction ligation reaction (Fig 1B), as well as exchange of the linker connecting both scFv domains if desired. This system can be used to easily customize the TCE design, allowing for efficient construction of a variety of TCEs and TCE compositions for testing. Our testing shows highly efficient exchange of both target antigen scFv and T cell antigen scFv can be achieved consistently using single pot restriction ligation as described in the methods section.

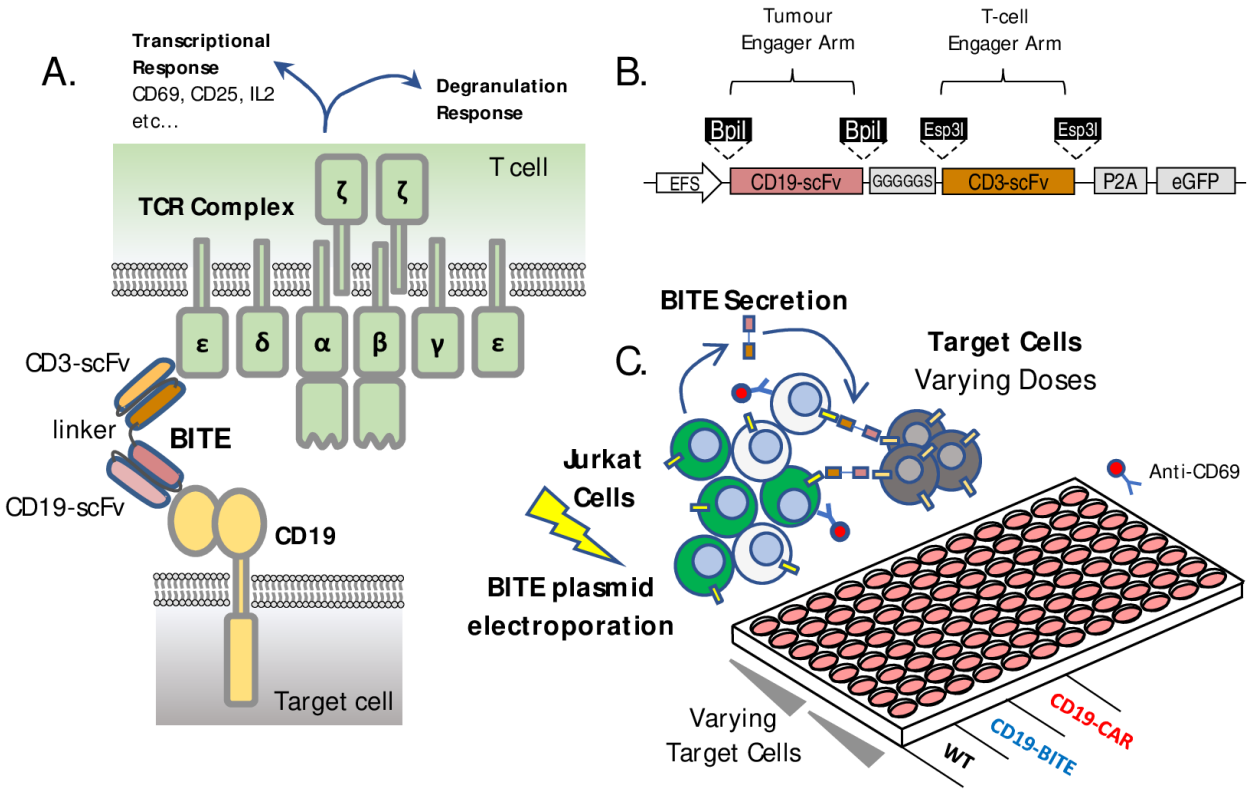

Figure 2.1. Modular TCE Plasmid and screening platform design.

(A) TCE mechanism of action relies on simultaneous engagement of target cell receptors usually located on tumour cells and the CD3 domains of the T-cell receptor on T cells. This results in forming an active immune synapse between the T cell and the cancer, leading to both transcriptional and direct degranulation responses within the T cells, and target cell death. (B) The transgene design for a dual-modular TCE plasmid incorporating type-IIs restriction enzyme cassettes on each scFv region to allow easy exchange of scFv domains via golden gate cloning, (C) TCE-Jurkat screening assay setup uses direct electroporation of TCE plasmids into Jurkat cells in co-culture with various target antigen positive or negative target cell lines.

2.4.2 TCE-J function first screening platform

Using the pTCE plasmid, we first tested a functional screening method using Jurkat electroporation to induce transient expression and secretion of the TCE molecule, similar to the method we have previously reported for screening novel chimeric antigen receptors[314]. Following TCE plasmid electroporation, Jurkat cells were co-incubated with target cells at varying effector to target ratios to produce a standard dose response curve,

with Jurkat cells acting as both the TCE producer and immune effector cell (Fig 1C). After co-incubation of Jurkat and target cells, cultures were stained with anti-CD69 and analyzed via flow cytometry to assess TCE activity. While we were able to detect consistent increases in Jurkat activation with TCE expression via this method (S1A Fig), activation of Jurkat cells expressing TCE was lower than that observed for Jurkat cells expressing a CD19-targeted CAR (S1B Fig). We hypothesized that the low activity of the TCE in this assay format might be due to relatively low electroporation efficiency and TCE production in Jurkat cells, thus we wished to examine a more traditional transient production of TCE proteins in HEK293T cells.

As a strategy to try to improve the signal to noise ratio for our TCE activity assay we next developed a transient TCE production method using HEK293T cells, which are widely used for production of recombinant proteins where a human cell source is desirable[267]. HEK293T cells were transfected with TCE plasmids using standard PEI transfection. Fluorescence microscopy confirms successful transfection due to expression of the pTCE GFP marker at day 1. HEK293T cells were then grown for 5–7 days before collecting the supernatant, using filtration to clear any remaining cells. Non-purified TCE supernatants were then assayed using co-cultures of Jurkat T cells and target cells similarly to the previous iteration of the TCE-J assay (Fig 2A). These co-cultures were left for either 16 or 40 hours, then analyzed via flow cytometry for CD69 upregulation on Jurkat cells. With this improved TCE production technique, we observed more consistent TCE-induced upregulation of CD69 in the presence of increasing numbers of CD19+ Raji or NALM6 target cells (Fig 2B). The addition of non-transfected HEK293T supernatant as a control had no effect on Jurkat activation.

As this production technique yielded a large volume of TCE supernatant, much more than necessary for Jurkat experiments, we were also able to rapidly proceed to testing the effects of CD19-TCE on co-cultures of primary human T cells and CD19+ Raji or Ramos target cells. Using live fluorescence microscopy (Incucyte), we monitored the relative growth of mKate2-labelled target cells in the presence of varying doses of CD19-TCE supernatant. We observed strong dose-dependent target cell killing with TCE treatment for both target cell types (Fig 2C). These results demonstrate that transient production in HEK293T cells followed by TCE-J assay represents a viable platform for testing of biological activity for TCE molecules.

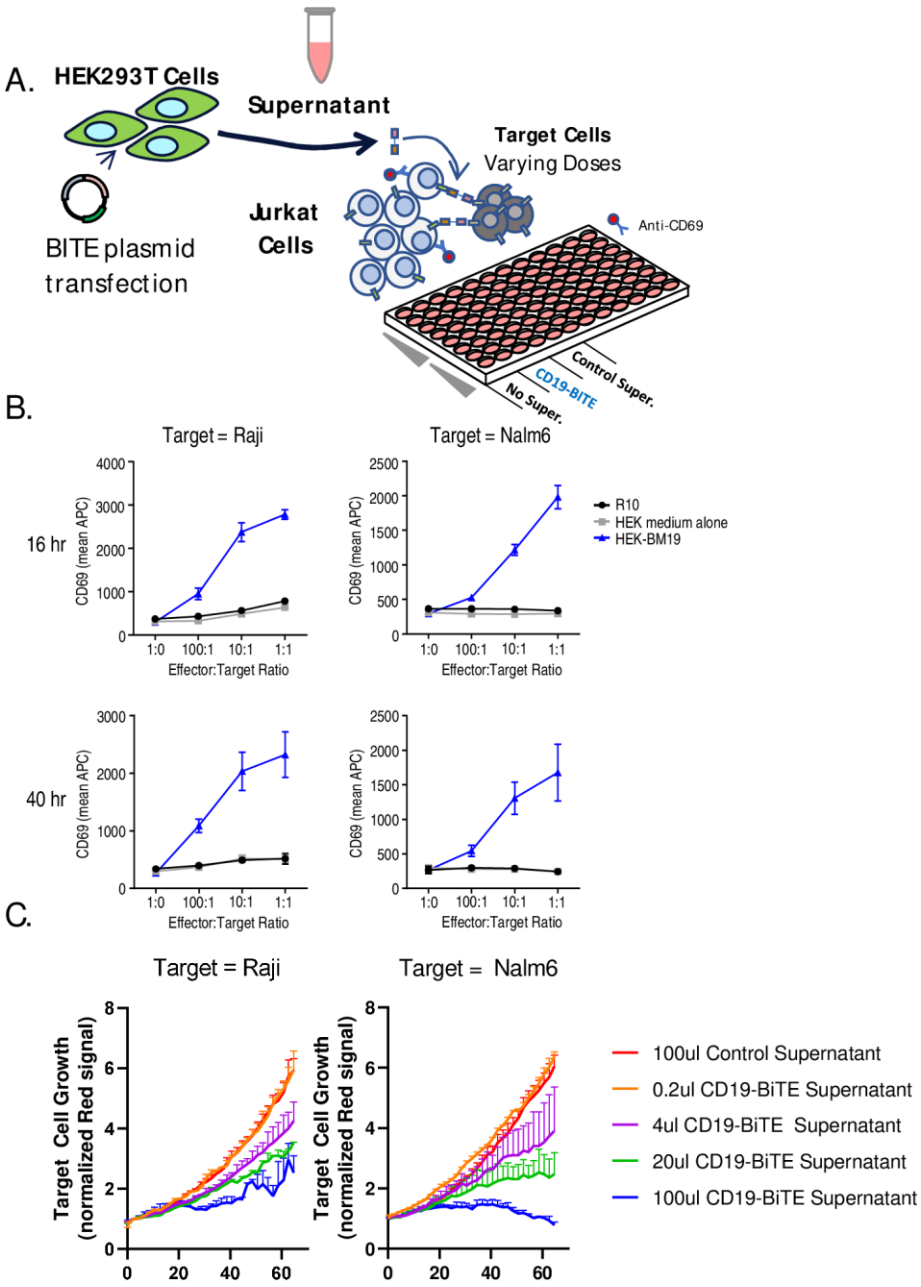

Figure 2.2. TCE-Jurkat assay using rapid HEK293T TCE production.

(A) A schematic illustration of the workflow for production of TCE supernatant using HEK293T cells and testing using Jurkat-target cell co-cultures is shown (B) HEK293T cells were transiently transfected with TCE plasmid as described in the methods section and supernatants were collected and frozen at -80°C. 50 000 Jurkat cells were placed in a 96-well plate in co-culture with varying numbers of CD19+ Raji or NALM6 with effector to target ratios as shown. 50ul of TCE supernatant or control supernatant was then added and co-cultures were incubated at 37°C overnight. Co-cultures were stained with anti-human CD69-APC and analyzed via flow cytometry. Graphs show the mean result from 4 experiments repeated in duplicate +/- SEM. (C) Primary human T cells were placed in co-culture with 10 000 human T cells and equal numbers of red fluorescently labelled CD19+ Raji or NALM6 cells, and varying doses of CD19-TCE supernatant was added. Co-cultures were then monitored at regular intervals using fluorescence microscopy and automated cell

counting via Incucyte. Graphs show the growth rate of red fluorescent target cells with varying TCE dose. Primary T cell results are from a single experiment performed in duplicate.

2.4.3 Swapping pTCE tumor engager arm

Next, we wished to test the flexibility of our TCE functional screening approach for different tumour antigen targeting domains. Using several mouse-derived single chain variable fragments (scFvs) targeting EGFRvIII, which we have previously reported to induce robust activity against EGFRvIII+ glioblastoma cells when combined in CAR proteins [20]. We thus generated novel EGFRvIII-TCE constructs using single pot restriction-ligation cloning with pTCE (Fig 3A). We then transiently transfected HEK293T cells with EGFRvIII-TCE plasmids and screened supernatants via Jurkat co-culture with EGFRvIII-positive U87vIII and DKMG glioblastoma target cell lines. Only two of the TCE plasmids generated (F269 and F263) resulted in positive CD69 upregulation when TCE supernatants were added to Jurkat/target cell co-cultures (Fig 3B). We then proceeded to testing using polyclonally expanded primary human T cells in co-culture with target antigen-positive U87-vIII target cells, or target antigen-negative U87-WT or Raji target cells. In this case, we observed rapid killing of EGFRvIII-positive target cells (Fig 3C) but not EGFRvIII-negative cells (Fig 3D and 3E). Overall, these results demonstrate that our modular plasmid platform allows rapid cloning and functional screening of novel TCE molecules for T-cell redirecting activity, identifying two candidate TCE molecules F263-OKT3 and F269-OKT3 for potential future development.

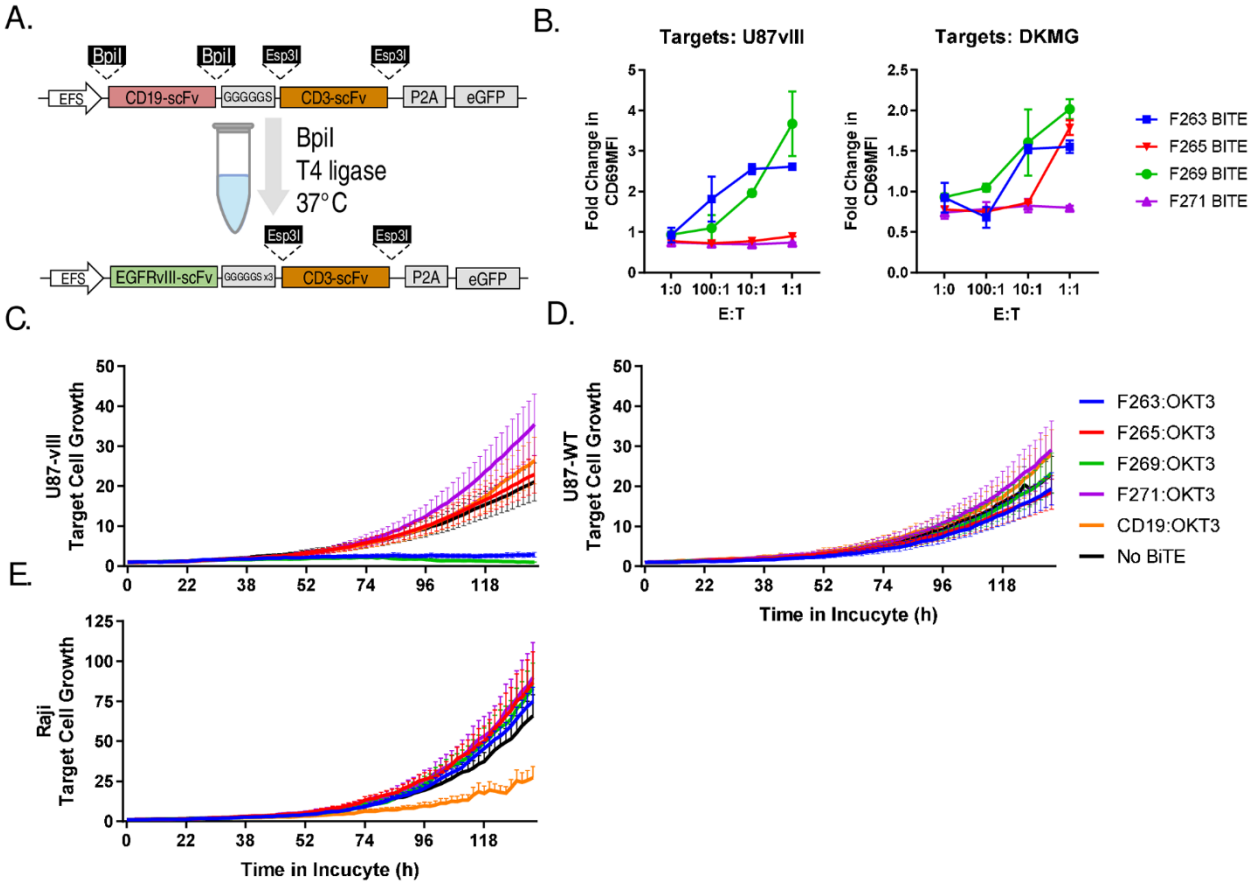

Figure 2.3. Production and screening of EGFRvIII targeted TCEs.

(A) A single-pot restriction ligation reaction with BpiI restriction enzyme was used to swap CD19-targeting arm with EGFRvIII-specific scFv sequences to generate EGFRvIII-TCE plasmids as described in the methods section. (B) HEK293T cells were transiently transfected with TCE plasmids and supernatant was collected and frozen. 50 000 Jurkat cells were placed in a 96-well plate in co-culture with varying numbers of EGFRvIII+ U87vIII or DKMG target cells as shown. 50ul of TCE supernatant or control supernatant was then added and co-cultures were incubated at 37°C overnight. Co-cultures were stained with anti-human CD69-APC and analyzed via flow cytometry. Graphs show the mean result from a single experiment performed in duplicate +/- SEM. Fresh EGFRvIII or CD19-specific TCE supernatants were then generated in HEK293T cells for testing in primary T cells. 10 000 human T cells were combined with 2000 (C) EGFRvIII+ CD19- U87vIII target cells, (D) EGFRvIII- CD19- U87WT cells, or (E) EGFRvIII- CD19+ Raji cells. Graphs show the relative fluorescent signal of red-fluorescent target cells over 5 days in co-culture. Results are derived from a single experiment but are representative of at least 3 repeated observations.

2.4.4 Swapping the CD3 targeting domain

We next sought to test our platform for flexibility with respect to screening novel T-cell engaging domains of the bispecific molecule. We developed a number of novel mouse monoclonal antibodies (mAbs) against human CD3 complex using a multi-antigen immunization strategy in mice and traditional hybridoma screening. Through this process, we were able to identify several monoclonal antibodies with reactivity to Jurkat cells (Fig 4A) and human T cells (Fig 4B). To assess whether scFvs derived from novel CD3-targeted mAbs would be functional within as part of a TCE molecule, we cloned 4 anti-human CD3 single chain variable fragments into CD19 or EGFRvIII specific TCE plasmids (Fig 4C). We then generated supernatants using transient transfection of HEK293T as described above. TCE supernatants were screened for activity using Jurkat cells in co-culture with EGFRvIII-expressing U87-VIII targets or CD19-expressing Raji cells. Previously tested constructs using OKT3 CD3-engager arms showed activity with both EGFRvIII and CD19 specific TCEs, whereas we detected activity for only one of our novel CD3-engager TCEs and only when combined with an EGFRvIII-specific scFv (Fig 4D). To confirm these results, we repeated TCE production and Jurkat co-culture screening of CD19 and EGFRvIII targeted TCE molecules incorporating OKT3 or the novel 1E2 CD3-targeting single chain variable fragment. Whereas EGFRvIII TCEs incorporating an scFv derived from the 1E2 mAb or OKT3 showed specific reactivity against EGFRvIII expressing U87-vIII cells, only CD19-OKT3 showed reactivity to CD19-expressing Raji cells (Fig 4E). These results indicate that the novel CD3-targeting 1E2-scFv is functional only for an EGFRvIII-targeting TCE but not a

CD19-targeting TCE, likely due to the specific binding characteristics of the CD19 or EGFRvIII scFv elements.

Finally, to assess whether the wholly novel EGFRvIII-1E2 TCE molecule identified here can induce genuine functional interaction between human T cells and target cells, we proceeded to screening these molecules for activity in co-cultures of polyclonally expanded human T cells with U87-VIII or Raji target cells. Human T-cells quickly killed EGFRvIII+ target cells when treated with a TCE combining EGFRvIII-scFv with OKT3 or our novel CD3-specific 1E2 scFv, but not CD19-targeted TCEs (Fig 4F, S1–S4 Videos). In contrast, a CD19-specific scFv in combination with only OKT3 showed activity against Raji cells, but not a similar CD19-1E2 or EGFRvIII-specific TCEs (Fig 4G, S5–S8 Videos). Overall, these results indicate that we have established a flexible platform for high-throughput functional screening of novel TCE molecules wherein either the tumour targeting or immune targeting arm can be recombined and screened for biological activity.

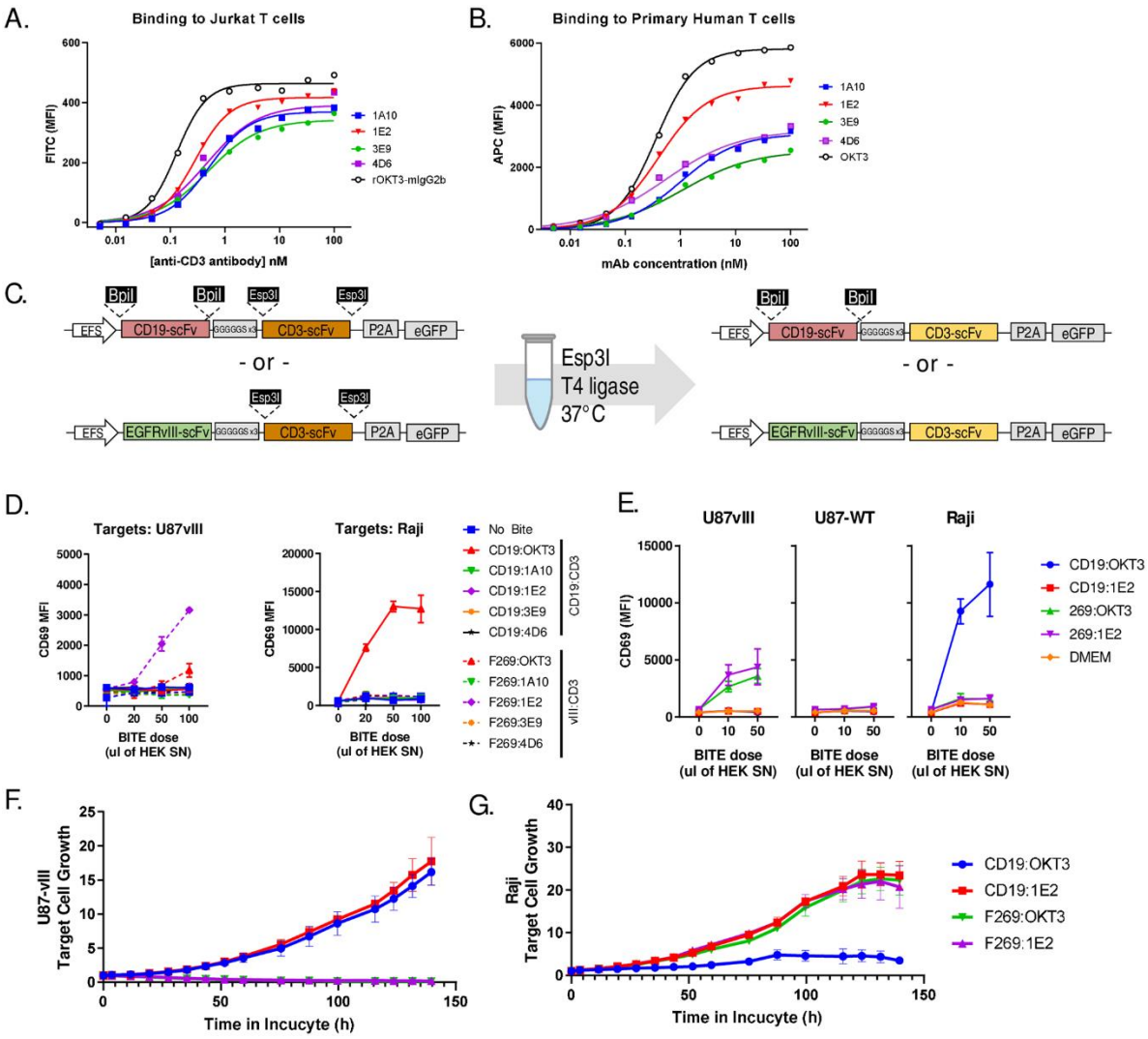

Figure 2.4. Production and screening of TCE molecules incorporating novel CD3 targeting scFvs.

Novel monoclonal antibodies were generated via mouse immunization and hybridoma screening. Four monoclonal antibodies are shown which have high reactivity to (A) Jurkat T cells and (B) primary human T cells. Following this, antibody heavy and light chains were sequenced. (C) scFv DNA was then synthesized and assembled into CD19 or EGFRvIII TCE molecules using single-pot restriction ligation with Esp3I restriction enzyme. (D) Ten unique CD19 or EGFRvIII TCE plasmids were then transfected into HEK293T cells and supernatants were tested using Jurkat cells in 1:1 co-cultures with EGFR-vIII+ U87vIII cells (*left*) or CD19+ Raji cells (*right*) using varying doses of TCE supernatant as shown. (E) Four TCE plasmids found to produce active TCE molecules were tested again against EGFRvIII+ U87-vIII cells, EGFRvIII- U87-WT cells, or CD19+ Raji cells. (F) TCE supernatants for CD19 or EGFRvIII targeted molecules incorporating the 1E2 CD3-scFv were added to co-cultures with 10 000 primary human T cells and 2000 target cells. Graphs show the relative fluorescent signal of red-fluorescent target cells over 5 days in co-culture. Results are derived from a single experiment but are representative of at least 3 repeated observations.

2.5 Discussion

Monoclonal antibody therapies targeting many cancer-associated antigens can effectively induce antibody dependent cellular cytotoxicity (ADCC) through simultaneous engagement of target antigens via their variable domains and immune cells via the Fc domain. Many recombinant antibodies have been shown to mediate their activity through ADCC both in pre-clinical and clinical studies of CD20-targeting rituximab[315], Her2-targeting trastuzumab[316], or CD38 targeting daratumumab[317], among others. While these therapies have had remarkable success in treatment of many cancers, NK-mediated ADCC lacks the aggressively proliferative, tumour-penetrating, and inflammatory responses that can be mediated by antigen-specific T cell responses. Thus, bi-specific T cell engaging antibodies were envisioned as a means of redirecting more potent T cell responses against tumours, leading to the development of blinatumomab, a CD19-CD3 TCE used to treat acute lymphoblastic leukemia, as well as other TCE therapeutics at various stages of pre-clinical and clinical development[301]. While TCE therapeutics show strong potential for treatment of many different cancer types, their complex structure makes discovery and development costly and unpredictable. Thus, we sought to establish a flexible and cost-efficient platform for rapid identification of promising TCE molecules.

The system presented here provides a full overview of our development work for TCE screening, including: design of a bi-modularized TCE plasmid, scFv swapping of either tumor or T-cell engaging elements, transient production in HEK293T cells, and TCE-J screening of supernatants. This establishes a complete method for high throughput functional screening of novel TCE molecules which can be readily replicated in other labs

interested to develop their own TCEs. Other systems have been previously reported for TCE screening, but all are dependent on production of purified high-quality proteins; such as the dock and lock system used by Rossi et al. to screen multi-functional antibodies[318]; the work of Zappala et al. where antibodies are covalently linked to a CD3-specific scFv[319]; or that by Hofmann et al.[320] wherein intein mediated dimerization of antibodies is used. Whereas these methods offer a compelling means to mix and match many different binding domains for their activity in dimerized format, all require purified antibody proteins, which may increase the complexity and cost of screening. Furthermore, some methods may not be predictive of activity for TCEs incorporated in a single molecule for downstream production. It should be noted that while the TCE-J method presented here does not require a purification step to screen and evaluate generated TCEs, purification will ultimately be necessary for downstream testing using *in vivo* models. Given that the plasmid we developed here does not code for an Fc region, similar to blinatumomab, making standard protein G purification not possible. Thus, we intend to investigate alternate versions of this platform in future, for example we have developed a version of this TCE screening plasmid containing a His-tag to allow downstream purification via IMAC column.

Sugiyama et al have demonstrated a similar workflow wherein more than 52 individual bi-specific antibody molecules were generated and screened in both heavy/light chain orientations[321]. We propose that the plasmids established here provide a more flexible cloning system, as the application of single-pot restriction ligation cloning would allow users with limited molecular biology knowledge to generate novel TCE assemblies via

golden gate cloning, while also minimizing the synthesis costs for labs employing these tools. Downstream of bi-specific antibody generation and purification, most previous reports have focused on some form of T-cell Dependent Cellular Cytotoxicity (TDCC) assay[322], typically using a viability measurements such as MTS or Luciferase reporting systems. These assays can be effective; however, we find that assessment of CD69 on Jurkat cells to be the most easily scalable method of measuring T cell activation activity. Jurkat testing also removes the need for donor cells and provides a consistent, standardized cell line for screening TCEs. For testing with primary T cells, we find that live microscopy provides a simple method of evaluating active tumor control and killing, although flow cytometry can also be applied to yield similar results.

Other more advanced and higher throughput approaches to screening and analysis of bi-specific antibodies based on single cell droplet based microfluidics fluorescence sorting have also been reported.[323,324] As such approaches combine both antibody panning and antibody activation into a singular assay, they are compatible with the screening of polyclonal libraries of bi-specific molecules. The plasmids we have developed here also incorporate elements necessary for lentiviral production, and thus would be compatible with the generation of polyclonal Jurkat-TCE cell libraries. In future, we will investigate suitable methods for downstream functional assessment such as single cell sorting and screening, or microwell entrapment of TCE producing and target cells.

While other methods of TCE screening such as those discussed above are have been developed, many of these methods require significant investment and access to specialized equipment and the use of costly consumables. TCE-J was designed not only to

allow for quick TCE discovery and optimization, but also to provide tools and protocols to academic labs, which can be performed with minimal protein production and purification costs, and with minimal DNA synthesis costs. We hope that the ease of access and relatively low entrance cost of TCE-J allows more researchers to contribute to the development and optimization of bi-specific therapeutics, the development of novel synthetic biology applications for TCE molecules, and to apply these tools more broadly to biological research.

This work also extends our insights into the specific EGFRvIII-specific antibodies tested here, which we have previously reported on for CAR activity[314]. The four EGFRvIII-specific scFv molecules tested all showed some activity in CAR format, both in the activation of CAR-expressing Jurkat cells or for inducing primary CAR-T killing of U87-VIII target cells. In contrast to this, we find that only two molecules showed significant activity here when tested in TCE format. As the screening approach employed here does not incorporate any characterization of TCE production, it is possible that low biological activity for these molecules may have been due to low productivity within HEK293T cells, and thus we cannot state conclusively that these molecules would not be functional if produced and purified in other formats. While this may be the case, low production yield is also an important category for considering whether TCE molecules are suitable for therapeutic development and thus would need to be considered in molecular hit selection regardless.

Similarly, we also find that only one of the novel CD3-targeting scFvs tested here showed activity in TCE format, and even then, activity was restricted to combination with EGFRvIII-targeting scFv and not with a CD19-specific scFv. Again, we have no insight into the failure

rate for TCE molecules in this assay, as the intent of this assay is to provide a rapid means for testing biological activity rather than focusing on various aspects of antibody characterization. We are currently undertaking molecular studies to test whether incorporating different linker domains may be able to improve the activity of TCEs using the novel CD3-scFv reported to have activity here, something that may provide further insight into the design constraints for these TCE molecules.

The fully novel EGFRvIII-CD3 engaging molecules identified at the end of the manuscript provides a proof of principle example for high throughput discovery of novel TCE therapeutics. As this molecule shows strong activity in mediating T-cell killing of antigen-positive tumour cells and little to no off-target activity, it also shows potential for downstream development as a therapeutic to target EGFRvIII-expressing tumours, such as glioblastoma. In the future, we intend to expand on this platform to better understand the design space and study the biology of bi-specific antibody therapeutics that mediate active engagement of T-cells or other immune cells with target cells.

2.6 Supplemental Material

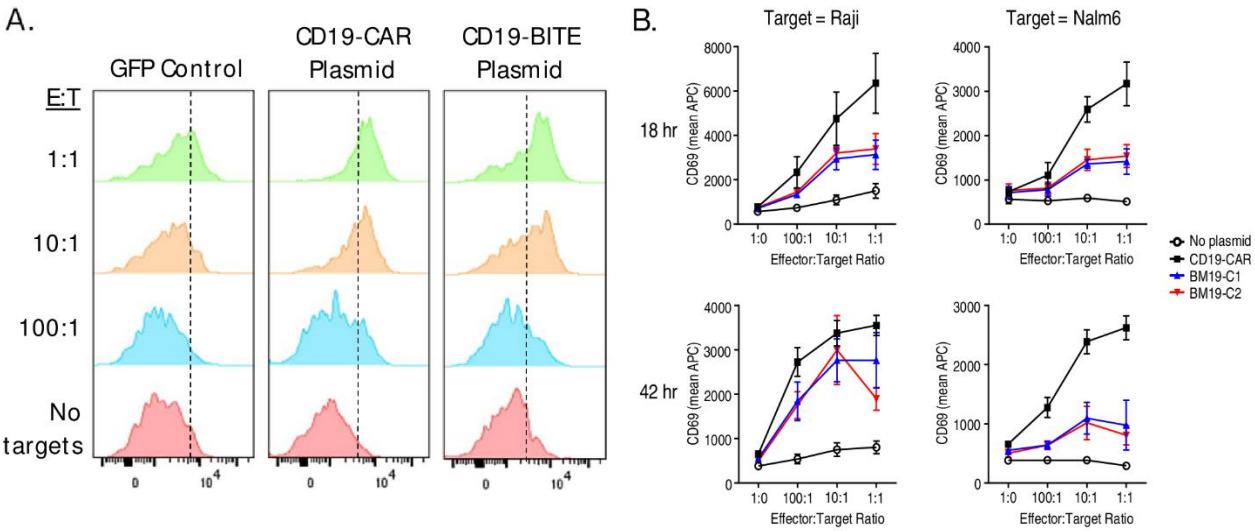

Supplementary Figure 2.1: TCE-Jurkat Assay using direct electroporation in Jurkats.

(A) Human Jurkat T cells were electroporated with CD19-targeted TCE or CAR plasmids as described in the methods section. Following recovery, electroporated Jurkat cells were then placed in co-culture with fluorescently labelled CD19-expressing target cells at various effector to target ratios and incubated at 37°C overnight. Co-cultures were stained with anti-human CD69-APC and analyzed via flow cytometry. Results are representative of 3 repeated experiments. (B) The mean fluorescent intensity for CD69-APC staining on gated Jurkat cells is shown for Jurkat-CD19-TCE or Jurkat-CD19-CAR cells in co-culture with CD19+ Raji or NALM6 cells for 18 hours (top) or 42 hours (bottom). Graphs show the mean result from 3 experiments repeated in duplicate +/- standard error of the mean (SEM).

CHAPTER 3: EVALUATING THE EFFECT OF TRANSITIONING A SINGLE TARGET CAR TO A MULTI-TARGETING FORMAT

Note: This Chapter is a manuscript submitted to Frontiers in Immunology. Confirmation of this submission can be found in Appendix 1.

Co-transduced EGFR and Mesothelin NanoCARs Superior to Tandem-CAR in H292 Lung Cancer Xenograft

Alex Shepherd[2], Bigitha Bennychen[2], Laura Tamblyn[1], Shalini Raphael[1], Henk van Faassen[1], Greg Hussack[1], Mehdy Elahi[1], Nasha Nassoury[1], Jennifer J. Hill[1,4], Sameer Zulfiqar[1], Ahmed Zafer[1], Qin Zhu[1], Tina Nguyen[1], Robert A. Pon[1], Risini D. Weeratna[1], Mehdi Arbabi-Ghahroudi[1,2], and *Scott McComb[1-4]

Affiliations:

1. Human Health Therapeutics Research Centre, National Research Council Canada, Ottawa, ON, Canada
2. Department of Biochemistry, Microbiology and Immunology, Faculty of Medicine, University of Ottawa, Ottawa, ON, Canada
3. Centre for Infection, Immunity, and Inflammation, University of Ottawa, Ottawa, ON, Canada
4. Ottawa Institute for Systems Biology, Ottawa ON Canada

*Correspondence: scott.mccomb@nrc-cnrc.gc.ca

3.1 - Abstract:

The development of chimeric antigen receptor T-cell (CAR-T) therapies typically involves a trial-and-error approach, with many candidate CARs failing to activate effective responses *in vitro* or *in vivo*. The complex structure-function relationship that makes CARs unpredictable is amplified when combining multiple CAR molecules; thus, we have established a platform approach to rapidly screen multi-antigen-targeted combinations (multiCAR), either in tandem or co-expression formats. High-throughput CAR-Jurkat assessment demonstrates functional responses against individual antigens similar to single-target CARs, with multi-antigen CAR signals dominated by the more potent CAR. Using this platform, we combine a sub-optimal mesothelin nanobody-based CAR (MSLN-VHH-CAR), which can slow but not eliminate human lung cancer in a xenograft model, with

a high-potency EGFR-VHH-CAR. When tested in primary CAR-T cells, both tandem and co-transduced EGFR/MSLN-CARs exhibited similar *in vitro* tumour suppression capabilities and higher antigen sensitivity than single target CARs. However, *in vivo,* co-transduction proved to be significantly more effective against H292 lung cancer xenografts compared to a tandem MSLN/EGFR-VHH-CAR. Ultimately, use of our multiCAR screening platform reveals that, as with single target CARs, *in vitro* screening of multi-antigen targeting CARs is a relatively poor predictor of *in vivo* efficacy. Furthermore, this work highlights the importance of considering multiCAR therapies as novel entities with unique emergent properties, which cannot be reliably predicted by the effects of single-target CARs.

3.2 - Introduction:

Chimeric antigen receptor (CAR) T cells have become a powerful treatment option for relapsed hematological malignancies, with more than seven therapies approved for the treatment of blood cancers by the US FDA, Health Canada, and other international health regulators by 2025. Current market approved therapies target CD19 and BCMA to combat relapsed B-cell lymphoma/leukemia and multiple myeloma, respectively [325]. CAR-T therapies have thus far shown limited effectiveness against solid tumours due to multiple challenges that include: the absence of safe tumour-specific targets, tumour-induced immunosuppression, antigen heterogeneity, antigen escape, and inadequate tumour infiltration of CAR-T cells, among others.

Given the challenges facing CAR-T therapies, it has been proposed that engineering CAR molecules that simultaneously target multiple antigens could improve efficacy through broadening the ability of CAR-T cells to recognize tumour antigens, mitigating both antigen

heterogeneity and antigen escape [326–329]. Two strategies used to achieve this are: (1) tandem CAR, wherein two separate antigen binding domains (ABDs) are combined in a single CAR molecule, and (2) multiCAR co-expression, wherein two separate CAR proteins are expressed on a single cell. MultiCAR co-expression can be achieved a single bi-cistronic gene construct or using co-transduction of T cells with two or more viral vectors expressing different CAR molecules. Clinical trial results for multi-antigen targeting CARs have shown some promise, with generally similar toxicity to single target CARs and high complete response, but clear advantage over single targeting CARs has not been consistently demonstrated [330–333].

The majority of commercially approved CAR therapies utilize single-chain variable fragment antibodies derived from conventional antibodies (scFvs), though a growing body of evidence shows that single domain antibodies (known as sdAbs, nanobodies, or VHHs) can also be used to create highly functional CAR molecules. VHHs, which do not contain a variable light chain, can be isolated from synthetic libraries or from natural heavy-chain only antibodies found in camelid species, such as llamas and camels [334]. The single gene structure of VHHs makes the process of genetic isolation, assembly, and testing of multiple CAR molecules quicker and more predictable than for scFvs [335]. Furthermore, the single molecular structure of VHHs is also thought to result in lower propensity for aggregation that could drive tonic signaling or other undesirable effects found in multi-scFv CAR molecules. Thus, we sought here to establish a screening platform through which we could further explore strategies to combine VHH-CARs targeting multiple antigens.

One cancer antigen that has been explored in CAR-T pre-clinical studies and clinical trials for solid tumour cancers is mesothelin (MSLN). MSLN is a glycosylphosphatidylinositol (GPI) anchored protein, which is typically expressed at a lower level and restricted to specific areas in healthy tissue [336–338]. MSLN becomes highly upregulated and non-localized in several solid tumour malignancies such as lung, ovarian, pancreatic, and triple negative breast cancer, among others [339]. MSLN-based CAR-T therapies have demonstrated some efficacy in clinical trials, though severe pulmonary toxicities have also occurred [246,340,341]. Similar to MSLN, epidermal growth factor receptor (EGFR) is another highly studied solid tumour target for CAR-T [342,343], including previous work wherein we explored the use of an anti EGFR-VHH domain as a CAR-T targeting moiety [153]. Here, we generated and tested multi-antigen targeting CAR-T cells that react to both EGFR and MSLN, a combination of antigens that is overexpressed in a wide range of malignancies such as lung, stomach and pancreatic cancers [286,344,345].

We report here the development of a screening platform for multi-antigen targeting CARs and exploring their functionality using *in vitro* and *in vivo* models. Specifically, we generate both tandem and co-transduced multi-antigen CAR-T cells that combine MSLN and EGFR VHH-based targeting elements. Similarly to our previous experience with single target CD22 VHH-CARs[201], *in vitro* screening with multi-antigen VHH-CARs revealed consistently strong antigen responses, but subtle molecular properties led to remarkably divergent outcomes in *in vivo* tests using a xenograft model of human lung cancer. Despite similar *in vitro* functionality, co-transduced EGFR/MSLN CAR-T cells significantly outperformed tandem CAR-T treatments *in vivo*. Overall, our findings underscore the unpredictable

nature of CAR molecules and further emphasize the importance of designing and optimizing multi-targeted CAR-T therapies as unique entities.

3.3- Results:

3.3.1 - Designing and cloning a multi-antigen-targeting CAR screening platform

We have previously reported the development of modularized CAR backbone plasmids that allow rapid recombination and screening of novel CAR molecules [346]. Here we wished to extend these methods and tools to facilitate the evaluation of multi-antigen targeting CARs (Supplemental Figure 1A). To this end, we developed modular CAR plasmids which incorporate different fluorescent markers: TagBFP, mKate2, or iRFP720, alongside our previous CAR plasmids incorporating NeonGreen fluorescent protein. These plasmids could allow for the assessment of up to four distinct CARs using flow cytometry, either individually or in combination (Supplementary Figure 2). Electroporation of a previously reported CD22-VHH-CAR [201], using either blue or green fluorescent protein (BFP or GFP) expressing CAR plasmids into Jurkat cells demonstrated independent expression of each reporter and expression of the dual reporters when co-electroporated. Notably, co-electroporation of CAR plasmids invariably resulted in coordinated expression of both plasmids (Figure 1A). As expected, CD22-CAR-Jurkat cells showed similar response to CD22+ target cells across all CAR plasmids (Figure 1B), as indicated by target cell dose dependent upregulation of the activation marker CD69 on CAR-Jurkat cells.

Next, we sought to confirm the multi-antigen responsiveness using an orthogonal antigen system that combines antigens not normally co-expressed on target cells. We thus selected two solid tumour targeting VHH-CARs (MSLN or EGFR) and two hematological

cancer targeting VHH-CARs (CD22-or BCMA). As predicted, single CAR electroporation resulted in selective responses against solid tumour cells (H292 lung cancer, EGFR+/MSLN+) or hematological tumour targets (Ramos lymphoma, CD22+/BCMA+) [Figure 1C], while co-electroporation resulted in consistent responses against both solid and hematological cancer targets (Figure 1D). Importantly, the magnitude of response between single and co-transduced CAR cells was maintained across orthogonal targets, with the relatively weakly reactive CD22-CAR showing similarly low responses in single or multi-target format. Collectively, this data shows that, we have established a platform that allows for many CAR variants to be rapidly generated and tested in multi-antigen targeting format.

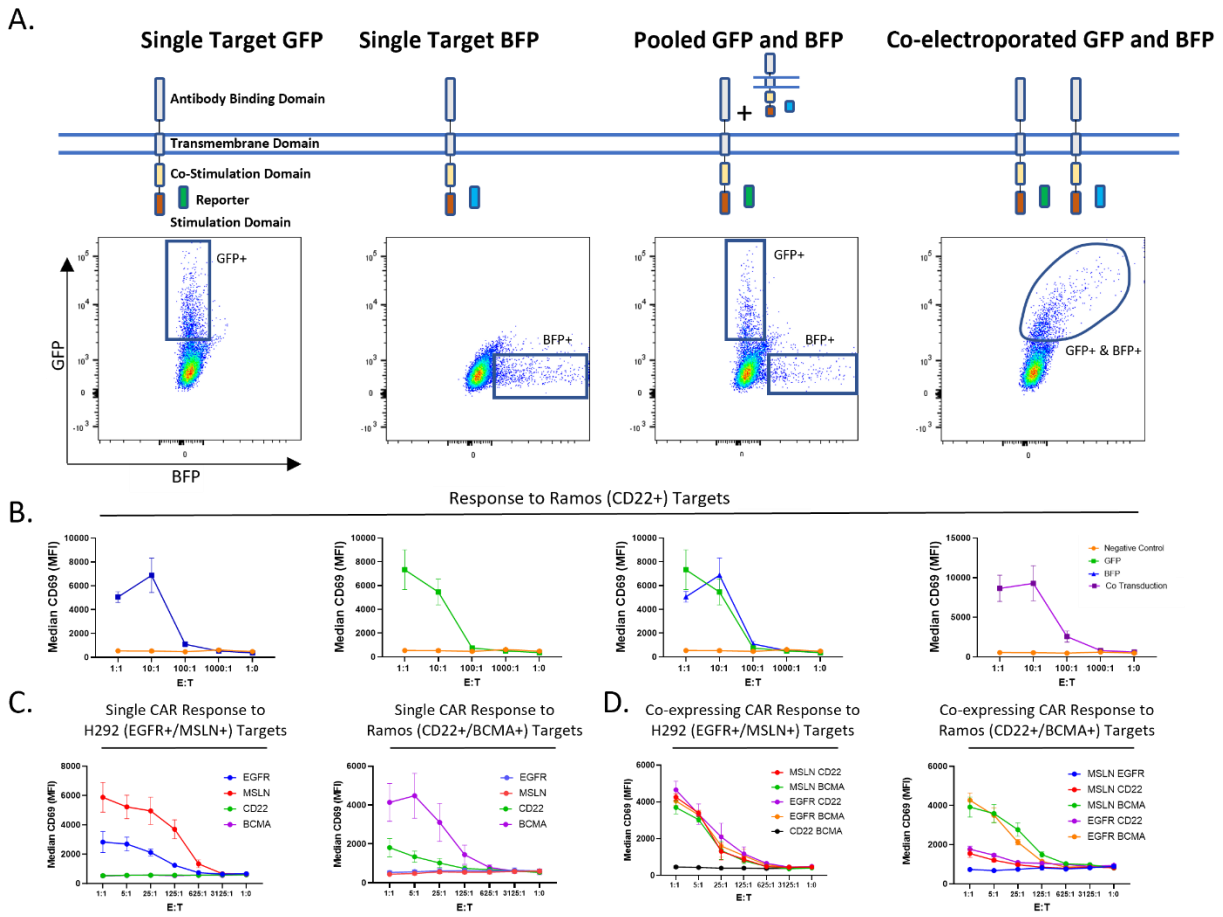

Figure 3.1. Co-expression of multi-coloured CAR plasmids demonstrates parallel response to multiple antigens

A. Multi-colour reporter combination flow cytometry assessment. Wild type Jurkats e6.1 cells were electroporated with 4µg of DNA encoding GFP, BFP or 2µg of both plasmids. After recovering for 4 hours, cells were assessed by flow cytometry. **B.** Multi-colour CAR-Jurkat functionality verified using a CAR-J assay. Jurkat wild type cells were electroporated with a previously reported CD22 CAR as shown above and co-cultured with Ramos Nuclight cells (CD22+) at 1:1 E:T as compared to unmodified control cells with the same targets. After overnight co-culture, cells were stained with anti-human CD69 and assessed via flow cytometry. **C and D.** Non naturally occurring combinations of CD22 or BCMA (Blood) and EGFR or MSLN (Solid tumor) were tested in various combinations. Jurkats were electroporated as described above then run in a CAR-J for 24 hours against either Ramos Nuclight (CD22+ and BCMA+) or H292 Nuclight (EGFR+ and MSLN+) target cells. After overnight co-culture, cells were stained with anti-human CD69 and assessed via flow cytometry. Graphs show CAR-Jurkat response without a secondary CAR **(C)** and with combined plasmids **(D)** when challenged with a single relevant antigen. Data presented as the median + SEM, n = 3.

3.3.2 - Incorporating Tandem CAR as an alternative strategy for multi-antigen targeting

While co-expression of multiple CARs is an apparently straightforward method to achieve multi-antigen targeting, combining multiple antigen targeting moieties in a single tandem CAR offers an alternative strategy, with the potential benefit of minimizing the molecular/cellular complexity by incorporating two binding elements in a single CAR molecule. Thus, we also wished to create a dual-modular tandem CAR plasmid that would allow rapid recombination of either of two antigen binding domains within a single tandem CAR plasmid (Supplemental Figure 1B). Using the same orthogonal solid/hematological CAR test system described above to test various tandem CAR formats, we found that tandem CARs did not entirely mirror the single target CARs. When compared to the single target CARs (Figure 2A), tandem CARs exhibited somewhat higher CD69 expression against both solid and hematological tumour targets (Figure 2B), though this was not true for every construct or every antigen target. These results indicate that tandem-CARs maintain responsiveness to multiple targets but can result in somewhat unpredictable changes in the magnitude of response for any given tandem CAR, which seemed mostly correlated with the higher response in the membrane distal binder.

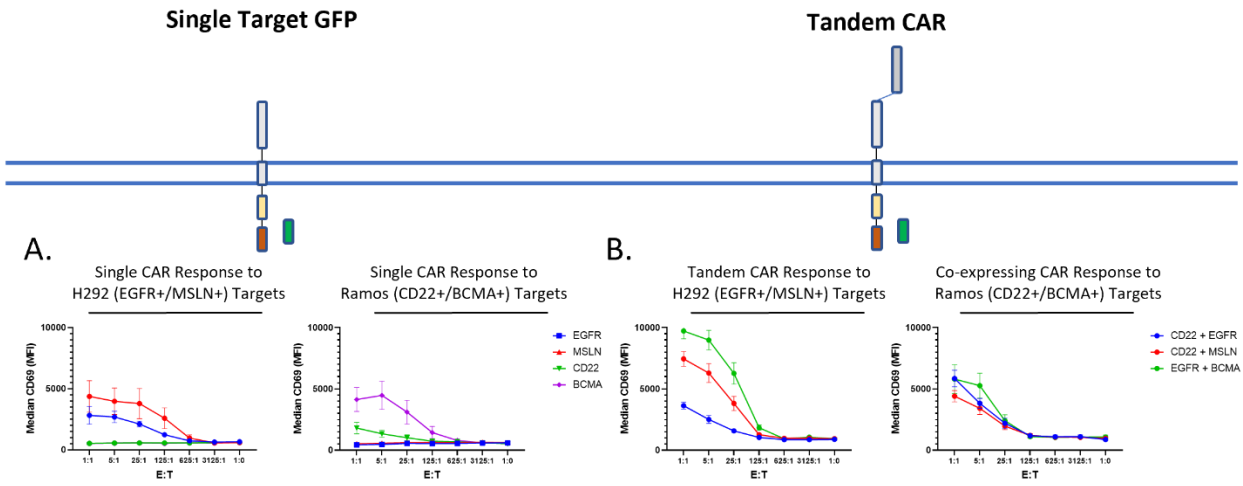

Figure 3.2. Tandem multi-CAR platform reveals unpredictable multi-antigen responses

Novel Tandem CAR plasmid tested using non naturally occurring combinations of CD22 or BCMA (Blood) and EGFR or MSLN (Solid tumor). Plasmids were electroporated into wild type Jurkat cells at 4µg of DNA per million cells and given 4 hours to rest. Post recovery the CAR-Jurkat cells were run in a CAR-J with a co-culture of Ramos Nuclight (CD22+ and BCMA+) or H292 Nuclight (EGFR+ and MSLN+) target cells in a 1/5 serial dilution starting at 1:1. After overnight co-culture, cells were stained with anti-human CD69 and assessed via flow cytometry. Graphs show CAR-Jurkat response without a secondary CAR and with using a tandem plasmid when challenged with a single relevant antigen. Data presented as the median + SEM, n = 3

3.3.3 - MSLN-sdCAR shows partial in vivo efficacy in single target format

To validate our multi-CAR development platforms, we next focused on biologically relevant antigen combinations for solid tumours. EGFR and MSLN are two targets that have been extensively explored in CAR-T pre-clinical development and clinical trials, with co-occurrence of these antigens in many tumour types. Recently, we performed an immunization campaign to identify a panel of llama-derived VHHs targeting MSLN [347]. Surface plasmon resonance (SPR) measurements of anti-MSLN VHHs binding to immobilized MLSN-extracellular ligand-binding domain (ECD) reveals equilibrium dissociation constants (K_Ds) ranging between 0.23 to 408 nM for human MSLN (Figure 3A). Next, the VHHs were cloned into a modular CAR backbone using single-pot restriction ligation as previously described[346], confirming their assembly via Sanger sequencing. Jurkat

cells expressing various MSLN-VHH-CARs were co-cultured with target cell lines with varying levels of MSLN expression: HT1080 (MSLN-neg), SKOV3 (MLSN-low), and H292 (MSLN-high) [Supplementary Figure 3], demonstrating both the functionality of these MSLN-VHH-CARs and low tonic signal/autoactivation (Figure 3B). This response was further characterized to demonstrate a dose-dependent CAR response using a serial dilution of H292 cells with a constant number of CAR-Jurkat cells. Overall, we identified three categories of MSLN-VHH-CARs: 4 strong responders, 1 medium responder, and 5 weak/negative responders (Figure 3C). Notably, none of the MSLN CARs showed signs of strong tonic signaling within Jurkat cells in the absence of target antigen.

To further evaluate CAR functionality, we selected a representative set of high, medium, and low responding MSLN-CARs for testing in primary T cells. Donor human T cells were isolated from whole blood, polyclonally activated, and transduced with a MSLN-VHH-CAR lentiviral vector. The resulting CAR-T cells were tested via long-term co-culture with repeated challenges using MSLN-high H292 lung cancer cells expressing mKate2, allowing continual monitoring of target cell growth through live fluorescence microscopy over 5 weeks. Both the medium and low responding CARs TP7-50 and TP7-49 showed minimal effect on H292 target cell growth (Figure 3D), while high responding CARs all showed relatively similar killing of H292 cells. We also examined the response against different target cells with varying MSLN and EGFR expression (Supplemental Figure 3), with TP7-56 standing out for an ability to eliminate MSLN-low MCF7 target cells after several target challenges (Supplemental Figure 4). None of the MSLN-CARs showed significant response

against MSLN-negative Raji or Ramos cells (Supplemental Figure 4). Overall, these results identify a number of potential candidates MSLN CARs with antigen specific activity.

MSLN-TP7-9, TP7-38 and TP7-56 VHH-CARs were selected for further *in vivo* testing alongside our previously reported highly potent EGFR-VHH-CAR [153]. Groups of 5 female NOD/SCID/IL2r-gamma-chain deficient (NSG) mice received a subcutaneous (SC) injection of $6x10^6$ H292 tumour cells, followed by intravenous treatment with 5×10^6 VHH-CAR T cells or an equivalent total number of untransduced (mock) T cells at day 15 post-tumour challenge. Of the MSLN targeting CARs tested, only MSLN-TP7-56-VHH-CAR achieved moderate tumour suppression with extended survival which was not statistically significant over groups receiving mock T cells (P=.25). As previously shown, EGFR1-VHH-CAR demonstrated highly potent tumour suppression with significant survival benefit over the groups receiving mock T cells (P=0.03) at the CAR-T dose tested (Figure 3E,F). The majority of non-treated mice and those treated with mock T cells reached humane endpoint by day 90. Mice treated with MSLN-TP7-56-VHH-CAR began reaching the humane endpoint around day 75 and continued to be sacrificed until the end of the experiment. By contrast, surviving EGFR-VHH-CAR T cell-treated mice showed no detectable tumour burden even at the end of the study (Figure 3E). Thus, despite potent *in vitro* activity, most MLSN-CARs showed no *in vivo* activity, with only MSLN-TP7-56-VHH-CAR having a modest therapeutic effect.

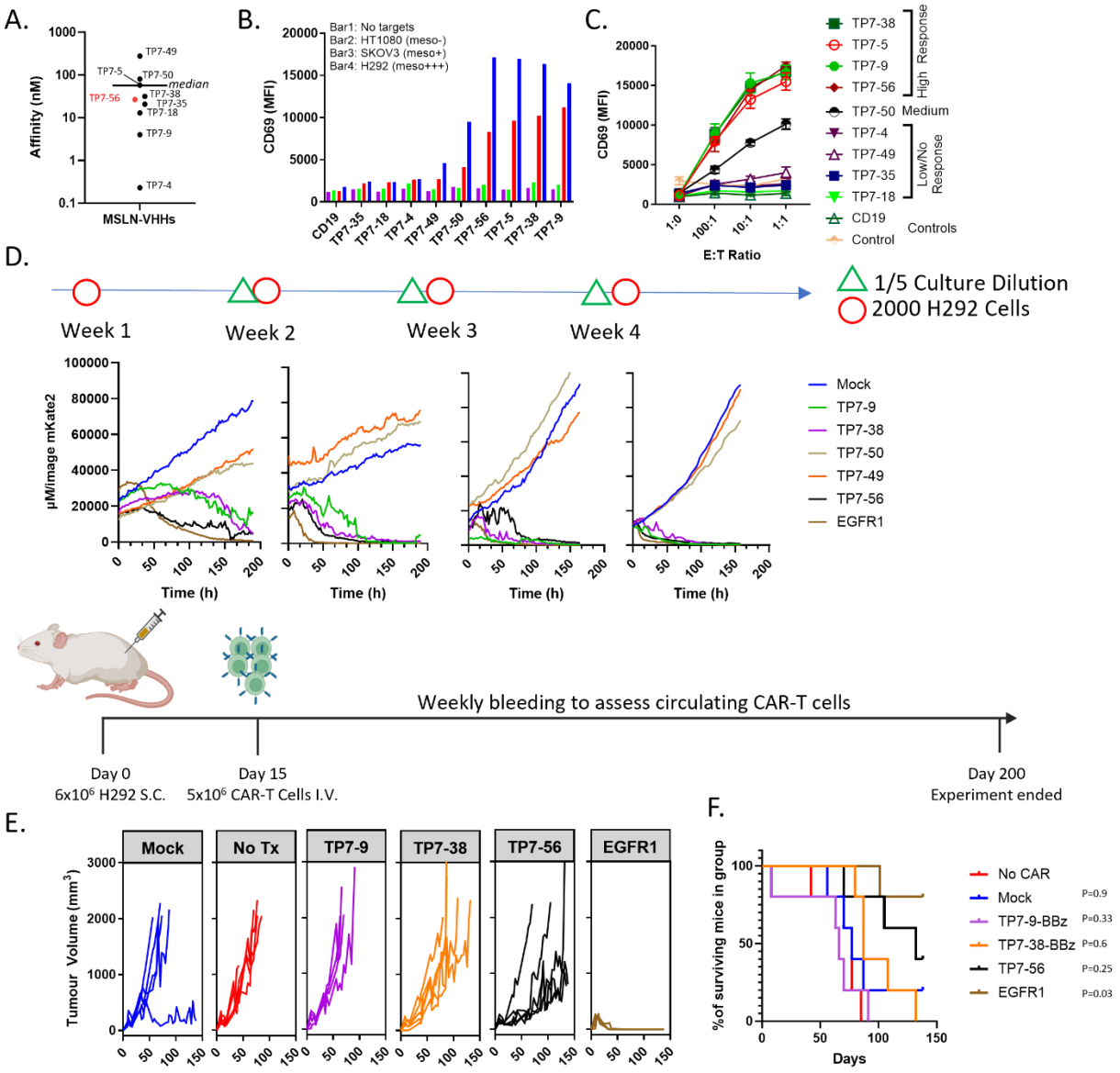

Figure 3.3. MSLN nanobody CARs show long term tumor control in vitro, moderate tumor suppression in vivo

A. Affinities of the MSLN-VHH binders. Affinity of the lead MSLN TP7-56 highlighted in red. **B and C.** MSLN sdAbs were transferred directly from phagemid-VHH vectors into pSLCAR screening backbone via PCR and tested for CAR-Jurkat assay. Resultant MSLN-sdAb CAR proteins were run in a CAR-J assay by electroporating 2-4µg of DNA into Jurkat cells and were allowed to rest for 4 hours. Post recovery CAR-Jurkat cells were co-cultured for 24 hours against HT1080 (MSLN-), SKOV3(MSLN low) and H292 (MSLN High) cells lines **(B)**, or a 1/10 serial dilution of H292 (MSLN High) target cells **(C)**. Post co-culture cells were stained with anti-human CD69 assessed via flow cytometry. Graphs reported as mean+SEM, n=3. **D.** *In vitro* killing efficacy assessment via Incucyte live imagine system. Donor primary CAR-T cells at Day 9 were thawed and allowed to recover for 16 hours before being co-cultured 5:1 with H292-Nuclight cells. Killing was assessed through

reduction in %red area (tumor cells) over the course of the initial challenge and three subsequent rechallenges. Each rechallenge was accompanied by a 1 in 5 split. **E and F.** NSG Mice were given a subcutaneous injection of H292- Nuclight cells, which were allowed to develop over the course of 15 days. Once the tumor was established and developed(~15 days), aliquots containing ~5M CAR-T cells (approximately 15-20M total T cells) or equivalent Mock T cells were thawed, then injected intravenously through the tail vein. Tumor volume was assessed weekly using calipers. Mice were monitored and sacrificed if they reached pre-determined humane endpoints. P values show log-rank test for Kaplan Meier survival curve comparison with untreated (No CAR) group (n = 5 mice/group).

3.3.4 - Creation of EGFR and MSLN Tandem or Co-transduced CARs and confirmation of response to both targets

Although MSLN-TP7-56-VHH-CAR was inferior to EGFR1-VHH-CAR in this model, we wished to test whether a multi-CAR targeting strategy might further improve both CARs. We generated lentiviral vectors encoding EGFR or MSLN single target CARs, or tandem CAR molecules combining EGFR and MSLN binders in two orientations (Supplemental Figure 1C and D). We then generated Jurkat cells with stable expression of EGFR, MSLN, co-transduction with both EGFR and MSLN-CARs, or two tandem EGFR/MSLN CARs; CAR-Jurkat cells were sorted to ensure uniform expression of MSLN, EGFR, tandem-EGFR/MSLN, or both MSLN and EGFR CARs (co-transduced). Testing CAR-Jurkat response to H292 target cells, a target that expresses both MSLN and EGFR at a high level (Figure 4A-B), resulted in responses for all EGFR/MSLN CAR combinations. Given its similar response of EGFR-MSLN or MSLN-EGFR tandem-CARs, MSLN-EGFR-VHH-CAR was selected for further testing described below.

To verify the relative responses of the tandem and co-transduced MSLN/EGFR-VHH-CARs against individual target proteins, we developed an artificial system with exclusive MSLN or EGFR expression. HEK293T cells, which are normally devoid of these targets, were transfected using a piggyback plasmid to express either EGFR or MSLN on their surface and sorted for ensure uniform expression (Figure 4C,D) In a dose response CAR-J assay, tandem MSLN-EGFR-VHH-CAR and co-transduced MSLN/EGFR-VHH-CAR demonstrated similar levels of activation to EGFR or MSLN single target CARS when combined with the HEK293-

EGFR or HEK293-MSLN target lines respectively (Figure 4E). Importantly, single target EGFR or MSLN CARs showed no response to the opposite target, similar to a BCMA-CAR which was used as an irrelevant target control. Collectively, these results confirm that that both antigen binding domains maintain capacity to signal independently with one or both of the antigens present.

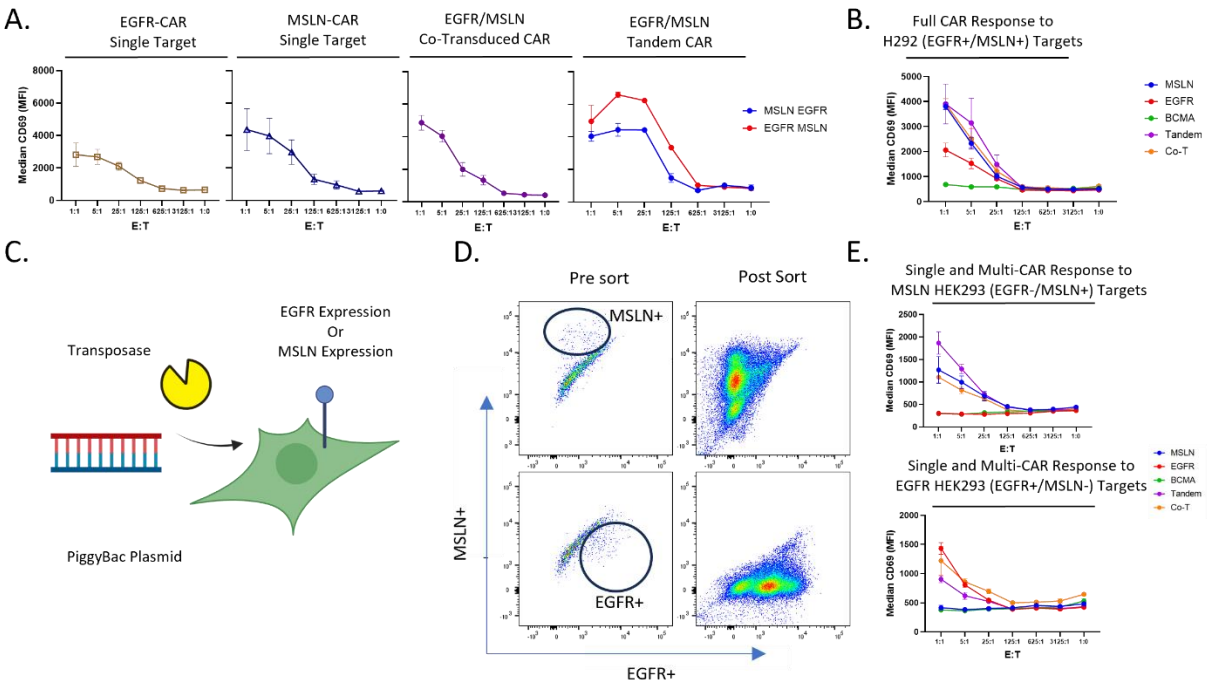

Figure 3.4. EGFR/MSLN Multi-CARs Maintain Single-target response

A and B. Solid tumor relevant combination of MSLN and EGFR tested in both Co-Transduced and Tandem formats. Jurkat Wild Type cells were electroporated using 4µg of MSLN, EGFR or both orientation MSLN/EGFR Tandem CAR, or 2µg of both MSLN and EGFR CAR plasmids and allowed for recover for 4 hours. Post recovery a CAR-J assay was run using a co-culture of H292 cells (MSLN+ and EGFR+) using a 1/5 serial dilution. After 24 hours in co-culture, cells were stained with anti-human CD69 and assessed via flow cytometry. Graphs display individual results of both single target and multi-targeting CARs **(A)** or overlays to show the comparative effect **(B)** using a BCMA targeting CAR as a negative control. **C and D.** Outline of the process of creating single target antigen HEK392T cells. HEK293T cells were transfected using a combination of either EGFR or MSLN surface expression encoding piggybac plasmid alongside a transposase. **(C)** Cells were cultured and assessed every 2-3 days for stable antigen expression. Once stable expression of MSLN or EGFR on the cell surface of HEK293T was confirmed, cells were sorted for expression of the chosen antigen **(D)** and cultured to ensure continued expression. **E.** Assessment of relevant combination with only a single target present. Jurkat Wild Type cells were electroporated as shown above and co-cultured with either EGFR+ or MSLN+ modified HEK293T cells overnight. Cells were then stained with anti-human CD69 and assessed via flow cytometry. Graphs show CAR-Jurkat response to either EGFR+/MLSN- or EGFR-/MSLN+ cells confirming functionality of individual binders. Results presented as median + SEM, n=3.

3.3.5 - Primary CAR-T cell cytotoxic response demonstrates higher antigen sensitivity in multi-targeting formats

Having confirmed single and multi-antigen EGFR/MSLN CAR functionality, we next tested these constructs using human primary T cells *in vitro*. As above, CAR-T cells were derived from healthy donor PBMCs, allowed to expand for 9 days and cryopreserved. Single or multi-targeting MSLN/EGFR CAR-T cells were then tested in long-term co-culture assay using target cells exhibiting varying levels of EGFR and MSLN antigens (Supplemental Figure 3). As described for MSLN single target experiments above, co-cultures were split 1:5 and rechallenged with fresh targets at day 7 and examined for an additional 7 days. All single target and combination EGFR/MSLN CAR-T cells successfully supressed MLSN-high/EGFR-high H292 cells (Figure 5). Focusing on responses to MSLN-low/EGFR-med SKOV-3 and MSLN-low/EGFR-low MCF-7, we observed reduced responses with single targets, but both co-transduced and tandem EGFR/MSLN CARs showed more potent restriction of target cell growth. Despite the increased antigen sensitivity, co-transduced and tandem MSLN/EGFR-VHH-CARs did not exhibit any off-target response towards MSLN-neg/EGFR-neg Ramos lymphoma cells.

Overall, this *in vitro* data suggests that both co-transduction and tandem MSLN/EGFR-VHH-CAR enhance sensitivity to targets with low antigen expression, without any increase in non-specific activity against irrelevant targets.

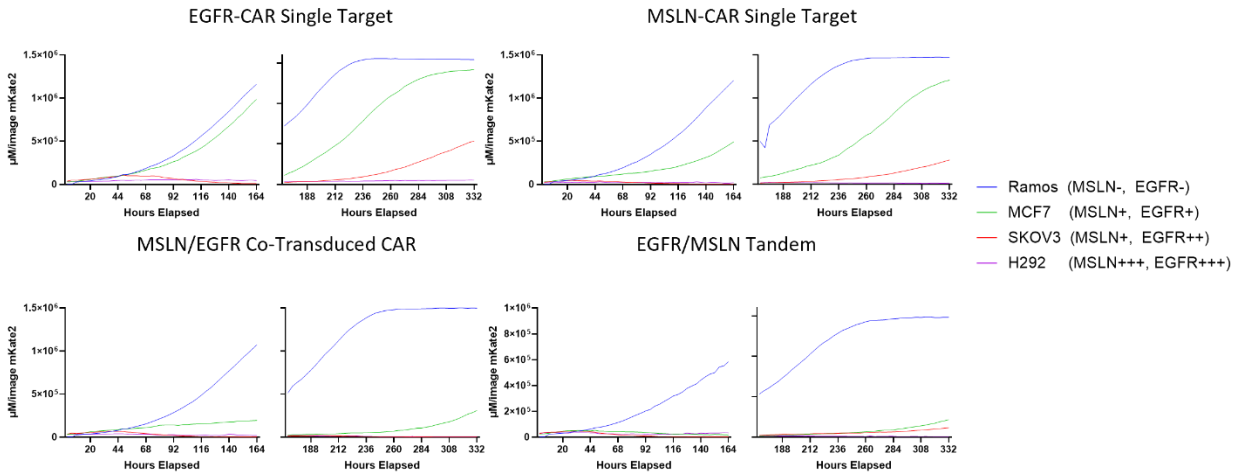

Figure 3.5. In vitro testing shows effective tumor cytotoxicity

In vitro killing efficacy assessment via Incucyte live imagine system. Donor Primary CAR-T cells at Day 9 were thawed and allowed to recover for 16 hours. CAR-T cells were then placed in low-density culture (1:5) with IL-7/IL-15 supplementation and examined for red fluorescent target cell growth (%red area) over the course of the initial challenge and subsequent rechallenge. Each rechallenge was accompanied by a 1 in 5 split. Each graph presents the mean of 2 duplicate wells from a single experiment.

3.3.6 - Co-transduced MSLN/EGFR-VHH-CAR exhibits sustained, long-term efficacy in NSG mice

Although there is an expanding array of *in vitro* assays to evaluate CAR-T activity, xenograft mouse models continue to be vital for assessing the therapeutic efficacy of CAR-T cells in the context of a living animal. As previously, female NSG mice were injected S.C. with $6x10^6$ H292 tumour cells and allowed 15 days for tumour engraftment. Mice were then treated intravenously with a high dose ($5x10^6$) of CAR-T cells expressing either single target, co-transduced (unsorted) or tandem MSLN/EGFR VHH-CARs. Control mice (untreated/vehicle) exhibited consistent tumour growth, reaching the humane endpoint (>2000mm^3) as early as day 76. Mice treated with CAR-T cells demonstrated anticipated tumour suppression, consistent with prior testing (Figure 6A-C). As before, single-target EGFR VHH-CAR-T cell treated mice displayed significantly lower tumour growth and

improved survival compared to MSLN- VHH-CAR -T cell-treated mice (Figure 6A-C), though we note reduced activity with EGFR-CARs from this donor compared to previous experiment. There was no significant difference between single target MSLN CAR and tandem MSLN/EGFR VHH-CAR, nor did they have a significant impact on mice survival or tumour burden when compared to vehicle control (Figure 6B-C). In contrast, co-transduced MSLN/EGFR VHH-CAR-T treated mice achieved near complete and immediate control of tumour growth, with a significant improvement in survival relative to untreated control mice (Figure 6C). While neither day 76 tumour burden, nor survival was statistically significantly higher for co-transduced EGFR/MSLN relative to EGFR single target, two mice showed late emergence of tumours with EGFR CAR-T treatment, but no such tumours were seen with the EGFR/MSLN co-transduced group (Figure 6A-C).

To evaluate the response of the multi-targeting CARs under more strenuous conditions, the trial was repeated with a reduced dose of CAR-T cells (1×10^6 CAR-T cells) [Figure 6D-F], resulting in a much-diminished response for all CAR constructs. However, co-transduced EGFR/MSLN VHH-CAR-T treated mice demonstrated a significant delay in tumour growth from untreated, with 100% survival over 200 days, and one mouse showing complete tumour eradication (Figure 6D). Despite apparent benefit, statistical divergence between EGFR single target and EGFR/MSLN co-transduced CAR-T treatment was not significant for either tumour burden or survival (Figure 6D-F).

To better understand the nature of different CAR-T treatments we also examined circulating T and CAR-T cells in the blood throughout the high ($5x10^6$) and low ($1x10^6$) dose VHH-CAR-T treatment experiments. In low dose CAR-T treated mice, too few cells were recorded

consistently for useful evaluation and thus could not be analyzed. In mice that received a high dose, we note significantly fewer overall human CD45+ circulating T cells in mice treated with EGFR-CAR than MSLN-CAR (Figure 6G and Supplemental Figure 5A). Tandem and Co-transduced CAR treated mice showed higher numbers of circulating T cells, similar to MSLN CAR-T. Restricting our analysis to circulating human-CD45+ cells with positive staining for VHH-CAR, we see similar results, albeit with lower statistical significance (Figure 6H and Supplemental Figure 5B). This difference in expansion can also be seen when examining reporter fluorescence, which confirms the presence of both MSLN-GFP and EGFR-BFP CAR-T cells (Supplemental Figure 5C). Despite differences observed in T cell and VHH-CAR-T cell numbers, minimal variation was observed in CAR-T cell differentiation or CD8/CD4 cell ratios across groups on day 61, which marked the highest cell expansion (Supplemental Figure 5D and E). Overall, our findings show that co-transduction results in a superior response compared to single-target MSLN VHH-CAR or tandem MSLN/EGFR VHH-CAR-T, and is associated with higher CAR expansion than EGFR-CAR-T cells in this model of human lung cancer treatment.

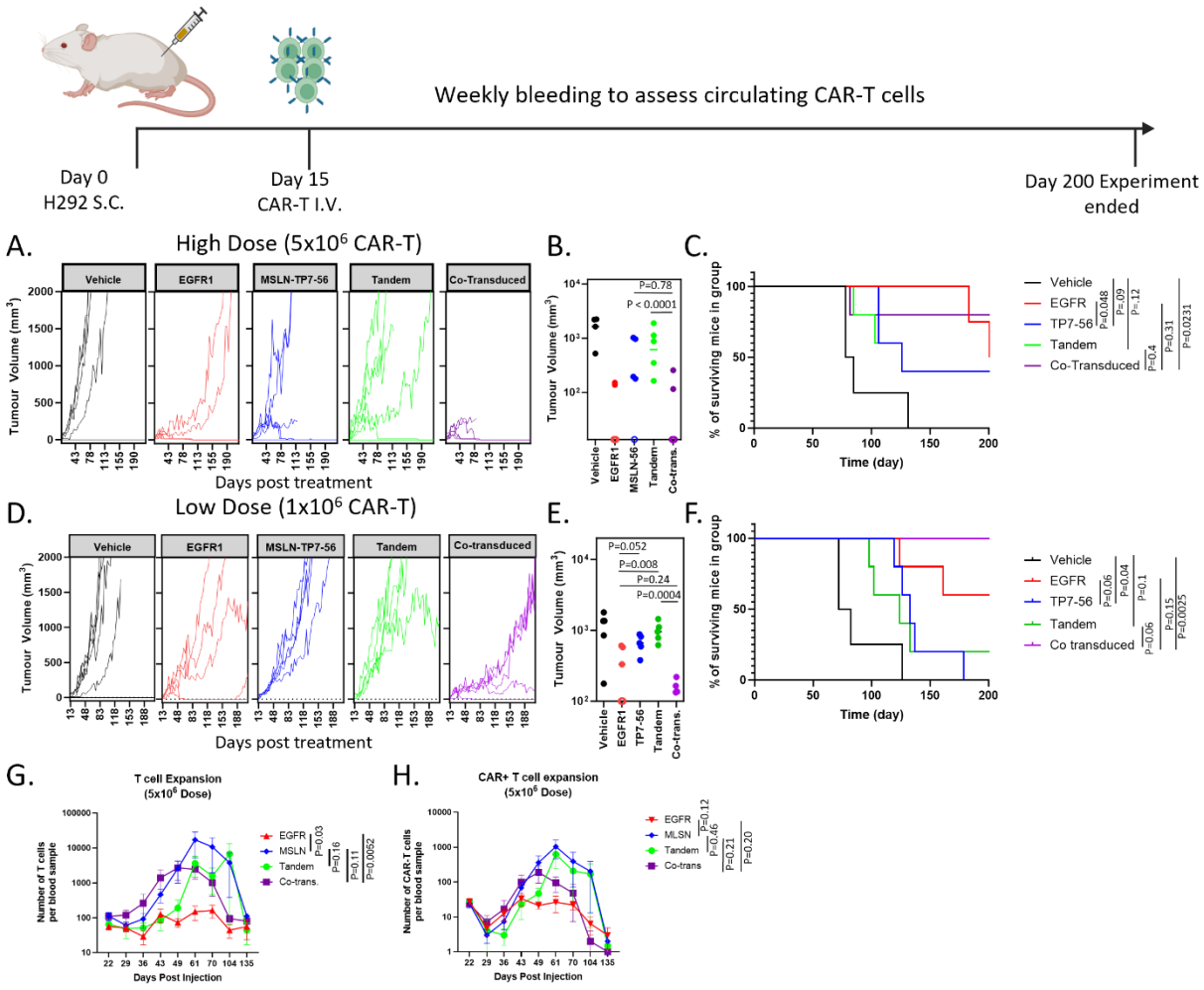

Figure 3.6. NSG in vivo testing demonstrates durable long-term response from co-transduced CAR-T at low dose

Assay performed on Female NOD/SCID/IL2r-gamma-chain^{null} (NSG) mice in groups of 5. Mice were given a subcutaneous dose of 6×10^6 H292 tumor cells. Once the tumor was established (~15 days) 5×10^6 CAR-T Cells (High dose), 1×10^6 CAR-T cells (Low dose) or vehicle control were delivered via IV injection into the tail vein after being thawed. Mouse tumor burden was assessed daily **(A and D),** with the last with all mice alive in each group being day 76 **(B)** and day 79 **(E)** respectively. P values show differences between tumor mass using Student's t test. Mice were euthanized at tumour burden >2000 mm^3, weight loss >20%, or if mice displayed severe signs of distress or discomfort during regular monitoring as per the NRC-HHT Institutional Animal Care Committee protocol. P values show log-rank test for Kaplan Meier survival curve **(C and F).** Circulating blood cells were assessed weekly through cheek bleeds and tumor volume through callipers. Circulating blood cell analysis through FACS included investigation of total circulating T cells. **(G)** and total circulating CAR-T cells **(H)** for high dose. Low dose FACS analysis was performed but showed insufficient cells for analysis. P values show comparisons between curves using 2-way ANOVA.

3.4 - Discussion:

Despite being synthetically engineered, the inherent complexity of T cells means that the biology of novel CAR-T cells is not completely understood or entirely predictable. Here we developed an efficient platform to quickly combine and screen multi-antigen targeting combinations in Jurkat cells, allowing functional validation of antigenic response before committing to the more intensive process of lentiviral vector production and testing in primary human T cells. Use of this platform allowed us to combine single target CARs targeting MSLN and EGFR, two antigens often co-expressed on solid tumours, in both co-transduced and tandem multi-CAR formats. Our results show that MSLN-TP7-56-VHH-CAR could be effectively combined with an EGFR-CAR to create a multiantigen CAR which maintains response to both targets; more specifically demonstrating that co-transduction of an EGFR/MSLN CAR-T led to slower tumour growth and longer survival than a tandem EGFR/MSLN CAR strategy in an *in vivo* model of human lung cancer cells with high expression of both targets. The successful establishment of a multiCAR screening platform could lead to further CAR optimization and development of logic gating CARs, allowing for engineered AND gated CARS (requiring both signals to activate) to reduce the risk of toxicity from these or other binders, or NOT gating (one binder inhibits signal if bound) to prevent potential off tumour toxicities [348].

While our results highlighted the effectiveness of co-transduced CAR-T cells relative to a tandem multi-antigen CAR strategy, we believe this result should not be generalized to other CAR combinations. Indeed, previous research has shown that tandem CARs can be

effective in some cases. For example, a study by Qin et al using a CD19xCD20 multi-antigen CAR showed the inverse of our observations here, with the tandem CAR outperforming a co-transduced CAR-T of the same combination [227]. Several other preclinical studies have also shown that the tandem CAR format does not negatively impact performance *in vivo* and can mitigate antigen loss in xenograft mouse models of hematological malignancies [235,236,349–351]. Furthermore, others showed increased proliferation from tandem CAR-T when exposed to either antigen in blood cancers [350,352], and for solid tumour models *in vitro* [329,353,354]. Despite this wealth of positive data supporting tandem CAR approaches, there is also evidence of potential deleterious effects in some tandem CARs. For example, it was reported that compromised downstream signaling and binding for a tandem-CAR reduced CD3ζ phosphorylation and subsequent T cell signaling [349]. Like other multiCAR strategies, tandem CAR appears to also perform well in clinical trials, with several studies reporting high objective response rates in multiple myeloma, acute lymphoblastic leukemia and non-Hodgkins lymphoma patients, though not necessarily demonstrating clear superiority over single target CARs [355–359].

Co-transduced CAR-T has also been tested in various clinical trials with similar response rates as seen in single target CAR-T [226,360], though few if any have made direct clinical comparison between single and multi-target CARs. Interestingly, co-transduction should by design reduce the risk of antigen-loss following CAR-T treatment but this does not seem to lead to better overall response rates[226,361], suggesting that the beneficial effects of co-transduction fail to address the central causes of CAR-T treatment failure. A third strategy for multi-antigen CAR based on multi-cistronic expression of multiple CARs within a single

vector was not tested in our work presented here; though this strategy has been tested in pre-clinical research and clinical trials [362,363]. Overall, clinical data to date does seem to provide adequate support to indicate that a combination of two effective single antigen will necessarily result in a superior multi-antigen CAR-T therapeutic, regardless of the molecular strategy employed.

Having tested many VHH-CARs targeting several different antigens, we were interested in utilizing our *in vitro* multi-CAR screening platforms to better understand how combinatorial CARs might impact the response profile of different CARs. Our orthogonal antigen testing system, allowed us to confirm that co-expression of multiple CARs led to similar antigen response to that seen with single CAR expression. In contrast, we find that tandem format seems to lead to altered CAR responses relative to single target CARs, with somewhat less predictable effects than the simpler strategy of co-expression through co-transduction. We speculate that this change in response magnitude may be due to better antigen access for the more distal of the tandem antigen binding domains, a result which mirrors the data seen in our previous work studying the role of spacer/linker design in the same EGFR-VHH CAR studied here [153]. Previous work from others with a tandem HER2/IL13Rα2 CAR proposed a similar explanation of differential antigen responses [364]. Given our observations here, we feel that similar to single target CARs, discovery and development of multi-targeting CARs must also be tackled empirically, as each multi-CAR represents a unique therapeutic entity whose *in vitro* or *in vivo* response properties cannot yet be adequately predicted.

While our *in vivo* data demonstrates superiority of co-transduced over tandem format for EGFR/MSLN CAR, the mechanism underlying this effect remains unclear. Given that both MSLN-single target and MSLN-tandem CARs showed dramatically higher T cell and CAR-T expansion relative to EGFR single target CARs in our *in vivo* studies, we hypothesize that the particular MSLN-CAR molecule (TP7-56) employed here may induce T cell signaling that favours cellular expansion over functional cytolytic activity. This result somewhat mirrors what was reported for at least one clinical trial examining MSLN CAR-T, wherein clear expansion of MSLN based CAR-T cells was shown despite minimal effect on disease progression[340,341]. MSLN-based CARs have also been shown to have poor persistence in other trials[340,365], potentially indicating that the nature of the MSLN antigen might somehow impact CAR-T fitness. Conversely to MSLN CAR-T, we noted remarkably few circulating single-target EGFR T cells and CAR-T cells, despite high overall efficacy, possibly due to a lack of proliferation. Similar to MSLN CAR-T, tandem MSLN/EGFR CAR resulted in higher expansion and poor tumour control, with co-transduced MSLN/EGFR CAR CAR-T showing an apparent intermediate phenotype of medium expansion and good tumour control. Thus, we hypothesize that the variable responses possible with a co-transduced mixture of MSLN and EGFR CARs may result in a favourable mixture of proliferation and cytolytic response, unlike tandem EGFR/MSLN CAR wherein cells would by nature embody a single response type.

Finally, our data also adds to a long and growing list of scFv and VHH-based CARs which we and others have tested using *in vitro* and *in vivo* models [153,201]. We find that both Jurkat cell screening and primary T cell data indicated similar capacity for these molecules to repress

target cells over multiple weeks *in vitro*, despite the significant differences we later observed *in vivo*. This result mirrors our findings with CD22-CAR-Ts wherein we observed only subtle differences in *in vitro* responses and dramatically divergent *in vivo* functionality [201]. While the list of *in vitro* characterization assays for novel CAR molecules continues to expand, beyond confirming antigen-specific reactivity and assessing tonic signaling, these methods appear to be of limited predictive value for *in vivo* testing, emphasising a clear need for improved CAR screening methods.

3.5 - Methods and Material:

3.5.1 SPR binding

SPR assays were used to determine anti-MSLN VHH kinetics and, affinities. Before SPR, all VHHs were size exclusion chromatography (SEC) purified using a Superdex 75 Increase 10/300 GL column (Cytiva, Vancouver, Canada) in HBS-EP running buffer (10 mM HEPES, 150 mM NaCl, 3 mM EDTA, 0.005% Tween 20, pH 7.4) at a flow rate of 0.8 mL/min and 500 µL fractions collected. SPR experiments were performed on a Biacore T200 (Cytiva) at 25°C using Series S CM5 sensor chips (Cytiva). Recombinant human MSLN (R&D Systems, Minneapolis, MN, Cat: 3265-MS) was amine-coupled in 10 mM acetate buffer, pH 4 (Cytiva), resulting in ~370 resonance units (RUs) immobilized with a theoretical maximum binding response (R_{max}theo) of 168 RUs. VHHs were injected (40 µL/min) at various concentration ranges (0.625 – 10 nM to 125 – 2000 nM, depending on the VHH) for 180 s of contact time followed by 180 s of dissociation time. Human MSLN surfaces were regenerated with a 30 s pulse of 10 mM glycine, pH 1.5, at 100 µL/min. Binding responses from an ethanolamine-blocked reference flow cell were subtracted and single-cycle

kinetics sensorgrams fit to a 1:1 interaction model using BIAevaluation Software v3.2 (Cytiva), in order to calculate k_a, k_d and K_D.

3.5.2 Multi-CAR Cloning

New reporter and tandem CAR sequences were cloned into a modularized CAR backbone with the design based on all human structural domains combined with llama-derived VHHs. The specific structure was as follows: [CD28 signal peptide]-[VHH]-[(G4S)3linker]-[CD8hinge domain]-[CD28 transmembrane domain]-[41BB-signaling domain]-[CD3z signaling domain]-[P2A]-[NeonGreen Fluorescent Protein], similarly as first reported by Bloemberg et al.[346] To clone the multicolour plasmid library DNA sequences containing each new reporter were obtained from Twist Bioscience (California, USA). For multicolour CAR screening plasmids, the original plasmid was digested to remove the original NeonGreen reporter, then the new fluorescent reporter genes were added using Gibson cloning as described in the text. To clone the tandem CAR, the original plasmid was digested to remove the original CAR binding sequence, then a DNA fragment containing two distinct type II restriction enzyme cassettes (Esp3I or BpiI) for each CAR, as well as a small G4S linker between the two modularized binders, was added using Gibson cloning. Plasmids were then miniprepped to isolate purified BFP, mKate2 and iRFP720 plasmids, or the new modular tandem plasmid and the sequences were confirmed using sanger sequencing.

3.5.3 CAR-J assay

High-throughput assessments of CAR function were performed by the CAR-Jurkat assay according to our previous report [346]. Briefly, WT Jurkat cells were incubated at RT with either 4μg of a single lentiviral CAR plasmid (pSLCAR) or 2μg of multiple pSLCAR plasmids, or with no plasmid control in Immunocult-XF T Cell Expansion Medium (STEMCELL Technologies). Cells and plasmid DNA in solution were transferred into 0.2cm electroporation cuvettes (Bio-Rad Gene Pulser; Bio-Rad) and electroporated using the Nepagene Super Electroporator NEPA21 with the following settings: 2 poring pulses of 175 V, pulse length 5, interval 50, decay rate 10, and polarity positive; followed by 5 transfer pulses of 20 V, pulse length 50, interval 50, decay rate 40, polarity +/−. Cells were then immediately transfer to prewarmed recovery media (RPMI containing 20% FBS, and 2 mM L-glutamine) and allowed to recover for 1 to 4 hours before co-culturing with various targets at varying effector to target ratios, as specified in text. Electroporated Jurkat cells were mixed with varying numbers of target cells in round-bottom 96-well plates in varying effector-to-target (E:T) ratios as specified in each figure. Co-cultured cells were incubated overnight at 37°C, 5% CO_2 before being stained with allophycocyanin (APC)-conjugated anti-human-CD69 antibody (BD Biosciences). Flow cytometry acquisition was performed using a BD LSRFortessa™ (BD Biosciences), and data were analyzed using FlowJo software and visualized using GraphPad Prism software.

3.5.4 Cell Lines and Cell Culture

All of the cell lines were monitored regularly for mycoplasma contamination using an in-house PCR assay [312]. In preparation for the cell assays, healthy cultures of Jurkat E6-1 cells (catalog no. TIB-152, American Type Culture Collection [ATCC]#) were maintained in RPMI complete (RPMI 1640 supplemented with 10% fetal bovine serum (FBS), 2 mM L-glutamine, and 100U/mL penicillin and 100 µg/mL streptomycin). All of the target cell lines described in this paper were modified using Nuclight Red Lentivirus Puro (catalog no. 4625, Sartorius) to generate stable red fluorescent cells, so that they can be easily differentiated from effector cells in flow cytometry or live microscopy analyses. Specific target lines used were as follows: Ramos (catalog no. CRL-1596, ATCC), SK-OV-3 (catalog no. HTB-77, ATCC), MCF-7 (catalog no. HTB-22, ATCC), H292 (catalog no. CRL-5878, ATCC) and HT-1080 (catalog no. CCL-121, ATCC). Target cell lines were cultured in varying media conditions, as recommended by the ATCC cell repository. Co-cultures were always performed in appropriate T cell supportive media conditions.

3.5.5 Creation of EGFR and MSLN expressing HEK293T

HEK293T (Clone 17; ATCC) were plated in a tissue culture-treated plate prior to transfection. After cell adherence, the media was replaced with DMEM with no additives. A transfection mix of 9µg of linearized polyethyleneimine (PEI) per 4µg of DNA (2ug of piggyBac plasmid and 2µg of transposase) was added to HEPES buffer was prepared and allowed to incubate at room temperature for 20 minutes before addition to the cells. Cells were incubated with the transfection mix for 4-6 hours at 37˚C, before the media was replaced with DMEM complete (DMEM supplemented with 10% FBS, 2 mM L-glutamine,

and 100U/mL penicillin and 100 µg/mL streptomycin) for 24 hours. Cells were stained with Fluorescein isothiocyanate (FITC)-anti-human EGFR and Phycoerythrin (PE) anti-human MSLN and accessed for EGFR and MSLN surface expression by flow cytometry. Once confirmed to be present, EGFR and MLSN were assessed over 3 weeks to ensure expression was stable. MSLN or EGFR expressing cells were selected via cell sorting using the Sony MA900 Multi-Application Cell Sorter. (Sony Biotechnology)

3.5.6 Lentivirus Production

All lentiviruses were produced using the 293SF-PAC-LV-IIIb-3D4 packaging cell line [366]. Briefly, the packaging cells were transfected with a mixture of PEI and the required plasmids. Four hours post-transfection, cumate and coumermycin were added to induce the production of lentiviral elements. The following day, the cells were concentrated fourfold in medium containing cumate, coumermycin, and sodium butyrate. Three days post-transfection, the culture supernatant was collected, concentrated approximately 600-fold by ultracentrifugation, and titrated using a gene transfer assay in permissive cells with flow cytometry-based readout.

3.5.7 CAR-T cell production

Primary human T cells were isolated from whole blood obtained from healthy human volunteers under informed consent and approval through the Ottawa Hospital Research Institute Research Ethics Board. In brief, T cells were isolated from peripheral blood mononuclear cells (PBMCs) freshly isolated from healthy blood donors via negative

magnetic selection. The T cells were activated with MACS GMP TransAct CD/CD28 beads (Miltenyi Biotec) and cultured in Stemcell Technologies ImmunoCult™-XF T Cell Expansion Medium supplemented with 20U IL-2 (Proleukin, Norvartis). Activated T cells were transduced with CAR-GFP and/or CAR-BFP lentiviral vectors, 24h post-stimulation and expanded with strict maintenance of cell concentrations below $5x10^5$ cells/mL. All cell counting were performed using Cellometer Auto 2000 Cell Viability Counter (Nexcelom) to assess live/dead counts using acridine orange (AO)/propidium iodide (PI) staining. Efficiency of transduction was assessed at day 7 by flow cytometry and at day 10 the CAR-T cells were used for assays. Mock T cells underwent the same treatment as CAR-transduced T cells, skipping only addition of lentivirus step. Cell acquisition was performed using BD® LSR-Fortessa™. Post-acquisition analysis was performed using FlowJo software.

3.5.8 Continuous live-cell imaging co-culture assay

Short-term killing response of CAR-T cells was assayed using a Sartorius Incucyte® S3. Tumour target cells were resuspended in Stemcell Technologies ImmunoCult™-XF T Cell Expansion Medium supplemented with 20 U/mL human IL-2 and plated in a flat-bottom tissue culture-treated plate. CAR-T cells or control T cells were revived 24 hours prior the assay start and cultured in Stemcell Technologies ImmunoCult™-XF T Cell Expansion Medium supplemented with 10% FBS and 20 U/ml human IL-2. The CAR-T or control cells were then added to the plate containing the target cells at an E:T ratio of 5:1 (10 000 total T cells with 2000 target cells) for each well against the respective targets. Images were taken

at regular intervals in phase-contrast and examining red (excitation [ex]. 565–605 nm; emission [em]. 625–705 nm) or green fluorescence (ex. 440–480 nm; em. 504–544 nm). Automated cell counting of red (target) or green (CAR-T) cells was performed using Incucyte analysis software, and data were graphed using GraphPad Prism software. Cell dilution at a 1 in 5 split with fresh media, and addition of 2000 fresh target cells in their respective wells were performed weekly for cocultures that were maintained beyond 7 days.

3.5.9 Repetitive CAR-T cell stimulation assay

This assay was adapted from the a previously reported STAR assay protocol for CAR-T exhaustion [367]. Briefly, tumour target cells were resuspended ImmunoCult™-XF T Cell Expansion Medium supplemented with 20U IL-2 and plated in a 24-well tissue culture-treated plate at 100,000 target cells per well. CAR-T cells or control T cells were thawed 24 hours prior to the assay start and cultured in ImmunoCult™-XF T Cell Expansion Medium supplemented with 10% FBS and 20 U/mL human IL-2. CAR-T cells or control T cells were added to plated target cells at 100,000 cells per well. Wells received an additional 100,000 target cells in each well every 2 days until endpoint. A 1 in 5 media dilution passage and media feed were performed alongside every 4 additions (~every 8 days). An aliquot of T cells was analysed with each stimulation via flow cytometry with the following antibodies: BV786-CD69, PE-Cy7-CD25, BV421-PD1 (all from BD Biosciences), and VHH-CAR surface expression via anti-VHH staining [in house antibody as reported in [368]].

3.5.10 Animal Studies

Eight-week-old NOD/SCID/IL-2Rγ$^{-/-}$ (NSG; strain no. 005557, The Jackson Laboratory) mice were engrafted subcutaneously with 6x10^6 H292-Nuclight cells on day 0. The tumour was allowed to develop for 15 days, at which point mice were randomized for cage assignment. Cages were randomly assigned CAR-T treatments. All randomization was done using the Microsoft Excel RAND() function. On day 15 post tumour cell injection, mice were treated with either 5x10^6 CAR-T cells (~30-40 million total T cells) for a high dose treatment, or 1x10^6 (~5-10 million total T cells) for a low dose treatment, or an equivalent number of total untransduced mock control T cells by intravenous injection. Tumour growth was measured weekly after tumour engraftment by a digital caliper, and the weight and signs of distress were monitored. Weekly bleeding was also performed to monitor and phenotype circulating CAR-T via flow cytometry. Isolated T cells from the blood were assessed with the following antibody stains: BV786-hCD69, BV711 anti-mouse CD45, BV650-hCD45RA, BV421-hPD1, PerCP-Cy5.5-hCD8, Pe-Cy7-hCD25,PE-CF594-hCD45RO, PE-hCCR7, APC-H7-hCD45, BUV395-hCD4 and anti-VHH [in house as per [368]]. Mice were euthanized at tumour burden >2000 mm^3, weight loss >20%, or if mice displayed severe signs of distress or discomfort during regular monitoring as per the NRC-Human Health Therapeutics (HHT) Institutional Animal Care Committee protocol. Weekly bleeding was also performed to monitor and phenotype circulating CAR-T via flow cytometry. Anaesthesia where required was performed using inhalation of 4% isofluorane, and euthanasia was performed via exsanguination or cervical dislocation of fully anesthetized animals. The study design was

approved by the NRC-HHT Institutional Animal Care Committee and was conducted in accordance with Canadian Council on Animal Care guidelines. Tumour growth and survival (humane endpoint) curves were generated using GraphPad Prism 9.

3.6 – Supplemental Data

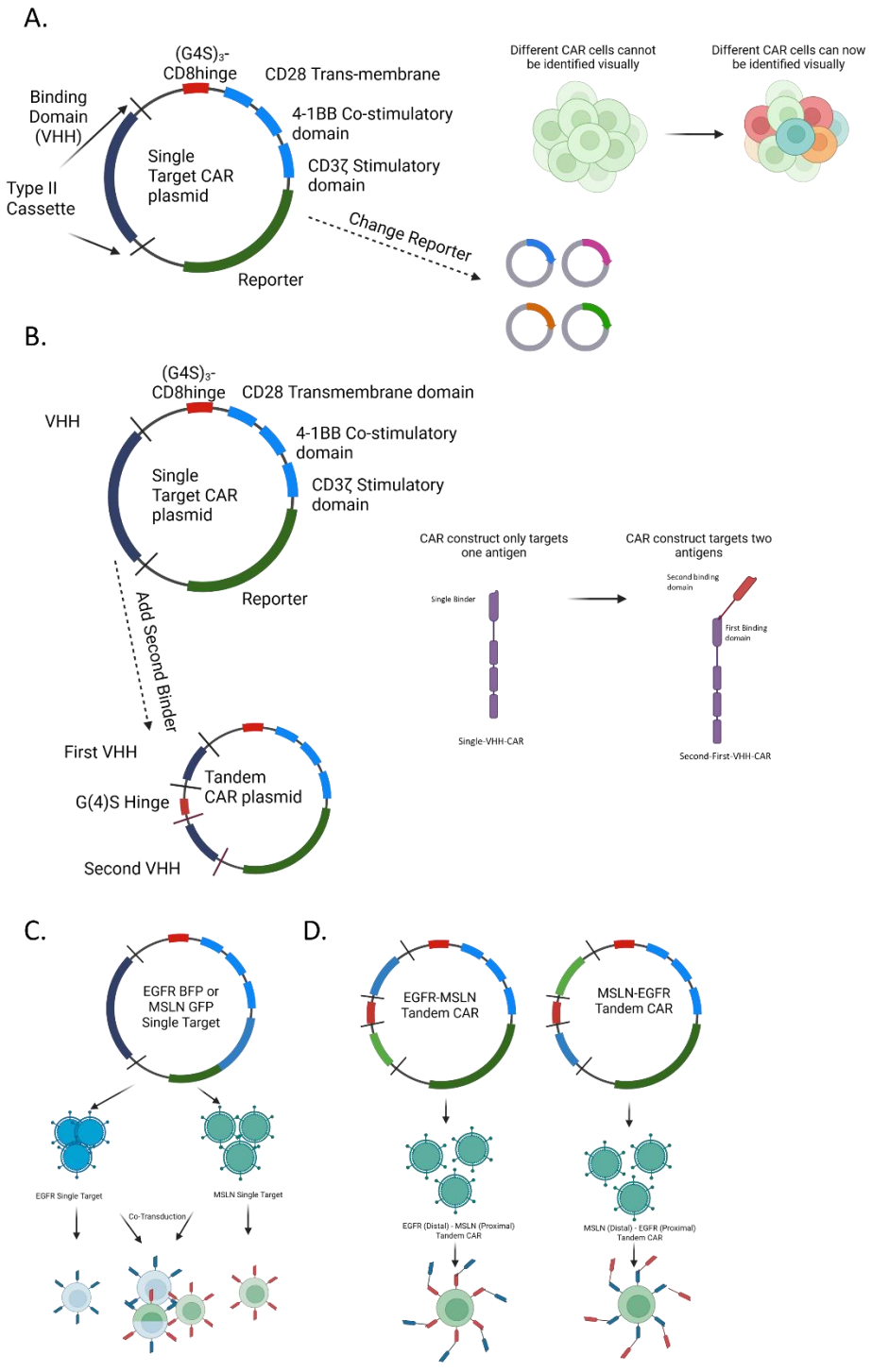

Supplementary Figure 3.1. Layout of multi-car and Tandem CAR plasmids

Basic plasmid layout of the multi-colour plasmid platform **(A)** and tandem CAR **(B).** Modification to the plasmids performed using Gibson assembly. Complete plasmid layout and map can be found at addgene.com **(C)** Results of lentiviral transduction and co-transduction of single target virus or **(D)** transduction of tandem virus

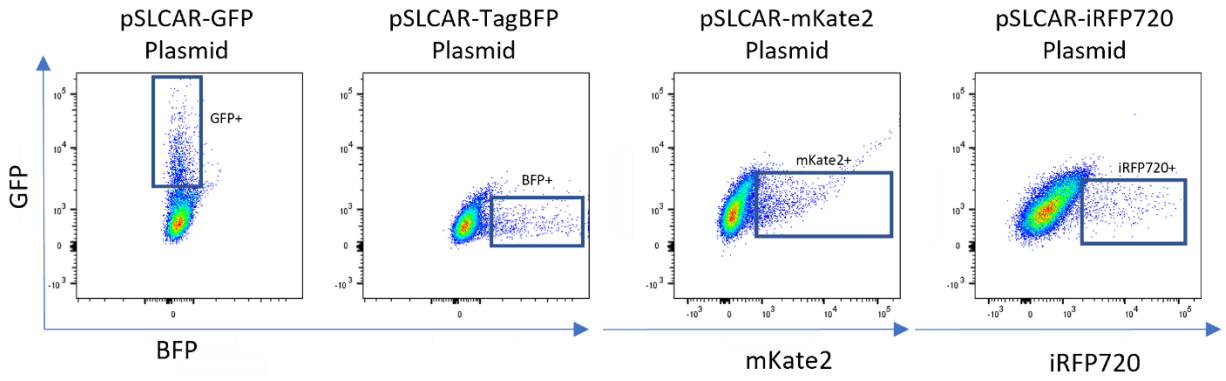

Supplementary Figure 3.2. All functional multi-colour reporters

Wild Type Jurkat e6.1 cells were electroporated with 4ug of plasmid, allowed to recover for 24 hours, then assessed by flow cytometry. Flow plots show electroporation efficiency and functionality of new reporter.

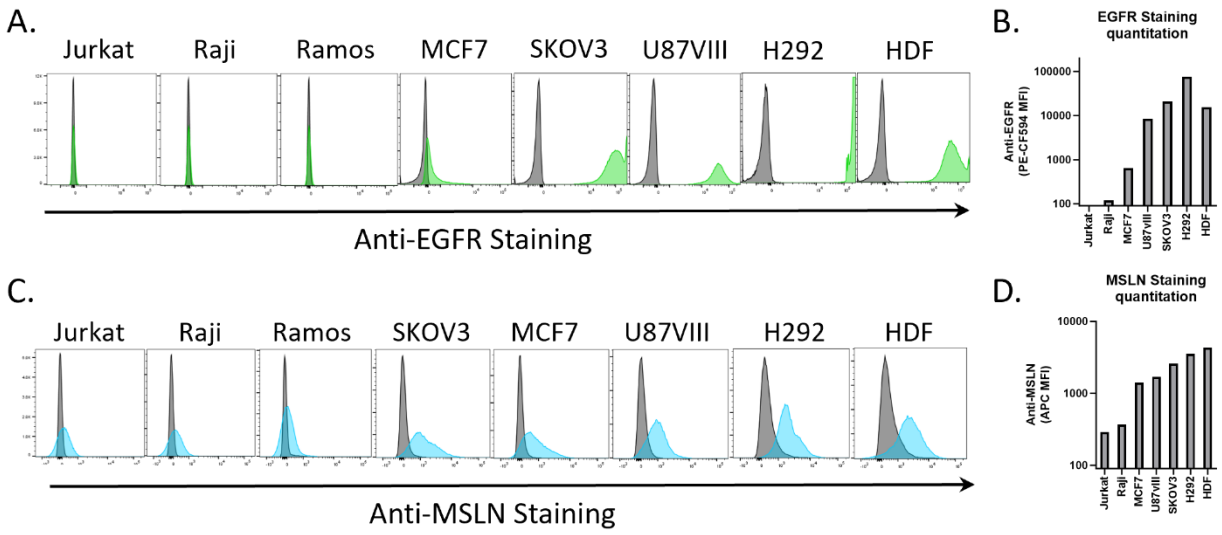

Supplementary Figure 3.3. EGFR and MLSN expression level assessed through flow cytometry

Various targets were stained for MSLN and EGFR at .25µl/ml and assessed through flow cytometry to record the level of EGFR and MSLN present on the cell surface. Cells stained were as follows: Human Dermal Fibroblasts (HDF), H292 – Human lung mucoepidermoid carcinoma, U87VIII - human glioblastoma line modified to express EGFRvIII, MCF7 – human metastatic breast adenocarcinoma, SKOV3 – human ovarian serous cystadenocarcinoma, Ramos – human Burkitt's lymphoma, Raji – Human Burkitt's lymphoma, and Jurkat e6.1 – Human T cell lymphoma. All cells besides HDF and Jurkat were modified with Nuclight Red nuclear stain. Histograms show staining as compared to control [**A** and **C**]. Graphs show MFI of Anti-EGFR **(B)** or Anti-MSLN **(D).** Ramos has been removed from bar graph due to redundancy with Raji.

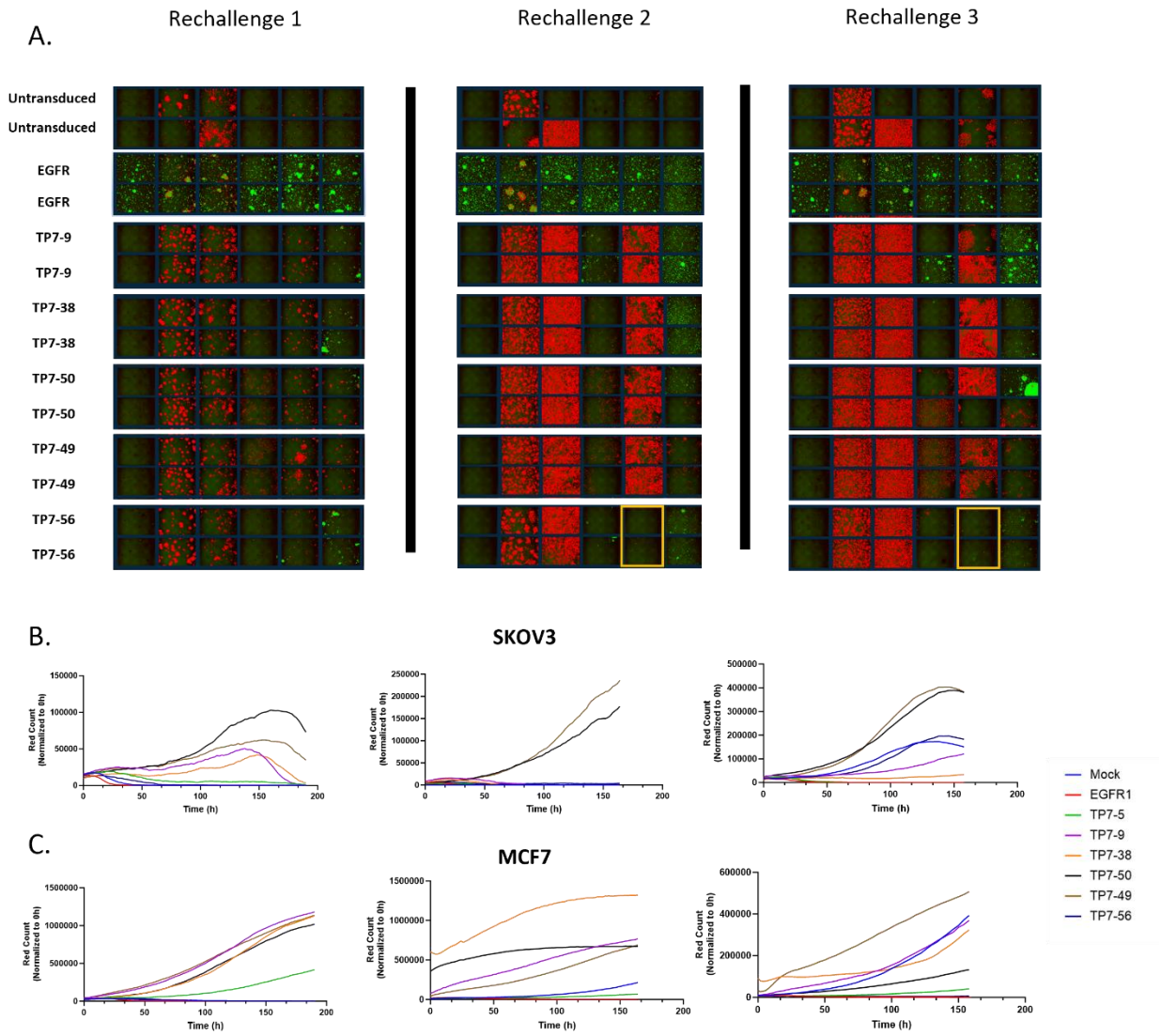

Supplementary Figure 3.4. Single Target MSLN CAR in vitro killing against varying level of MSLN expression

A-C. *In vitro killing* efficacy assessment via Incucyte live imagine system. Donor Primary CAR-T cells at Day 9 were thawed and allowed to recover for 16 hours. CAR-T cells were then placed in low-density culture (1:5) with IL-7/IL-15 supplementation. CAR-T were co-cultured 5:1 against Raji (MSLN-), Ramos (MSLN-), SKOV3 (MSLN++). MCF7(MSLN+), and H292 (MSLN+++). All target cells were stained with the nuclight nuclear stain. Raji included as a secondary negative control due to its tendency to induce tonic signaling. Co-cultures were examined for red fluorescent target cell growth (%red area) over the course of the initial challenge and subsequent rechallenges. Each rechallenge was accompanied by a 1 in 5 split. CAR-T able to clear MCF7 cells by the end of week 4 highlighted in yellow **(A)**. Graphs show specific target cell growth of lower MSLN expression targets Skov3 (MSLN low) **[B]** and MCF7 (MLSN very low) **[C]**. Graphs display mean of multiple duplicate wells of a single experiment.

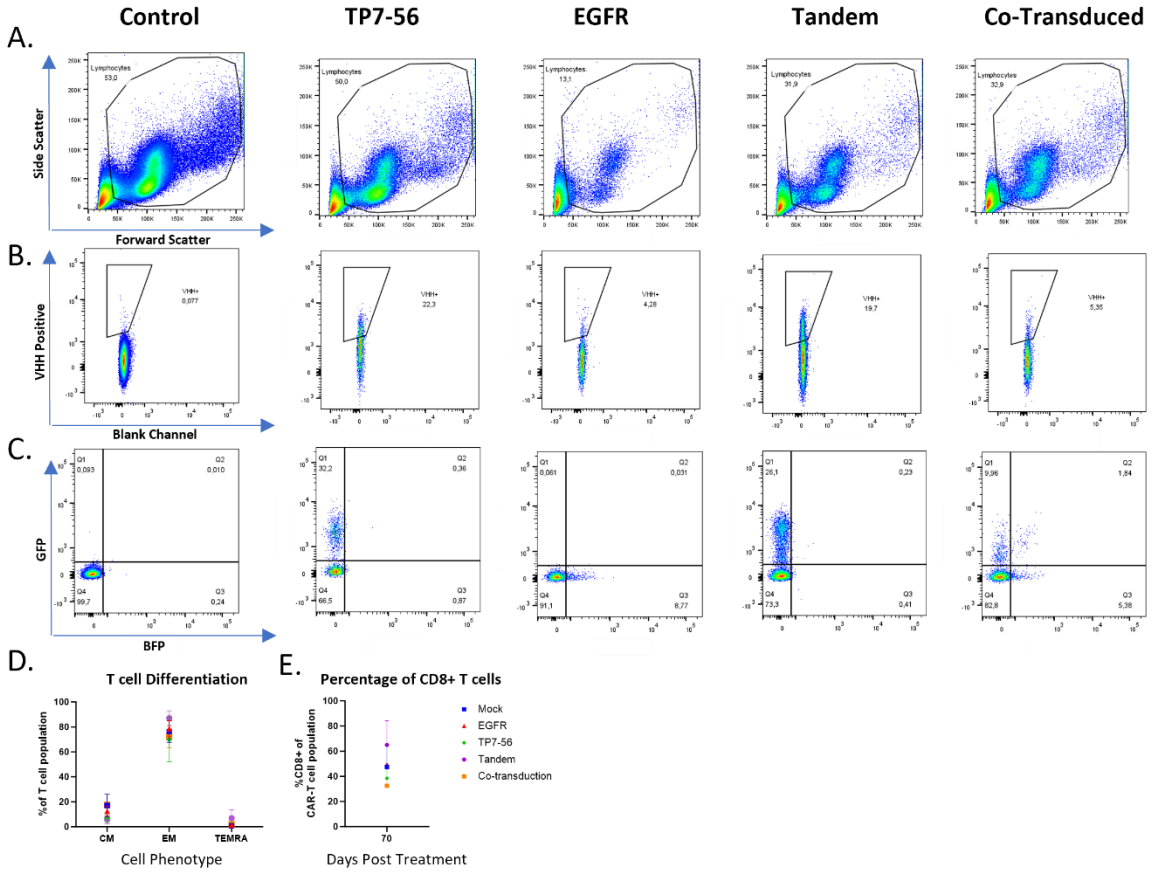

Supplementary Figure 3.5. In vivo blood T cell expansion and differentiation

Blood taken via weekly cheek bleeds from all surviving mice in each group. **(A-C)** Flow cytometry scatter plots of samples from each group. All samples show day 61 (Highest expansion of both T cell and CAR-T recorded) from the high dose trial. T cells were isolated from blood samples and stained with a complete staining panel including anti-VHH, anti-CD8/4 and anti-CD25 among other. Scatter plots show the percentage of total lymphocytes T cells as assessed by size (**A**), total CAR-T cells as shown with an anti-VHH stain (**B**) and total CAR-T cells as shown by individual reporter, BFP (Q3), GFP (Q1) and both (Q2) (**C**). **D and E.** Graphs show differentiation of T cells at the same time point (Day 61) [**D**] and CD8% of the T cell population (**E**). Graphed data presented at median +SEM, n=5.

CHAPTER 4: EVALUATING CAR-T USING CELLULAR AVIDITY

Note: This Chapter contains a manuscript submitted to Bioprotocol. Additional data and discussion have been added which add context and expands on findings but did not fit within the scope of the publication.

A Flow Cytometry–Based Method for Assessing CAR Cell Binding Kinetics Using Stable CAR Jurkat Cells

Alex Shepherd[1, 3], Bigitha Bennychen[1, 3], Ahmed Zafer[1], Risini D. Weeratna[1] and Scott McComb[1, 2, 3, *]

[1]Human Health Therapeutics Research Centre, National Research Council, Ottawa, ON, Canada

[2]Centre for Infection, Immunity and Inflammation, University of Ottawa, Ottawa, ON, Canada

[3]Department of Biochemistry, Microbiology, and Immunology, University of Ottawa, Ottawa, ON, Canada

*Correspondence: scott.mccomb@nrc-cnrc.gc.ca

4.1 – Abstract

Chimeric antigen receptors (CARs) are synthetic fusion proteins that can reprogram immune cells to target specific antigens. CAR-expressing T cells have emerged as an effective treatment method for hematological cancers; despite this success, the mechanisms and structural properties that govern CAR responses are not fully understood. Here, we provide a simple assay to assess cellular avidity using a standard flow cytometer. This assay measures the interaction kinetics of CAR-expressing T cells and targets antigen-expressing target cells. By co-culturing stably transfected CAR Jurkat cells with target positive and negative cells for short periods of time in a varying effector– target gradient, we were able to observe the formation of CAR-target cell doublets, providing a readout of actively bound cells. When using the optimized protocol reported here, we observed unique cellular binding curves that varied between CAR constructs with differing antigen

binding domains. The cellular binding kinetics of unique CARs remained consistent, were dependent on specific target antigen expression, and required active biological signaling. While existing literature is not clear at this time whether higher or lower CAR cell binding is beneficial to CAR therapeutic activity, the application of this simplified protocol for assessing CAR binding could lead to a better understanding of the proximal signaling events that regulate CAR functionality.

4.2- Key Features

• Determines CAR receptor cellular interaction kinetics using a Jurkat cell model. • Can be used for a wide variety of CAR target antigens, including both hematological and solid tumor targets.

• Experiments can be performed in under two hours with no staining using a standard flow cytometer.

• Requires stable CAR Jurkat cells and target cells with stable fluorescent marker expression for optimal results.

Keywords: CAR-T, Jurkat, Screening, T cell, Cellular avidity, High throughput, Flow cytometry, Cell-to-cell interaction, Cellular kinetics

This protocol is used in: Front Immunol (2022), DOI: 10.3389/fimmu.2022.864868

4.3 – Graphical Overview

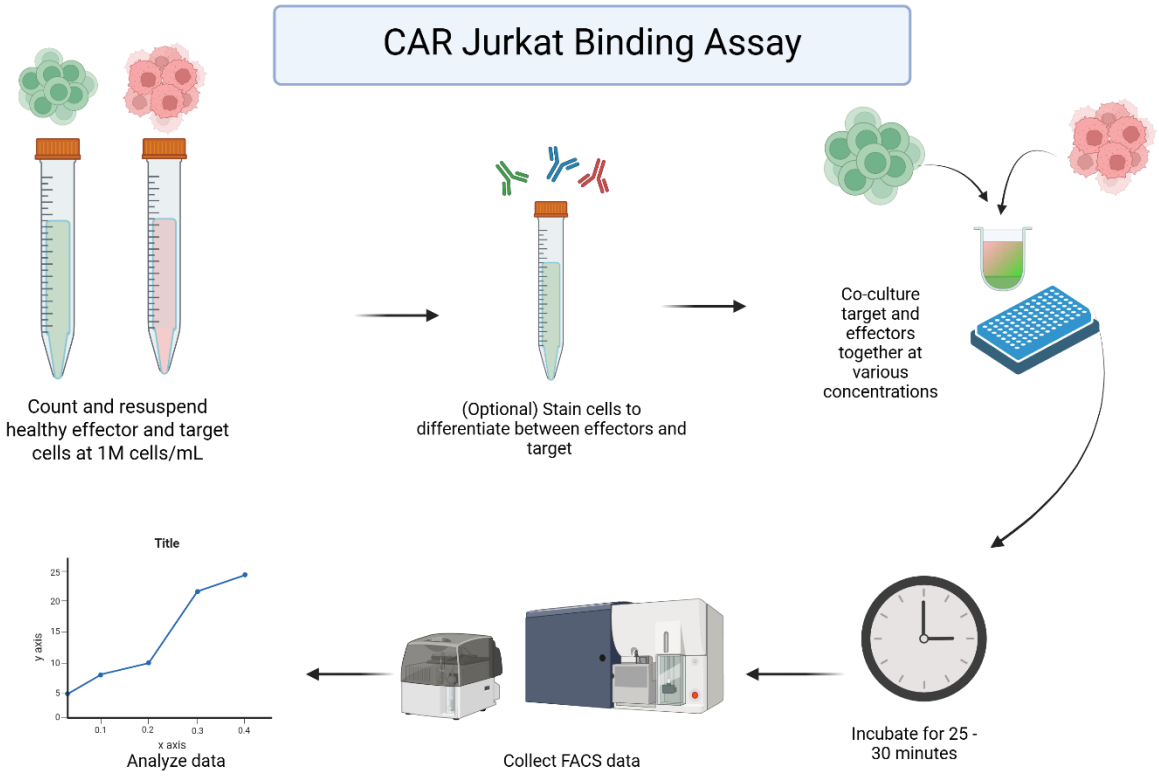

4.4 – Background

Chimeric antigen receptor (CAR) T-cell therapy is an engineered cellular cancer therapy that reprograms a patient's T cells to target a specific protein, mimicking natural T-cell receptor (TCR) function but redirected toward antigens found on the surface of cancer cells. CAR-T cells have emerged as a highly successful tool for providing robust therapeutic responses against refractory or relapsed hematological cancers, with ongoing research across many domains of immunology to extend the range and efficacy of CAR-T treatments for solid tumor malignancies[369–371]. Many advancements have been made in understanding the novel biology of CAR-modified T cells; however, CART-cell screening models still struggle to choose candidate binding elements based on in vitro assessments of CART

activation and cytotoxicity assays. Whilst activation markers, such as CD69, are well-documented using CARJurkat and primary CAR-T-cell screening methods, it is unclear how well these markers can predict in vivo efficacy of the CAR-T cells[153,372]. Recently, cellular avidity was recognized as a property of CAR-expressing cells that varies between different CAR constructs and correlates with important functional properties such as CAR expansion, CAR-activated trogocytosis, and CAR-T exhaustion[373–375]. Cellular avidity is defined by the total sum of cell-to-cell interactions, encompassing the whole immunological synapse and many cellular adhesion processes[376]. Given that cell binding is a near-immediate consequence of CAR signaling and proximal T-cell response processes, understanding the nature of this interaction and how it differs between standard TCR interaction vs. CARs is an important area of research. Investigating how cellular avidity changes with different CAR binding domains or structural designs is also vital for improving CAR discovery and development. It is important to note that while the specific properties of an antibody used to create a CAR impact the overall cellular avidity, the affinity and avidity of an antibody are entirely distinct from the complete cell-to-cell interaction that defines “cellular avidity”. For soluble proteins such as antibodies, avidity is defined as the overall accumulated strength of interaction through multiple interactions, but it can vary widely depending on the nature of the target antigen and the specific conditions of the assay. The measured avidity of an antibody is usually reported as the half-maximal binding concentration observed over a titrated binding assay, this property being referred to as the apparent affinity (KD). In contrast to antibodies, using the assay described herein, we have observed that the half-maximal binding of CAR-expressing cells over a titrated range of

target cell concentration does not vary between CAR proteins; rather, we find that CAR cells consistently reach a point of saturated maximal binding, wherein a varying proportion of CAR-expressing cells will form a strong bond with target cells (we refer to this as a CAR-target doublet). The strength of this interaction, while not encompassing the entirety of the kinetics, approximates what is commonly called functional avidity. This observation of a varying binding rate between CAR-expressing and target cells has similarly been reported using an assay based on a resonance force ramp microscopy using the Lumicks zMovi device[373], which directly tests the strength of interaction by attempting to measure the force at which CAR-target pairs are dissociated. We find that the rate of CAR-target doublet formation increases with higher target cell density, eventually reaching a saturation point. Furthermore, we find the rate of doublet formation varies between different CARs[201] or CAR designs[153]. While this assay does not directly test the strength of interaction and therefore is only an approximation of overall cellular avidity, we believe the unique target binding properties for each CAR serve as valuable metrics for CAR screening and assessment. As such, this assay could be used as a replacement to, or in conjunction with, direct avidity assays for optimal CAR selection. Here, we provide a complete description of our cellular binding assay that serves as a quick, high-throughput addition to CAR-T screening workflows using a standard flow cytometer. Through the quantification of cell/target doublets formed within CAR Jurkat target cell co-cultures over a wide range of effector-to-target ratios, the unique cell binding properties associated with each CAR can be determined. This assay provides consistent results and can be employed with both solid tumors (see validation of protocol) and hematological tumor models.

4.5 – Materials and Reagents

4.5.1 - Biological materials

1. Jurkat e6.1 (ATCC, catalog number: TIB 152) expressing a variety of CAR proteins

2. Ramos (ATCC, catalog number: CRL-1596) or other relevant target tumor cell line(s)

Target cells have been engineered with Nuclight Lenti-Red (Sartorius, Germany; 4476). It is also possible to use non-fluorescent cells for this assay, but antibody prestaining of targets or effectors is recommended as detailed in section B.

4.5.2 – Reagents

1. Fetal Bovine Serum (FBS) (Sigma Life Sciences, catalog number: F2442-500ML)

2. L-Glutamate (Gibco, catalog number: 25030-081)

3. Penicillin/Streptomycin (Pen/Strep) (Gibco, catalog number: 15140-122)

4. RPMI 1640 (Gibco, catalog number: 21870-076)

5. Dulbecco's phosphate-buffered saline (DPBS) (Gibco, catalog number: 14190-144)

6. VHH or scFv-specific fluorescent antibody (optional) (generated in-house) a. An analogous anti-VHH polyclonal product (Jackson Laboratories, catalog number: 128-605-232) b. For other CARs, various anti-scFv or anti-linker antibodies are available

7. CD45 or other Jurkat/T-cell specific antibody (optional) (BD Pharmingen, catalog number: 560178)

8. CD19 or other target-specific antibody (optional) (BD Horizon, catalog number: 612938)

4.5.3 – Solutions

1. R10 complete (see Recipes)

4.5.4 – Recipes

1. Table 4.1 – R10 Complete recipe

Reagent	Final concentration	Quantity or Volume
RPMI 1640		500 mL
FBS	100ml/L	50ml
L-Glutamate	10ml/L	5ml
Pen/strep	10ml/L	5ml

4.5.5 Laboratory Supplies

1. 96-well U-bottom plate (Falcon, catalog number: 353077)

4.6 – Equipment

1. BD LSRFortessa flow cytometer

2. BD LSRFortessa flow cytometer HTS plate reader

4.7 – Software and datasets

1. FACS Diva

2. FlowJo

3. GraphPad Prism 10

4.8 -Procedure

4.8.1 – Stable CAR Jurkat Preparation

Notes: 1) This assay has been optimized to use both target and effector cells to sort for 100% CAR or reporter-positive cells. Doing so will significantly improve data analysis and data quality.

2) We also recommend testing any cells being used for mycoplasma before use in this assay.

3) CAR Jurkat cells and target cells should be in healthy log-phase growth conditions prior to initiating the avidity assay, as described below. This can be accomplished by splitting cells 1–2 days before use.

4) If using adherent cells, aim to have cells with a confluency of 70%–80%.

5) Jurkat cells can be visually assessed for cell health (healthy Jurkat cells will be round and form small clumps) alongside a viability stain when counting. Do not use cells that are less than 80% viable. We have found that cell health can have a major impact on the consistency of results for this assay.

1. Cells used to make stable CAR Jurkat or Nuclight target cells should be healthy, log-phase cells prior to lentivirus exposure. Lentiviral transduction should only be performed by trained professionals and handled with all safety protocols in mind. A full lentivirus creation and transduction protocol can be found in Tandon et al.[377]. Please note that all work using active lentivirus requires BSL2+ safety and training. While details are not provided here, a general workflow for generating stable CAR Jurkat cells involves the following steps: CAR-lentiviral particle production as per linked protocol; (optional) lentiviral concentration using high-speed centrifugation; transduction of Jurkat cells with CAR-lentiviral particles; cell sorting to isolate a pure population of CAR Jurkat cells; and (optional) cryopreservation of the CAR Jurkat cell line for various downstream analyses, such as the one described here

2. Once transduced cells are viral vector–free (typically after three media changes and at least 7 days at 37 °C), cells can be safely sorted for 100% CAR or fluorescent marker

expression for best results. To generate target cells with stable Nuclight-Lenti (Sartorius, USA) expression, puromycin selection can be used. For stable cells with no resistance genes, the best option is the derivation of single-cell clone populations using cell sorting or limiting dilutions.

4.8.2 – CAR Jurkat binding assay plate setup

1. Remove your target and stable CAR Jurkat cells from the incubator and count them, ensuring cells have at least 80% viability and are in the log phase of growth. We recommend not using cells that have been in culture for more than three months.

2. Spin down and bring CAR Jurkat and target cells to 1 million cells/mL in separate suspensions in R10 complete media. To enhance discrimination between effector cells, target cells, or doublets, you may use prestaining with antibodies that are specific to effector cells (e.g., CD45 or anti-VHH/scFv) or target cells (e.g., CD19). This is especially helpful if you are not using cells with stable fluorescent protein expression, as shown in Figure 4.1. If you are using an antibody stain for your CAR or target cells, spin down and stain your cells now.

> **a.** For staining, resuspend the cell pellet in 100 µL of R10 complete medium, stain, and leave in the dark at room temperate for 15 min before washing off the excess stain. To wash, add 5 mL of 1× PBS and spin down the cells at 500× g for 3 min before removing the PBS and resuspending the cells in R10 complete medium, bringing the cell concentration back up to 1 M/mL.

b. Exemplary data provided here uses the Ramos human lymphoma cell line as the target cell line, although this assay can be successfully performed with a wide variety of adherent and non-adherent target cells.

3. Add 50 µL of R10 complete medium to each well of your 96-well plate.

4. Add target cells to each well at the ratio described in Table 1 below. An example plate map is also given in Table 2.

Table 4.2 - Effector-to-target dilution chart

Ratio	# of cells (effector/target)	Vol needed at 1M cell/mL-Effector (µL)	Vol needed at 1M cell/mL Target (µL)	Row letter
1:10	5000/45000	5	45	A
1:5	10000/40000	10	40	B
1:2	15000/30000	15	30	C
1:1	25000/25000	25	25	D
2:1	30000/15000	30	15	E
5:1	40000/10000	40	10	F
10:1	45000/5000	45	5	G

Table 4.3 - Example plate map

E:T		CAR Samples											
		CAR1		CAR2		CAR3		CAR4		CAR5		Control (Irrelevant CAR)	
	1:10												
	1:5												
	1:2												
	1:1												
	2:1												
	5:1												

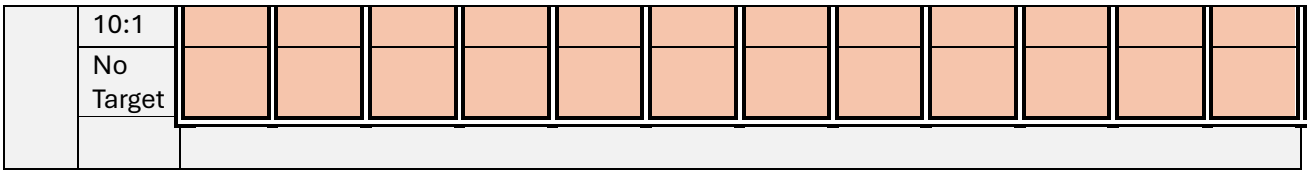

5. Plate Jurkat cells at the appropriate concentration as shown above. If done correctly, all wells should contain 100 µL of sample. Manually and gently shake the plate from side to side.

6. Place the 96-well plate in an incubator at 37 °C and 5% CO2 for 30 min.

a. If desired, this assay can be run at 4 °C as a control. Doublets should not form at this temperature.

b. This assay has been performed in as little as 10 min and as long as 4 h. Thirty minutes is our recommended minimum time for best results. It should be noted that, if this assay is being performed with an adherent target cell line, the incubation should not last long enough for cells to adhere.

4.8.3 – CAR Jurkat avidity flow cytometry

1. During the plate incubation, start up the flow cytometer and perform Cytometer Setup and Tracking (CS&T) and a system prime of the high-throughput sampler (HTS) to ensure the flow cytometer is functioning properly.

2. Once the incubation period has elapsed, run the plate on the flow.

a. This assay is optimized for an HTS setup for the BD LSRFortessa. Depending on your equipment, some modifications may be necessary.

b. While some settings may vary, those used for our setup are as follows:

1) Samples were run on a 96-well U-bottom plate, collecting 75 µL of sample or 50,000 events per well.

2) Cells were mixed by the cytometer and collected at a rate of 3 µL/s. The relevant voltage settings are as follows:

a) FSC 180 V

b) SSC 250 V

c) FITC 480 V

d) PerCP-Cy5-5 730 V

e) APC 600 V

4.9 – Data analysis

Data analysis of the raw flow data should be performed in the latest version of FlowJo but could be similarly performed with alternative flow cytometry analysis software. To start, gate out dead cells or cellular debris using forward and side scatter (Figure 4.1, top left). From here, analysis can be performed in two separate ways to obtain cellular avidity reading. If you are using stained cells or cell lines with a reporter, set your laser reading to display your cellular stains for the CAR and your target cell line with acceptable signal strength. The example shown below uses stable fluorescent markers: NeonGreen (FITC) for the CAR and Nuclight Red (or mKate2; PerCP Cy5.5) for the target cell lines. Should the cells bind, this should show three or four separate populations: unbound CAR Jurkat cells, unbound target cells, and bound doublets that express both the CAR and target colors (Figure 4.1, top middle). If your stable population of CAR Jurkat is unsorted, you may see an unstained population of non-CAR expressing Jurkats as well.

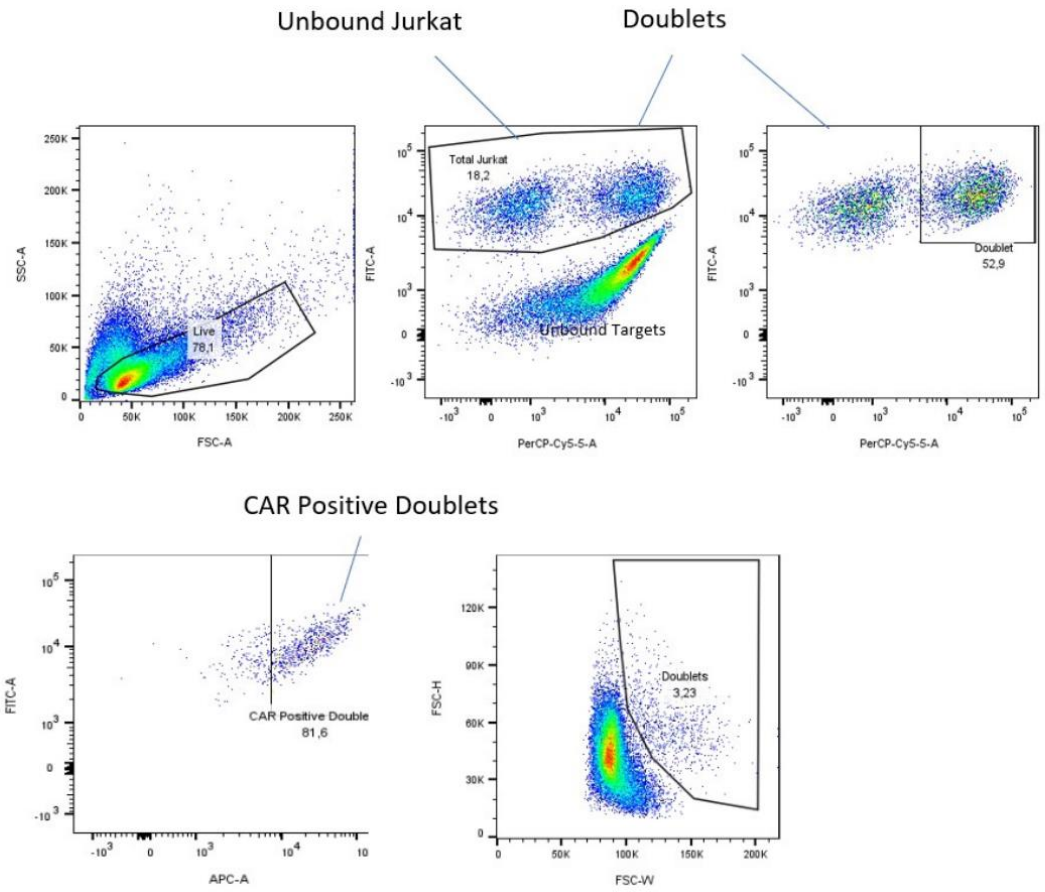

Figure 4.1. Gating method for fluorescently labeled and sorted cells.
Dead cells and debris are gated out (top left), then unbound targets are removed (top middle). Finally, doublets are separated from unbound chimeric antigen receptor (CAR) Jurkat cells and displayed as a percentage of parent (top right). CAR confirmation of doublets can be confirmed using a CAR-specific surface stain (APC channel here), removing auto-fluorescent false positives from doublets that are dead cells or cellular debris (bottom, left). An alternative method of analyzing doublets using their increased size on forward scatter (bottom, middle). This method will require some additional calculations to find the number of living Jurkat cells.

If you do not have stains in your CAR or target cells, instead display the forward scatter height by the forward scatter width. Cell doublets present in the well should be wider than the rest of the cells and can be selected alongside the other unbound Jurkats to give a similar result (see Figure 4.1, bottom middle). It should be noted that if the target cells are significantly bigger than the Jurkat cells, this method may not work as well, so we

recommend using a staining method if possible. To generate a CAR:target curve, use flow cytometry analysis software to exclude unbound target cells and then record your doublet population as a percentage of parents of the entire Jurkat population in the well (Figure 4.1, right). This will give the percentage of the CAR Jurkat population bound at that time and ratio. The ratio of bound doublet cells to free CAR Jurkat can be calculated manually as follows:

$$\frac{Number\ of\ CAR\ positive\ bound\ cells}{Total\ numbler\ of\ living\ CAR-Jurkat\ cells}\ x\ 100\%$$

This data can be graphed using appropriate data visualization software such as GraphPad PRISM 10, resulting in a curve with maximum binding occurring in an excess of target cells (>1:10–1:25 effector:target ratio) (see Figure 4.2).

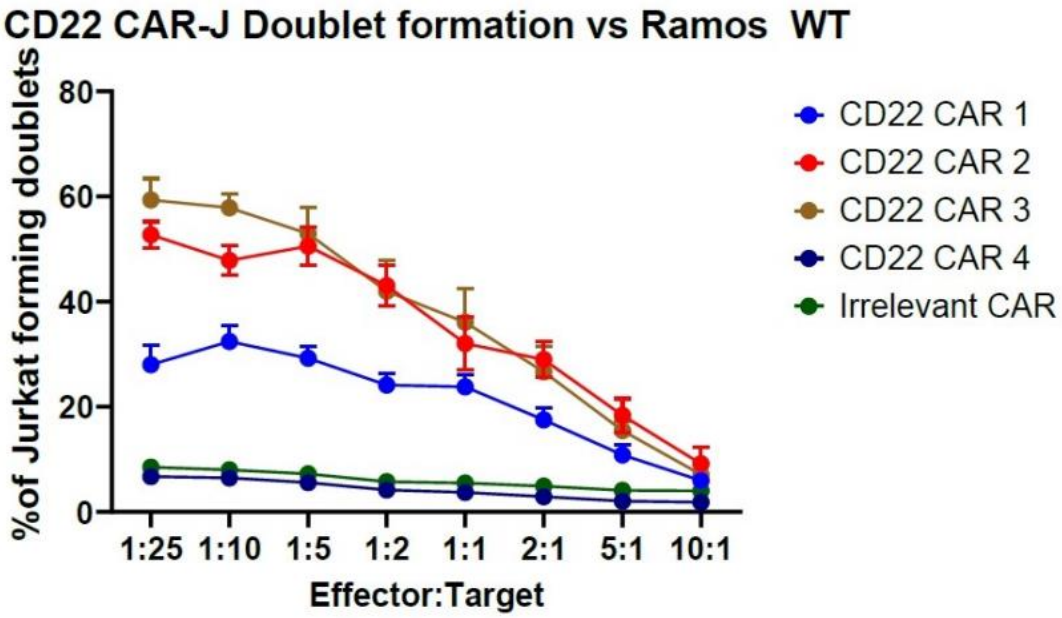

Figure 4.2. Exemplary data of CD22 chimeric antigen receptor (CAR) Jurkat binding kinetics against Ramos WT cells. The data displayed was performed in triplicate and displays data plus standard error of mean (SEM). Note that the "Irrelevant CAR" data set (green) has been nudged up two data points for visibility. Exported data was imported into PRISM 10 and graphed in the "grouped" format.

4.10 – General notes and troubleshooting

4.10.1 – General notes

1. As mentioned above, this assay is biological in nature and requires active cellular signaling to induce cell-to cell interaction. No cell-to-cell binding will occur at 4 °C, as signaling processes are inactive at this temperature. This can be used to test for non-specific binding and establish a background (Figure 4.3). Additionally, we recommend running the assay in parallel with a negative cell line and a non-specific/irrelevant specificity CAR to establish non-specific binding control.

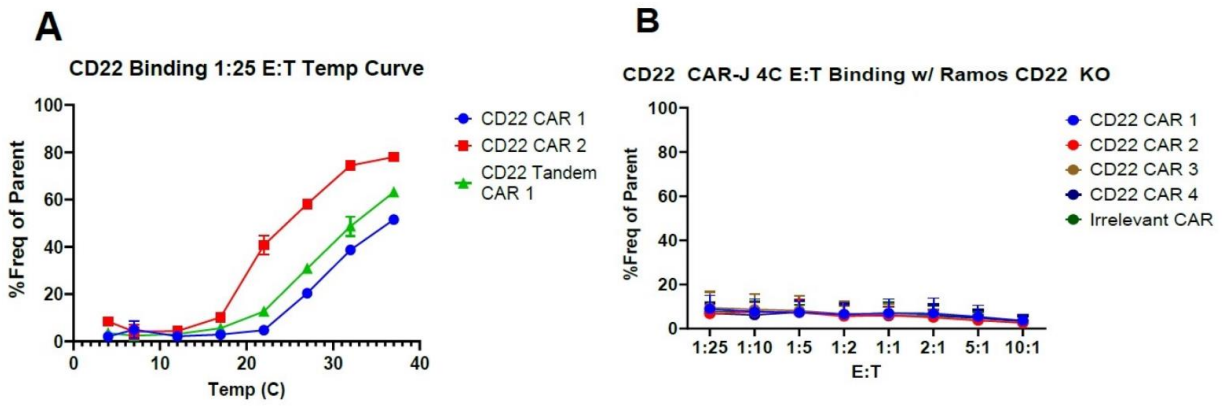

Figure 4.3. Chimeric antigen receptor (CAR)-Jurkat binding assessment using a temperature curve. (A) CD22 CAR-J cells were run first at 1:25 effector:target starting at 4 °C and incrementing the temperature gradually until 37 °C. Then, the binding assay was repeated in full at 4 °C. CAR-J cells cannot bind targets at 4 °C and only begin to show binding at approximately 21 °C. (B) The standard assay described above performed with target antigen negative cells. Experimental data was performed in triplicate. Error bars show standard error of mean (SEM).

2. This assay is not CAR exclusive. This can work with any biological that causes T cells to bind, such as bispecific T cell engagers (TCEs), that cause cell binding and T-cell synapse formation.

3. We are currently working on a version of this assay using lentiviral-transduced T cells. The primary cell version can be successful, but the nature of expanded donor T cells requires additional attention to experimental details to yield consistent results. Specifically, the proliferation state, transduction rate, and donor source are all key variables that can interfere with the measurement of CAR cellular avidity. Thus, we feel that this assay is best measured using Jurkat T cells for several reasons: (1) Jurkat cells lack a cytotoxic response and have limited cytokine activity, with no risk of the bound cell dying before passing through the flow cytometer; (2) Jurkat CAR cells can be sorted to 100% CAR cells without issues due to their steady proliferation; (3) Jurkat cells maintain a consistent

differentiation profile, while primary T cells can vary widely throughout manipulations. For these reasons, we recommend using Jurkat cells for performing this assay

4.10.2 - Troubleshooting

Problem 1: Cells do not form doublets in co-culture within 30 min.

Possible cause: Wrong culture plate used.

Solution: Change the assay plate to a 96-well treated U-bottom plate. This assay is optimized for U-bottom 96-well plates. Attempts in larger wells or wells with flat bottoms generally result in sub-optimal results.

Possible cause: Cells are unhealthy.

Solution: Re-attempt assay with cells in log-phase of growth. Cell health has been shown to have a direct impact on the speed and count of doublets in solution.

Problem 2: Cells do not form doublets ever.

Possible cause: Incubation is performed in untreated plastic or the wrong plastic type.

Solution: Ensure the assay is performed in a 96-well plate made of non-pyrogenic vacuum gas plasma-treated polystyrene. Incubations done in polypropylene tubes such as PCR tubes or 1.5 mL Eppendorf or in untreated polystyrene have been unsuccessful, as it appears the cells adhere to the plastic and have difficulty binding.

4.11 – Additional Results

4.11.1 – Further exploration of the biologic component in binding

In addition to the data included within the published protocol paper, further investigation of CAR based antigen binding has been undertaken. As demonstrated above, CAR proteins cannot bind to their target antigen at 4°C. To further explore this, we first attempted to co-culture the cells at 4°C for 30 minutes at the maximum E:T ratio (1:25) with Ramos Nuclight target cells, assessed the avidity of the cells, and then moved them back to 37°C for an additional 30 minutes. (Figure 4.4) All of the stable CAR-Jurkat cells recovered and were able to successfully form doublets once placed at the proper temperature, suggesting that similar to TCR binding, there is a large component of CAR binding that cannot activate below a certain threshold, and binds optimally at 37°C. Furthermore, this provides assurance that the lack of binding was temporary and not due to cell death or dysfunction from being held at lower temperatures for extended periods of time.

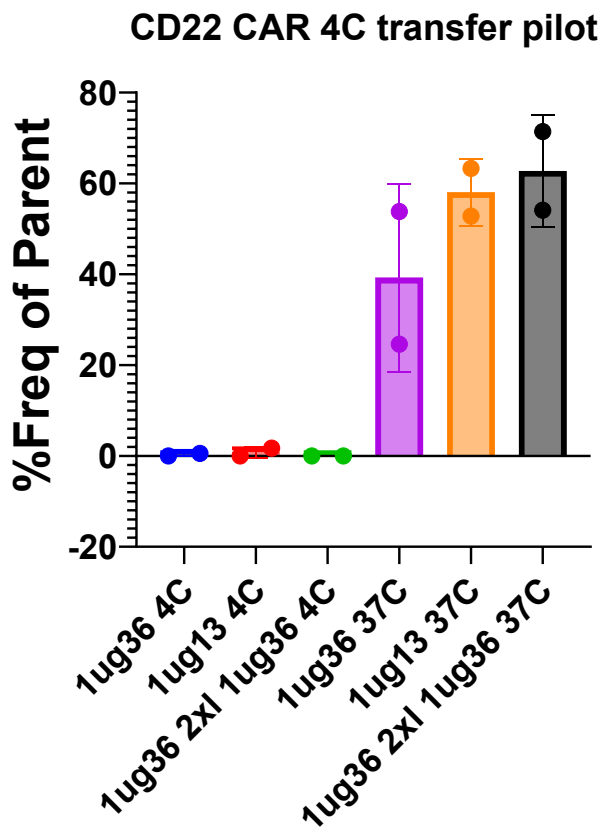

Figure 4.4. CD22 CAR binding post-recovery from 4°C co-culture
Graph shows doublet format of CD22 CAR-J cells at 1:25 effector target ratio after incubation at 4°C and after a secondary incubation at 37°C. Results presented in duplicate as mean + SD.

4.11.2 – CAR avidity in CARs with multiple binders

Next, we decided to investigate how CAR avidity changed in the context of multi-CAR. First, to establish a baseline, a full spectrum of CD22 CARs was tested for avidity. (Figure 4.5.) This separated the CARs into three major groups: high avidity, low avidity and non-binders. These avidities also appeared to correlate with the proximity of epitope of the target antigen being bound, with higher avidity CARs binding to more distal epitopes and low avidity CARs

binding to proximal epitopes (Not shown but can been seen in Figure 5.1). Additionally, it was observed that changes to the transmembrane domain could also affect the cellular avidity, as seen in the differences between the testing and BCRx (Clinical) backbones with the change from standard testing backbone to BCRx resulting in an approximately 10% increase in avidity. Next, we combined these CD22 CARs into a multi-antigen format to observe the change in avidity when combined. Given that it would be impossible to know which antigen binding region was binding when with this setup in a co-transduced CAR, it was decided that tandem CARs with two separate CD22 binders would be cloned for this assay. The CD22 CARs chosen for these combinations were the high avidity 1ug74 and low avidity 1ug36, as well as the low avidity 1ug10. 1ug36 is the current clinical lead and thus the most highly documented of the three, it was used as base, and combined with each other CAR, as well as itself. The tandem CAR was also cloned with a longer linker region than previous CARs to ensure that steric hindrance was less of a concern. When combined CARs with similar avidities remained at the same avidity, however when a high and a low CARs were combined in a tandem format, the resulting avidity was the average of the two, suggesting that each CAR has an equal opportunity to bind and influence the binding maxima when binding to an antigen with the equal surface expression.(Figure 4.6) Interestingly, when 1ug36 was combined with itself, its avidity increased. While this could be due to changes from the format, it is also possible that 1ug36 is self reactive and the resulting autoactivation caused an increase in binding.

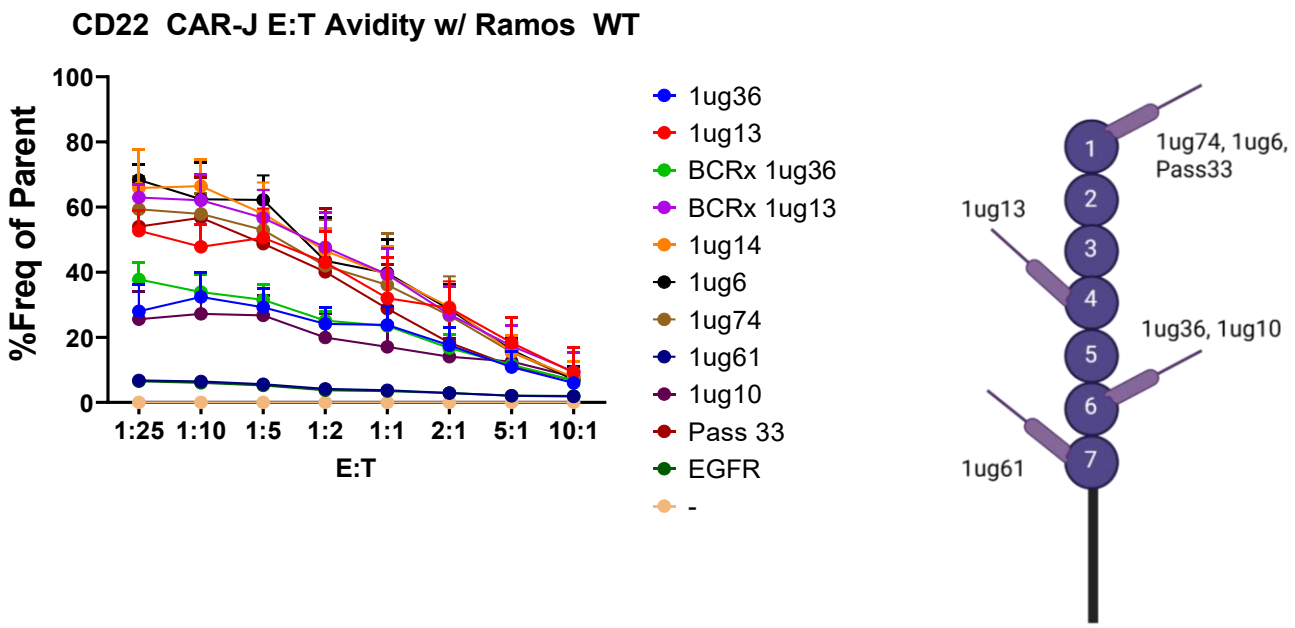

Figure 4.5. Full CD22 CAR Avidity Test

Full cohort of CD22s CAR-Jurkat cells tested to determine avidity. Stable CD22 CAR-Jurkat cells were co-cultured with Ramos Nuclight cells as described in the method above and assessed via flow cytometry. Graph shows avidity response in doublet formation as reported as % frequency of parent. Results reported in triplicate, data presented as mean + SEM. Picture shows CD22 binding epitopes of notable CD22 CARs

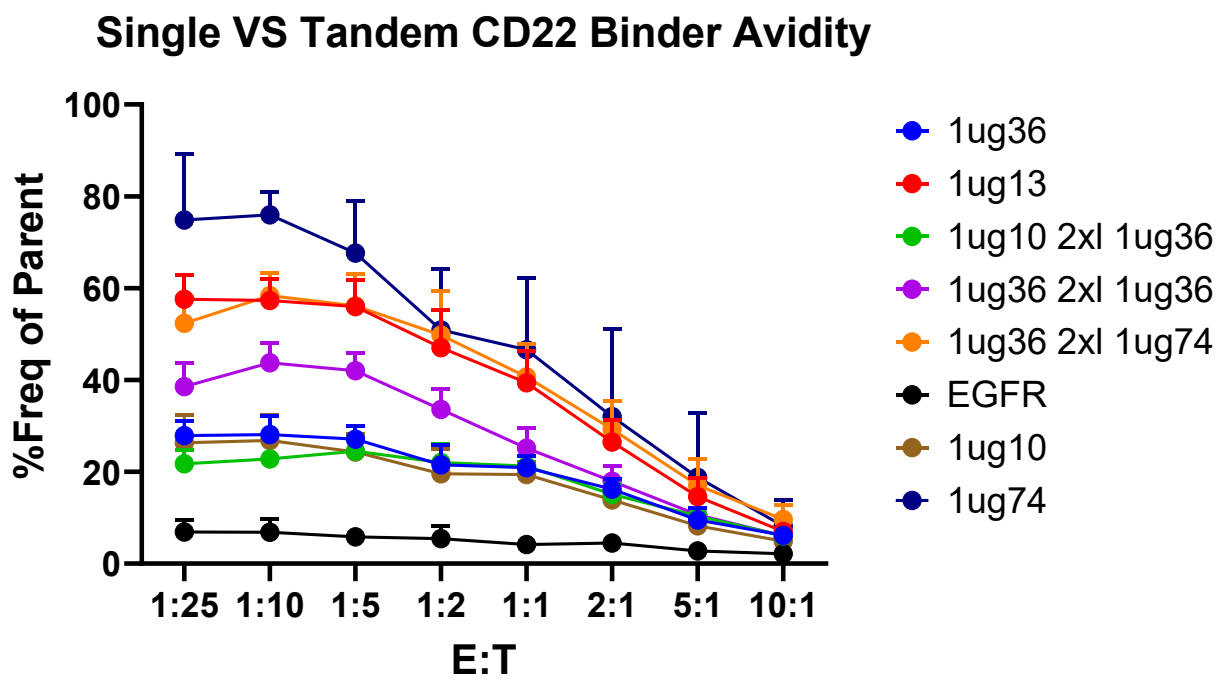

Figure 4.6. Tandem CAR avidity comparison
Single and Tandem 2XL (Double linker size) tested to determine avidity. Stable CD22 single target and XL Tandem CAR-Jurkat cells were co-cultured with Ramos Nuclight target cells as described in the method above and assessed via flow cytometry Graph shows avidity response in doublet formation as reported as % frequency of parent. Results reported in triplicate, data presented as mean + SEM.

4.11.3– CAR maximal binding is held in check by an equilibrium

Finally, one key observation noted during the creation and testing of this assay is that each CAR tested showed a unique binding maxima – a point at which once a certain number of CAR-Jurkats in a co-culture were bound no other cells would form doublets. To better understand these interactions, we ran a standard CAR avidity assay with three CD22 candidates, a high avidity CAR (1ug74), a low avidity CAR (1ug36) and a non binding CAR (1ug61) as a negative control in a 1:1 co-culture with Ramos NL cells. Once doublets had formed, each co-culture was selectively sorted used as SONY MA900 Multi-Application

Cell Sorter (Sony Biotechnology) into actively bound doublets and unbound cells. The unbound cells were then placed in a new co-culture with fresh Ramos cells at the same ratio and both groups were allowed to incubate for an additional 30 minutes. (Figure 4.7) When assessed by flow cytometry post incubation we observed that the sorted unbound cells actively bound the newly introduced targets, while the 100% doublet population binding to dissociate from their previously bound partners in order to regain equilibrium and remain at the binding maxima. The lower avidity CAR appeared to dissociate faster than the higher avidity CARs.

Figure 4.7. CAR-Jurkat binding maximum held in check by equilibrium.
High, low and non-binding CD22 CAR-Jurkat cells assessed to determine maximum binding pre and post sorting into unbound and bound cells. Stable CD22 CAR-Jurkat cells were co-cultured with Ramos Nuclight cells as described in the method above and assessed via flow cytometry. The remaining culture was sorted into 100% bound population or 100% unbound population. The unbound population was supplemented with an equivalent amount of target cells and both groups were incubated for an additional 30 minutes before reassessment. Graph shows avidity response in doublet formation as reported as % frequency of parent. Data presented as mean + SEM.

4.12 – Discussion

Being a synthetic protein, CAR constructs incorporate attributes from both antibodies and the TCR. While the signaling components built into the CAR are those of a T cell, the binding region uses an scFv or VHH to facilitate interaction and binding to activate the T cell. While cellular avidity is impacted by all of the design choices made, or at the very least

those made above the cellular membrane, the results here show that the antibody binding region plays a large role in determining how the CAR and the cell its combined with will bind to a target.

While understudied in CAR-T, TCR binding kinetics and the downstream consequences of how and how long TCR bind for has been studied. TCR complexes have been shown to be extremely sensitive, requiring small numbers of pMHC complexes in order to trigger cell lysis through CTL.[378,379] Part of the reason that T cells are able to signal with such low density of engagers is through serial engagement, where a TCR-pMHC forms, triggers TCR signalling, then detaches and rebinds another TCR to re-initiate signal.[380] For this process to work efficiently however, the binding and dissociation must be fast enough as to not let the initial signal fade.[381] This follows the T cell kinetic proofreading model, which postulates that TCR interactions require a minimum half-life or interaction time in order to produce a productive signal.[382] This model is generally supported with it having been shown that, in most cases, the potency of TCR ligands is determined by the half life of the resulting complex.[383] This correlation between interaction half-life and TCR activation does not appear to extend forever, with some peptide variants showing weakened activity with a longer half-life.[384,385] When directly examined it was shown that TCR activation could be impaired by decreasing and increasing the duration that the TCR remained bound, showing that TCR activation has an optimal amount of time an antigen should remain bound for, for efficient T cell activation.[204] This is known as optimal dwell time.

Given that CAR-T cells signal through the same mechanisms as the TCR, namely CD3ζ, it stands to reason that CAR proteins may also have an optimal dwell time. However, while

TCRs are already heavily regulated by the body to have optimized dwell time, the CARs are synthetic and thus their cellular avidity and consequentially dwell time appears to be largely determined by the binding region chosen.[204] This suggests that CAR-T have a sweet spot – an antigen binding region that binds enough to allow for efficient T cell activation through serial engagement, but limits the interaction and dwell time as to not impact the signal. Unlike TCR, however, CAR-T development does not undergo the same rigorous optimization and selection process to help optimize this interaction, meaning each unique CAR has its own specific interaction with its antigen, only some of which will land in the optimal range. While only a single example, this theory is supported by our experiments with CD22 CARs, with the lead CAR 1ug36 being much lower avidity than the other CARs tested *in vivo,* with the tumor suppression shown being correlated to lower avidity in Jurkats.

Unfortunately, these cellular interactions are still not fully understood. We have shown here that this process is biologically driven and not purely kinetic, however the driving force that determines the equilibrium uncovered here is still unknown. These doublets are consistently formed until this maximum is reached even in an extreme excess of targets as shown in the 1:25 effector to target ratio presented. Even when forced to forms doublets above this percentage, we observed rapid bond dissolution in order to return to equilibrium. This limit is currently under investigation, however one possible hypothesis for this is quorum regulation through CD28 and CTLA-4, which modulate T cell culture density.[386]

Finally, it should be recognized that CARs are not TCRs. While forming similar structures to the TCRs immune synapse, the structures formed in CAR binding are formed more rapidly, with less structure and regulation, and less reliance of LFA-1 with no distinct adhesion rings forming. Additionally, LCK does not form a supercluster and instead forms several microclusters.[82] This results in more rapid on and off rates for CARs when compared to TCRs as well faster cytotoxic response. These distinct differences from TCRs make it all the more clear that CAR-T binding and activation require more study in order to be fully understood. Determining how to control and optimize this key point of interaction will be important in improving CAR discovery and screening.

4.13 – Supplementary Materials

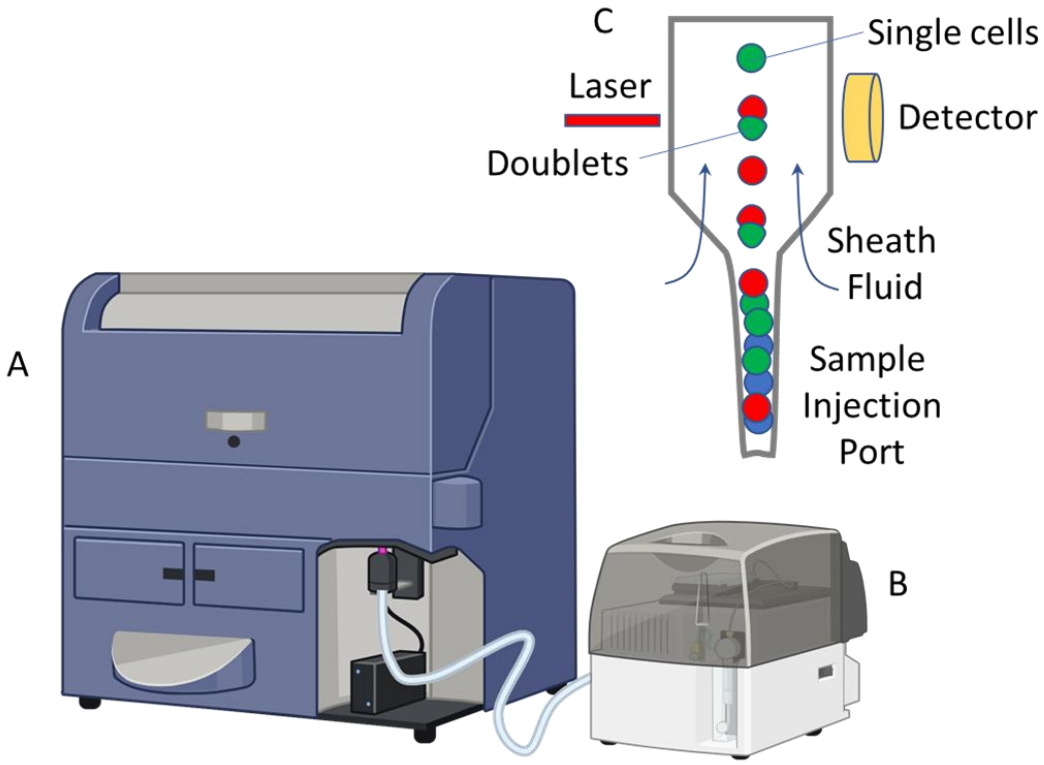

Figure S4.1. Cytometer and HTS setup.

Setup of BD LSRFortessa (A) with the High Throughput Sampler (HTS). The sampler (B) connects to the cytometer via a flexible tube attached to the sample injection port on the cytometer. The sampler automatically mixes and uptakes samples that are chosen via FACS Diva software. Samples are acquired during movement through the flow cell, where tangential flow of sheath fluid causes hydrodynamic focusing of the cells in order to allow acquisition of single cells, or strongly bound cell pairs.

CHAPTER 5: USING CELL SURFACE PROTEOMICS, PHOSPHOPROTEOMICS AND TRANSCRIPTOMICS TO EXPLORE CAR ONTOLOGY

Note: This Chapter contains a manuscript prepublication data which we intend to publish in a future manuscript once adequate data has been collected.

5.1 – Abstract

The development process of CAR-T is primarily results oriented, with screening and testing focused on finding potentially viable constructs for clinical use, rather than exploring the structure-function relationship of CAR molecules. While the assays used in standard CAR development are necessary, they often fail to translate early results in screening to *in vivo* success. To better understand what properties lead to CARs which consistently achieve tumor clearance, we have begun developing methodologies to assess different CAR constructs during target engagement to better understand how the differences in binding domain affect downstream CAR signaling and efficacy. While initial tests produced low confidence data that was difficult to assess, refinement and optimization of the assays by narrowing the assessed area, as well as modifying the analysis methods allowed for clearer, more specific data that can show important insight into how small changes to CAR-T structure impact efficacy downstream. Assessment of the current CD22 clinical lead 1ug36 against other CD22 CARs, while still preliminary, revealed potential differences in CD28 and LCK phosphorylation in for 1ug74 and 1ug13 suggesting that CD45 may not be effectively re-engaging the synapse leading to increased signal through CD28 leading to less cytotoxicity. In contrast, 1ug36 appears to show upregulations of NFAT and MAPK pathways, even more so when examined with a CD8 transmembrane domain instead of the CD28TM version. Ultimately, while these results have yet to be confirmed, they clearly

show the potential key insight that multi-omic assessment can provide. Should these results prove to be consistent across repeats, the data provided may lead to new screening targets, and overall, more reliable, consistent CAR-T development in the future.

5.2 – Introduction

CAR-T therapy has seen major success against hematological cancers, providing rapid clearance and durable response to otherwise untreatable malignancies. Despite this, the ability to consistently create safe, effective CARs remains out of reach, as our understanding of the mechanisms and properties that define this response profile is still incomplete. Given that CAR molecules have been shown to harness several major T cell functions, such as cytotoxicity and survival, it stands to reason that a comprehensive understanding of the underlying signals would benefit CAR-T development and optimization. Additionally, while it was previously though that CARs and TCR had similar signaling pathways, as CAR proteins are constructed from endogenous TCR proteins, recent data suggests that CAR-T signal through a combination of canonical TCR pathways and CAR specific ones.[387–389] Proteomic assessment has also presented new data regarding the differences between co-stimulatory domains and their resulting downstream signals[390]

These previous studies often focus on CARs in a T cell environment; however, the majority of our early testing is done in the pseudo-T cell Jurkat model. While not a complete facsimile to T cells, Jurkats provide a cheap, consistent T cell like line that it easy to manipulate and test, making for an ideal screening environment. Additionally, as demonstrated above in chapter 4, cell-to-cell contact is an important factor in how CAR

cells respond. Many approaches utilize modification to their target lines such as stable isotope labeling (SILAC)[391], fixation and removal of the T cells from culture for examination, or stimulation of the cells using beads or another synthetic source.[390] While this makes data analysis easier we speculated that this might modify the results as it would not be a clear depiction of true CAR-Target interaction. Thus, in order to better understand our screening model, as well as identify potential new early screening targets, we attempted to explore CAR-Jurkat through the lens of proteomic, phosphoproteomic and transcriptomic analysis while actively engaging target cells. Unlike flow cytometry, this combination of analytical methods would theoretically allow us an overview of the CAR engagement and activation process, allowing us to pinpoint differences in protein, phosphate and gene expression.

Before proteomics can be further discussed however, it is important to understand the context in which these experiments were performed. The metrics that determine CAR and CAR-T success in early screening are often not very indicative of how a CAR will perform in later phases of testing. While screening for functionality and *in vitro* tumor control are necessary steps, evaluation of several different CAR we have produced shows that these tests often only identify whether a CAR is functional.[153,201] Even *in vivo* testing in the current form, while important, may fail to translate to the human body. This is not always the case: studies such as 1XX CD19 CAR showed favourable results when moving from mice into phase 1 clinical trials, however in many cases mice often serve a poor substitute for the human body.[392,393] The most commonly used mouse model, xenograft, gives an incomplete immune response due to being immunodeficient. More accurate models, such as

humanized mice may be to expensive for the majority of labs, and still don't full represent a complete immune profile, as these mice lack human stroma or any immune memory.[393] From a metadata standpoint, failed transitions from mice to human are also likely underreported, as negative results are published far less often that positive ones.[394] Despite this, these tests will remain as an essential part of CAR screening and approval process for the time being and do fulfill an important role in identifying promising candidates, but more precise and in-depth screening is required to have a screening platform that can identify success earlier and be confident that that success will continue into the future.

In an attempt to better understand the factors that contribute to a clinically viable CAR we decided to examine the most successful CAR that we have produced thus far: 1ug36, a CD22 targeting CAR which is now the lead of the CLIC-2201 clinical study. Given its success, 1ug36 presents a unique opportunity to examine a clinically viable CAR within the context the other CARs it has been tested with. This allows for the unique properties of 1ug36 to be identified by observing the differences between it and each of the other CD22 CARs tested. These CARs will be assessed in two different contexts – alone, as a stable CAR expressing Jurkat cell, and actively interacting with a target cell across several timepoints. The former acts as a good baseline and control, allowing for changes in expression and phosphorylation to be observed when the cell is activated from a resting state. Additionally, recent studies have found that certain levels of tonic CAR signaling are actually beneficial to CAR performance, and the examination of the baseline CAR-jurkat cell may reveal some previously unknown markers that could be used to identify this

characteristic in early screening.[395] For the latter, gaining a better understanding of how the specific pathways and proteins differ in clinically effective CAR mediated cell activation is critical to being able both screening and design CAR constructs. As demonstrated in chapters 3 and 4, small changes in the binding region or regions can significantly impact the corresponding signal and fate of the cell, determining how well it kills a target, how well it proliferates and how it binds to its target, among others. Using a combination of mass spectrometry, RNAseq, and flow cytometry, we hope to identify targets that indicate a potentially successful candidate in the most accessible form of CAR, CAR-jurkats, allowing for a more diverse and reliable screening platform.

Through these studies we hope to understand what different kinds of CAR signals look like in a cell, potentially allowing for more targeted and specific screening in future development. As an example, perhaps you want to design a CAR that is very aggressive: highly cytotoxic and proliferates rapidly during the initial treatment. Normally, this might pose a safety concern, however, with a better understanding of CAR signaling and its relationship with its structure you could also design the CAR to not persist and to burn out quickly without sustaining itself, limiting its exposure to healthy tissue long term. With an even higher level of understanding it could be possible to tune the response to be more focused on tumor killing through perforin and granzyme and less on cytokine release, limiting the possibility of CRS. With the knowledge of what physiological changes lead to what downstream signals and effects, you could theoretically specifically select for this or any CAR and be confident that the end result will be what you designed it to be. By

understanding how different phenotypes of CARs signal, a CAR customized to target specific kinds of malignancy could be a possibility.

Another important piece of context in which these CARs are examined is their structure. The other CD22 CARs vary from our chosen baseline of 1ug36 in one of two ways. Primarily, these CARs vary from 1ug36 only in terms of binding region: the transmembrane domain, co-stimulatory domain and CD3ζ are identical. This means that all differences in efficacy and signal are due to difference only from this domain. While this may seem obvious, it is important to understand just how small the differences in sequence as highlighted in Table 5.1, with an average of 10 animo acid (AA) changes in the CDR3 region and the overall sequence length. As demonstrated above, these small changes in the sequence can significantly influence how and where the CAR binds to its target, as well as the downstream signal. The other way in which we are evaluating 1ug36, it through comparison from its screening version to its clinical one. While this backbone contains the same co-stimulation and CD3ζ regions, it does have a CD8 transmembrane domain instead of CD28 and the promoter region used to promote the CAR is the full version of EF1α instead of the shortened one. The comparison will allow us to identify how the transition to the clinical version impacts its downstream signal both at baseline, as well as when actively engaging a target.

Name	Sequence	Amino acid Difference from 1ug36
1ug36	QVQLVESGGGLVQAGGSLRVSCEASGITFSRAAMGWYRQRPGKERERVAVVNSDSSTIYADS VKGRFTISRDNAKNTVYLQMNSLEPEDTAVYYCWSPGFGSYWGQGTQVTVSSPLRDDGGGG SGGGGSGGGGSGGTTTPAPRPPTPAPTIASQPLSLRPEACRPAAGGAVHTRGLDFACDVVS	CDR1 region length:8AA CDR 2 region length:7AA CDR 3 region length: 8AA Non CDR AA Difference: N/A Total Length: 184

1ug13	QVQLVESGGGLVQAGDSLRLSCAGSGGSFSSVTMAWFRQAPGKDREFVAAITWSSPSTYYA DSVKGRFTISRDNAKNTVYLQMNSLKPEDTAVYYCAGGRTGRGTSADTDEYNYWGQGTQVTV SSPLRDDGGGGSGGGGSGGGGSGGTTTPAPRPPTPAPTIASQPLSLRPEACRPAAGGAVHT RGLDFACDVVS	CDR1 region length:8AA CDR 2 region length:9AA CDR 3 region length: 18AA Non CDR AA Difference:11AA Total Length:195
1ug74	QVQLVESGGGLVQAGGSLRLSCAGSGFTFDDYAMGWFRQAPGKEREVVSCMGSSDGATYY ADSVKGRFTISRDNAKNTVYLQMNSLKPEDTAIYYCAVDKPFYDGGYRYTCPVDFGSWGQGT QVTVSSPLRDDGGGSGGGGSGGGGSGGTTTPAPRPPTPAPTIASQPLSLRPEACRPAAGG AVHTRGLDFACDVVS	CDR1 region length:8AA CDR 2 region length:8AA CDR 3 region length: 21AA Non CDR AA Difference:8AA Total Length:198
1ug61	QVQLVESGGGLVQAGGSLRLSCAASMSSFSQYVMYWYRQAPGKQRELVATITSYSNTNYADS VKGRFTISRDNAKSIAYLQMDSLKPEDTAVYYCNAQYGSTFIRNHWDDWGQGTQVTVSSPLR DDGGGGSGGGGSGGGGSGGTTTPAPRPPTPAPTIASQPLSLRPEACRPAAGGAVHTRGLDF ACDVVS	CDR1 region length:8AA CDR 2 region length:7AA CDR 3 region length: 15AA Non CDR AA Difference:8AA Total Length:191

Table 5.1 Sequence variation in CD22 VHH sequences used in CAR constructs

5.3 – Evolution of methodology and prospective work

5.3.1 – CD22 CAR testing reveals 1ug36 as lead clinical candidate

The NRCs cancer immunology team has created a CD22 targeting CAR-T that has recently begun phase one clinical trials. While pre-clinical assessment definitively showed that the lead candidate, 1ug36, had superior *in vivo* efficacy, it has provided relatively little insight as to why this CAR was superior to the others tested alongside it. To better understand why 1ug36s successfully treated *in vivo* murine blood cancer, while the other CD22 CARs produced could not, it was decided that we would assess 1ug36 using proteomics. While the development process of all the CD22 CARs has been fully documented in *Discovery and preclinical development of a therapeutically active nanobody-based chimeric antigen receptor targeting human CD22* by McComb et al.[201] it will be described here in brief as well. 20 anti-CD22 nanobodies were generated from a male llama which was immunized with purified recombinant human CD22- extra cellular domain protein. The specificity of these sdAbs was confirmed using ELISA and SPR and showed that monomeric sdAbs had

equilibrium dissociation constants (K_D; binding affinity) ranging between 0.03 and 250 nM, with a median value of 3.6 nM. (Figure 5.1A) Next, anti-CD22 sdAb sequences were transferred into a modular CAR plasmid backbone via scarless cloning, as described above in chapter 3. These CARs were confirmed to be reactive to CD22+ positive Ramos and Raji cells, but not against CRISPR modified CD22 knockout Ramos cells, SKOV3 or K562 wild type cells both of which are CD22 negative.(Figure 5.1B) This was followed up with a live cell imaging cytotoxicity assay which produced variable results for both tumor suppression and proliferation based likely based on donor variability (not shown) and chromium release cytotoxicity assay which identified 1ug36 as the sole candidate who had comparable specific toxicity to the CD22 benchmark m971.(Figure 5.1C) This was followed by a pilot *in vivo* test using 1ug13 and 1ug36 in NSG mice. While mice treated here showed significantly higher survival in 1ug36 as compared to the unmodified T cell control, no group has above 50% survival past day 30. (Figure 5.1D) Based on these preliminary assessments, 4 CD22 CARs were chosen for further assessment: 1ug36, 1ug13, 1ug74 and Pas33 in a different backbone which was currently being used for a CD19 clinical trial, with the most significant change being that the transmembrane domain was changed from CD28 to CD8. When tested in a fully blind *in vivo* test, only NSG mice treated with 1ug36 or m971 had significantly increased survival when compared to unmodified control and only 1ug36, 1ug13 and m971 showing significantly lower tumor engraftment. (Figure 5.1E) 1ug36 also showed the highest rate of CAR-T expansion when examined in blood samples.[201] Based on these results, 1ug36 was selected as the lead candidate.

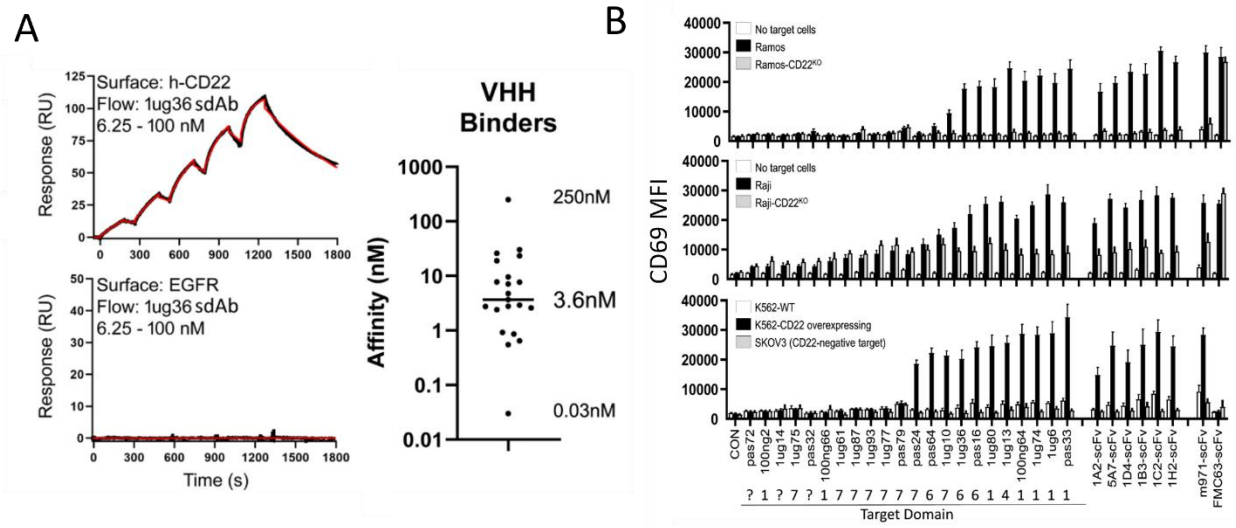
A
Surface: h-CD22
Flow: 1ug36 sdAb
6.25 - 100 nM
Response (RU)
Surface: EGFR
Flow: 1ug36 sdAb
6.25 - 100 nM
Response (RU)
Time (s)
VHH Binders
Affinity (nM)
250nM
3.6nM
0.03nM
B
No target cells
Ramos
Ramos-CD22KO
No target cells
Raji
Raji-CD22KO
K562-WT
K562-CD22 overexpressing
SKOV3 (CD22-negative target)
CD69 MFI
CON
pas72
100ng2
1ug14
1ug75
pas32
100ng66
1ug61
1ug87
1ug93
1ug77
pas79
pas24
pas64
1ug10
1ug36
pas16
1ug80
1ug13
100ng64
1ug74
1ug6
pas33
1A2-scFv
5A7-scFv
1D4-scFv
1B3-scFv
1C2-scFv
1H2-scFv
m971-scFv
FMC63-scFv
? 1 ? 7 ? 1 7 7 7 7 7 7 6 7 6 6 1 4 1 1 1 1 1
Target Domain

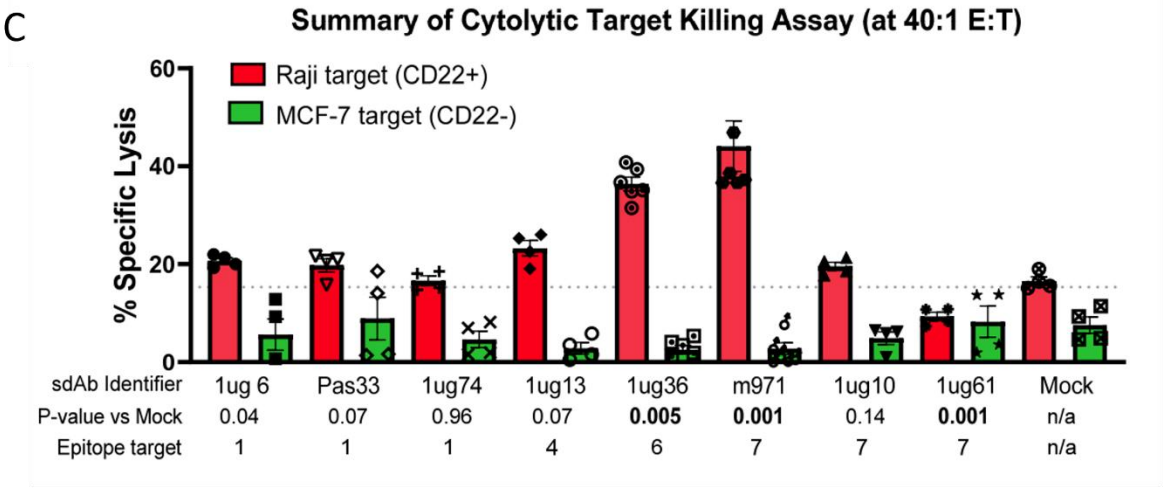
C
Summary of Cytolytic Target Killing Assay (at 40:1 E:T)
Raji target (CD22+)
MCF-7 target (CD22-)
% Specific Lysis
sdAb Identifier 1ug 6 Pas33 1ug74 1ug13 1ug36 m971 1ug10 1ug61 Mock
P-value vs Mock 0.04 0.07 0.96 0.07 0.005 0.001 0.14 0.001 n/a
Epitope target 1 1 1 4 6 7 7 7 n/a

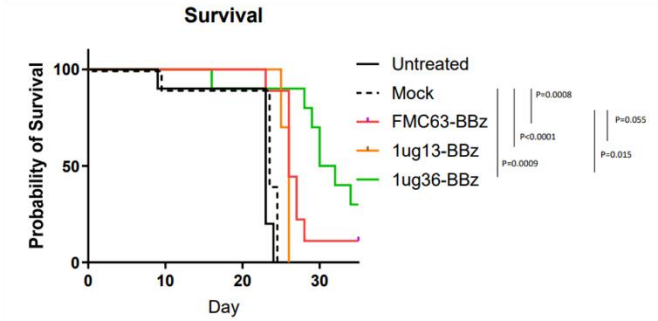
D
Survival
Probability of Survival
Day
Untreated
Mock
FMC63-BBz
1ug13-BBz
1ug36-BBz
P=0.0008
P<0.0001
P=0.0009
P=0.055
P=0.015

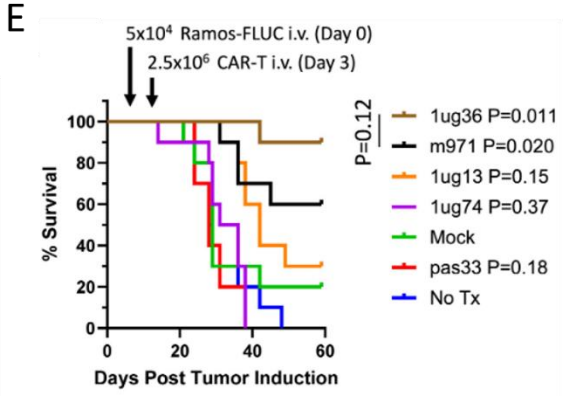
E
5x10⁴ Ramos-FLUC i.v. (Day 0)
2.5x10⁶ CAR-T i.v. (Day 3)
% Survival
Days Post Tumor Induction
P=0.12
1ug36 P=0.011
m971 P=0.020
1ug13 P=0.15
1ug74 P=0.37
Mock
pas33 P=0.18
No Tx

Figure 5.1 Summary of CD22-sdCAR lead selection

Summary of data regarding CD22 lead selection. **(A)** Representative SPR sensorgrams showing specific sdAb binding to immobilized CD22-ECD and distribution of 20 anti-CD22 sdAb equilibrium K_Ds. **(B)** Jurkat cells were electroporated with various CD22-sdCAR, CD22-scFv-CAR, or control scFv-CAR plasmids and immediately mixed at 1:1 E:T with various red fluorescent protein-marked target cells: Ramos or Ramos-CD22KO cells, Raji or Raji-CD22KO cells and K562-WT, K562-CD22-overexpressing, or irrelevant SKOV3 cells. After overnight coculture, cells were stained with anti-human CD69 antibody and assessed via flow cytometry. **(C)** CD22sdCAR-T cells tested for short-term cytolytic response via chromium release assay. Graph shows the mean cytolysis at 40:1 E:T ratio from both donors +/- SEM, P-values shows the result of a student T test comparison of specific Raji killing with unmodified (mock) T cells. **(D)** Preliminary in vivo testing with CD22sdCAR-T cells. Nod-SCID-IL2Rγ-null (NSG) mice were injected with 5x104 Ramos-FLUC cells and randomly assigned to cages, at day 3 post-tumor mice were injected with 5 x 106 total T cells for various CAR-T products or unmodified (mock) T cells (n=10 mice per group). Mice were monitored for by distress and euthanized at pre-determined humane endpoints. The number of surviving mice at each timepoint after tumour challenge is shown in survival graphs. P values show the comparison of survival for treatment groups via Log-Rank test. **(E)** Testing of CD22 CARs using CD8 transmembrane domain modification. Nod-SCID-IL-2Rγ-null (NSG) mice were then injected with 5×10^4 Ramos-FLUC cells and randomly assigned to cages. At day 3, cage groups were randomly assigned to treatment groups with 2.5×10^6 CD22 CAR-T cells or equivalent total dose of unmodified (mock) T cells (n = 10 mice per group). Mice were monitored for by distress and euthanized at predetermined humane endpoints. Graphs show the number of surviving mice at various time points. p values show the comparison of survival for treatment groups to untransduced mock T cells via the log-rank test. Figure adapted from *Discovery and preclinical development of a therapeutically active nanobody-based chimeric antigen receptor targeting human CD22* by McComb et al.[201]

5.3.2 – Trial of unlabeled co-culture analysis

To assess the unique properties of 1ug36, we initially evaluated it against its closest non-benchmark competitor in *in vivo* testing, 1ug13, while actively engaging targets. We prepared a sample of 100% CAR expression Jurkat cells with similar levels of CAR present on the cell surface by sorting the cells using a SONY MA900 Multi-Application Cell Sorter (Sony Biotechnology) combined with an anti-VHH stain whose MFI correlated with CAR surface expression. Enough CAR-Jurkat cells to produce a sufficient amount of protein for mass spectrometry analysis (~5 million cells) were then combined in a 1:1 co-culture with wild type Ramos cells, or CRISPR-Modified Ramos CD20/CD22 knockout cells. Cells were either combined and immediately, centrifuged, dried and flash frozen using dry ice (0 minutes of target exposure), or allowed to sit in co-culture at 37°C, 5% CO^2 for either 10 minutes, 30 minutes, 1,2,4,6,8,12,16,20 or 24 hours before undergoing the same procedure. Cells were then lysed in 2% SDS, and the protein was precipitated. A small portion of the protein was QCed and quantified using a Brantford assay to ensure that enough material was present. Sample protein was then digested using SP3 digest and the trypsin release fragment was recovered for analysis. 4138 unique proteins and 14313 phospho-peptides were identified, although the data sets often contained missing values making validation difficult. Some possible trends could be seen, including some differences between 1ug36 and 1ug13 between early exposure and late exposure, however the noise in the data made our confidence low (Figure 5.2). Additionally, while notable proteins of interest and controls such as CD69 could be seen being upregulated only

during later timepoint, the majority of the data, including those with notable differences appeared largely unrelated to T cell response. Large portions of the proteins identified were housekeeping or structural proteins, with many of the proteins of interest that have been known to be apart of the CAR signaling pathway were missing. It also became clear that using CD22- negative cells would not be sufficient as a control. Overall, the data produced was unwieldy, and difficult to parse with confidence, however we were able to demonstrate that assessing proteomic data was possible using an unmodified co-culture. Despite this, it was clear that modifications needed to be made to glean and useful information and additional controls were needed.

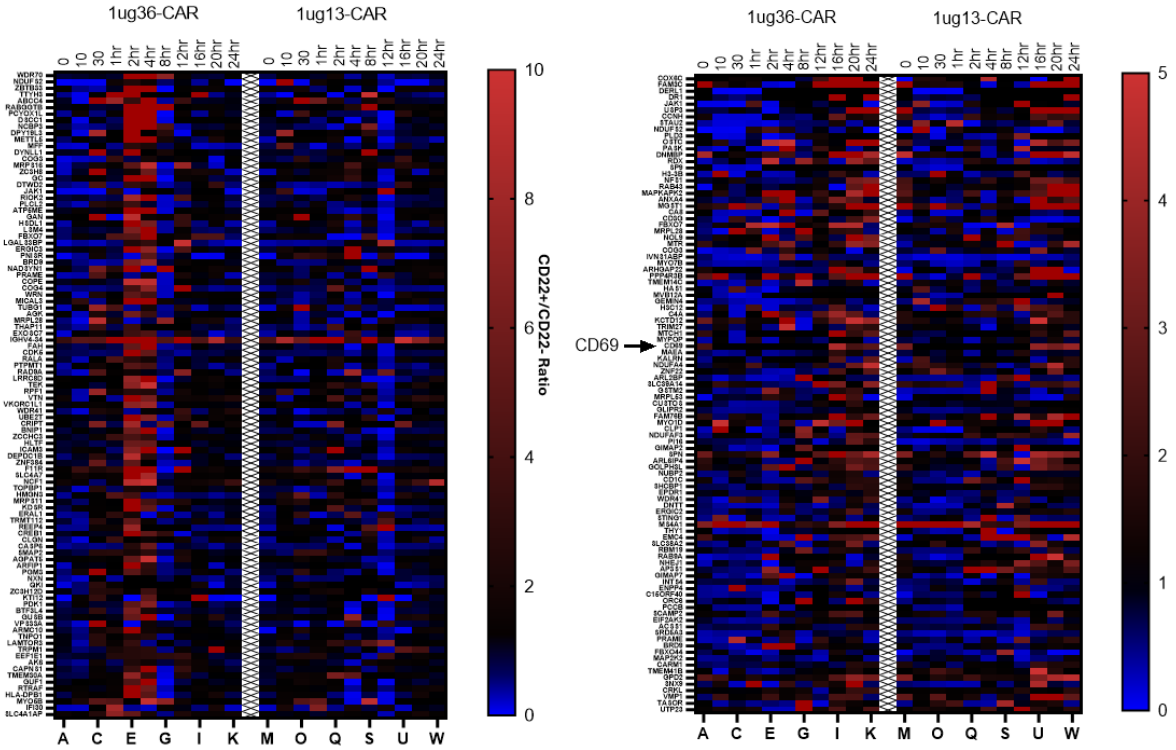

Figure 5.2. Early and Late Timepoint fold difference of top 100 expressing proteins in 1ug36 and 1ug13 with Ramos WT or CD22- Knockout co-culture

CAR-Jurkat cells were co-cultured with either Ramos wild type or CRISPR Ramos CD22 Knockout cell for 0 minutes, 10 minutes, 30 minutes, 1 hour, 2 hours, 4 hours, 8 hours, 12 hours, 16 hours, 20 hours, or 24 hours, before being flash frozen and prepared for mass spectrometer analysis. Samples analyzed using a Thermo Fisher Orbitrap Eclipse Tribrid Mass spectrometer using DDA analysis and normalized and identified using MatchRx. Heatmaps display top 100 proteins for the early timepoints (0 minutes to 4 hours) [left] and the late timepoints (16 hours to 24 hours) [right].

5.3.3 – Inclusion of additional CD22 CAR and transcriptomics to proteomic approach

In order to make the data clearer and easier to analyze, we decided upon adding several additional CAR-Jurkat samples for analysis, in the hopes that having several other comparators would allow for common trends to be found, as well as adding two controls a non-functional CAR, as well as unmodified jurkats. These were 1ug74, an extremely high

signaling CD22 CAR which was essentially non-functional *in vivo,* 1ug61, a CD22 CAR who antibody can bind CD22, but whose CAR cannot, Jurkat wild type cells, and 1ug36 and 1ug13 with the modifications made for clinical use (BCRx). Additionally, we added transcriptomic analysis, in the hope that common pathways could be found and correlated between analysis methods. Unfortunately, results were similar to the first round of analysis, with some potentially interesting trends being seen both in the transcriptomic and proteomic data, however issues with clarity and confidence made any follow up impossible; without more concise data or the ability to do volcano plot analysis using context provided from the proteomics data set it would be extremely difficult to glean any useful information that we could be confident in. Similar to the previous attempt, the data generated suffered from issues with large portions of the dataset being unrelated to the goal of the study, making trends difficult to observe as while potentially important markers such as CD22 or Cytotoxic and regulatory T cell molecule (CRTAM) can be assessed, the majority of the highly expressed markers found provide little to no relevant data. (Figure 5.3). While the value of the additional transcriptomic data and the additional CD22 clones was clear, it became apparent that data sets would have to be performed at a higher clarity, with more replicates in order to be useful.

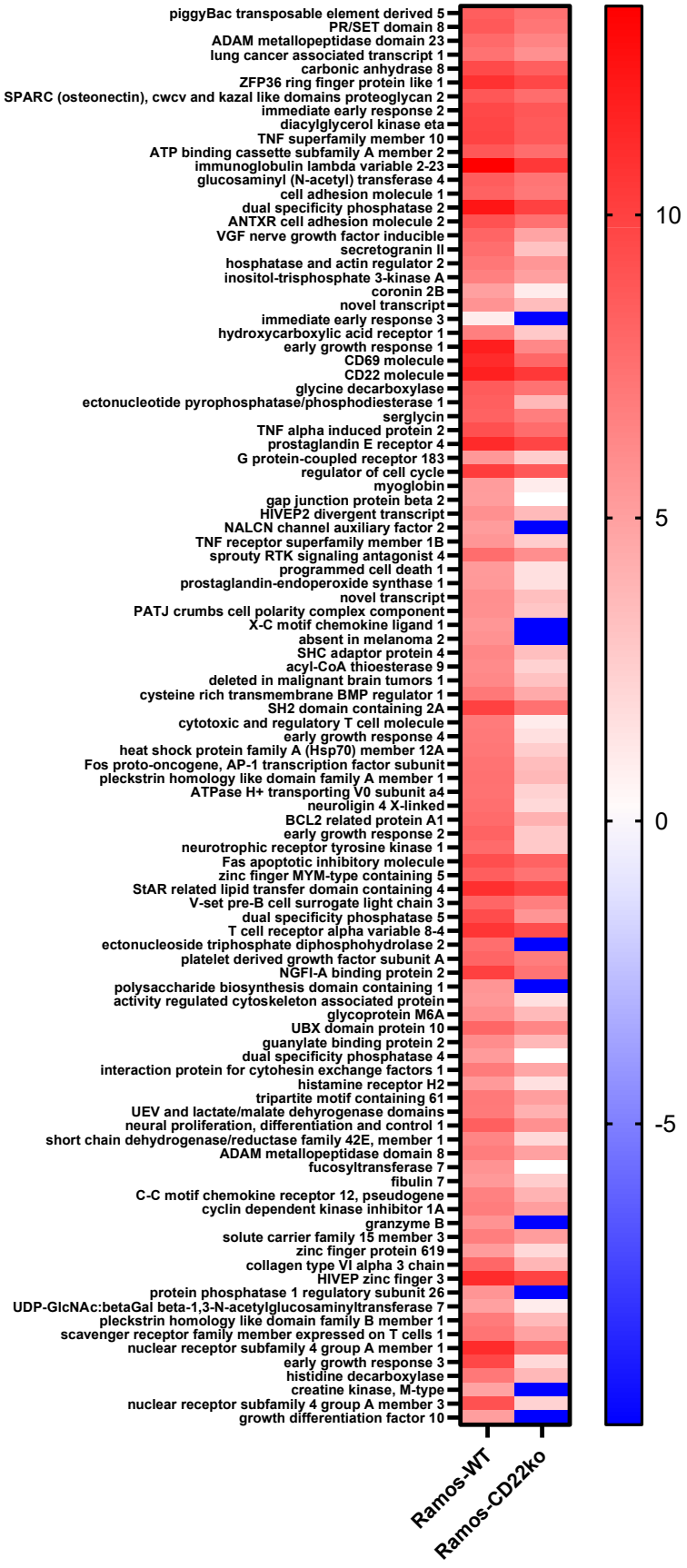
piggyBac transposable element derived 5
PR/SET domain 8
ADAM metallopeptidase domain 23
lung cancer associated transcript 1
carbonic anhydrase 8
ZFP36 ring finger protein like 1
SPARC (osteonectin), cwcv and kazal like domains proteoglycan 2
immediate early response 2
diacylglycerol kinase eta
TNF superfamily member 10
ATP binding cassette subfamily A member 2
immunoglobulin lambda variable 2-23
glucosaminyl (N-acetyl) transferase 4
cell adhesion molecule 1
dual specificity phosphatase 2
ANTXR cell adhesion molecule 2
VGF nerve growth factor inducible
secretogranin II
hosphatase and actin regulator 2
inositol-trisphosphate 3-kinase A
coronin 2B
novel transcript
immediate early response 3
hydroxycarboxylic acid receptor 1
early growth response 1
CD69 molecule
CD22 molecule
glycine decarboxylase
ectonucleotide pyrophosphatase/phosphodiesterase 1
serglycin
TNF alpha induced protein 2
prostaglandin E receptor 4
G protein-coupled receptor 183
regulator of cell cycle
myoglobin
gap junction protein beta 2
HIVEP2 divergent transcript
NALCN channel auxiliary factor 2
TNF receptor superfamily member 1B
sprouty RTK signaling antagonist 4
programmed cell death 1
prostaglandin-endoperoxide synthase 1
novel transcript
PATJ crumbs cell polarity complex component
X-C motif chemokine ligand 1
absent in melanoma 2
SHC adaptor protein 4
acyl-CoA thioesterase 9
deleted in malignant brain tumors 1
cysteine rich transmembrane BMP regulator 1
SH2 domain containing 2A
cytotoxic and regulatory T cell molecule
early growth response 4
heat shock protein family A (Hsp70) member 12A
Fos proto-oncogene, AP-1 transcription factor subunit
pleckstrin homology like domain family A member 1
ATPase H+ transporting V0 subunit a4
neuroligin 4 X-linked
BCL2 related protein A1
early growth response 2
neurotrophic receptor tyrosine kinase 1
Fas apoptotic inhibitory molecule
zinc finger MYM-type containing 5
StAR related lipid transfer domain containing 4
V-set pre-B cell surrogate light chain 3
dual specificity phosphatase 5
T cell receptor alpha variable 8-4
ectonucleoside triphosphate diphosphohydrolase 2
platelet derived growth factor subunit A
NGFI-A binding protein 2
polysaccharide biosynthesis domain containing 1
activity regulated cytoskeleton associated protein
glycoprotein M6A
UBX domain protein 10
guanylate binding protein 2
dual specificity phosphatase 4
interaction protein for cytohesin exchange factors 1
histamine receptor H2
tripartite motif containing 61
UEV and lactate/malate dehyrogenase domains
neural proliferation, differentiation and control 1
short chain dehydrogenase/reductase family 42E, member 1
ADAM metallopeptidase domain 8
fucosyltransferase 7
fibulin 7
C-C motif chemokine receptor 12, pseudogene
cyclin dependent kinase inhibitor 1A
granzyme B
solute carrier family 15 member 3
zinc finger protein 619
collagen type VI alpha 3 chain
HIVEP zinc finger 3
protein phosphatase 1 regulatory subunit 26
UDP-GlcNAc:betaGal beta-1,3-N-acetylglucosaminyltransferase 7
pleckstrin homology like domain family B member 1
scavenger receptor family member expressed on T cells 1
nuclear receptor subfamily 4 group A member 1
early growth response 3
histidine decarboxylase
creatine kinase, M-type
nuclear receptor subfamily 4 group A member 3
growth differentiation factor 10
10
5
0
-5
Ramos-WT
Ramos-CD22ko

Figure 5.3. Exemplary transcriptomic data of 1ug36 at 6 hours post co-culture
Comparison of 1ug36 CAR-Jurkat transcriptomic data from 6 hour co-culture with Ramos Nuclight wild type (left) or Ramos CD22 Crispr knockout (right). Samples were resuspended in Trizol solution before being flash frozen in dry ice before storage. RNASeq read generated using NextSeq500 with paired-end reads (2 x 75bp), targeting approximately 10 million reads per sample.

5.3.4 – Modifying approach to Data Independent Analysis and Cell Surface capture

Having done two consecutive trials which both resulted in noisy, difficult to parse data sets, it was clear that a more focused, specific approach was needed for proteomics. Instead of doing analysis of both cells in their entirety, we decided to focus our observations on the CAR molecule and the surrounding area, namely the cell surface. To do this, we used a technique called glyco-oxidization hydrazide capture. This is a modification of cell surface capture, known as direct cell surface capture. Here the cell surface proteins are oxidized using sodium meta periodate. This results in aldehyde groups which can be immobilized using hydrazide on a gel-based bead. These immobilized glycoproteins can then be digested with trypsin, or chymotrypsin and then peptides containing an N-linked glycosylation site can be released using PNGaseF. This change in preparation and digestion protocol allows for the majority of the cell to be excluded from analysis, resulting in a smaller, clearer data set, which focuses on the CAR and the interacting proteins.

The second change is with the analysis of the data by the mass spectrometer itself. Previous data sets processed with the mass spectrometer using an acquisition process known as Data Dependent Acquisition or DDA. In DDA the spectrometer performs MS1 analysis as normal and selects the most intense peptide ions to be fragmented and further analyzed in MS2. While this works for simple analyses, the spectrometers' decision to select proteins for MS2 analysis based on abundance can often lead to important, but less prevalent proteins being ignored. Given the complexity of the systems at play, as well as the lower relative abundance of the CAR proteins and its collaborators, it was possible that some important proteins were deprioritized. Thus, we changed the analysis to Data

Independent Analysis or DIA for the cell surface proteomics data. DIA uses Sequential window acquisition of all theoretical mass spectra (SWATH-MS), which uses a first quadrupole isolation window to step across mass ranges and collect a high resolution, full composite MS2 scan at each step. This ensures that all proteins are fully analyzed. While this does increase the amount of data, and the complexity of the data generated, it does increase clarity, and the size of the sample set should be offset by reduction in total protein count from the high specificity capture technique. For the phosphoproteomics data, a combination of DIA and DDA was used. While the DIA provided a more comprehensive data suite, the DDA software includes estimates for which site is being phosphorylated in the case of multiple potential sites in any given peptide. This combined approach allows for better overall analysis of phosphorylation patterns.

The latest approach combined the new methods above with two separate sample sets. The first was an unstimulated, triplicate sample set with each CAR but no targets. The other was a stimulated, triplicate sample set with four time points, 0 minutes, 10 minutes, 6 hours and 24 hours. Each of the samples for these sets were collected individually and underwent quality control testing prior to undergoing lysis and hydrazide capture or RNA extraction. Quality control testing included cell viability at time of sampling, CAR-Jurkat cell activation as assessed CD69 surface expression through flow cytometry and exact ratios of effector to target. The quality control measurement can be seen in figure 5.4.

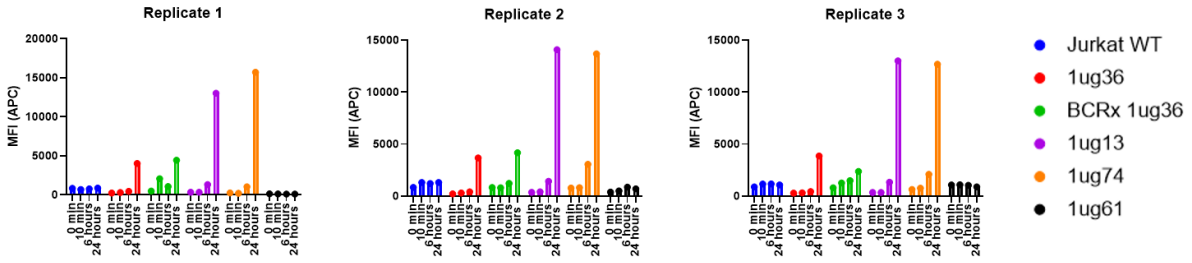

Figure 5.4. QC data for Triplicate Glyco-oxy cell surface samples
Data of triplicate quality control samples taken as an aliquot from the total volume before oxidization. Sample were immediately placed on at 4°C to halt any cell to cell interaction and kept at this temperature until stained with mouse anti-human CD69 APC antibody and assessed via flow cytometry. Samples that did not pass QC were immediately discarded. The full QC sheet can be found in Appendix 2.

5.3.5 – Prospective work for Glyco-oxy cell surface capture, phosphoproteomics and transcriptomics CAR-Jurkat data

While still in progress, some patterns can be observed in the initial data from each analysis method. The phosphorylation data found 6516 unique phosphorylation sites. Overall, the baseline set showed little difference between sample sets, with the changes between groups of samples being small enough to highlight differences between individuals of the same CAR. (Appendix 4) When examining preliminary findings from the stimulated samples sets several notable differences between CARs were noted. Using the standard KEGG TCR activation pathway and the cell signaling technology CAR signaling network pathways as reference points we could detect active phosphorylation in 21 of the total 43 proteins commonly associated with CAR or TCR signaling (~48%) [Appendix 4 A].[396] Of those that could not be found, five interactors could be found instead (ie. Calcineurin binding protein 1 [CABIN1] but no Calcineurin) and four similar proteins to those found in the standard signal pathway could be found (ie. Tumor necrosis factor associated factor 4 [TRAF4] but not TRAF2). Although not all the exact phosphorylation sites can be identified notable

differences in signaling between both binding site variation (36 vs 13 vs 74 vs 61) and transmembrane domains (CD28 vs CD8a) could be observed. These observations included higher CD28 phosphorylation of the y191 sites in higher signaling and binding CARs 1ug13 and 1ug74, indicating higher CD28 SH2 activity and PI3K recruitment.[397] While PI3K was not reported, this can be seen with the phosphorylation of a downstream protein, AKT, which shows higher activity in 1ug13 and 1ug74 post initial binding interaction(0 minutes). These CARs also had higher phosphorylation of LCK y505, a down regulatory tyrosine, which may indicate less CD45 activity with these CARs (Appendix 4 B and C). Another notable difference could be found in NFATc2 phosphorylation wherein all CD28 transmembrane domain CARs showed downregulated phosphorylation when compared to WT while the CD8a transmembrane domain BCRx 1ug36 was upregulated. An opposite effect was observed with ICAM-3 phosphorylation, with CD28TM 1ug36 showing higher signaling than its CD8a counterpart. Finally, 1ug36 showed higher LAT phosphorylation (likely s224) than all other samples, possibly indicating higher IL2 production.[398] 1ug36 also shows higher level of phosphorylation in several MAP kinases, as well as PLCγ1 (Figure 5.4B-C). It should also be noted that some of these pathways overlap with B cell pathways meaning that the target cell line used, Ramos, may be contributing to some of the increases in data seen, given that it is Burkitt's lymphoma B cell line. In theory, this can contribution can be equalized across all samples by normalizing the data using the ratio of targets to effectors as recording in the full QC measurements (Appendix 2), however it should be kept in mind while assessing the data. While still preliminary, these and other undiscussed changes in the data highlight critical differences in the CARs examined, allowing for better

understanding of the relationship between CAR structure and its impact on downstream signaling and function.

5.4 – Methods and Materials

5.4.1 Cell Surface Oxidization sample preparation

Solutions of 10mM sodium-meta-periodate and 200mM sodium sulphite were prepared using 6.5 pH PBS in advance. 100 million Jurkat WT cells and 100 million Ramos WT cells with a minimum viability 85% were combined in a co-culture, with 25 million of each cell being combined on ice (0-minute timepoint) and the remaining being combined in a T175 cell culture flask and returned to the incubator. Additional aliquots were taken at 10 minutes, 6 hours, and 24 hours post combination and immediately placed on ice to halt the reaction, 1ml samples were taken from the aliquots for quality control and transcriptomics. Aliquots were centrifuged on a pre-cooled centrifuge at 200g for 5 minutes at 4°C. The supernatant was removed, and the cell pellet was resuspended in 18mL of the sodium-meta-periodate solution, and tube was then covered in reflective foil to protect the solution from light. The resuspended pellet was transferred to a rotator for 10 minutes at 4°C. After 10 minutes had elapsed, add 1900ul of the sodium sulphite and place back on the rotator for another 6 minutes at 4°C. After the 6 minutes had passed, the sample was placed back in the pre-cooled centrifuge and centrifuged at 200g for 5 minutes at 4°C. The supernatant was removed, and the pellet was resuspended in cold 6.5 pH PBS. The sample was then centrifuged again at 800g for 3 minutes at 4°C. The supernatant was completely removed

from the pellet and the sample was then flash frozen using dry ice. Samples were stored at -80°C until ready for lysis. Quality control samples were stained with APC anti-CD69 and assessed by flow cytometry to ensure proper activation as well as record exact ratio of Ramos to Jurkat cells.

5.4.2 Cell lysis of non-oxidized pellets

Thaw cell pellets individually for lysis. Cell pellets should not be thawed unless immediately beginning lysis treatment to prevent proteins and phosphoprotein degradation. Cell pellets were lysed in 150µl of 2% SDS in PBS and 1/200 dilution of phosphatase inhibitor. Once lysis was underway 0.5µl of benzonase was added. The lysed pellet was then homogenized by passing it through a 1ml syringe, and the solution was then placed on a rotator for 15 minutes at room temperature. Next, the solution was centrifuged at max speed for 10 minutes to pellet any cellular debris and unbroken cells. A 40µl aliquot of the supernatant was taken for quantification and the remaining transferred to new 1.5ml tubes. Quantification was done using a standard detergent compatible protein assay.

5.4.3 Cell lysis of oxidized pellets

Thaw cell pellets individually for lysis. Cell pellets should not be thawed unless immediately beginning lysis treatment to prevent proteins and phosphoprotein degradation. Hydrazide coupling buffer of 100mM NaOAc, pH 5.5 and 150mM NaCl was prepared in advance. Cell pellets were lysed in 150µl of 2% SDS in hydrazide coupling buffer and 1/200 dilution of phosphatase inhibitor. Once lysis was underway 0.5µl of benzonase was added. The lysed pellet was then homogenized by passing it through a 1ml

syringe, and the solution was then placed on a rotator for 30 minutes at room temperature. Next, the solution was centrifuged at max speed for 10 minutes to pellet any cellular debris and unbroken cells. A 40µL aliquot of the supernatant was taken for quantification and the remaining transferred to new 1.5ml tubes. Quantification was done using a standard detergent compatible protein assay.

5.4.4 SP3 Digest

50µg of protein was transferred from each cell lysis sample into a new tube and the volume was brough to 50µl using 2% SDS in PBS. 1/10th of the volume (5µL) of 100mM dithiothreitol (DTT) solution [0.015g/ml in tetraethylammonium bromide, pH 8.5 or 50mM ammonium bicarbonate] was added to all samples, which were then heated to 80°C to reduce them, then allowed to cool to RT. Next, samples were alkylated by adding 1/10th of the volume (5.5µl) of 250mM iodoacetamide solution (0.015g/ml in tetraethylammonium bromide, pH 8.5 or 50mM ammonium bicarbonate) and incubated at room temperature in the dark for 30 minutes. The alkylation was then quenched using 1/10th of the volume (6µl) of 100mM DTT solution and incubating samples at room temperature for 15 minutes. During the quench, two types of SpeedBead Magnetic Carboxylate-modified particles (Cat# 65152105050250 & 45152105050250, Sigma) were combined in 1:1 ratio and washed twice with water, then resuspended in 625µl of water to make the concentration 20mg/ml. Beads were prepared so that 400µg of beads were available for each sample. Beads were added to each sample at a 10:1 ratio (~ 25µl) and homogenized using a pipette, then transferred to a 96 deep-well plate and covered using a foil plate cover for each of the remaining incubations. To induce binding to the beads the same volume (~91.5µl) of 100%v/v ethanol

was added to each protein/mag bead mixture and immediately mixed by pipetting up-down four times. This was then incubated at room temperature for 15 minutes, mixing again with the pipette at the 5-minute mark. Then a magnetic plate was used to bring the beads to the side of each well. The supernatant was removed, and the beads were washed three times using 250µl of 80% ethanol, letting each wash sit with the beads for at least 10 minutes. After the final wash two tubes of sequencing grade trypsin was added to 1325µl of 100mM HEPES buffer pH 8.5 and 63µl was added to each sample. The aggregated beads were then re-suspended in the trypsin solution and the plate was sealed with a heat-sealing film. Samples were incubated at 37°C overnight to full digest the proteins into peptides. Once the digestion was complete, the plate was quickly spun to ensure all liquid was in the wells and the liquid digested was separated from the beads using a mag plate and transferred to 1.5ml tubes and sorted at -80°C until ready to be placed on the mass spectrometer.

5.4.5 Hydrazide Capture

1mg of proteins was transferred from each sample to a new 2ml tube, then diluted to an SDS concentration of ~0.55% in 1300µl of hydrazide coupling buffer. Next hydrazide-gel beads were prepared. 50µl of beads were prepared per sample. To prepare, the beads were transferred to 1.5ml tubes using a P1000 with a cut tip to increase the size of the hole. This ensure the beads would not be broken when pipetted. Beads were washed three times in the maximum amount of volume of hydrazide coupling buffer, centrifuging at 1000g for 15 seconds between washes. The beads were divided equally into 1.5ml tubes and a final hydrazide coupling buffer wash was added and the beads were allowed to settle using gravity before use. When ready, the coupling buffer was removed from the beads using

p200 and the beads were resuspending in 600µ of sample using a cut p1000 tip. Beads were then mixed using gentle flicking and inversion before being incubated on a rotator overnight at room temperature. Following capture, the beads were allowed to settle using gravity, then the supernatant containing the unbound proteins was removed and stored at -80°C. Using a cut p1000 tip, resuspend the beads in 500µl of UREA buffer (8M UREA and 0.4M ammonium bicarbonate in water) and transfer to a mini-spin column. Then a vacuum manifold was used to wash the beads eight times using 500µl of UREA buffer and four times using 50mM ammonium bicarbonate. Next, 10mM DTT solution (0.015g/ml in tetraethylammonium bromide, pH 8.5 or 50mM ammonium bicarbonate) and 25mM iodoacetamide solution (0.015g/ml in tetraethylammonium bromide, pH 8.5 or 50mM ammonium bicarbonate) were prepared. 600µl of DTT solution was added to each sample, which were then inverted to mix and incubated for 1 hour at 56°C. The DTT was then spun out with a 15 second centrifugation at 0.8 rpm. Then 600µl of iodoacetamide solution was added, inverted to mix it, and then incubated at room temperature in the dark for 1 hour. The iodoacetamide was then spun out with a 15 second centrifugation at 0.8 rpm. The beads were then washed four times with 100mM HEPES buffer, pH 8.5, using the last wash and a cut p1000 tip to transfer the beads to a new 1.5ml tube. Next, 10 tubes of sequencing grade trypsin were mixed with 3.5ml of 100mM HEPES buffer, pH 8.5. The beads were centrifuged at 0.8 rpm for 15 seconds and all of the remaining buffer was removed, then the beads were resuspending in 300ul of trypsin solution. The beads were then incubated at 37°C overnight without rotation. While the incubation was ongoing, new mini-spin columns were incubated overnight at 4°C with 600ul 100mM HEPES buffer. Post

incubation, the storage buffer was spun out and column was rinsed twice with 100mM HEPES buffer. The trypsin digested beads were then transferred to the prewetted column using a cut p1000 tip. The trypsin release fragment was then collected with a 15-minute spin at 0.8 rpm. This was stored at -80°C. The beads then underwent the following washes, with a centrifugation at 0.8 rpm to remove each wash solution: three washes with 600µl of 1.5M NaCl, three washes with 600µl 60% ACN, 0.1% TFA solution in PBS, three washes with 600µl Methanol and finally six washes with 500µl of 50mM ammonium bicarbonate. After washing the beads were transferred to new 1.5ml tubes using 500µl of 50mM ammonium bicarbonate. Then, 50mM ammonium bicarbonate (100µl/sample) and PNGase F (2 µl/sample) were mixed and added to the beads, after the transfer buffer was removed. The beads were then mixed by flicking and incubating at 37°C in a rack with no rotation overnight. Finally, the digested supernatant was transferred to a new 1.5ml tube. The beads were washed twice with 100ul of 50mM ammonium bicarbonate and the resulting supernatant combined with the previously removed supernatant. The supernatant was then run through pre-wetted (50mM ammonium bicarbonate) mini-spin column using a 20 second, 0.8 rpm spin to remove any gel particles. The samples were then speed-vacced down to ~60µl and 2µl of trypsin was added to the sample to digest any remaining PNGase F. This is the N-linked fragment, which was stored at -80°C until analysis.

5.4.6 RNA extraction

Note: this protocol is a version of the official protocol for the Direct-zol™ RNA Miniprep Kit (Zyme Research Cat #R2070T,R2070, R2071 R2072 or R2073) which has been shortened for brevity. The full version of this protocol can be found here: https://files.zymoresearch.com/protocols/_r2070t_r2070_r2071_r2072_r2073_direct-zol_rna_miniprep_plus_kit.pdf

Samples were placed and stored in Trizol® Solution during collection, thus step II (Sample preparation) as outlined in the protocol has been omitted here

Buffer preparation was performed on a per kit basis due to the varying level of preparation needed per kit.

An 300µl of 95-100% ethanol was added to each sample and mixed thoroughly. Samples were then transferred into a Zymo-Spin™ IIICG Column in a collection tube and centrifuged at max speed until the entire volume had passed through the column (~30 seconds). The flow through was then discarded. 400µl of RNA Wash buffer was added and spun through the column. 5µl of DNase1 and 75µl DNA Digestion Buffer were added directly to the column matrix and incubated at room temperature for 15 minutes. 400µl of Direct-zol™ RNA PreWash was added to the column and spun through. The supernatant was discarded, and this wash was repeated an additional time. 700µl of RNA Wash Buffer was added to the column and was centrifuged for 1 minute at maximum speed. The flow through was discarded. The column was moved to an RNase-free tube and 100µl of DNase/RNase-free water was added directly to the column matrix and centrifuged. The flow through was set aside until library construction.

5.4.7 RNA library construction

Note: this protocol is a version of the official protocol for the NEBNext UltraExpress® RNA Library Prep Kit (NEB #E3330S/L) which has been shortened for brevity. The full version of this protocol can be found here: https://www.neb.com/en-ca/-/media/nebus/files/manuals/manuale3330.pdf?rev=3e4fe10bb8b34f0c90d36a5055eda1a1&sc_lang=en-ca&hash=C167D4A37CEE85421FCC32C62BB5A635

The express protocol (1A) was used for this assay. All manufacturers' instructions were followed.

Before performing this protocol, RNA quality should be assessed. Only RNA with an RNA Integrity Number (RIN) of 7 or higher should be used.

RNA samples were diluted to a final volume of 50µl in a nuclease-free 0.2 ml PCR tube and kept on ice. 20µl of NEBNextOligo DT25 beads were added a separate 1.5ml tube (one per sample), mixed, then placed on a magnetic rack at room temperature until the solution became clear. The supernatant was removed, and the beads were washed with 50µl of NEBNext RNA binding buffer (2X) and placed back on the magnetic rack until the solution became clear. The supernatant was removed, and 50µl of NEBNext RNA binding buffer (2X) was added to the beads and mixed until homogeneous. 50µl of beads was added to each RNA sample. Each sample was then heated using a thermal cycler with the following program: 2 minutes at 80°C, 5 minutes at 25°C, Hold at 25°C. Samples were then placed back on the magnetic rack until the solution became clear. Supernatant was removed, and the samples were washed using 200µl of NEBNext Wash Buffer. The buffer was then removed, and the beads were suspended in a mix of 50µl of NEBNext Tris Buffer and 50µl of NEBNext RNA Binding Buffer (2X). The tubes were then heated using a thermal cycler with the following program: 2 minutes at 80°C, 5 minutes at 25°C, Hold at 25°C. Samples were then placed back on the magnetic rack until the solution became clear. Supernatant was removed, and the samples were washed using 200µl of NEBNext Wash Buffer. The buffer was then removed, and the samples were removed from the magnetic rack. 6.5µl of 1X Fragmentation Master Mix was added to each sample and mixed. Samples were then heated using a thermal cycler with the following program: 15 minutes at 94°C, Hold at 4°C.

Samples were quickly spun in a microcentrifuge and 5µl of supernatant was transferred into a fresh nuclease free tube.

Next, a master mix of NEBNext UltraExpress Strand Specificity Reagent (4µl per sample) and NEBNext UltraExpress First Strand Enzyme Mix (1µl per sample) was prepared and added to each sample. Samples were mixed, then headed using a thermal cycler with the following program: 10 minutes at 25°C, 10 minutes at 42°C, 5 minutes at 70°C, Hold at 4°C. 30µl of NEBNext UltraExpress Second Strand Master Mix was added to each sample, mixed then heated using a thermal cycler with the following program 30 minutes at 16°C, Hold at 4°C.

72µl of AMPure or SPRIselect Beads were added to each sample, mixed, then incubated at room temperate for 5 minutes. Samples were then placed on a magnetic rack, and the supernatant was removed. Samples were then washed 3 times using 200µl of 80% ethanol, after which the beads were allowed to air dry. Samples were then removed from the magnetic rack and 22µl of 0.1X TE buffer was added to each sample then vortexed. Samples were incubated for 2 minutes at room temperature, then placed back on the magnetic rack. Once the solution became clear, the 20µl of supernatant was transferred to a new tube. 2.5µl of NEBNext UltraExpress End Prep Reaction Buffer and 1.5µl of NEBNext UltraExpress End Perp Enzyme Mix were added to each sample. Samples were mixed, then heated using a thermal cycler with the following program: 5 minutes at 20°C, 10 minutes at 65°C, Hold at 4°C.

2µl of Diluted Adaptor and 12µl of NEBNext UltraExpress Ligation Master Mix were added to each sample, mixed, then heated using a thermal cycler with the following program: 15 minutes at 20°C, Hold at 4°C. 2µl of NEBNext UltraExpress USER Enzyme was added to each sample which was then heated using a thermal cycler with the following program: 5 minutes at 37°C, Hold at 4°C.

Next, 50µl of NEBNext MSTC High Yield Master Mix and either 5µl of Index (X) Primer and Universal Primer or 10µl of Index Primer Mix were added to each sample depending on which product was available. Samples were mixed, then underwent the following PCR cycling conditions in a thermal cycler: 98°C for 30 seconds (1 cycle), 98°C for 10 seconds, then 65°C for 75 seconds (12 cycles), 65°C for 5 minutes (1 cycle), Hold at 4°C

Finally, 70µl of AMPure or SPRIselect Beads (Same as previous step) were added to each sample, mixed, then incubated at room temperate for 5 minutes. Samples were placed on a magnetic rack, and once the mix became clear, the supernatant was removed and discarded. Beads were then resuspended in 50µ of 0.1X TE buffer and 40µl of NEBNext Bead Reconstitution Buffer, vortexed and incubated at room temperature for 5 minutes. Samples were placed on a magnetic rack, and once the mix became clear, the supernatant was removed and discarded. Samples were then washed 3 times using 200µl of 80% ethanol, after which the beads were allowed to air dry. 23µl of 0.1X TE buffer was added to each sample then vortexed. Samples were incubated for 2 minutes at room temperature, then placed back on the magnetic rack. Once the solution became clear 20µl was transferred to a fresh tube and stored at -20°C.

5.5 – Discussion

Despite its success as a patient specific therapeutic, the key factors which differentiate an effective CAR from those that fail in pre-clinical or clinical testing remain unknown. Proteomic and phosphoproteomic analysis have emerged as key methods in better understanding CAR signaling pathways, but often heavily rely on bead-based antigen display for stimulation, or isotope labeling and/or cell sorting in order isolate T cells for clearer results.[387,399] These studies also primarily focus on focus on mapping existing signaling pathways in comparison to the TCR, or focus on domains such as co-stimulatory with only short term timepoints used for sampling, examining the differences between on and off, as opposed variations between CARs.[400,401] Here, we have begun developing methodology to successfully examine the signaling and abundance patterns in CAR proteins using live, unmodified cells during co-culture. With further improvement, this should allow for a complete examination of CAR-Target interaction, including immune synapse formation, and should result in a more complete signal analysis. While still under investigation, we hope that the results of this trial and future improvements will yield insights into how the binding domain of the CAR affects the cytotoxic and proliferative function of the CAR but also identifies proteins of interest which can used to better select CAR proteins during early screening and discovery.

Due to the complexity of combining two separate cell samples with no internal labeling, a standard bulk proteomics approach proved to not be feasible. As such, narrowing down the field of analysis to the n-linked fragment produced by glycol-oxy cell surface capture produced a somewhat happy medium, allowing for focus on the CAR protein and its

immediate interactors near the cell surface while excluding the majority of the cell. This, combined with a DIA approach to data collection, gave us a clearer, focused data set containing the CAR and some of its interactors. This approach does come with some limitations, however. To start, while identifying many proteins and phosphorylation sites, this approach was only able to record half of the commonly understood signaling pathway, including many transcription factors. While this may be a sampling issue, it is likely that the exclusion of the majority of the cell removes access to some of these important pathways, specifically those that are not transported to the cell surface during activation. The inclusion of RNAseq transcriptomic analysis may be able to supplement this missing data however this analysis comes at significant cost, both in terms of time of money. Cell surface capture also adds several layers of difficulty to the process of sample preparation, with the capture process requiring upwards of 72 hours and requiring the use of fragile agar-based beads. Despite these limitations, we believe this method provides the most informative and accurate detection of effector target interactions, minimizing interventions that might cause changes to cell viability or activity, and allowing for true assessment of cell-to-cell interaction and downstream signaling; capturing minutia that may not be present with antigen bound beads. Using the lead CD22 CAR 1ug36 as a comparator for other CD22 CARs, our preliminary data seems to identify changes in protein and phosphorylation patterns which diverge from other CARs and may allow us to identify key proteins of interest to include in future screening.

CHAPTER 6: DISCUSSION AND CONCLUDING THOUGHTS

6.1 – Improving CAR-T through better binding domain selection

As has hopefully become clear from the work discussed in the above chapters, subtle properties of the CAR-T binding domain determine how a CAR behaves in the absence or presence of target antigen and have a major impact on the overall efficacy of a CAR based therapeutic. We see in the results reported here and in published works,[201] that CD22 1ug36 results in an exceptional *in vivo* response, unlike the other CD22 CARs tested alongside it, but we do not have complete understanding of what subtle properties underlie its functional superiority. Similar trends can be seen the MSLN data presented in chapter 3, with the subtle properties of TP7-56 that are not apparent in *in vitro* screening leading to better *in vivo* effect. Both studies also find very little correlation between standard antibody assessment metrics such as affinity (K_D) and how they perform in the context of a CAR ABD, presenting a clear need for CAR specific ways to evaluate the ABD.

To this end the avidity testing developed in Chapter four presents a novel method to evaluate a new quality in CARs which directly involves the ABD and how it binds: cellular avidity. Unlike affinity, which has been commonly used to evaluate CAR-T in the past, cellular avidity assesses the CAR in a cell to cell interaction, not solely as an antibody.[402–404] Here I report on my work to develop a novel method for determining CAR cell avidity allowing for insight into the biological and kinetic interactions between the binding domain and the antigen epitope to which it binds, an evaluation metric which has recently become more prevalent for CAR-T.[373,405] This work uncovered a unique quality which seems to emerge from subtle properties of the binding domain, namely the maximum binding

capacity of the CAR-T cell. This maximum binding capacity is defined by the point where an equilibrium is reached between bound CAR cells in doublets, and unbound CARs in the presence of a super excess of antigen positive targets, although the underlying mechanisms enforcing this equilibrium still remains unclear. These results shown in chapter four, combined with the data generated in chapter five's multi-omics approach, suggest that where and how CAR cells bind to their target directly impacts downstream cell signaling, and ultimately how well a CAR can respond long term to a malignancy.

The immediate impact of a different binder can be directly seen with the differences seen between 1ug13/1ug74 and 1ug36 with the multi-omics data showing differences in how CARs with a high binding maximum (13 and 74) may potentially have less CD45 re-engagement, reducing signaling through LCK and increasing signalling through CD28. Although still preliminary, it is tempting to speculate about the relationship between binding properties and downstream signaling. As observed in TCR binding and discussed above[204], CARs may have an optimal on-off rate for binder engagement, also known as dwell time, which changes depending on the avidity of the binder being used. Higher avidity CARs with easier epitope access may over engage their targets too quickly generating an incomplete signal though CD3ζ. CARs with lower avidity and less accessible epitopes, have a more optimal dwell time, and adequate off time between serial engagements. This is supported by the preliminary finding from the omics data set, showing high LCK y505 phosphorylation on 1ug13 and 1ug74, while 1ug36 shows high LAT and MAPK phosphorylation, suggesting that the higher avidity CARs do not allow CD45 to dephosphorylate LCK post bind, reducing the extent to which LCK and ZAP70 are

phosphorylated and instead phosphorylating CD28. Should the omics results prove consistent, this hypothesis could be further explored through the study of 1ug10, another CD22 CAR which binds the same epitope as 1ug36 and has similar levels of avidity, but less cytotoxicity. Notably, these insights may be CD22 specific and may indicate that binder access and avidities effect on CAR signaling and dwell time requires investigation for each antigen. Antigens such as mesothelin, which are GPI anchored and have large, easily accessible extra cellular domains, may have similar levels of avidity across all binders, or may have avidity change based on yet unknown qualities of the ABD.

6.2 – The impact of additional binding domains on CAR-T function

In addition to exploring the role of the binding domain in CAR signal and function, this thesis also examines the effects of how the presence of multiple binding domains, in either co-expression or tandem, changes the efficacy and functionality of a CAR. The platform created allows for the high throughput screening of both combination types but highlights the effectiveness of the co-transduced format of multi-car *in vivo,* although the tandem format has been shown to be successful by other groups.[227,235,350,353]Here, the subtle nature of CAR traits appears again, with the platform clearly demonstrating that combining two or more CARs always impacts the final product in unpredictable ways that are only apparent in more complex *in vivo* studies. While I cannot report any consistency in the changes brought about by combination, what is clear is the need to individually assess combinations as a new, unique treatment option. Additionally, while the subtle changes introduced by the combination of CARs remain difficult to predict, I have demonstrated that these changes can both improve and hinder CAR-T *in vivo* effect.

6.3 – CAR-T screening, assessment and evaluation

Based on the experimental results outlined in this document it is clear that we are still far from the optimal way to assess and develop CAR-T. The current testing paradigm is primarily comprised of testing *in vitro* and *in vivo* efficacy through killing cancer cells in various states. Despite the heavy use of these assays, we continually see very little consistency between how a CAR performs in Jurkat functionality screening, primary cell *in vitro* cytotoxicity and *in vivo* tumor burdens and mouse survival.[153,201,406] This makes CAR-T development analogous to playing slots; we go through the necessary steps to get the wheels to spin, showing that the construct is functional and can kill a tumor in a dish and maybe in a mouse, but we haven't opened the machine up to examine the insides so we can tilt the odds in our favour. Differences in CARs can be noted but currently are not informative enough to act upon in a meaningful way without further understanding of the system in which they occur and are often so subtle that they remain undetected until *in vivo* studies or later. The current CAR-T testing paradigm also ignores the major differences between *in vitro* and *in vivo* studies, as the transition from a dish to a living breathing organism marks a massive shift in complexity.[407] *In vitro* studies represent an optimized environment in which CAR-T cells are forced to interact with their target and provided an excess of nutrients, while *in vivo* present a complex, dynamic system in which CAR-T must locate and traffic to the tumor. Once the T cells have infiltrated the TME they then face a host physiological barriers such as hypoxia and competition for resources, along side immunosuppressant chemokines, receptors and toxic metabolites, all of which are extremely difficult to replicate outside of a body.[407,408] The gap between these systems are

also difficult to close; our own attempts to improve the scope of *in vitro* testing by continuously stimulating CAR-T cells to more closely mimic a tumor environment resulted in failure; CAR-T cells generated from multiple donors failed to response to targets or display any sort of exhaustion markers over the course of 6 weeks, despite showing favourable *in vivo* results. Overall, while improving *in vitro* is by no means impossible, it is clear that other metrics of assessment are also needed to better understand the response profile of a CAR-T therapy. Currently, the standard screening platform for CAR-T can only really assess whether a CAR can function, but not how or in what way. This is still important; ensuring a CAR is functional and responsive allows us to screen out non-functional candidates and allows us to test several important metrics such as transduction efficiency, but should be part of a more intensive process, not the entirety of it.

Through the work performed in the latter half of this thesis, I hope to assist in the process of deeper examination into the inner working of CAR-T, bettering our understanding by introducing new tools and methodologies for examining an extremely complicated, living, moving system. While the steps outlined above are necessary for the testing of CARs, identifying new ways to assess CARs and new targets or pathways of interest for screening is key to both making CAR-T to uncovering and understanding the difference which separate successful candidates from the rest. To this end, I have worked to develop multiple novel screening targets, using cellular avidity and identifying potentially key signaling markers in early cell signalling that help identify how a CAR will perform against a tumor. These assays and markers have the potential to not only find functional CARs but also give some insight into how the CAR signal will influence the cell and are a step in the

direction of a CAR fully designed for a specific target. As an additional upside, avidity testing is extremely fast, requiring only 30 minutes of incubation time, as opposed to the 24 hours required for CAR-J or the 2 weeks required for most *in vitro* testing. Based on the preliminary data from the multi-omics testing, the markers highlighted there could also be assessed quickly, as most phosphorylation occurs very quickly after binding.

A prime example of the potential of these tools and methods is my deep examination of the lead CD22 CAR 1ug36 alongside the rest of the CD22 cohort. As briefly described in chapter 5.3.1, 1ug36 was chosen as the CD22 lead after significantly better performance *in vivo* than the other CD22 CARs tests along side it. Despite this, the majority of the *in vitro* testing performed showed most of the CD22 CARs as relatively equal, with only Cr^{51} release showing any major differences. When tested using avidity, a notable difference in 1ug36 was immediately identified, showing it as a low to medium avidity CAR while all but one of the other CARs showed high avidity. Unlike affinity, which is antibody specific, cellular avidity's assessment of the entire cell to cell interaction allowed us to recognize that the manor in which 1ug36 was binding to CD22 was different from the other CARs and may contribute to its success *in vivo*. When combined with the analysis done in chapter five, we can potentially identify certain differences in how 1ug36 signals and interacts with its targets, with notable differences in CD45 associated phosphorylation sites and regulatory adhesion proteins such as ICAM3. 1ug36 differing activity as demonstrated in chapter 5 lends credence to the previously postulated goldilocks zone: that too strong of a signal, like those of 1ug74 and 1ug13, is actually detrimental to CAR activity. The ease of access to epitopes 1 through 4 likely allows for either too much signal, or too rapid reengagement of

the CAR, changing the downstream signals as CD45 cannot fulling reengage and dephosphorylate LCK. Conversely, 1ug61s lack of binding as seen in chapter 4, provides an easy explanation for the lack of change seen in chapter 5; the CAR cannot access the binding site, likely due to steric hinderance, or if it can, it cannot bind effectively enough to stimulate a T cell response. Finally, 1ug36 lands in the sweet spot: the less accessible epitope of CD22 epitope 6 give it a lower overall signal as seen in chapter 5, but its lower overall activity and lower avidity allow for the CAR to upregulated different signaling pathways, signaling through MAP kinases and LAT, as CD45 is allowed enough time to full reengage. While still preliminary, the data and context provided by both avidity testing and the various omic assessments may provide a much clearer picture as to why 1ug36 performed better *in vivo* than other CD22 CARs. Should these observations remain consistent throughout repetitions, this optimal signaling range will impact how we assess CARs in early screening. If an optimal signaling zone can be determined, CARs can be screened for properties that give it the highest chance of landing in that spot, as opposed to the previous methodology which simply tests for functionality and high activation.

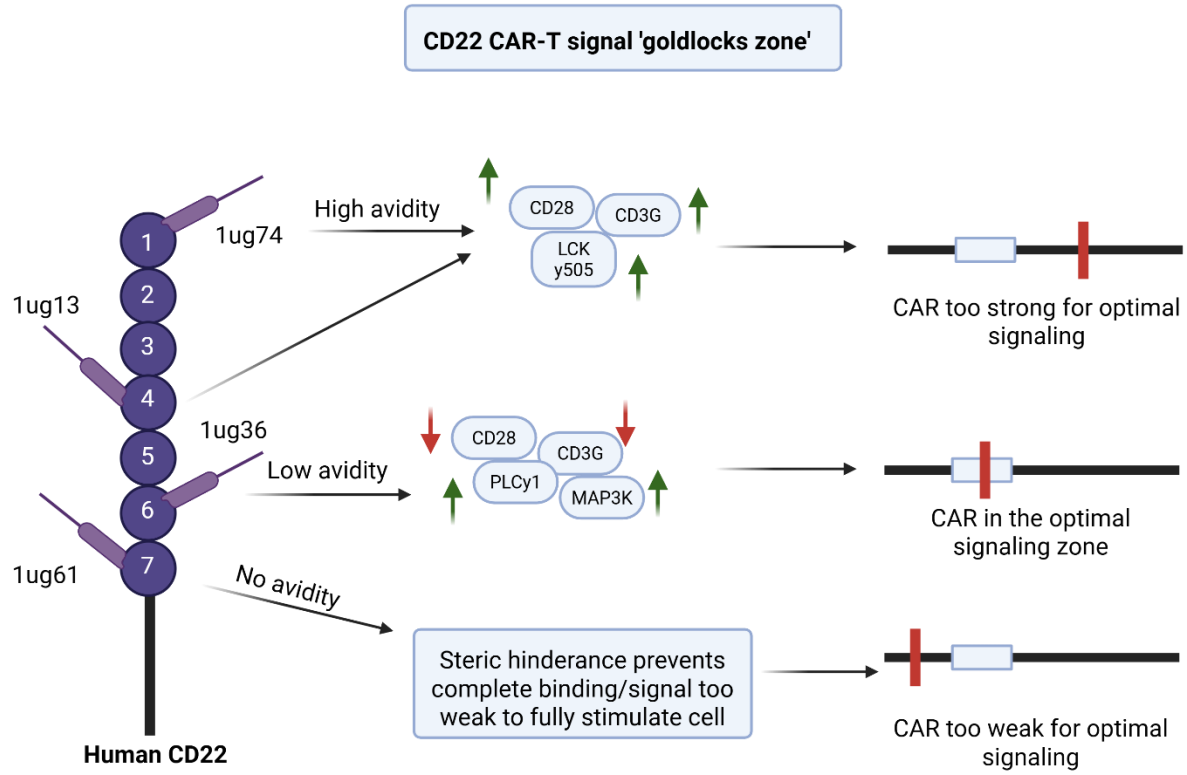

Figure 6.3 – Representation of the goldilocks zone for CAR signaling.

6.4 – The relationship between structure of a CAR and its function

One of the central problems with CAR-T and its development is that the relationship between the structure of a CAR and how it is going to function is unknown. While we possess surface level knowledge on the subject, we lack a deeper understanding about why these functional changes result in a certain phenotype. The CAR co-stimulatory domain is a primary example of this with 4-1BB often resulting in persistent, longer lasting CARs, and CD28-CAR typically results in aggressive, shorter live cells. Differences in cytokine release and varying adverse effects have been observed between the two as

well.[409] The differences between how this change in co-stimulatory domain affect CARs function has been studied extensively, however the reason as to why 4-1BB or CD28 as a co-stimulatory domain result in these phenotypes has only recently begun to be studied thoroughly.[410] The same can be said for the observations made regarding the binding region; we have observed differences in avidity, cytotoxicity, proliferations and cytokine release caused exclusively by a change in the binding region but are just beginning to explore why these changes occur. Due to this, we currently lack the knowledge required to make meaningful decisions in development for either of these regions.

Another important distinction that is necessary to recognise is that CAR is a cellular therapy. Unlike most chemical pharmaceuticals which interact the same way with a given receptor every time for the vast majority of people, a CAR is a synthetic protein which harnesses a complicated system inside a cell that is unique to the patient. As such, examining changes brought about by a modification of the CAR protein must be presented in the context of the entire cell. We can see from table 1.1 that the literature shows that every part of the CAR can impact every relevant part of the signal it produces, and thusly a change to any part, affects every part. A better understanding of the entirety of the signal and the contributions of each individual domains impact is the key to designing and producing CARs that are safe, effective, and specific. To this end, data presented in the fifth chapter of this thesis, along with similar studies, should hopefully serve as a stepping off point, allowing for key differences CAR binders and transmembrane domains to be observed. From here, these differences can be further studies with the goal of identifying what specific signaling changes specific changes to each domain impact.

6.5 – Defining a ‘good’ CAR protein

Ultimately, the work here is a contribution towards defining what it meant to be a ‘good’ CAR protein. The current definition is hazy at best: a good CAR achieves durable, complete remission in a patient with a malignancy that highly expresses the targeted antigen and is safe enough to administer without a high risk of severe side effects. This definition, however, lacks substance: a way to define CARs beyond the long-term survival rates, and does not lump all CAR into a singular category, regardless of context or disease treated. To better clarify how to define a good CAR we require a better understanding of how physiological changes affect how the CAR and cell function, as well as how the molecule itself interacts with both the cell it is a part of and the target molecule. Additionally, there are several questions that should be included, such as how much bystanding killing should a CAR engage in? How much persistence should a CAR have? When should a CAR be administered? A clearly defined set of characteristics which makes a CAR ‘good’ has some semblance of shape, but currently there are still too many unknowns to truly define it.

It can also be argued that being able to better define what a good CAR is or improving CAR-T design philosophy requires a reimagining of what success for CAR-T looks like. While current CAR-T therapy is often described as ‘personalized’, the treatment is still very much a general, one size fits all approach. As such, CAR-T, like most other treatment options a CAR that is a ‘good’ CAR for some patients, may do nothing for others. This makes defining a good CAR impossible by these standards; a treatment is only good if it works consistently. Instead, future CAR-T treatment and design could be focused around actual personalized therapeutics; by understanding how modifications to each part of the CAR affect its

function it could be possible to design a custom CAR that is best suited to treat the disease at hand. In this model, a malignancy and the patients cells could be phenotyped and a CAR designed and created specifically targeting that cancer, allowing for the most effective and precise therapeutic with the highest chance of success.[411] Moving from designing 'good' CARs to designing the right CAR will require a shift in both how the field examines and designs CARs, but also how we ascribe a treatment to a disease. We will need a much more complete understanding of how CAR-T functions, as well as how the components fit together to make that function happen. However, with this approach, I truly believe that CAR-T could become the personalized therapeutic we claim it to be.

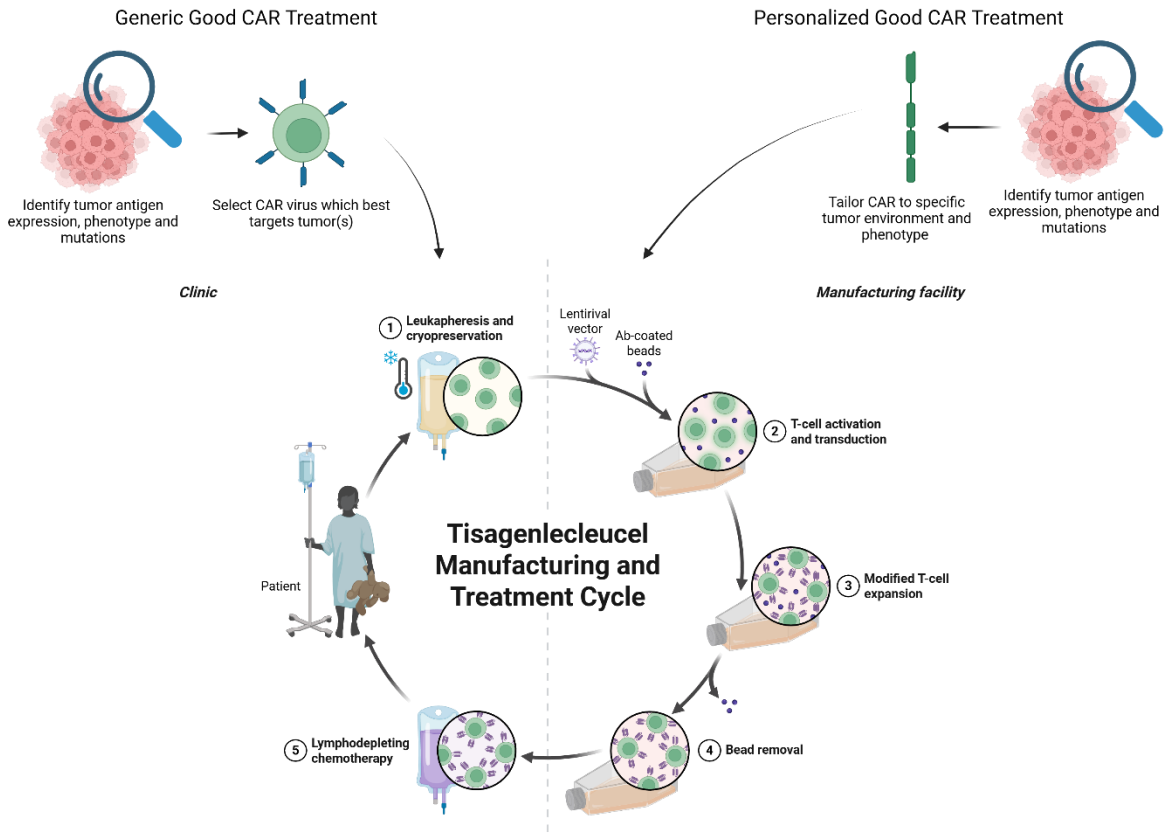

Figure 6.5 – Application of generic and personalised CAR-T approaches

6.6 – Concluding thoughts

The challenge presented here is immense and will require thousands upon thousands of hours of work and study to reach even a fraction of the goal. To further this goal, I have presented tools to quickly screen and tested bi-specific T cell engagers, combined single target CAR-T, assess CAR-T avidity and provided a library of proteomic, phosphoproteomic and transcriptomic data to better define CAR-T signals. This will provide access to cheap, high throughput methods to create and assess single and multi-antigen target synthetic immune stimulatory treatment options and as well as new ways to assess, understand and optimize the treatments being created. The emphasis on Jurkat cell-based assessment further increases accessibility, allowing labs to easily integrate the methods and data presented in cheap, consistent and easy to learn system. Through our own testing data presented from the use of these tools has thus far uncovered potential new screening opportunities and presented novel tools to help us gain a more comprehensive understanding of own synthetic immune stimulating therapeutics. Using these tools and data presented here we plan to continue to explore and improve these therapeutics, hopefully leading to a clearer, more precise design philosophy. I hope that these tools aid in the advancement of knowledge regarding T cell engaging biologics, creating more effective, specific therapeutics that are designed for a purpose instead of brute forced into existence.

REFERENCES

1. Milestones in Cancer Research and Discovery - NCI. https://www.cancer.gov/research/progress/250-years-milestones (2015).
2. Hunter, P. The fourth pillar. *EMBO Rep* **18**, 1889–1892 (2017).
3. Dobosz, P. & Dzieciątkowski, T. The Intriguing History of Cancer Immunotherapy. *Front Immunol* **10**, 2965 (2019).
4. Oiseth, S. J. & Aziz, M. S. Cancer immunotherapy: a brief review of the history, possibilities, and challenges ahead. *jcmt* **3**, 250–261 (2017).
5. A Brief History of Immunotherapy. **3**, (2014).
6. McCarthy, E. F. The Toxins of William B. Coley and the Treatment of Bone and Soft-Tissue Sarcomas. *Iowa Orthop J* **26**, 154–158 (2006).
7. Isaacs, A., Lindenmann, J. & Andrewes, C. H. Virus interference. I. The interferon. *Proceedings of the Royal Society of London. Series B - Biological Sciences* **147**, 258–267 (1997).
8. Burnet, M. Cancer—A Biological Approach: III. Viruses Associated with Neoplastic Conditions. IV. Practical Applications. *Br Med J* **1**, 841–847 (1957).
9. Billingham, R. E., Brent, L. & Medawar, P. B. Quantitative Studies on Tissue Transplantation Immunity. III. Actively Acquired Tolerance. *Philosophical Transactions of the Royal Society of London Series B* **239**, 357–414 (1956).
10. Prehn, R. T. & Main, J. M. Immunity to Methylcholanthrene-Induced Sarcomas. *JNCI: Journal of the National Cancer Institute* **18**, 769–778 (1957).

11. Old, L. J., Clarke, D. A. & Benacerraf, B. Effect of Bacillus Calmette-Guérin Infection on Transplanted Tumours in the Mouse. *Nature* **184**, 291–292 (1959).
12. Allison, J. P., McIntyre, B. W. & Bloch, D. Tumor-specific antigen of murine T-lymphoma defined with monoclonal antibody. *J Immunol* **129**, 2293–2300 (1982).
13. Köhler, G. & Milstein, C. Continuous cultures of fused cells secreting antibody of predefined specificity. *Nature* **256**, 495–497 (1975).
14. van der Bruggen, P. *et al*. A Gene Encoding an Antigen Recognized by Cytolytic T Lymphocytes on a Human Melanoma. *Science* **254**, 1643–1647 (1991).
15. Tsao, L.-C., Force, J. & Hartman, Z. C. Mechanisms of therapeutic anti-tumor monoclonal antibodies. *Cancer Res* **81**, 4641–4651 (2021).
16. PhD, C. J. 25 Years of Trastuzumab: A Legacy of Innovation. *American Association for Cancer Research (AACR)* https://www.aacr.org/blog/2023/10/17/25-years-of-trastuzumab-a-legacy-of-innovation/ (2023).
17. Witzig, T. E. *et al*. Treatment With Ibritumomab Tiuxetan Radioimmunotherapy in Patients With Rituximab-Refractory Follicular Non-Hodgkin's Lymphoma. *JCO* **20**, 3262–3269 (2002).
18. Kothari, M. *et al*. A Comprehensive Review of Monoclonal Antibodies in Modern Medicine: Tracing the Evolution of a Revolutionary Therapeutic Approach. *Cureus* https://doi.org/10.7759/cureus.61983 (2024) doi:10.7759/cureus.61983.
19. Zahavi, D. & Weiner, L. Monoclonal Antibodies in Cancer Therapy. *Antibodies* **9**, 34 (2020).
20. MYLOTARGTM (gemtuzumab ozogamicin) for injection.

21. Tsao, L.-C., Force, J. & Hartman, Z. C. Mechanisms of therapeutic anti-tumor monoclonal antibodies. *Cancer Res* **81**, 4641–4651 (2021).
22. Gardner, T. A., Elzey, B. D. & Hahn, N. M. Sipuleucel-T (Provenge) autologous vaccine approved for treatment of men with asymptomatic or minimally symptomatic castrate-resistant metastatic prostate cancer. *Hum Vaccin Immunother* **8**, 534–539 (2012).
23. Mansh, M. Ipilimumab and Cancer Immunotherapy: A New Hope for Advanced Stage Melanoma. *Yale J Biol Med* **84**, 381–389 (2011).
24. Marei, H. E., Hasan, A., Pozzoli, G. & Cenciarelli, C. Cancer immunotherapy with immune checkpoint inhibitors (ICIs): potential, mechanisms of resistance, and strategies for reinvigorating T cell responsiveness when resistance is acquired. *Cancer Cell International* **23**, 64 (2023).
25. Cancer Vaccines: The Types, How They Work, and Which Cancers They Treat | Memorial Sloan Kettering Cancer Center. https://www.mskcc.org/cancer-care/diagnosis-treatment/cancer-treatments/immunotherapy/cancer-vaccines.
26. Saxena, M., van der Burg, S. H., Melief, C. J. M. & Bhardwaj, N. Therapeutic cancer vaccines. *Nat Rev Cancer* **21**, 360–378 (2021).
27. Omolekan, T. O. *et al*. Viral warfare: unleashing engineered oncolytic viruses to outsmart cancer's defenses. *Front. Immunol.* **16**, (2025).
28. Fukuhara, H., Ino, Y. & Todo, T. Oncolytic virus therapy: A new era of cancer treatment at dawn. *Cancer Sci* **107**, 1373–1379 (2016).
29. Fischbach, M. A., Bluestone, J. A. & Lim, W. A. Cell-Based Therapeutics: The Next Pillar of Medicine. *Sci Transl Med* **5**, 179ps7 (2013).

30. Lim, W. A. Designing Customized Cell Signaling Circuits. *Nat Rev Mol Cell Biol* **11**, 393–403 (2010).

31. Pryciak, P. M. Designing new cellular signaling pathways. *Chem Biol* **16**, 249–254 (2009).

32. Choi, D., Kim, T.-G. & Sung, Y. C. The Past, Present, and Future of Adoptive T Cell Therapy. *Immune Netw* **12**, 139–147 (2012).

33. Rosenberg, S. A., Restifo, N. P., Yang, J. C., Morgan, R. A. & Dudley, M. E. Adoptive cell transfer: a clinical path to effective cancer immunotherapy. *Nat Rev Cancer* **8**, 299–308 (2008).

34. Braendstrup, P., Levine, B. L. & Ruella, M. The Long Road to the First FDA Approved Gene Therapy: Chimeric Antigen Receptor T Cells Targeting CD19. *Cytotherapy* **22**, 57–69 (2020).

35. First Cancer TCR Cell Therapy Approved by FDA - NCI. https://www.cancer.gov/news-events/cancer-currents-blog/2024/fda-tecelra-synovial-sarcoma-mage-a4 (2024).

36. Lifileucel First Cellular Therapy Approved for Cancer - NCI. https://www.cancer.gov/news-events/cancer-currents-blog/2024/fda-amtagvi-til-therapy-melanoma (2024).

37. Sun, L., Su, Y., Jiao, A., Wang, X. & Zhang, B. T cells in health and disease. *Sig Transduct Target Ther* **8**, 235 (2023).

38. Rothenberg, E. V., Moore, J. E. & Yui, M. A. Launching the T-cell-lineage developmental programme. *Nat Rev Immunol* **8**, 9–21 (2008).

39. Yang, Q., Jeremiah Bell, J. & Bhandoola, A. T-cell lineage determination. *Immunological Reviews* **238**, 12–22 (2010).

40. Dutta, A., Zhao, B. & Love, P. E. New insights into TCR β-selection. *Trends in Immunology* **42**, 735–750 (2021).

41. Aifantis, I., Buer, J., Boehmer, H. von & Azogui, O. Essential Role of the Pre-T Cell Receptor in Allelic Exclusion of the T Cell Receptor β Locus. *Immunity* **7**, 601–607 (1997).

42. Klein, L., Kyewski, B., Allen, P. M. & Hogquist, K. A. Positive and negative selection of the T cell repertoire: what thymocytes see and don't see. *Nat Rev Immunol* **14**, 377–391 (2014).

43. Brugnera, E. *et al.* Coreceptor Reversal in the Thymus: Signaled CD4+8+ Thymocytes Initially Terminate CD8 Transcription Even When Differentiating into CD8+ T Cells. *Immunity* **13**, 59–71 (2000).

44. Singer, A. New perspectives on a developmental dilemma: the kinetic signaling model and the importance of signal duration for the CD4/CD8 lineage decision. *Current Opinion in Immunology* **14**, 207–215 (2002).

45. Yu, Q., Erman, B., Bhandoola, A., Sharrow, S. O. & Singer, A. In Vitro Evidence That Cytokine Receptor Signals Are Required for Differentiation of Double Positive Thymocytes into Functionally Mature CD8+ T Cells. *Journal of Experimental Medicine* **197**, 475–487 (2003).

46. Singer, A., Adoro, S. & Park, J.-H. Lineage fate and intense debate: myths, models and mechanisms of CD4- versus CD8-lineage choice. *Nat Rev Immunol* **8**, 788–801 (2008).

47. He, X. *et al.* The zinc finger transcription factor Th-POK regulates CD4 versus CD8 T-cell lineage commitment. *Nature* **433**, 826–833 (2005).
48. ThPOK acts late in specification of the helper T cell lineage and suppresses Runx-mediated commitment to the cytotoxic T cell lineage | Nature Immunology. https://www.nature.com/articles/ni.1652.
49. Setoguchi, R. *et al.* Repression of the Transcription Factor Th-POK by Runx Complexes in Cytotoxic T Cell Development. *Science* **319**, 822–825 (2008).
50. Taniuchi, I. *et al.* Differential Requirements for Runx Proteins in CD4 Repression and Epigenetic Silencing during T Lymphocyte Development. *Cell* **111**, 621–633 (2002).
51. Hernández-Hoyos, G., Anderson, M. K., Wang, C., Rothenberg, E. V. & Alberola-Ila, J. GATA-3 Expression Is Controlled by TCR Signals and Regulates CD4/CD8 Differentiation. *Immunity* **19**, 83–94 (2003).
52. Park, J.-H. *et al.* Signaling by intrathymic cytokines, not T cell antigen receptors, specifies CD8 lineage choice and promotes the differentiation of cytotoxic-lineage T cells. *Nat Immunol* **11**, 257–264 (2010).
53. Conteduca, G., Indiveri, F., Filaci, G. & Negrini, S. Beyond APECED: An update on the role of the autoimmune regulator gene (AIRE) in physiology and disease. *Autoimmun Rev* **17**, 325–330 (2018).
54. Romagnani, S. Th1/Th2 cells. *Inflamm Bowel Dis* **5**, 285–294 (1999).
55. Luckheeram, R. V., Zhou, R., Verma, A. D. & Xia, B. CD4+T Cells: Differentiation and Functions. *Clin Dev Immunol* **2012**, 925135 (2012).

56. Murray, H. W., Rubin, B. Y., Carriero, S. M., Harris, A. M. & Jaffee, E. A. Human mononuclear phagocyte antiprotozoal mechanisms: oxygen-dependent vs oxygen-independent activity against intracellular Toxoplasma gondii. *J Immunol* **134**, 1982–1988 (1985).

57. Alberts, B. *et al.* Helper T Cells and Lymphocyte Activation. in *Molecular Biology of the Cell. 4th edition* (Garland Science, 2002).

58. Wuest, T. Y., Willette-Brown, J., Durum, S. K. & Hurwitz, A. A. The influence of IL-2 family cytokines on activation and function of naturally occurring regulatory T cells. *J Leukoc Biol* **84**, 973–980 (2008).

59. Vignali, D. A. A., Collison, L. W. & Workman, C. J. How regulatory T cells work. *Nat Rev Immunol* **8**, 523–532 (2008).

60. Andersen, M. H., Schrama, D., Straten, P. thor & Becker, J. C. Cytotoxic T Cells. *J Invest Dermatol* **126**, 32–41 (2006).

61. Bhat, P., Leggatt, G., Waterhouse, N. & Frazer, I. H. Interferon-γ derived from cytotoxic lymphocytes directly enhances their motility and cytotoxicity. *Cell Death Dis* **8**, e2836 (2017).

62. Nagata, S. Fas-mediated apoptosis. *Adv Exp Med Biol* **406**, 119–124 (1996).

63. Call, M. E., Pyrdol, J., Wiedmann, M. & Wucherpfennig, K. W. The Organizing Principle in the Formation of the T Cell Receptor-CD3 Complex. *Cell* **111**, 967–979 (2002).

64. Shah, K., Al-Haidari, A., Sun, J. & Kazi, J. U. T cell receptor (TCR) signaling in health and disease. *Sig Transduct Target Ther* **6**, 1–26 (2021).

65. Dupic, T., Marcou, Q., Walczak, A. M. & Mora, T. Genesis of the αβ T-cell receptor. *PLoS Comput Biol* **15**, e1006874 (2019).

66. Krishna, C., Chowell, D., Gönen, M., Elhanati, Y. & Chan, T. A. Genetic and environmental determinants of human TCR repertoire diversity. *Immunity & Ageing* **17**, 26 (2020).

67. Courtney, A. H., Lo, W.-L. & Weiss, A. TCR SIGNALING: MECHANISMS OF INITIATION AND PROPAGATION. *Trends Biochem Sci* **43**, 108–123 (2018).

68. Liu, D., Hu, X., Chen, Z., Wei, W. & Wu, Y. Key links in the physiological regulation of the immune system and disease induction: T cell receptor -CD3 complex. *Biochemical Pharmacology* **227**, 116441 (2024).

69. Bettini, M. L. *et al.* CD3 ITAM diversity is required for optimal T cell receptor signaling and thymocyte development. *J Immunol* **199**, 1555–1560 (2017).

70. Rossy, J., Williamson, D. J. & Gaus, K. How does the kinase Lck phosphorylate the T cell receptor? Spatial organization as a regulatory mechanism. *Front Immunol* **3**, 167 (2012).

71. Wange, R. L. LAT, the Linker for Activation of T Cells: A Bridge Between T Cell-Specific and General Signaling Pathways. *Science's STKE* **2000**, re1–re1 (2000).

72. Paz, P. E. *et al.* Mapping the Zap-70 phosphorylation sites on LAT (linker for activation of T cells) required for recruitment and activation of signalling proteins in T cells. *Biochem J* **356**, 461–471 (2001).

73. Balagopalan, L., Coussens, N. P., Sherman, E., Samelson, L. E. & Sommers, C. L. The LAT Story: A Tale of Cooperativity, Coordination, and Choreography. *Cold Spring Harb Perspect Biol* **2**, a005512 (2010).

74. Zhang, W. *et al.* Association of Grb2, Gads, and Phospholipase C-γ1 with Phosphorylated LAT Tyrosine Residues: EFFECT OF LAT TYROSINE MUTATIONS ON T CELL ANTIGEN RECEPTOR-MEDIATED SIGNALING *. *Journal of Biological Chemistry* **275**, 23355–23361 (2000).

75. Liu, S. K., Fang, N., Koretzky, G. A. & McGlade, C. J. The hematopoietic-specific adaptor protein Gads functions in T-cell signaling via interactions with the SLP-76 and LAT adaptors. *Current Biology* **9**, 67–75 (1999).

76. Andreotti, A. H., Schwartzberg, P. L., Joseph, R. E. & Berg, L. J. T-Cell Signaling Regulated by the Tec Family Kinase, Itk. *Cold Spring Harb Perspect Biol* **2**, a002287 (2010).

77. Das, J. *et al.* Digital signaling and hysteresis characterize Ras activation in lymphoid cells. *Cell* **136**, 337–351 (2009).

78. Onnis, A. & Baldari, C. T. Orchestration of Immunological Synapse Assembly by Vesicular Trafficking. *Front. Cell Dev. Biol.* **7**, (2019).

79. Dustin, M. L., Chakraborty, A. K. & Shaw, A. S. Understanding the Structure and Function of the Immunological Synapse. *Cold Spring Harb Perspect Biol* **2**, a002311 (2010).

80. Yi, J., Wu, X. S., Crites, T. & Hammer, J. A. Actin retrograde flow and actomyosin II arc contraction drive receptor cluster dynamics at the immunological synapse in Jurkat T cells. *Mol Biol Cell* **23**, 834–852 (2012).

81. Monks, C. R. F., Freiberg, B. A., Kupfer, H., Sciaky, N. & Kupfer, A. Three-dimensional segregation of supramolecular activation clusters in T cells. *Nature* **395**, 82–86 (1998).

82. Davenport, A. J. *et al.* Chimeric antigen receptor T cells form nonclassical and potent immune synapses driving rapid cytotoxicity. *Proc Natl Acad Sci U S A* **115**, E2068–E2076 (2018).

83. Campi, G., Varma, R. & Dustin, M. L. Actin and agonist MHC–peptide complex–dependent T cell receptor microclusters as scaffolds for signaling. *J Exp Med* **202**, 1031–1036 (2005).

84. Grakoui, A. *et al.* The Immunological Synapse: A Molecular Machine Controlling T Cell Activation. *Science* **285**, 221–227 (1999).

85. Lee, K.-H. *et al.* The Immunological Synapse Balances T Cell Receptor Signaling and Degradation. *Science* **302**, 1218–1222 (2003).

86. Lee, K.-H. *et al.* T Cell Receptor Signaling Precedes Immunological Synapse Formation. *Science* **295**, 1539–1542 (2002).

87. Varma, R., Campi, G., Yokosuka, T., Saito, T. & Dustin, M. L. T Cell Receptor-Proximal Signals Are Sustained in Peripheral Microclusters and Terminated in the Central Supramolecular Activation Cluster. *Immunity* **25**, 117–127 (2006).

88. Wiedemann, A. *et al.* T-cell activation is accompanied by an ubiquitination process occurring at the immunological synapse. *Immunology Letters* **98**, 57–61 (2005).

89. Yi, J., Balagopalan, L., Nguyen, T., McIntire, K. M. & Samelson, L. E. TCR microclusters form spatially segregated domains and sequentially assemble in calcium-dependent kinetic steps. *Nat Commun* **10**, 277 (2019).

90. Binder, C. *et al.* CD2 Immunobiology. *Front. Immunol.* **11**, (2020).

91. Liu, S. J., Hahn, W. C., Bierer, B. E. & Golan, D. E. Intracellular mediators regulate CD2 lateral diffusion and cytoplasmic Ca2+ mobilization upon CD2-mediated T cell activation. *Biophysical Journal* **68**, 459–470 (1995).

92. Davis, S. J. & van der Merwe, P. A. The kinetic-segregation model: TCR triggering and beyond. *Nat Immunol* **7**, 803–809 (2006).

93. Naor, D., Sionov, R. V. & Ish-Shalom, D. CD44: Structure, Function and Association with the Malignant Process. in *Advances in Cancer Research* (eds Vande Woude, G. F. & Klein, G.) vol. 71 241–319 (Academic Press, 1997).

94. Alisson-Silva, F. *et al.* CD43 sialoglycoprotein modulates cardiac inflammation and murine susceptibility to Trypanosoma cruzi infection. *Sci Rep* **9**, 8628 (2019).

95. Tong, J. *et al.* CD43 Regulation of T Cell Activation Is Not through Steric Inhibition of T Cell–APC Interactions but through an Intracellular Mechanism. *Journal of Experimental Medicine* **199**, 1277–1283 (2004).

96. Hermiston, M. L., Xu, Z. & Weiss, A. CD45: A Critical Regulator of Signaling Thresholds in Immune Cells. *Annual Review of Immunology* **21**, 107–137 (2003).

97. Fischer, E. H., Charbonneau, H., Cool, D. E. & Tonks, N. K. Tyrosine phosphatases and their possible interplay with tyrosine kinases. *Ciba Found Symp* **164**, 132–140; discussion 140-144 (1992).

98. Chang, V. T. *et al.* Initiation of T cell signaling by CD45 segregation at 'close-contacts'. *Nat Immunol* **17**, 574–582 (2016).

99. Pingel, J. T. & Thomas, M. L. Evidence that the leukocyte-common antigen is required for antigen-induced T lymphocyte proliferation. *Cell* **58**, 1055–1065 (1989).

100. Sieh, M., Bolen, J. B. & Weiss, A. CD45 specifically modulates binding of Lck to a phosphopeptide encompassing the negative regulatory tyrosine of Lck. *EMBO J* **12**, 315–321 (1993).

101. McAdam, A. J., Schweitzer, A. N. & Sharpe, A. H. The role of B7 co-stimulation in activation and differentiation of CD4+ and CD8+ T cells. *Immunol Rev* **165**, 231–247 (1998).

102. Bian, Y. *et al.* The capacity of the natural ligands for CD28 to drive IL-4 expression in naïve and antigen-primed CD4+ and CD8+ T cells. *International Immunology* **17**, 73–83 (2005).

103. Acuto, O. & Michel, F. CD28-mediated co-stimulation: a quantitative support for TCR signalling. *Nat Rev Immunol* **3**, 939–951 (2003).

104. Ho, A. & Dowdy, S. F. Regulation of G1 cell-cycle progression by oncogenes and tumor suppressor genes. *Current Opinion in Genetics & Development* **12**, 47–52 (2002).

105. Boonen, G. J. J. C. *et al.* CD28 induces cell cycle progression by IL-2-independent down-regulation of p27kip1 expression in human peripheral T lymphocytes. *European Journal of Immunology* **29**, 789–798 (1999).

106. Kovalev, G. I., Franklin, D. S., Coffield, V. M., Xiong, Y. & Su, L. An Important Role of CDK Inhibitor p18INK4c in Modulating Antigen Receptor-Mediated T Cell Proliferation. *J Immunol* **167**, 3285–3292 (2001).

107. Lea, N. C. *et al.* Commitment Point during G0→G1 That Controls Entry into the Cell Cycle. *Mol Cell Biol* **23**, 2351–2361 (2003).

108. Appleman, L. J., van Puijenbroek, A. A. F. L., Shu, K. M., Nadler, L. M. & Boussiotis, V. A. CD28 Costimulation Mediates Down-Regulation of p27kip1 and Cell Cycle Progression by Activation of the PI3K/PKB Signaling Pathway in Primary Human T Cells1. *The Journal of Immunology* **168**, 2729–2736 (2002).

109. Diehn, M. *et al.* Genomic expression programs and the integration of the CD28 costimulatory signal in T cell activation. *Proc Natl Acad Sci U S A* **99**, 11796–11801 (2002).

110. Vinay, D. S. & Kwon, B. S. 4-1BB signaling beyond T cells. *Cell Mol Immunol* **8**, 281–284 (2011).

111. Hehlgans, T. & Pfeffer, K. The intriguing biology of the tumour necrosis factor/tumour necrosis factor receptor superfamily: players, rules and the games. *Immunology* **115**, 1–20 (2005).

112. Cannons, J. L., Choi, Y. & Watts, T. H. Role of TNF Receptor-Associated Factor 2 and p38 Mitogen-Activated Protein Kinase Activation During 4-1BB-Dependent Immune Response1. *The Journal of Immunology* **165**, 6193–6204 (2000).

113. Shuford, W. W. *et al.* 4-1BB Costimulatory Signals Preferentially Induce CD8+ T Cell Proliferation and Lead to the Amplification In Vivo of Cytotoxic T Cell Responses. *J Exp Med* **186**, 47–55 (1997).

114. Lee, H.-W. *et al.* 4-1BB Promotes the Survival of CD8+ T Lymphocytes by Increasing Expression of Bcl-xL and Bfl-11. *The Journal of Immunology* **169**, 4882–4888 (2002).

115. Croft, M. Costimulation of T cells by OX40, 4-1BB, and CD27. *Cytokine & Growth Factor Reviews* **14**, 265–273 (2003).

116. Pieper, K., Grimbacher, B. & Eibel, H. B-cell biology and development. *Journal of Allergy and Clinical Immunology* **131**, 959–971 (2013).

117. Alberts, B. *et al.* B Cells and Antibodies. in *Molecular Biology of the Cell. 4th edition* (Garland Science, 2002).

118. Aziz, M., Iheanacho, F. & Hashmi, M. F. Physiology, Antibody. in *StatPearls* (StatPearls Publishing, Treasure Island (FL), 2025).

119. Charles A Janeway, J., Travers, P., Walport, M. & Shlomchik, M. J. The complement system and innate immunity. in *Immunobiology: The Immune System in Health and Disease. 5th edition* (Garland Science, 2001).

120. Charles A Janeway, J., Travers, P., Walport, M. & Shlomchik, M. J. The structure of a typical antibody molecule. in *Immunobiology: The Immune System in Health and Disease. 5th edition* (Garland Science, 2001).

121. Mejias-Gomez, O. *et al.* A window into the human immune system: comprehensive characterization of the complexity of antibody complementary-determining regions in functional antibodies. *mAbs* **15**, 2268255 (2023).

122. Mosch, R. & Guchelaar, H.-J. Immunogenicity of Monoclonal Antibodies and the Potential Use of HLA Haplotypes to Predict Vulnerable Patients. *Front Immunol* **13**, 885672 (2022).

123. Chen, X., Zaro, J. & Shen, W.-C. Fusion Protein Linkers: Property, Design and Functionality. *Adv Drug Deliv Rev* **65**, 1357–1369 (2013).

124. Shen, Z., Yan, H., Zhang, Y., Mernaugh, R. L. & Zeng, X. Engineering Peptide Linkers for scFv Immunosensors. *Anal Chem* **80**, 1910–1917 (2008).

125. Kim, D.-J. *et al.* Production and characterisation of a recombinant scFv reactive with human gastrointestinal carcinomas. *Br J Cancer* **87**, 405–413 (2002).

126. Rossotti, M. A., Bélanger, K., Henry, K. A. & Tanha, J. Immunogenicity and humanization of single-domain antibodies. *The FEBS Journal* **289**, 4304–4327 (2022).

127. Hamers-Casterman, C. *et al.* Naturally occurring antibodies devoid of light chains. *Nature* **363**, 446–448 (1993).

128. Sabir, J. S. M. *et al.* Construction of naïve camelids VHH repertoire in phage display-based library. *Comptes Rendus Biologies* **337**, 244–249 (2014).

129. Bae, J. & Song, Y. Engineering a cell-penetrating hyperstable antibody scFv(Ras) – An extraordinary approach to cancer therapeutics. *Synth Syst Biotechnol* **6**, 343–350 (2021).

130. Li, Z. *et al.* Influence of molecular size on tissue distribution of antibody fragments. *MAbs* **8**, 113–119 (2015).

131. Keyaerts, M. *et al.* Phase I Study of 68Ga-HER2-Nanobody for PET/CT Assessment of HER2 Expression in Breast Carcinoma. *J Nucl Med* **57**, 27–33 (2016).

132. Hutt, M., Färber-Schwarz, A., Unverdorben, F., Richter, F. & Kontermann, R. E. Plasma Half-life Extension of Small Recombinant Antibodies by Fusion to Immunoglobulin-binding Domains. *J Biol Chem* **287**, 4462–4469 (2012).

133. Kunz, P. *et al.* The structural basis of nanobody unfolding reversibility and thermoresistance. *Sci Rep* **8**, 7934 (2018).

134. Lou, H. & Cao, X. Antibody variable region engineering for improving cancer immunotherapy. *Cancer Commun (Lond)* **42**, 804–827 (2022).

135. Audenhove, I. V. & Gettemans, J. Nanobodies as Versatile Tools to Understand, Diagnose, Visualize and Treat Cancer. *eBioMedicine* **8**, 40–48 (2016).

136. Hussack, G., MacKenzie, C. R. & Tanha, J. Characterization of Single-Domain Antibodies with an Engineered Disulfide Bond. in *Single Domain Antibodies: Methods and Protocols* (eds Saerens, D. & Muyldermans, S.) 417–429 (Humana Press, Totowa, NJ, 2012). doi:10.1007/978-1-61779-968-6_25.

137. Asaadi, Y., Jouneghani, F. F., Janani, S. & Rahbarizadeh, F. A comprehensive comparison between camelid nanobodies and single chain variable fragments. *Biomarker Research* **9**, 87 (2021).

138. Wu, Z. *et al.* Screening and evaluation of TROP2-targeted scFv tracers for cancer diagnosis. *Journal of Nuclear Medicine* **66**, 251163–251163 (2025).

139. Nikkhoi, S. K. *et al.* Bispecific killer cell engager with high affinity and specificity toward CD16a on NK cells for cancer immunotherapy. *Front Immunol* **13**, 1039969 (2022).

140. Meckler, J. F., Levis, D. J., Vang, D. P. & Tuscano, J. M. A Novel bispecific T-cell engager (BiTE) targeting CD22 and CD3 has both in vitro and in vivo activity and synergizes with blinatumomab in an acute lymphoblastic leukemia (ALL) tumor model. *Cancer Immunol Immunother* **72**, 2939–2948 (2023).

141. Hassani, M. *et al.* Construction of a chimeric antigen receptor bearing a nanobody against prostate a specific membrane antigen in prostate cancer. *Journal of Cellular Biochemistry* **120**, 10787–10795 (2019).

142. Baer, R., Chen, K. C., Smith, S. D. & Rabbitts, T. H. Fusion of an immunoglobulin variable gene and a T cell receptor constant gene in the chromosome 14 inversion associated with T cell tumors. *Cell* **43**, 705–713 (1985).

143. Kuwana, Y. *et al.* Expression of chimeric receptor composed of immunoglobulin-derived V regions and T-cell receptor-derived C regions. *Biochem Biophys Res Commun* **149**, 960–968 (1987).

144. Gross, G., Waks, T. & Eshhar, Z. Expression of immunoglobulin-T-cell receptor chimeric molecules as functional receptors with antibody-type specificity. *Proc Natl Acad Sci U S A* **86**, 10024–10028 (1989).

145. Kalos, M. *et al.* T Cells with Chimeric Antigen Receptors Have Potent Antitumor Effects and Can Establish Memory in Patients with Advanced Leukemia. *Sci Transl Med* **3**, 95ra73 (2011).

146. Kohn, D. B. *et al.* CARs on Track in the Clinic. *Mol Ther* **19**, 432–438 (2011).

147. First-Ever CAR T-cell Therapy Approved in U.S. *Cancer Discov* **7**, OF1 (2017).

148. Asmamaw Dejenie, T. *et al.* Current updates on generations, approvals, and clinical trials of CAR T-cell therapy. *Hum Vaccin Immunother* **18**, 2114254.

149. Chmielewski, M. & Abken, H. TRUCKs: the fourth generation of CARs. *Expert Opinion on Biological Therapy* **15**, 1145–1154 (2015).

150. Till, B. G. *et al.* CD20-specific adoptive immunotherapy for lymphoma using a chimeric antigen receptor with both CD28 and 4-1BB domains: pilot clinical trial results. *Blood* **119**, 3940–3950 (2012).

151. Morgan, R. A. *et al.* Case Report of a Serious Adverse Event Following the Administration of T Cells Transduced With a Chimeric Antigen Receptor Recognizing ERBB2. *Molecular Therapy* **18**, 843–851 (2010).

152. Fujiwara, K. *et al.* Hinge and Transmembrane Domains of Chimeric Antigen Receptor Regulate Receptor Expression and Signaling Threshold. *Cells* **9**, 1182 (2020).

153. McComb, S. *et al.* Programmable Attenuation of Antigenic Sensitivity for a Nanobody-Based EGFR Chimeric Antigen Receptor Through Hinge Domain Truncation. *Front. Immunol.* **13**, (2022).

154. Muller, Y. D. *et al.* The CD28-Transmembrane Domain Mediates Chimeric Antigen Receptor Heterodimerization With CD28. *Front. Immunol.* **12**, (2021).

155. Alabanza, L. *et al.* Function of Novel Anti-CD19 Chimeric Antigen Receptors with Human Variable Regions Is Affected by Hinge and Transmembrane Domains. *Mol Ther* **25**, 2452–2465 (2017).

156. Ying, Z. *et al.* Parallel Comparison of 4-1BB or CD28 Co-stimulated CD19-Targeted CAR-T Cells for B Cell Non-Hodgkin's Lymphoma. *Mol Ther Oncolytics* **15**, 60–68 (2019).

157. Priceman, S. J. *et al.* Co-stimulatory signaling determines tumor antigen sensitivity and persistence of CAR T cells targeting PSCA+ metastatic prostate cancer. *Oncoimmunology* **7**, e1380764 (2017).

158. Kawalekar, O. U. *et al.* Distinct Signaling of Coreceptors Regulates Specific Metabolism Pathways and Impacts Memory Development in CAR T Cells. *Immunity* **44**, 380–390 (2016).

159. Drent, E. *et al.* Combined CD28 and 4–1BB costimulation potentiates affinity-tuned Chimeric Antigen Receptor-engineered T cells. *Clin Cancer Res* **25**, 4014–4025 (2019).

160. Tammana, S. *et al.* 4-1BB and CD28 Signaling Plays a Synergistic Role in Redirecting Umbilical Cord Blood T Cells Against B-Cell Malignancies. *Human Gene Therapy* **21**, 75–86 (2010).

161. Carpenito, C. *et al.* Control of large, established tumor xenografts with genetically retargeted human T cells containing CD28 and CD137 domains. *Proceedings of the National Academy of Sciences* **106**, 3360–3365 (2009).

162. Velasco Cárdenas, R. M.-H. *et al.* Harnessing CD3 diversity to optimize CAR T cells. *Nat Immunol* **24**, 2135–2149 (2023).

163. Ding, L., Li, Y., Li, J., ter Haak, M. & Lamb, L. S. Gamma-Delta (γδ) CAR-T Cells Lacking the CD3z Signaling Domain Enhance Targeted Killing of Tumor Cells and Preserve Healthy Tissues. *Blood* **142**, 6835 (2023).

164. Kekre, N. *et al*. CLIC-01: Manufacture and distribution of non-cryopreserved CAR-T cells for patients with CD19 positive hematologic malignancies. *Front Immunol* **13**, 1074740 (2022).

165. Which Cell and Gene Therapies Are Approved to Treat Cancer? *Alliance for Cancer Gene Therapy* https://acgtfoundation.org/for-patients/approved-cell-and-gene-therapies/.

166. Research, C. for B. E. and. KYMRIAH. *FDA* https://www.fda.gov/vaccines-blood-biologics/cellular-gene-therapy-products/kymriah (2024).

167. Research, C. for B. E. and. ABECMA (idecabtagene vicleucel). *FDA* https://www.fda.gov/vaccines-blood-biologics/abecma-idecabtagene-vicleucel (2024).

168. Research, C. for B. E. and. TECARTUS. *FDA* https://www.fda.gov/vaccines-blood-biologics/cellular-gene-therapy-products/tecartus (2024).

169. Research, C. for B. E. and. YESCARTA. *FDA* https://www.fda.gov/vaccines-blood-biologics/cellular-gene-therapy-products/yescarta (2024).

170. Research, C. for B. E. and. BREYANZI (lisocabtagene maraleucel). *FDA* https://www.fda.gov/vaccines-blood-biologics/cellular-gene-therapy-products/breyanzi-lisocabtagene-maraleucel (2024).

171. Research, C. for B. E. and. CARVYKTI. *FDA* https://www.fda.gov/vaccines-blood-biologics/cellular-gene-therapy-products/carvykti (2024).

172. Research, C. for B. E. and. AUCATZYL. *FDA* https://www.fda.gov/vaccines-blood-biologics/aucatzyl (2025).

173. Brudno, J. N. & Kochenderfer, J. N. Toxicities of chimeric antigen receptor T cells: recognition and management. *Blood* **127**, 3321–3330 (2016).

174. Gabelli, M. *et al.* Maintenance therapy for early loss of B-cell aplasia after anti-CD19 CAR T-cell therapy. *Blood Advances* **8**, 1959–1963 (2024).

175. Cappell, K. M. & Kochenderfer, J. N. Long-term outcomes following CAR T cell therapy: what we know so far. *Nat Rev Clin Oncol* **20**, 359–371 (2023).

176. Laetsch, T. W. *et al.* Three-Year Update of Tisagenlecleucel in Pediatric and Young Adult Patients With Relapsed/Refractory Acute Lymphoblastic Leukemia in the ELIANA Trial. *J Clin Oncol* **41**, 1664–1669 (2023).

177. Martin, T. *et al.* Ciltacabtagene Autoleucel, an Anti–B-cell Maturation Antigen Chimeric Antigen Receptor T-Cell Therapy, for Relapsed/Refractory Multiple Myeloma: CARTITUDE-1 2-Year Follow-Up. *J Clin Oncol* **41**, 1265–1274 (2023).

178. Flugel, C. L. *et al.* Overcoming on-target, off-tumour toxicity of CAR T cell therapy for solid tumours. *Nat Rev Clin Oncol* **20**, 49–62 (2023).

179. Beatty, G. L. & O'Hara, M. Chimeric antigen receptor-modified T cells for the treatment of solid tumors: Defining the challenges and next steps. *Pharmacol Ther* **166**, 30–39 (2016).

180. Palazón, A., Aragonés, J., Morales-Kastresana, A., de Landázuri, M. O. & Melero, I. Molecular Pathways: Hypoxia Response in Immune Cells Fighting or Promoting Cancer. *Clinical Cancer Research* **18**, 1207–1213 (2012).

181. Watson, M. J. & Delgoffe, G. M. Fighting in a wasteland: deleterious metabolites and antitumor immunity. *J Clin Invest* **132**, e148549.

182. Bronte, V. & Zanovello, P. Regulation of immune responses by L-arginine metabolism. *Nat Rev Immunol* **5**, 641–654 (2005).

183. Connolly, J. L. *et al.* Tumor Structure and Tumor Stroma Generation. in *Holland-Frei Cancer Medicine. 6th edition* (BC Decker, 2003).

184. Zhang, E., Gu, J. & Xu, H. Prospects for chimeric antigen receptor-modified T cell therapy for solid tumors. *Mol Cancer* **17**, 7 (2018).

185. McGowan, E. *et al.* PD-1 disrupted CAR-T cells in the treatment of solid tumors: Promises and challenges. *Biomedicine & Pharmacotherapy* **121**, 109625 (2020).

186. Chen, N., Li, X., Chintala, N. K., Tano, Z. E. & Adusumilli, P. S. Driving CARs on the uneven road of antigen heterogeneity in solid tumors. *Curr Opin Immunol* **51**, 103–110 (2018).

187. Kekre, N. *et al.* CLIC-01: Manufacture and distribution of non-cryopreserved CAR-T cells for patients with CD19 positive hematologic malignancies. *Front. Immunol.* **13**, (2022).

188. Negishi, S. *et al.* Treatment strategies for relapse after CAR T-cell therapy in B cell lymphoma. *Front. Pediatr.* **11**, (2024).

189. Zhang, Y. & Pastan, I. High Shed Antigen Levels within Tumors: An Additional Barrier to lmmunoconjugate Therapy. *Clin Cancer Res* **14**, 7981–7986 (2008).

190. Sterner, R. C. & Sterner, R. M. CAR-T cell therapy: current limitations and potential strategies. *Blood Cancer J.* **11**, 1–11 (2021).

191. Shaikh, S. & Shaikh, H. CART Cell Therapy Toxicity. in *StatPearls* (StatPearls Publishing, Treasure Island (FL), 2025).

192. Si, S. & Teachey, D. T. Spotlight on Tocilizumab in the Treatment of CAR-T-Cell-Induced Cytokine Release Syndrome: Clinical Evidence to Date. *Ther Clin Risk Manag* **16**, 705–714 (2020).

193. Bhaskar, S. T., Dholaria, B., Savani, B. N. & Oluwole, O. The Evolving Role of Bridging Therapy during CAR-T Therapy. *Clin Hematol Int* **6**, 9–16.

194. Roddie, C. *et al.* Effective bridging therapy can improve CD19 CAR-T outcomes while maintaining safety in patients with large B-cell lymphoma. *Blood Adv* **7**, 2872–2883 (2023).

195. CAR-T Clinical Trials: Potentially Moving CAR T Into Earlier Lines of MM Treatment. *Cancer Network* https://www.cancernetwork.com/view/car-t-clinical-trials-potentially-moving-car-t-into-earlier-lines-of-mm-treatment (2025).

196. *Moving CAR-T into Earlier Lines of Therapy in Multiple Myeloma*. (2024).

197. Sanber, K., Savani, B. & Jain, T. Graft-versus-host disease risk after chimeric antigen receptor T-cell therapy: the diametric opposition of T cells. *British Journal of Haematology* **195**, 660–668 (2021).

198. Canada, H. Good manufacturing practices guide for drug products (GUI-0001). https://www.canada.ca/en/health-canada/services/drugs-health-products/compliance-enforcement/good-manufacturing-practices/guidance-documents/gmp-guidelines-0001/document.html (2018).

199. Cliff, E. R. S. *et al.* High Cost of Chimeric Antigen Receptor T-Cells: Challenges and Solutions. *Am Soc Clin Oncol Educ Book* e397912 (2023) doi:10.1200/EDBK_397912.

200. Choi, G., Shin, G. & Bae, S. Price and Prejudice? The Value of Chimeric Antigen Receptor (CAR) T-Cell Therapy. *Int J Environ Res Public Health* **19**, 12366 (2022).

201. McComb, S. *et al.* Discovery and preclinical development of a therapeutically active nanobody-based chimeric antigen receptor targeting human CD22. *Molecular Therapy Oncology* **32**, (2024).

202. Zhang, Z. *et al.* Modified CAR T cells targeting membrane-proximal epitope of mesothelin enhances the antitumor function against large solid tumor. *Cell Death Dis* **10**, 476 (2019).

203. James, S. E. *et al.* Antigen sensitivity of CD22-specific chimeric T cell receptors is modulated by target epitope distance from the cell membrane. *J Immunol* **180**, 7028–7038 (2008).

204. Kalergis, A. M. *et al.* Efficient T cell activation requires an optimal dwell-time of interaction between the TCR and the pMHC complex. *Nat Immunol* **2**, 229–234 (2001).

205. Long, A. H. *et al.* 4-1BB Costimulation Ameliorates T Cell Exhaustion Induced by Tonic Signaling of Chimeric Antigen Receptors. *Nat Med* **21**, 581–590 (2015).

206. Labbé, R. P., Vessillier, S. & Rafiq, Q. A. Lentiviral Vectors for T Cell Engineering: Clinical Applications, Bioprocessing and Future Perspectives. *Viruses* **13**, 1528 (2021).

207. Milone, M. C. & O'Doherty, U. Clinical use of lentiviral vectors. *Leukemia* **32**, 1529–1541 (2018).

208. Funke, S. *et al.* Targeted Cell Entry of Lentiviral Vectors. *Mol Ther* **16**, 1427–1436 (2008).

209. Escors, D. & Breckpot, K. Lentiviral vectors in gene therapy: their current status and future potential. *Arch Immunol Ther Exp (Warsz)* **58**, 107–119 (2010).

210. Liang, M. *et al*. Targeted Transduction via CD4 by a Lentiviral Vector Uses a Clathrin-Mediated Entry Pathway. *J Virol* **83**, 13026–13031 (2009).

211. Rabson, A. B. & Graves, B. J. Synthesis and Processing of Viral RNA. in *Retroviruses* (eds Coffin, J. M., Hughes, S. H. & Varmus, H. E.) (Cold Spring Harbor Laboratory Press, Cold Spring Harbor (NY), 1997).

212. Poletti, V. & Mavilio, F. Interactions between Retroviruses and the Host Cell Genome. *Mol Ther Methods Clin Dev* **8**, 31–41 (2017).

213. Meng, B. & Lever, A. M. Wrapping up the bad news – HIV assembly and release. *Retrovirology* **10**, 5 (2013).

214. Broussau, S. *et al*. Packaging cells for lentiviral vectors generated using the cumate and coumermycin gene induction systems and nanowell single-cell cloning. *Mol Ther Methods Clin Dev* **29**, 40–57 (2023).

215. Haas, D. L., Case, S. S., Crooks, G. M. & Kohn, D. B. Critical factors influencing stable transduction of human CD34(+) cells with HIV-1-derived lentiviral vectors. *Mol Ther* **2**, 71–80 (2000).

216. Vink, C. A. *et al*. Eliminating HIV-1 Packaging Sequences from Lentiviral Vector Proviruses Enhances Safety and Expedites Gene Transfer for Gene Therapy. *Mol Ther* **25**, 1790–1804 (2017).

217. Huehls, A. M., Coupet, T. A. & Sentman, C. L. Bispecific T-cell engagers for cancer immunotherapy. *Immunology & Cell Biology* **93**, 290–296 (2015).

218. Klein, J. S. *et al.* Examination of the contributions of size and avidity to the neutralization mechanisms of the anti-HIV antibodies b12 and 4E10. *Proceedings of the National Academy of Sciences* **106**, 7385–7390 (2009).

219. Brischwein, K. *et al.* Strictly Target Cell-dependent Activation of T Cells by Bispecific Single-chain Antibody Constructs of the BiTE Class. *Journal of Immunotherapy* **30**, 798 (2007).

220. Amann, M. *et al.* Antitumor Activity of an EpCAM/CD3-bispecific BiTE Antibody During Long-term Treatment of Mice in the Absence of T-cell Anergy and Sustained Cytokine Release. *Journal of Immunotherapy* **32**, 452 (2009).

221. Offner, S., Hofmeister, R., Romaniuk, A., Kufer, P. & Baeuerle, P. A. Induction of regular cytolytic T cell synapses by bispecific single-chain antibody constructs on MHC class I-negative tumor cells. *Molecular Immunology* **43**, 763–771 (2006).

222. Osada, T. *et al.* Metastatic colorectal cancer cells from patients previously treated with chemotherapy are sensitive to T-cell killing mediated by CEA/CD3-bispecific T-cell-engaging BiTE antibody. *Br J Cancer* **102**, 124–133 (2010).

223. Dreier, T. *et al.* Extremely potent, rapid and costimulation-independent cytotoxic T-cell response against lymphoma cells catalyzed by a single-chain bispecific antibody. *International Journal of Cancer* **100**, 690–697 (2002).

224. Manzke, O., Titzer, S., Tesch, H., Diehl, V. & Bohlen, H. CD3×CD19 bispecific antibodies and CD28 costimulation for locoregional treatment of low-malignancy non-Hodgkin's lymphoma. *Cancer Immunol Immunother* **45**, 198–202 (1997).

225. Roddie, C. *et al.* Dual targeting of CD19 and CD22 with bicistronic CAR-T cells in patients with relapsed/refractory large B-cell lymphoma. *Blood* **141**, 2470–2482 (2023).

226. Ghorashian, S. *et al.* CD19/CD22 targeting with cotransduced CAR T cells to prevent antigen-negative relapse after CAR T-cell therapy for B-cell ALL. *Blood* **143**, 118–123 (2024).

227. Qin, H. *et al.* Preclinical Development of Bivalent Chimeric Antigen Receptors Targeting Both CD19 and CD22. *Molecular Therapy - Oncolytics* **11**, 127–137 (2018).

228. Brillembourg, H. *et al.* The role of chimeric antigen receptor T cells targeting more than one antigen in the treatment of B-cell malignancies. *British Journal of Haematology* **204**, 1649–1659 (2024).

229. Kumar, M., Keller, B., Makalou, N. & Sutton, R. E. Systematic Determination of the Packaging Limit of Lentiviral Vectors. *Human Gene Therapy* **12**, 1893–1905 (2001).

230. Cordoba, S. *et al.* CAR T cells with dual targeting of CD19 and CD22 in pediatric and young adult patients with relapsed or refractory B cell acute lymphoblastic leukemia: a phase 1 trial. *Nat Med* **27**, 1797–1805 (2021).

231. Fergusson, N. J., Adeel, K., Kekre, N., Atkins, H. & Hay, K. A. A systematic review and meta-analysis of CD22 CAR T-cells alone or in combination with CD19 CAR T-cells. *Front. Immunol.* **14**, (2023).

232. Li, W. *et al.* APRIL CAR-T Cell Therapy for Relapsed/Refractory Multiple Myeloma: A Phase I Clinical Trial. *Blood* **144**, 7229 (2024).

233. Grada, Z. *et al.* TanCAR: A Novel Bispecific Chimeric Antigen Receptor for Cancer Immunotherapy. *Molecular Therapy - Nucleic Acids* **2**, (2013).

234. Zah, E., Lin, M.-Y., Silva-Benedict, A., Jensen, M. C. & Chen, Y. Y. T Cells Expressing CD19/CD20 Bispecific Chimeric Antigen Receptors Prevent Antigen Escape by Malignant B Cells. *Cancer Immunology Research* **4**, 498–508 (2016).

235. Li, H. *et al.* CAR-T cells targeting CD38 and LMP1 exhibit robust antitumour activity against NK/T cell lymphoma. *BMC Med* **21**, 330 (2023).

236. Kang, L. *et al.* Characterization of novel dual tandem CD19/BCMA chimeric antigen receptor T cells to potentially treat multiple myeloma. *Biomark Res* **8**, 14 (2020).

237. Holland, E. M. *et al.* CAR T-cells as Salvage Therapy for post CAR T-cell Failure. *Transplant Cell Ther* **29**, 574.e1-574.e10 (2023).

238. Xu, K. Sequential infusion of two different chimeric antigen receptor T cells: induction of a deep and durable remission. *Blood Sci* **6**, e00177 (2024).

239. Meng, Y. *et al.* Short-Interval Sequential CAR-T Cell Infusion May Enhance Prior CAR-T Cell Expansion to Augment Anti-Lymphoma Response in B-NHL. *Front. Oncol.* **11**, (2021).

240. Furqan, F. & Shah, N. N. Multispecific CAR T Cells Deprive Lymphomas of Escape via Antigen Loss. *Annu Rev Med* **74**, 279–291 (2023).

241. Gardner, R. *et al.* Acquisition of a CD19-negative myeloid phenotype allows immune escape of MLL-rearranged B-ALL from CD19 CAR-T-cell therapy. *Blood* **127**, 2406–2410 (2016).

242. Jacoby, E. *et al.* CD19 CAR immune pressure induces B-precursor acute lymphoblastic leukaemia lineage switch exposing inherent leukaemic plasticity. *Nat Commun* **7**, 12320 (2016).

243. Orlando, E. J. *et al.* Genetic mechanisms of target antigen loss in CAR19 therapy of acute lymphoblastic leukemia. *Nat Med* **24**, 1504–1506 (2018).

244. Sotillo, E. *et al.* Convergence of Acquired Mutations and Alternative Splicing of CD19 Enables Resistance to CART-19 Immunotherapy. *Cancer Discov* **5**, 1282–1295 (2015).

245. Berchuck, A. *et al.* Heterogeneity of antigen expression in advanced epithelial ovarian cancer. *American Journal of Obstetrics & Gynecology* **162**, 883–888 (1990).

246. Haas, A. R. *et al.* Two cases of severe pulmonary toxicity from highly active mesothelin-directed CAR T cells. *Molecular Therapy* **31**, 2309–2325 (2023).

247. Tokarew, N., Ogonek, J., Endres, S., von Bergwelt-Baildon, M. & Kobold, S. Teaching an old dog new tricks: next-generation CAR T cells. *British Journal of Cancer* **120**, 26–37 (2019).

248. Nolan-Stevaux, O. & Smith, R. Logic-gated and contextual control of immunotherapy for solid tumors: contrasting multi-specific T cell engagers and CAR-T cell therapies. *Front. Immunol.* **15**, 1490911 (2024).

249. Bagley, S. J. *et al.* Intrathecal bivalent CAR T cells targeting EGFR and IL13Rα2 in recurrent glioblastoma: phase 1 trial interim results. *Nat Med* **30**, 1320–1329 (2024).

250. Tousley, A. M. *et al.* Co-opting signalling molecules enables logic-gated control of CAR T cells. *Nature* **615**, 507–516 (2023).

251. Kamata-Sakurai, M. *et al.* Antibody to CD137 Activated by Extracellular Adenosine Triphosphate Is Tumor Selective and Broadly Effective In Vivo without Systemic Immune Activation. *Cancer Discovery* **11**, 158–175 (2021).

252. Frey, G. *et al.* A novel conditional active biologic anti-EpCAM x anti-CD3 bispecific antibody with synergistic tumor selectivity for cancer immunotherapy. *MAbs* **16**, 2322562.

253. Fedorov, V. D., Themeli, M. & Sadelain, M. PD-1– and CTLA-4–Based Inhibitory Chimeric Antigen Receptors (iCARs) Divert Off-Target Immunotherapy Responses. *Sci Transl Med* **5**, 215ra172 (2013).

254. Manry, D., Bolanos, K., DiAndreth, B., Mock, J.-Y. & Kamb, A. Robust In Vitro Pharmacology of Tmod, a Synthetic Dual-Signal Integrator for Cancer Cell Therapy. *Front. Immunol.* **13**, (2022).

255. Jurkat, Clone E6-1 - TIB-152 | ATCC. https://www.atcc.org/products/tib-152.

256. Abraham, R. T. & Weiss, A. Jurkat T cells and development of the T-cell receptor signalling paradigm. *Nat Rev Immunol* **4**, 301–308 (2004).

257. Imboden, J. B. & Stobo, J. D. Transmembrane signalling by the T cell antigen receptor. Perturbation of the T3-antigen receptor complex generates inositol phosphates and releases calcium ions from intracellular stores. *Journal of Experimental Medicine* **161**, 446–456 (1985).

258. Tyrosine phosphatase CD45 is required for T-cell antigen receptor and CD2-mediated activation of a protein tyrosine kinase and interleukin 2 production. https://www.pnas.org/doi/epdf/10.1073/pnas.88.6.2037 doi:10.1073/pnas.88.6.2037.

259. Jutz, S. *et al.* Assessment of costimulation and coinhibition in a triple parameter T cell reporter line: Simultaneous measurement of NF-κB, NFAT and AP-1. *J Immunol Methods* **430**, 10–20 (2016).

260. Seminario, M.-C. & Wange, R. L. Signaling pathways of D3-phosphoinositide-binding kinases in T cells and their regulation by PTEN. *Seminars in Immunology* **14**, 27–36 (2002).

261. Astoul, E., Cantrell, D. A., Edmunds, C. & Ward, S. G. PI 3-K and T-cell activation: limitations of T-leukemic cell lines as signaling models. *Trends in Immunology* **22**, 490–496 (2001).

262. Shan, X. *et al*. Deficiency of PTEN in Jurkat T Cells Causes Constitutive Localization of Itk to the Plasma Membrane and Hyperresponsiveness to CD3 Stimulation. *Molecular and Cellular Biology* **20**, 6945–6957 (2000).

263. Ramos Cell Line - B-Cell Lymphoma Research. *Cytion* https://www.cytion.com/Knowledge-Hub/Cell-Line-Insights/Ramos-Cell-Line-B-Cell-Lymphoma-Research/.

264. RAJI Cells. *Cytion* https://www.cytion.com/RAJI-Cells/300359.

265. Singer, P. A. & Williamson, A. R. Cell surface immunoglobulin mu and gamma chains of human lymphoid cells are of higher apparent molecular weight than their secreted counterparts. *Eur J Immunol* **10**, 180–186 (1980).

266. HEK293T Cells. *Cytion* https://www.cytion.com/HEK293T-Cells/300189.

267. Tan, E., Chin, C. S. H., Lim, Z. F. S. & Ng, S. K. HEK293 Cell Line as a Platform to Produce Recombinant Proteins and Viral Vectors. *Front Bioeng Biotechnol* **9**, 796991 (2021).

268. NCI-H292 Cells. *Cytion* https://www.cytion.com/NCI-H292-Cells/305040.

269. SK-OV-3 [SKOV-3; SKOV3] - HTB-77 | ATCC. https://www.atcc.org/products/htb-77.

270. Comşa, Ş., Cîmpean, A. M. & Raica, M. The Story of MCF-7 Breast Cancer Cell Line: 40 years of Experience in Research. *Anticancer Research* **35**, 3147–3154 (2015).

271. Kim, K. *et al.* Epidermal Growth Factor Receptor vIII Expression in U87 Glioblastoma Cells Alters Their Proteasome Composition, Function, and Response to Irradiation. *Mol Cancer Res* **6**, 426–434 (2008).

272. CD19 CD19 molecule [Homo sapiens (human)] - Gene - NCBI. https://www.ncbi.nlm.nih.gov/gene/930.

273. Zelm, M. C. van *et al.* An Antibody-Deficiency Syndrome Due to Mutations in the CD19 Gene. *New England Journal of Medicine* **354**, 1901–1912 (2006).

274. Buhl, A. M., Pleiman, C. M., Rickert, R. C. & Cambier, J. C. Qualitative Regulation of B Cell Antigen Receptor Signaling by CD19: Selective Requirement for PI3-Kinase Activation, Inositol-1,4,5-Trisphosphate Production and Ca2+ Mobilization. *J Exp Med* **186**, 1897–1910 (1997).

275. Poe, J. C., Minard-Colin, V., Kountikov, E. I., Haas, K. M. & Tedder, T. F. A c-Myc and Surface CD19 Signaling Amplification Loop Promotes B Cell Lymphoma Development and Progression in Mice. *J Immunol* **189**, 2318–2325 (2012).

276. Cooper, L. J. N. *et al.* Development and application of CD19-specific T cells for adoptive immunotherapy of B cell malignancies. *Blood Cells, Molecules, and Diseases* **33**, 83–89 (2004).

277. CD22 associates with protein tyrosine phosphatase 1C, Syk, and phospholipase C-gamma(1) upon B cell activation. *J Exp Med* **183**, 547–560 (1996).

278. Meyer, S. J. *et al.* CD22 Controls Germinal Center B Cell Receptor Signaling, Which Influences Plasma Cell and Memory B Cell Output. *The Journal of Immunology* **207**, 1018–1032 (2021).

279. Séïté, J.-F. *et al.* IVIg modulates BCR signaling through CD22 and promotes apoptosis in mature human B lymphocytes. *Blood* **116**, 1698–1704 (2010).

280. Shah, N. N. *et al.* Characterization of CD22 Expression in Acute Lymphoblastic Leukemia. *Pediatr Blood Cancer* **62**, 964–969 (2015).

281. CLIC-2201 for the Treatment of Relapsed/Refractory B Cell Malignancies | Clinical Research Trial Listing. https://www.centerwatch.com/clinical-trials/listings/NCT06208735/clic-2201-for-the-treatment-of-relapsed-refractory-b-cell-malignancies/clic-2201-for-the-treatment-of-relapsed-refractory-b-cell-malignancies.

282. Tai, Y.-T. & Anderson, K. C. Targeting B-cell maturation antigen in multiple myeloma. *Immunotherapy* **7**, 1187–1199 (2015).

283. Moreaux, J. *et al.* BAFF and APRIL protect myeloma cells from apoptosis induced by interleukin 6 deprivation and dexamethasone. *Blood* **103**, 3148–3157 (2004).

284. Murphrey, M. B., Quaim, L., Rahimi, N. & Varacallo, M. A. Biochemistry, Epidermal Growth Factor Receptor. in *StatPearls* (StatPearls Publishing, Treasure Island (FL), 2025).

285. Tissue expression of EGFR - Summary - The Human Protein Atlas. https://www.proteinatlas.org/ENSG00000146648-EGFR/tissue.

286. Uribe, M. L., Marrocco, I. & Yarden, Y. EGFR in Cancer: Signaling Mechanisms, Drugs, and Acquired Resistance. *Cancers (Basel)* **13**, 2748 (2021).

287. Hanahan, D. & Weinberg, R. A. Hallmarks of Cancer: The Next Generation. *Cell* **144**, 646–674 (2011).

288. Witsch, E., Sela, M. & Yarden, Y. Roles for Growth Factors in Cancer Progression. *Physiology (Bethesda)* **25**, 85–101 (2010).

289. Hirsh, V. Managing treatment-related adverse events associated with egfr tyrosine kinase inhibitors in advanced non-small-cell lung cancer. *Curr Oncol* **18**, 126–138 (2011).

290. Cetuximab (Erbitux): Uses & Side Effects. *Cleveland Clinic* https://my.clevelandclinic.org/health/drugs/19538-cetuximab-injection.

291. Sok, J. C. *et al.* Mutant Epidermal Growth Factor Receptor (EGFRvIII) Contributes to Head and Neck Cancer Growth and Resistance to EGFR Targeting. *Clinical Cancer Research* **12**, 5064–5073 (2006).

292. Batra, S. K. *et al.* Epidermal growth factor ligand-independent, unregulated, cell-transforming potential of a naturally occurring human mutant EGFRvIII gene. *Cell Growth Differ* **6**, 1251–1259 (1995).

293. Wong, A. J. *et al.* Structural alterations of the epidermal growth factor receptor gene in human gliomas. *Proc Natl Acad Sci U S A* **89**, 2965–2969 (1992).

294. Faust, J. R., Hamill, D., Kolb, E. A., Gopalakrishnapillai, A. & Barwe, S. P. Mesothelin: An Immunotherapeutic Target beyond Solid Tumors. *Cancers (Basel)* **14**, 1550 (2022).

295. Tissue expression of MSLN - Summary - The Human Protein Atlas. https://www.proteinatlas.org/ENSG00000102854-MSLN/tissue.

296. Liu, X., Chan, A., Tai, C.-H., Andresson, T. & Pastan, I. Multiple proteases are involved in mesothelin shedding by cancer cells. *Commun Biol* **3**, 728 (2020).

297. Monoclonal antibody mechanisms of action in cancer | Immunologic Research. https://link.springer.com/article/10.1007/s12026-007-0073-4.

298. Tian, Z., Liu, M., Zhang, Y. & Wang, X. Bispecific T cell engagers: an emerging therapy for management of hematologic malignancies. *Journal of Hematology & Oncology* **14**, 75 (2021).

299. Amgen Research (Munich) GmbH. *An Open Label, Multicenter, Exploratory Phase II Study to Evaluate the Efficacy, Safety, and Tolerability of the BiTE® Antibody Blinatumomab in Adult Patients With Relapsed/Refractory B-Precursor Acute Lymphoblastic Leukemia (ALL)*. https://clinicaltrials.gov/study/NCT01209286 (2017).

300. Wu, J., Fu, J., Zhang, M. & Liu, D. Blinatumomab: a bispecific T cell engager (BiTE) antibody against CD19/CD3 for refractory acute lymphoid leukemia. *Journal of Hematology & Oncology* **8**, 104 (2015).

301. Wang, Q. *et al.* Design and Production of Bispecific Antibodies. *Antibodies (Basel)* **8**, E43 (2019).

302. Mechanism of Action | BLINCYTO® (blinatumomab). https://www.blincytohcp.com/mrd/moa.

303. Viardot, A., Locatelli, F., Stieglmaier, J., Zaman, F. & Jabbour, E. Concepts in immuno-oncology: tackling B cell malignancies with CD19-directed bispecific T cell engager therapies. *Ann Hematol* **99**, 2215–2229 (2020).

304. Blinatumomab. https://go.drugbank.com/drugs/DB09052.

305. Davis, M. W. & Jorgensen, E. M. ApE, A Plasmid Editor: A Freely Available DNA Manipulation and Visualization Program. *Front. Bioinform.* **2**, (2022).

306. Gibson, D. G. *et al.* Enzymatic assembly of DNA molecules up to several hundred kilobases. *Nat Methods* **6**, 343–345 (2009).

307. Engler, C., Kandzia, R. & Marillonnet, S. A One Pot, One Step, Precision Cloning Method with High Throughput Capability. *PLoS One* **3**, e3647 (2008).

308. Brinkmann, U. & and Kontermann, R. E. The making of bispecific antibodies. *mAbs* **9**, 182–212 (2017).

309. Mccomb, S. *et al.* Antigen-Binding Agents That Specifically Bind Epidermal Growth Factor Receptor Variant Iii. (2020).

310. Marcil, A., Jaramillo, M., Sulea, T., Moreno, M. & Wu, C. Anti-Egfrviii Antibodies and Antigen-Binding Fragments Thereof. (2020).

311. Marcil, A., Pon, R., Mccomb, S. & Iqbal, U. Anti-Cd3 Monoclonal Antibodies and Therapeutic Constructs. (2023).

312. Molla Kazemiha, V. *et al.* PCR-based detection and eradication of mycoplasmal infections from various mammalian cell lines: a local experience. *Cytotechnology* **61**, 117–124 (2009).

313. Chicaybam, L., Sodre, A. L., Curzio, B. A. & Bonamino, M. H. An Efficient Low Cost Method for Gene Transfer to T Lymphocytes. *PLOS ONE* **8**, e60298 (2013).

314. Bloemberg, D. *et al.* A High-Throughput Method for Characterizing Novel Chimeric Antigen Receptors in Jurkat Cells. *Molecular Therapy - Methods & Clinical Development* **16**, 238–254 (2020).

315. Reff, M. *et al.* Depletion of B cells in vivo by a chimeric mouse human monoclonal antibody to CD20. *Blood* **83**, 435–445 (1994).

316. Understanding the Mechanisms Behind Trastuzumab Therapy for Human Epidermal Growth Factor Receptor 2–Positive Breast Cancer | Journal of Clinical Oncology. https://ascopubs.org/doi/10.1200/JCO.2009.22.1507.

317. Casneuf, T. *et al.* Effects of daratumumab on natural killer cells and impact on clinical outcomes in relapsed or refractory multiple myeloma. *Blood Advances* **1**, 2105–2114 (2017).

318. Rossi, E. A. *et al.* Stably tethered multifunctional structures of defined composition made by the dock and lock method for use in cancer targeting. *Proc Natl Acad Sci U S A* **103**, 6841–6846 (2006).

319. Rapid, site-specific labeling of “off-the-shelf” and native serum autoantibodies with T cell–redirecting domains | Science Advances. https://www.science.org/doi/10.1126/sciadv.abn4613.

320. Full article: Intein mediated high throughput screening for bispecific antibodies. https://www.tandfonline.com/doi/full/10.1080/19420862.2020.1731938.

321. Sugiyama, A. *et al.* A semi high-throughput method for screening small bispecific antibodies with high cytotoxicity. *Sci Rep* **7**, 2862 (2017).

322. Nazarian, A. A. *et al.* Characterization of bispecific T-cell Engager (BiTE) antibodies with a high-capacity T-cell dependent cellular cytotoxicity (TDCC) assay. *J Biomol Screen* **20**, 519–527 (2015).

323. Wang, Y. *et al.* High-throughput functional screening for next-generation cancer immunotherapy using droplet-based microfluidics. *Sci Adv* **7**, eabe3839 (2021).

324. Segaliny, A. I. *et al.* A high throughput bispecific antibody discovery pipeline. 2021.09.07.459213 Preprint at https://doi.org/10.1101/2021.09.07.459213 (2021).

325. FDA-approved CAR T-cell Therapies | UPMC Hillman. *UPMC HIllman Cancer Center* https://hillman.upmc.com/mario-lemieux-center/treatment/car-t-cell-therapy/fda-approved-therapies.

326. Jiao, C. *et al.* 4SCAR2.0: a multi-CAR-T therapy regimen for the treatment of relapsed/refractory B cell lymphomas. *Blood Cancer J.* **11**, 1–5 (2021).

327. Rafiq, S., Hackett, C. S. & Brentjens, R. J. Engineering strategies to overcome the current roadblocks in CAR T cell therapy. *Nat Rev Clin Oncol* **17**, 147–167 (2020).

328. Hegde, M. *et al.* Tandem CAR T cells targeting HER2 and IL13Rα2 mitigate tumor antigen escape. *J Clin Invest* **126**, 3036–3052 (2016).

329. Liang, Z. *et al.* Tandem CAR-T cells targeting FOLR1 and MSLN enhance the antitumor effects in ovarian cancer. *International Journal of Biological Sciences* **17**, 4365–4376 (2021).

330. Du, J. *et al.* Updated Results of a Phase I Open-Label Single-Arm Study of Dual Targeting BCMA and CD19 Fastcar-T Cells (GC012F) As First-Line Therapy for Transplant-Eligible Newly Diagnosed High-Risk Multiple Myeloma. *Blood* **142**, 1022 (2023).

331. Ren, H. *et al.* Bispecific CAR-iNKT Immunotherapy for High Risk MLL-Rearranged Acute Lymphoblastic Leukemia. *Blood* **142**, 766 (2023).

332. Tandem CD19/20 CAR-T Showed Durable Efficacy in Patients with Relapsed/Refractory B-Cell Lymphoma: Interim Results from a Multicenter Phase I/II Trial | Blood | American Society of Hematology. https://ashpublications.org/blood/article/144/Supplement%201/3132/533381/Tandem-CD19-20-CAR-T-Showed-Durable-Efficacy-in.

333. Shah, N. N. *et al.* P1082: RESULTS FROM A PHASE 1/2 STUDY OF TANDEM, BISPECIFIC ANTI-CD20/ANTI-CD19 (LV20.19) CAR T-CELLS FOR MANTLE CELL LYMPHOMA. *Hemasphere* **7**, e207658e (2023).

334. Arbabi-Ghahroudi, M. Camelid Single-Domain Antibodies: Promises and Challenges as Lifesaving Treatments. *Int J Mol Sci* **23**, 5009 (2022).

335. Asaadi, Y., Jouneghani, F. F., Janani, S. & Rahbarizadeh, F. A comprehensive comparison between camelid nanobodies and single chain variable fragments. *Biomarker Research* **9**, 87 (2021).

336. Ordóñez, N. G. Value of mesothelin immunostaining in the diagnosis of mesothelioma. *Mod Pathol* **16**, 192–197 (2003).

337. Frierson, H. F. *et al.* Large-scale molecular and tissue microarray analysis of mesothelin expression in common human carcinomas. *Human Pathology* **34**, 605–609 (2003).

338. Inaguma, S. *et al.* Comprehensive immunohistochemical study of mesothelin (MSLN) using different monoclonal antibodies 5B2 and MN-1 in 1562 tumors with evaluation of its prognostic value in malignant pleural mesothelioma. *Oncotarget* **8**, 26744–26754 (2017).

339. Klampatsa, A., Dimou, V. & Albelda, S. M. Mesothelin-targeted CAR-T cell therapy for solid tumors. *Expert Opinion on Biological Therapy* **21**, 473–486 (2021).

340. Haas, A. R. *et al.* Phase I Study of Lentiviral-Transduced Chimeric Antigen Receptor-Modified T Cells Recognizing Mesothelin in Advanced Solid Cancers. *Mol Ther* **27**, 1919–1929 (2019).

341. Castelletti, L., Yeo, D., van Zandwijk, N. & Rasko, J. E. J. Anti-Mesothelin CAR T cell therapy for malignant mesothelioma. *Biomarker Research* **9**, 11 (2021).

342. Maennling, A. E. *et al.* Molecular Targeting Therapy against EGFR Family in Breast Cancer: Progress and Future Potentials. *Cancers* **11**, 1826 (2019).

343. García-Foncillas, J. *et al.* Distinguishing Features of Cetuximab and Panitumumab in Colorectal Cancer and Other Solid Tumors. *Front. Oncol.* **9**, (2019).

344. Weidemann, S. *et al.* Mesothelin Expression in Human Tumors: A Tissue Microarray Study on 12,679 Tumors. *Biomedicines* **9**, 397 (2021).

345. Kachala, S. S. *et al.* Mesothelin Overexpression Is a Marker of Tumor Aggressiveness and Is Associated with Reduced Recurrence-free and Overall Survival in Early-Stage Lung Adenocarcinoma. *Clin Cancer Res* **20**, 1020–1028 (2014).

346. Bloemberg, D. *et al.* A High-Throughput Method for Characterizing Novel Chimeric Antigen Receptors in Jurkat Cells. *Molecular Therapy - Methods & Clinical Development* **16**, 238–254 (2020).

347. Arbabi-Ghahroudi, M., MCCOMB, S., Pon, R. & Weeratna, R. Anti-mesothelin (msln) single domain antibodies and therapeutic constructs. (2024).

348. Ebert, L. M., Yu, W., Gargett, T. & Brown, M. P. Logic-gated approaches to extend the utility of chimeric antigen receptor T-cell technology. *Biochem Soc Trans* **46**, 391–401 (2018).

349. Leung, I. *et al.* Compromised antigen binding and signaling interfere with bispecific CD19 and CD79a chimeric antigen receptor function. *Blood Adv* **7**, 2718–2730 (2022).

350. Dai, Z. *et al.* T cells expressing CD5/CD7 bispecific chimeric antigen receptors with fully human heavy-chain-only domains mitigate tumor antigen escape. *Signal Transduct Target Ther* **7**, 85 (2022).

351. Fernández de Larrea, C. *et al.* Defining an Optimal Dual-Targeted CAR T-cell Therapy Approach Simultaneously Targeting BCMA and GPRC5D to Prevent BCMA Escape–Driven Relapse in Multiple Myeloma. *Blood Cancer Discov* **1**, 146–154 (2020).

352. Wang, X.-Y. *et al.* Tandem bispecific CD123/CLL-1 CAR-T cells exhibit specific cytolytic effector functions against human acute myeloid leukaemia. *European Journal of Haematology* **112**, 83–93 (2024).

353. Yang, M. *et al.* Tandem CAR-T cells targeting CD70 and B7-H3 exhibit potent preclinical activity against multiple solid tumors. *Theranostics* **10**, 7622–7634 (2020).

354. Schmidts, A. *et al.* Tandem chimeric antigen receptor (CAR) T cells targeting EGFRvIII and IL-13Rα2 are effective against heterogeneous glioblastoma. *Neurooncol Adv* **5**, vdac185 (2022).

355. Zurko, J. C. *et al.* Long-term outcomes and predictors of early response, late relapse, and survival for patients treated with bispecific LV20.19 CAR T-cells. *Am J Hematol* **97**, 1580–1588 (2022).

356. Shah, N. N. *et al.* Phase 1 Trial of LV20.19 CAR T-Cells for Relapsed, Refractory CLL and Richter's Transformation. *Transplantation and Cellular Therapy* **30**, S35–S36 (2024).

357. Wang, Y. *et al.* A retrospective comparison of CD19 single and CD19/CD22 bispecific targeted chimeric antigen receptor T cell therapy in patients with relapsed/refractory acute lymphoblastic leukemia. *Blood Cancer J.* **10**, 1–3 (2020).

358. Qu, C. *et al.* Decitabine-primed tandem CD19/CD22 CAR-T therapy in relapsed/refractory diffuse large B-cell lymphoma patients. *Front. Immunol.* **13**, (2022).

359. Wang, L. *et al.* Bispecific CAR-T cells targeting CD19/20 in patients with relapsed or refractory B cell non-Hodgkin lymphoma: a phase I/II trial. *Blood Cancer J.* **14**, 1–13 (2024).

360. Gardner, R. *et al.* Early Clinical Experience of CD19 x CD22 Dual Specific CAR T Cells for Enhanced Anti-Leukemic Targeting of Acute Lymphoblastic Leukemia. *Blood* **132**, 278–278 (2018).

361. Bachiller, M. *et al.* ARI0003: Co-transduced CD19/BCMA dual-targeting CAR-T cells for the treatment of non-Hodgkin lymphoma. *Molecular Therapy* **33**, 317–335 (2025).

362. Shalabi, H. *et al.* CD19/22 CAR T cells in children and young adults with B-ALL: phase 1 results and development of a novel bicistronic CAR. *Blood* **140**, 451–463 (2022).

363. Xie, D. *et al.* Bicistronic CAR-T cells targeting CD123 and CLL1 for AML to reduce the risk of antigen escape. *Translational Oncology* **34**, 101695 (2023).

364. Hegde, M. *et al.* Tandem CAR T cells targeting HER2 and IL13Rα2 mitigate tumor antigen escape. *J Clin Invest* **126**, 3036–3052.

365. Ko, A. H. *et al.* Dual Targeting of Mesothelin and CD19 with Chimeric Antigen Receptor-Modified T Cells in Patients with Metastatic Pancreatic Cancer. *Molecular Therapy* **28**, 2367–2378 (2020).

366. Broussau, S. *et al.* Packaging cells for lentiviral vectors generated using the cumate and coumermycin gene induction systems and nanowell single-cell cloning. *Mol Ther Methods Clin Dev* **29**, 40–57 (2023).

367. Selli, M. E., Landmann, J. H., Arveseth, C. & Singh, N. Inducing T cell dysfunction by chronic stimulation of CAR-engineered T cells targeting cancer cells in suspension cultures. *STAR Protoc* **4**, 101954 (2023).

368. McComb, S. *et al.* Broadly Reactive Anti-VHH Antibodies for Characterizing, Blocking, or Activating Nanobody-Based CAR-T Cells. 2024.09.18.613561 Preprint at https://doi.org/10.1101/2024.09.18.613561 (2024).

369. Lu, J. & Jiang, G. The journey of CAR-T therapy in hematological malignancies. *Molecular Cancer* **21**, 194 (2022).

370. Marofi, F. *et al.* CAR T cells in solid tumors: challenges and opportunities. *Stem Cell Research & Therapy* **12**, 81 (2021).

371. Zhang, X., Zhu, L., Zhang, H., Chen, S. & Xiao, Y. CAR-T Cell Therapy in Hematological Malignancies: Current Opportunities and Challenges. *Front. Immunol.* **13**, (2022).

372. Lee, Y. G. *et al.* Regulation of CAR T cell-mediated cytokine release syndrome-like toxicity using low molecular weight adapters. *Nat Commun* **10**, 2681 (2019).

373. Halim, L. *et al.* Engineering of an Avidity-Optimized CD19-Specific Parallel Chimeric Antigen Receptor That Delivers Dual CD28 and 4-1BB Co-Stimulation. *Front. Immunol.* **13**, (2022).

374. Leick, M. B. *et al.* Non-cleavable hinge enhances avidity and expansion of CAR-T cells for acute myeloid leukemia. *Cancer Cell* **40**, 494-508.e5 (2022).

375. Olson, M. L. *et al.* Low-affinity CAR T cells exhibit reduced trogocytosis, preventing rapid antigen loss, and increasing CAR T cell expansion. *Leukemia* **36**, 1943–1946 (2022).

376. Erlendsson, S. & Teilum, K. Binding Revisited—Avidity in Cellular Function and Signaling. *Front. Mol. Biosci.* **7**, (2021).

377. Generation of Stable Expression Mammalian Cell Lines Using Lentivirus. https://bio-protocol.org/en/bpdetail?id=3073&type=0.

378. Sykulev, Y., Joo, M., Vturina, I., Tsomides, T. J. & Eisen, H. N. Evidence that a Single Peptide–MHC Complex on a Target Cell Can Elicit a Cytolytic T Cell Response. *Immunity* **4**, 565–571 (1996).

379. Garcia, K. C., Teyton, L. & Wilson, I. A. STRUCTURAL BASIS OF T CELL RECOGNITION. *Annual Review of Immunology* **17**, 369–397 (1999).

380. Valitutti, S., Müller, S., Cella, M., Padovan, E. & Lanzavecchia, A. Serial triggering of many T-cell receptors by a few peptide–MHC complexes. *Nature* **375**, 148–151 (1995).

381. Lanzavecchia, A., Iezzi, G. & Viola, A. From TCR Engagement to T Cell Activation: A Kinetic View of T Cell Behavior. *Cell* **96**, 1–4 (1999).

382. Kinetic proofreading in T-cell receptor signal transduction. https://www.pnas.org/doi/epdf/10.1073/pnas.92.11.5042 doi:10.1073/pnas.92.11.5042.

383. Kersh, G. J., Kersh, E. N., Fremont, D. H. & Allen, P. M. High- and Low-Potency Ligands with Similar Affinities for the TCR: The Importance of Kinetics in TCR Signaling. *Immunity* **9**, 817–826 (1998).

384. Hudrisier, D. *et al.* The efficiency of antigen recognition by CD8+ CTL clones is determined by the frequency of serial TCR engagement. *J Immunol* **161**, 553–562 (1998).

385. Degano, M. *et al.* A Functional Hot Spot for Antigen Recognition in a Superagonist TCR/MHC Complex. *Immunity* **12**, 251–261 (2000).

386. Zenke, S. *et al.* Quorum Regulation via Nested Antagonistic Feedback Circuits Mediated by the Receptors CD28 and CTLA-4 Confers Robustness to T Cell Population Dynamics. *Immunity* **52**, 313-327.e7 (2020).

387. Griffith, A. A. *et al.* SILAC Phosphoproteomics Reveals Unique Signaling Circuits in CAR-T Cells and the Inhibition of B Cell-Activating Phosphorylation in Target Cells. *J. Proteome Res.* **21**, 395–409 (2022).

388. Benmebarek, M.-R. *et al.* Killing Mechanisms of Chimeric Antigen Receptor (CAR) T Cells. *International Journal of Molecular Sciences* **20**, 1283 (2019).

389. Signaling from T cell receptors (TCRs) and chimeric antigen receptors (CARs) on T cells | Cellular & Molecular Immunology. https://www.nature.com/articles/s41423-020-0470-3.

390. MacMullan, M. A., Dunn, Z. S., Qu, Y., Wang, P. & Graham, N. A. Phospho-proteomic analysis of CAR-T cell signaling following activation by antigen-presenting cancer cells. 2022.02.24.481820 Preprint at https://doi.org/10.1101/2022.02.24.481820 (2022).

391. Frankenfield, A. M. *et al.* Benchmarking SILAC Proteomics Workflows and Data Analysis Platforms. *Mol Cell Proteomics* **24**, 100980 (2025).

392. Park, J. H. *et al.* Results From First-in-Human Phase I Study of a Novel CD19-1XX Chimeric Antigen Receptor With Calibrated Signaling in Large B-Cell Lymphoma. *J Clin Oncol* **43**, 2418–2428 (2025).

393. Duncan, B. B., Dunbar, C. E. & Ishii, K. Applying a clinical lens to animal models of CAR-T cell therapies. *Mol Ther Methods Clin Dev* **27**, 17–31 (2022).

394. Mlinarić, A., Horvat, M. & Šupak Smolčić, V. Dealing with the positive publication bias: Why you should really publish your negative results. *Biochem Med (Zagreb)* **27**, 030201 (2017).

395. Chen, J. *et al.* Tuning charge density of chimeric antigen receptor optimizes tonic signaling and CAR-T cell fitness. *Cell Res* **33**, 341–354 (2023).

396. KEGG PATHWAY: T cell receptor signaling pathway - Homo sapiens (human). https://www.kegg.jp/pathway/hsa04660.

397. Tian, R. *et al.* Combinatorial proteomic analysis of intercellular signaling applied to the CD28 T-cell costimulatory receptor. *Proc Natl Acad Sci U S A* **112**, E1594–E1603 (2015).

398. Rainwater, R. R. *et al.* DNA-PKcs governs LAT-dependent signaling in CD4+ and CD8+ T cells. 2025.03.06.641745 Preprint at https://doi.org/10.1101/2025.03.06.641745 (2025).

399. Salter, A. I. *et al.* Phosphoproteomic analysis of chimeric antigen receptor signaling reveals kinetic and quantitative differences that affect cell function. *Sci Signal* **11**, eaat6753 (2018).

400. MacMullan, M. A., Dunn, Z. S., Qu, Y., Wang, P. & Graham, N. A. Phospho-proteomic analysis of CAR-T cell signaling following activation by antigen-presenting cancer cells. 2022.02.24.481820 Preprint at https://doi.org/10.1101/2022.02.24.481820 (2022).

401. Salter, A. I. *et al.* Comparative analysis of TCR and CAR signaling informs CAR designs with superior antigen sensitivity and in vivo function. *Sci Signal* **14**, eabe2606 (2021).

402. Mao, R., Kong, W. & He, Y. The affinity of antigen-binding domain on the antitumor efficacy of CAR T cells: Moderate is better. *Front Immunol* **13**, 1032403 (2022).

403. Andreu-Saumell, I. *et al.* CAR affinity modulates the sensitivity of CAR-T cells to PD-1/PD-L1-mediated inhibition. *Nat Commun* **15**, 3552 (2024).

404. He, C. *et al.* CD19 CAR antigen engagement mechanisms and affinity tuning. *Sci Immunol* **8**, eadf1426 (2023).

405. Owens, G. L. *et al.* Preclinical Assessment of CAR T-Cell Therapy Targeting the Tumor Antigen 5T4 in Ovarian Cancer. *Journal of Immunotherapy* **41**, 130 (2018).

406. Kalaitsidou, M., Kueberuwa, G., Schütt, A. & Gilham, D. E. CAR T-cell Therapy: Toxicity and The Relevance of Preclinical Models. *Immunotherapy* **7**, 487–497 (2015).

407. Si, X., Xiao, L., Brown, C. E. & Wang, D. Preclinical Evaluation of CAR T Cell Function: In Vitro and In Vivo Models. *International Journal of Molecular Sciences* **23**, 3154 (2022).

408. Deng, X. *et al.* Antitumor activity of NKG2D CAR-T cells against human colorectal cancer cells in vitro and in vivo. *Am J Cancer Res* **9**, 945–958 (2019).

409. Cappell, K. M. & Kochenderfer, J. N. A comparison of chimeric antigen receptors containing CD28 versus 4-1BB costimulatory domains. *Nat Rev Clin Oncol* **18**, 715–727 (2021).

410. Roselli, E. *et al.* 4-1BB and optimized CD28 co-stimulation enhances function of human mono-specific and bi-specific third-generation CAR T cells. *J Immunother Cancer* **9**, e003354 (2021).

411. Sharma, P. *et al.* FDA Approval Summary: Idecabtagene Vicleucel for the Treatment of Triple-Class-Exposed, Relapsed or Refractory Multiple Myeloma. *Clin Cancer Res* **31**, 3362–3367 (2025).

412. CAR Signaling Networks Interactive Pathway | Cell Signaling Technology. https://www.cellsignal.com/pathways/car-signaling-networks?srsltid=AfmBOoouah2ciRsHgPIUECgPq7PNEvgjLQQCal6n8huwMpxRCCF-y7V9.

413. Cai, Y. C. *et al.* Selective CD28pYMNM mutations implicate phosphatidylinositol 3-kinase in CD86-CD28-mediated costimulation. *Immunity* **3**, 417–426 (1995).

414. Nyakeriga, A. M., Garg, H. & Joshi, A. TCR-induced T cell activation leads to simultaneous phosphorylation at Y505 and Y394 of p56(lck) residues. *Cytometry A* **81**, 797–805 (2012).

415. Vang, K. B. *et al.* CD28 and c-Rel-dependent Pathways Initiate Regulatory T Cell Development. *J Immunol* **184**, 4074–4077 (2010).

416. Ma, M. *et al.* TAK1 is an essential kinase for STING trafficking. *Molecular Cell* **83**, 3885-3903.e5 (2023).

417. Rainwater, R. R. *et al.* DNA-PKcs governs LAT-dependent signaling in CD4+ and CD8+ T cells. 2025.03.06.641745 Preprint at https://doi.org/10.1101/2025.03.06.641745 (2025).

418. Yeoh, W. J. & Krebs, P. SHIP1 and its role for innate immune regulation-Novel targets for immunotherapy. *Eur J Immunol* **53**, e2350446 (2023).

419. Induction of tyrosine phosphorylation during ICAM-3 and LFA-1-mediated intercellular adhesion, and its regulation by the CD45 tyrosine phosphatase. *J Cell Biol* **126**, 1277–1286 (1994).

APPENDICIES

Appendix 1: Confirmation of submission of Chapter 3 Manuscript: Screening and Testing EGFR and Mesothelin Nano-CARs for Multi-Antigen Targeting Solid Tumour Therapy

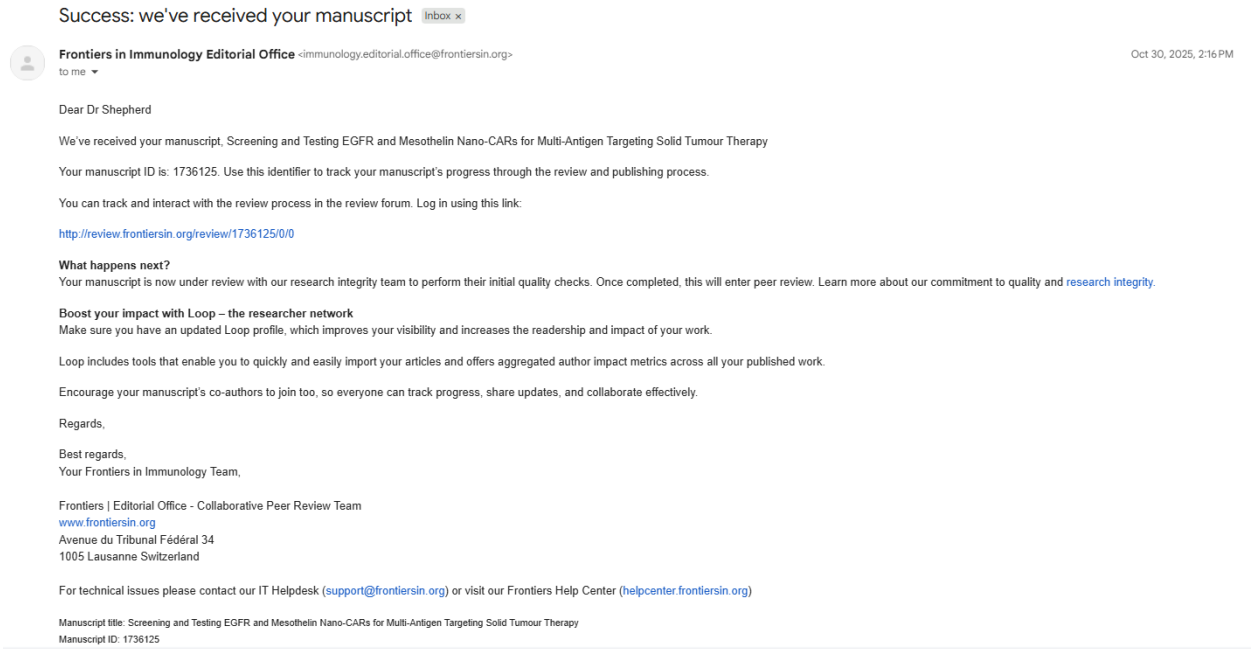

Success: we've received your manuscript Inbox ×

Frontiers in Immunology Editorial Office <immunology.editorial.office@frontiersin.org> Oct 30, 2025, 2:16 PM
to me

Dear Dr Shepherd

We've received your manuscript, Screening and Testing EGFR and Mesothelin Nano-CARs for Multi-Antigen Targeting Solid Tumour Therapy

Your manuscript ID is: 1736125. Use this identifier to track your manuscript's progress through the review and publishing process.

You can track and interact with the review process in the review forum. Log in using this link:

http://review.frontiersin.org/review/1736125/0/0

What happens next?
Your manuscript is now under review with our research integrity team to perform their initial quality checks. Once completed, this will enter peer review. Learn more about our commitment to quality and research integrity.

Boost your impact with Loop – the researcher network
Make sure you have an updated Loop profile, which improves your visibility and increases the readership and impact of your work.

Loop includes tools that enable you to quickly and easily import your articles and offers aggregated author impact metrics across all your published work.

Encourage your manuscript's co-authors to join too, so everyone can track progress, share updates, and collaborate effectively.

Regards,

Best regards,
Your Frontiers in Immunology Team,

Frontiers | Editorial Office - Collaborative Peer Review Team
www.frontiersin.org
Avenue du Tribunal Fédéral 34
1005 Lausanne Switzerland

For technical issues please contact our IT Helpdesk (support@frontiersin.org) or visit our Frontiers Help Center (helpcenter.frontiersin.org)

Manuscript title: Screening and Testing EGFR and Mesothelin Nano-CARs for Multi-Antigen Targeting Solid Tumour Therapy
Manuscript ID: 1736125

Appendix 2: Full quality control sheet for multi-omic sample preparation

	T0			T10		T6H		T24H	
	MFI (median AP	Average Viabil	Ramos/Jurk	MFI (median APC)	Ramos/Jurka	MFI (median APC	Ramos/Jurka	MFI (median APC	Ramos/Jurkat
1ug36-1	236	88.60%	Ramos: 46.7% Jurkat:	312	Ramos: 39.4% Jurkat:	465	Ramos: 47.9% Jurkat:	4032	Ramos: 53.3% Jurkat: 46.7%
1ug36-2	209	84.60%	Ramos: 49.9% Jurkat:	290	Ramos: 35.6% Jurkat:	401	Ramos: 33.7% Jurkat:	3671	Ramos: 39.5% Jurkat: 60.5%
1ug36-3	276	89.50%	Ramos: 44.7% Jurkat:	307	Ramos: 42.6% Jurkat:	437	Ramos: 51.4% Jurkat:	3854	Ramos: 49.3% Jurkat: 50.7%
1ug13-1	347	91.40%	Ramos: 59.7% Jurkat:	340	Ramos: 37.3% Jurkat:	1330	Ramos: 59.05% Jurkat:	13023	Ramos: 48.5% Jurkat: 51.5%
1ug13-2	361	89.30%	Ramos: 61.3% Jurkat:	401	Ramos: 39.8% Jurkat:	1423	Ramos: 55.4% Jurkat:	14089	Ramos: 55.6% Jurkat: 44.4%
1ug13-3	351	92.60%	Ramos: 56.5% Jurkat:	349	Ramos: 36.4% Jurkat:	1278	Ramos: 52.7% Jurkat:	13752	Ramos: 48.2% Jurkat: 51.8%
1ug61-1	147	85.50%	Ramos: 31.5% Jurkat: 68%	117	Ramos: 48.4% Jurkat:	109	Ramos: 45.2% Jurkat:	100	Ramos: 31.7% Jurkat: 67.8%
1ug61-2	387	89.90%	Ramos: 47.5% Jurkat:	491	Ramos: 35.3% Jurkat:	862	Ramos: 38.0% Jurkat:	690	Ramos: 31.7% Jurkat: 67.8%
1ug61-3	1068	85.70%	Ramos: 59.4% Jurkat:	1076	Ramos: 56.2% Jurkat:	1029	Ramos: 54.1% Jurkat:	875	Ramos: 52.1% Jurkat: 47.9%
1ug74-1	258	91.20%	Ramos: 25.2% Jurkat:	208	Ramos: 23.8% Jurkat:	1050	Ramos: 42.6% Jurkat:	15702	Ramos: 31.7% Jurkat: 67.8%
1ug74-2	764	91.90%	Ramos: 25.1% Jurkat:	801	Ramos: 23.0% Jurkat:	3058	Ramos: 38.0% Jurkat:	13690	Ramos: 21.1% Jurkat: 74.5%
1ug74-3	634	91.90%	Ramos: 46.4% Jurkat:	759	Ramos: 39.1% Jurkat:	2092	Ramos: 38.5% Jurkat:	12690	Ramos: 42.4% Jurkat: 57.6%
Jurkat -1	846	89.80%	Ramos: 34.6% Jurkat:	687	Ramos: 37.0% Jurkat:	782	Ramos: 38.0% Jurkat:	875	Ramos: 44.2% Jurkat: 55.8%
Jurkat -2	833	92.40%	Ramos: 27.2% Jurkat:	1307	Ramos: 47% Jurkat: 53%	1206	Ramos: 54.9% Jurkat:	1309	Ramos: 53.4% Jurkat: 46.6%
Jurkat -3	884	86.20%	Ramos: 32.8% Jurkat:	1154	Ramos: 25.1% Jurkat:	1174	Ramos: 44.1% Jurkat:	1065	Ramos: 56.6% Jurkat: 53.4%
BCRx 1u	484	85.20%	Ramos: 28.6% Jurkat:	2080	Ramos: 36.3% Jurkat:	1067	Ramos: 40.1% Jurkat:	4444	Ramos: 42..2% Jurkat: 57.8%
BCRx 1u	814	89.30%	Ramos: 39.7% Jurkat:	796	Ramos: 48.8% Jurkat:	1215	Ramos: 45.1% Jurkat:	4167	Ramos: 43.2% Jurkat: 56.8%
BCRx 1u	796	91.40%	Ramos: 27.8% Jurkat:	1256	Ramos: 40% Jurkat: 60%	1487	Ramos: 41.2% Jurkat:	2373	Ramos: 42.6% Jurkat: 57.4%

Appendix 3: Animal use protocol approval

National Research Council Canada
Human Health Therapeutics

Ottawa, Canada
K1A 0R6

Conseil national de recherches Canada

Produits thérapeutiques en santé humaine

February 27, 2023

Re: Scott McComb - Animal Care Committee approval

Dear Sir/Madam,

Dr. Scott McComb is a co-investigator on an Animal Use Protocol (NRC AUP#2020.04) entitled "Evaluation of Cellular and Biological Immunotherapy Using Mouse Models". The preclinical *in vivo* facility of the National Research Council (NRC) of Canada's Human Health Therapeutics (HHT) Research Centre holds a Good Animal Practice (GAP) certificate from the Canadian Council on Animal Care and has a dedicated Animal Care Committee (ACC) that oversee the ethical treatment of experimental animals used in research at NRC.

The ACC approved AUP 2020.04 in March 2020 and is renewable until March 2024. The protocol is in good standing. All animal experiments performed as described in AUP 2020.04 have been approved for ethical standards by the NRC ACC. The AUP is also subject to the Post-Approval Monitoring (PAM) program of the ACC. Specific experimental methods included in AUP 2020.04 include the use of murine tumour models, xenograft tumour models, and adoptive transfer of murine and human immune cells.

Information about our program, our ACC Terms of Reference and Policies and Procedures Manual is available online at: https://nrc.canada.ca/en/support-technology-innovation/human-animal-ethics

Should you require any further information, please do not hesitate to contact us.

Sincerely,

Weeratna, Risini
Digitally signed by Weeratna, Risini
Date: 2023.02.27 13:29:27 -05'00'

Risini Weeratna, PhD
ACC Chairperson, HHT-ACC

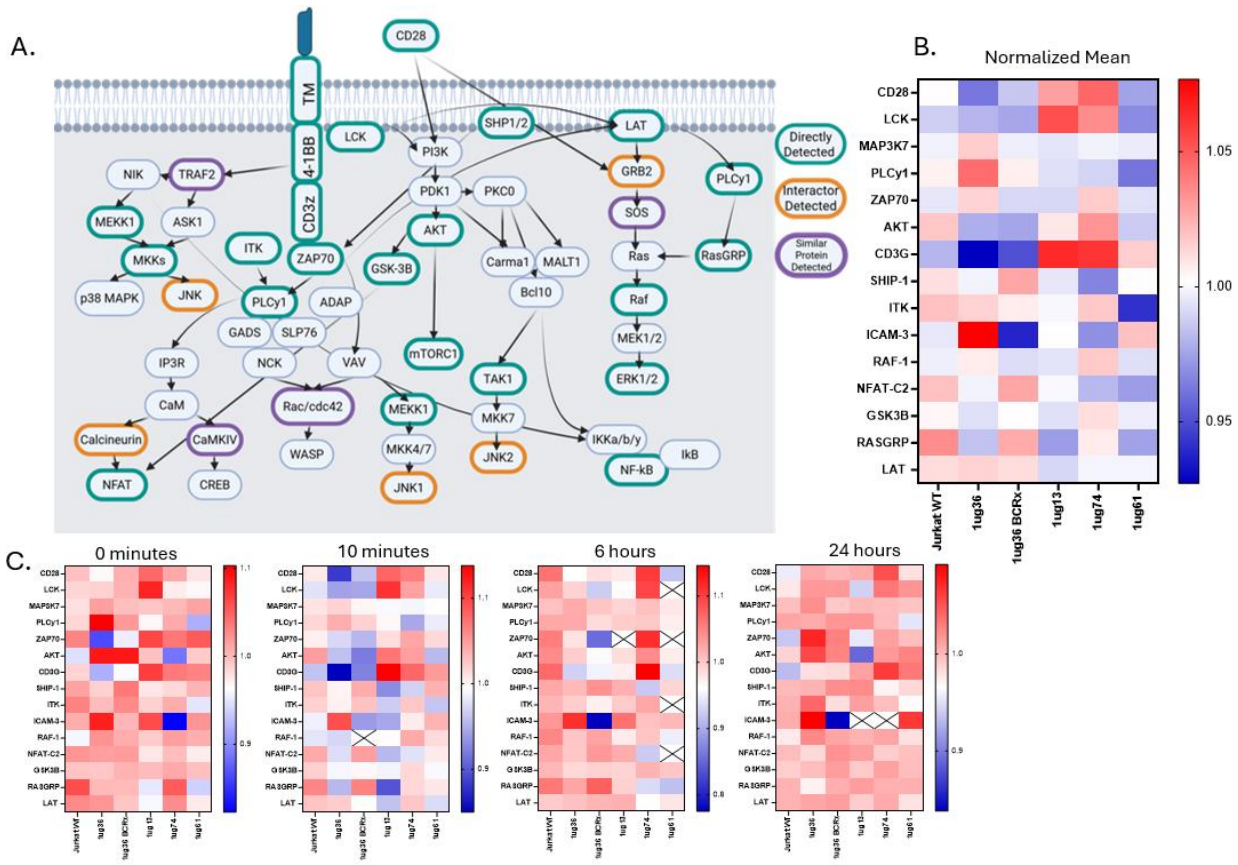

Appendix 4A Potential trends in CD22 CAR multi-omics analysis

Data presented samples from a single run of CD22 CARs after processing using DIA-NN analysis and normalization software. (A). Map of commonly associated CAR activation pathways and protein, indicating proteins observed during phosphoproteomic analysis, as well as adjacent and associated proteins observed when the exact protein could not be found. Map derived from the *Cell Signaling Technology – CAR Signaling Interactive Pathway*[412]. (B). Heap map of the mean abundance of all combined timepoints for each CAR for some of the notable proteins found within the phosphoproteomic dataset. Protein abundance normalized to the total mean of the entire dataset and presented in log2. (C). Heap map of the mean abundance over each separate timepoint for each CAR for some of the notable proteins found within the phosphoproteomic dataset. Protein abundance normalized to the total mean of each timepoint and presented in log2. Proteins that were observed in (A) but showed multiple missing datapoints (>30%) were omitted from heatmapping.

Appendix 4B. Discussion of interesting proteomic data

Although our approach was only able to identify approximately half of the commonly associated proteins with CAR and TCR signaling on this attempt, the proteins of interest identified reveal some interesting trends for both binder and transmembrane domain selection. As mentioned above, the higher binding 1ug13 and 1ug74 CARs showed notably higher phosphorylation of both CD28 y191 and LCK y505. This combinations of upregulated phosphorylation sites suggests that these CARs may have difficulty maintaining signal through CD3ζ and thusly must compensate with increased signaling through CD28.[413] The presence of LCK y505 specifically indicates that CD45 segregation

may be lasting longer than is optimal, allowing phosphate to build up on the inhibitory phosphorylation site, hampering the signal.[414] This line of thinking is supported by previously published data regarding binding; both 1ug13 and 1ug74 have much higher binding maximums than 1ug36 and may be binding for longer, resulting in extended CD45 segregation. The increase signaling seen in CD28 is shown to be on y191 or the PYAP region, a tyrosine directly associated with the SH2 region which stimulates the PI3K/AKT pathway, which promotes proliferation and survival rather than cytotoxicity.[413,415] This is further supported when examining AKT, in which similar phosphorylation patterns are seen. In contrast, 1ug36 shows higher signaling through LAT (likely s224) and the MAPK pathways, showing higher signaling through MAP3K7 or TAK1 s439. Instead of the increase proliferation and survival, these pathways simulate cytokine production and the upregulation of the NF-κB, JUN and ATF transcriptomic factors.[416,417]

Another notable difference between 1ug36 and 1ug13/74 is its CD69 signal. As seen in both Figures 5.1 and 5.3, 1ug36 activation is much lower than either of the other *in vitro* and *in vivo* candidates. This consistently low signal, combined with the differences in signaling that can be seen in the first replicate of the phosphoproteomic data set, suggests that higher signaling CARs may not be optimal candidates, at least in the case of CD69. While this further emphasizes the need for additional screening targets, it also may suggest that, at least for CD22, CAR-T may have an optimal level of signaling, something we have begun calling a 'goldilocks zone'. CAR-T with too high a signal may lead to inhibitory phosphate build up, as seen in Figure 5.5, or perhaps over engage a target too quickly, leading to unoptimized dwell times and an incomplete signal. To low of a signal, as seen in 1ug61, either fails to activate the cell, or it is too difficult to bind consistently to achieve serial engagement. While 1ug36 avidity and low CD69 response is not the only factor that make it unique; 1ug10 has a similar binding profile and CD69 response, but less CD^{51} release, optimizing CAR activity for a specific range, as opposed to maximal signaling presents a small but impactful potential shift in CAR-T screening and design process.

While the data presented here requires validation from additional data sets that are currently in production, it presents several promising possibilities for further testing and screening targets. First and foremost is CD28, with some preliminary experiments already being done to examine the further differences between transmembrane domains. Given the evidence supporting CD28 as a co-stimulatory molecule results in more aggressive, less persistent CAR cytotoxicity, and having CD28 as a transmembrane domain reduces the amount of free CD28 on the cell surface, it stands to reason that the non-CAR CD28s signaling may play an important role in how CARs signal.[154,409] When examining differences between CD28TM phosphorylation (Standard 1ug36) and CD8aTM (BCRx 1ug36) differences in the upregulation of SHIP1 and NFAT2 can be seen, suggesting that CD8aTM may direct CARs signaling towards cytotoxicity through NFAT and actively reduce proliferative signals by converting PI3K to PI2K through SHIP1 reducing AKT signaling.[418] Should this pattern of signaling be shown to be consistent, further examination of this interaction is warranted, either through an NFAT/AKT reporter to examine downstream signals, or through staining of the CD28 phosphorylation sites using phospho-flow. Secondly further investigation of the differences seen between 13/74 and 36. As seen in

Chapter 4, 13 and 74 fall into the high avidity CARs categories, while 36 has much lower avidity. This, combined with the differences in phosphorylation, suggests that this binding interaction may play a larger role than previously anticipated in how a CAR signals. Further testing of CD45 and LCK signaling is needed to better understand the impact epitope selection plays on CAR signal fate, as well as proper CD45 segregation during CAR binding. This can also be investigated through further investigation of ICAM3, which also shows higher phosphorylation in 1ug36, which has been shown to help regulate CD45.[419]